Purification, crystallization and structure determination of an azurin variant

A THESIS
SUBMITTED TO THE FACULTY OF THE GRADUATE SCHOOL
OF THE UNIVERSITY OF MINNESOTA
BY

Melanie Ann Ladd

IN PARTIAL FULFILLMENT OF THE REQUIREMENTS
FOR THE DEGREE OF
MASTER OF SCIENCE

Dr. Steven M. Berry

August 2012

Acknowledgements

I would like to thank Dr. Steve Berry for his patience and kindness toward me and for his enthusiasm for this research. He always made himself available for questions and any concerns I had, and his advice and expertise helped me accomplish my research goals. I would also like to thank Dr. Victor Nemykin and Dr. Pavel Solntsev for sharing their crystallography experience and familiarizing me with small molecule structure solution. Dr. Nemykin was instrumental in obtaining funding from the National Science Foundation for the Rigaku Rapid II Diffractometer which was crucial to the success of this work. Thank you also to Bryan Bandli for his time and his help in maintaining the instrument. Thanks to Dr. Ed Hoeffner and Dr. Carrie Wilmont at the Kahlert Structural Biology Laboratory on the University of Minnesota campus in the Twin Cities who gave of their time and shared their knowledge of macromolecular crystallography. I would also like to thank Dr. Clay Carter for his generosity in making his camera and microscope available to me to take photos of crystals. Thank you to Mr. and Mrs. Jim Swenson for providing the financial support that allowed me to gain experience working in a research laboratory during my undergraduate years. This experience spurred me on to continue this research. I would also like to thank those students who shared a workbench with me, specifically Audrey Schenework, Oleksandra Kniazieva, Erika Bladholm, Jacob Strange, Andy McCabe, Greg Reynolds and Stephani Lipps for all of their encouragement. Lastly, I would like to thank the Department of Chemistry and Biochemistry Faculty and Staff for this opportunity and for giving me the necessary guidance to complete this research.

Dedication

This thesis is dedicated to my Father in heaven who made this beautiful earth. Thank You for blessing this time in my life and giving me the opportunity to grow closer to You by learning more about Your creation.

Abstract

X-ray diffraction is a method that allows the three-dimensional structure of a molecule to be determined. To use this technique to study a protein model, high-quality crystals were grown. A biosynthetic approach was taken to model the mammalian protein peptidylglycine α-hydroxylating monooxygenase (PHM), which is a copper-binding protein that hydroxylates the α-carbon of a glycine residue in the production of peptide hormones. In order to understand the mechanism of this reaction, a model of the two copper sites involved in hydroxylation was created using the bacterial protein azurin as a scaffold (Az-PHM). To compare the structural similarity of the model to the native PHM system, Az-PHM crystals were grown for x-ray diffraction using various buffers, salts, polyethylene glycol (PEG) and excess copper. Dozens of the resulting crystals were diffracted, which had lower resolutions (~2.5 Å) and higher mosaicities (0.8 - 1.2° on average). Crystal dehydration and cryoprotection techniques were applied and consistently yielded higher resolution and lower mosaicity crystals. The crystal with the highest resolution and low mosaicity was grown in Tris buffer, lithium nitrate, PEG-2000 and copper chloride. Diffraction images for this crystal were collected on a Rigaku RAPID II X-ray Diffractometer using a copper radiation source with capillary optics and an R-AXIS image plate detector. Data were indexed to yield a $P2_12_12_1$ space group, which was then followed by integration, scaling and averaging using CrystalClear 2.1 software. Phases were determined using the Molecular Replacement method in the software CCP4. Finally, structural refinement of the model and electron density map in Coot yielded a 1.3 Å structure with an R_{factor} of 17.57% and an R_{free} of 20.70%.

TABLE OF CONTENTS

LIST OF TABLES

LIST OF FIGURES

CHAPTER 1

Chapter 1.1 Introduction

Biological inorganic chemistry is an exciting new field of chemistry that is devoted to exploring the role of metals in biological systems. Many metals such as vanadium, manganese, iron, cobalt, nickel, copper, zinc, molybdenum and tungsten have been found to play essential roles in the structure and function of metalloenzymes (1). After iron and zinc, copper is the third most abundant trace element in humans (2) and has many diverse functions in metalloenzymes as it can be involved in electron transfer, oxygen transport and even catalysis (1). With so many functional roles, surely the coordination around the copper plays a large part in fine-tuning its electronic structure and therefore, its function.

Copper sites in metalloproteins can be divided into six classes based on spectroscopic properties which depend on a copper's active site geometry, the types of ligands coordinated to the copper ion, the electronic structure of the copper atom and its resulting function. The first class is traditionally known as Type 1 (T1) and is characterized by proteins that bind a copper(II) ion that give an unusually strong signal in the UV-visible region near 600 nm (3). The signal is the direct result of the copper's strong covalent-like interaction with sulfur in a cysteine (4). The cysteine sulfur is one of three donors to bind in a trigonal fashion; the other ligands include two nitrogen atoms (Figure 1.1a). In addition, sometimes one or two axial ligands will also coordinate the copper center (sulfur from a methionine amino acid and/or oxygen from a backbone carbonyl group). Proteins containing a T1 site are often referred to as "blue copper proteins" and function in electron transfer (1). Type 2 (T2) is the name that defines the second class of copper sites which is expected to show a weaker blue color with absorption between ~575 and 800 nm when a copper(II) ion is bound to the active site. This weak absorption signal is due to the different geometry and ligand types normally found in T2 copper proteins (5). Typically, the ligands surrounding a T2 copper active site include four donors ("x" number of nitrogen atoms and "4-x" oxygen atoms from various amino acids) in a square planar coordination (Figure 1.1b) and on occasion, an axial donor (also usually a nitrogen or oxygen atom). Copper active sites classified as T2

are often involved in catalysis (1). Other classes of copper active sites are more rare and include Type 3 (T3), Copper A (Cu_A), Copper Z (Cu_Z) and copper chaperones.

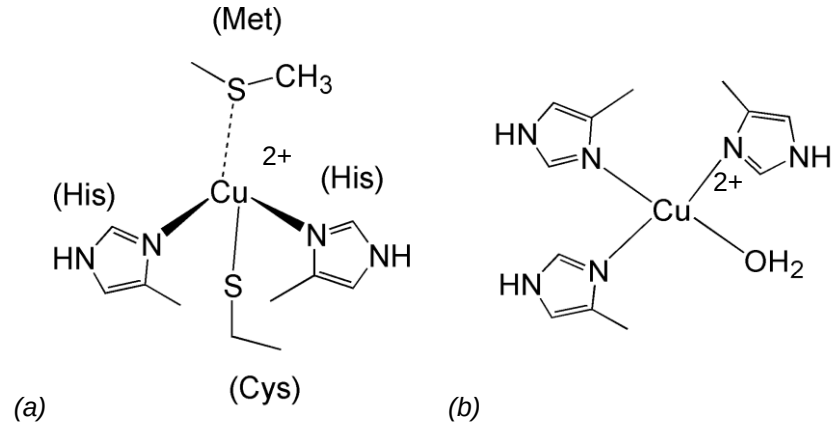

Figure 1.1. Typical coordination of (a) T1 and (b) T2 copper sites in biological molecules.

Understanding why the structure of different copper active sites gives rise to their function is at the heart of this research. Metalloprotein design is one way in which this relationship can be studied. In this study, metalloprotein design involves modeling a naturally-occurring metal site using a biosynthetic approach. Active site residues from the target metal site of interest are mutated into a native protein scaffold that is stable, easy to purify and well-characterized. By using an existing protein as a scaffold, the aqueous environment and common pH of the target system can be preserved. Also, because the number of possible active site residues is limited and their composition is the same as those ligands in the native system, certain aspects of metal coordination are maintained. In modeling the metal site of a target protein in this way, the end goal is to create a model that is a structural and functional mimic of the native system. Generally, native biological enzymes are so efficient and selective that few models can compare. In the future, the ability to mimic the structure and function of any enzyme by way of metalloprotein design will allow researchers to create protein molecules for any desired function (6).

Chapter 1.2 PHM and Azurin

The target protein of interest is peptidylglycine α-hydroxylating monooxygenase (PHM) which is a large metalloenzyme found in mammals. PHM is ~300 residues in

length (7) and is part of a larger protein complex called peptidylglycine α-amidating monooxygenase (PAM) which was first located in the pituitary gland (8). PHM contains two copper-binding sites that function in peptide hormone synthesis, catalyzing the oxidation of C-terminal glycine-extended peptides into α-hydroxylated products (9). These two copper sites are located across a solvent gap of ~11 Å (7) and each have different roles in that one of the coppers functions in electron transfer/electron storage (Cu_H) and the other participates in catalysis (Cu_M). The Cu_H site is thought to get its electrons from a physiological reductant, such as ascorbate, while the Cu_M site is thought to be where molecular oxygen and substrate bind prior to the hydroxylation reaction. One of the unknown questions about the roles of the copper ions in the mechanism is the nature of the reactive oxygen species generated at the Cu_M site (9).

Though the functions of these copper ions are characteristic of T1 and T2 copper active sites, structurally-speaking, both of these copper sites resemble the structure of T2 sites (Figure 1.2). Cu_H is bound by three histidines, 107, 108 & 172, and Cu_M is bound by two histidines, 242 & 244, and methionine 314 (the numbering is from human PHM) (9).

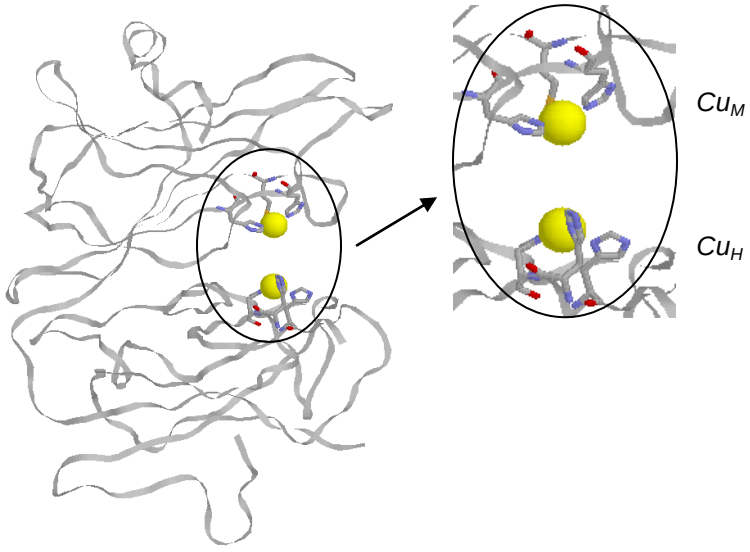

Figure 1.2. Copper active sites of PHM (PDB ID: 1PHM). The copper on the top, Cu_M, is bound by two histidine residues and a methionine and fuctions in electron transfer. The copper on the bottom, Cu_H, is bound by three histidines and is the site for catalysis.

Interestingly, PHM's copper(II) ions communicate when an electron is passed from Cu_H to Cu_M. This is puzzling given that the two copper ions are located across a solvent gap and are not coupled to one another. The shortest distance for the electron to travel is directly between the two copper centers in the solvent-filled gap that separates the copper ions (9). In order to better understand how the mechanism for electron transport occurs, to clarify the nature of the reactive oxygen species and to explore copper metalloprotein design parameters, a biosynthetic model was created using a protein called Azurin as the scaffold.

Azurin is small protein with a molecular weight of 14 kDa and a length of 128 residues (10). It is found in the soil bacteria *Pseudomonas aeruginosa* and is thought to play a role in the shuttling of electrons in the denitrification pathway (11, 12). It is a well-characterized blue copper protein, and historically, it's stable to mutations (13, 14), making it an ideal candidate to use for design. Azurin was also chosen because it possesses a native Type 1 copper binding site (His46, Cys112, His117 & Met121), shown in Figure 1.3. Using azurin as a scaffold, a Type 2 site was designed where three residues were mutated, namely Gln8Met, Gln14His and Asn16His, to create an Az-PHM variant (15). The overall protein fold of azurin contains mostly beta-sheet secondary structures with a looped section containing some alpha helical segments. Most of the amino acids supporting the T1 copper site are found on this loop section (Cys112, His117, Met 121) with the fourth ligand found on an internal strand of beta-sheet (His46) (16). The section of the protein where the T2 copper binding site was designed is a section that has three parallel strands of beta-sheet structure, with the amino acid residues Gln8Met, Gln14His, and Asn16His being found on two of these adjacent strands.

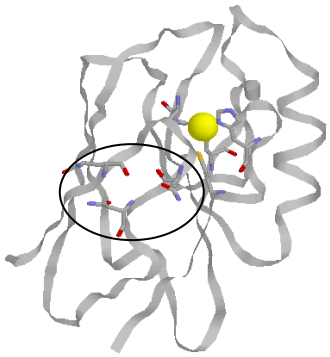

Figure 1.3. Azurin crystal structure (PDB ID: 4AZU) with a copper bound in the T1 copper site. The three residues circled were the amino acids that would be mutated to bind copper in the designed T2 site.

In order to study the function of the Az-PHM model, structural analysis must be carried out to identify whether or not the design of the T2 site allows a copper(II) ion to bind and to determine how closely the model recreates the native copper binding site structure. Protein structure can be determined qualitatively in several ways, however x-ray crystallography and NMR spectroscopy are the only two ways in which a high-resolution, three dimensional structure can be determined (17). In light of this, research began by purifying the protein in order to grow crystals of the mutant. Obtaining pure Az-PHM is vital because growing diffraction-quality crystals depends on the purity of the protein sample (18).

Chapter 1.3 Az-PHM Purification

Az-PHM was purified from BL21* *E. coli* cells previously infected with a pET9a expression vector containing a gene for the azurin preprotein from the bacterium *Pseudomonas aeruginosa* (15). Cell colonies were cultured for 5-8 hours in LB media containing Kanamycin in a shaking incubator at 37°C and then again overnight in a 2x yeast-tryptone (2xYT) medium containing 16 g bactotryptone, 10 g yeast extract, 5 g sodium chloride and 50 mg kanamycin per liter of media for 12-14 hours at 30°C. After cells reached an optical density of >1.5 at 600 nm, the cultures were induced with isopropyl β-D-1-thiogalactopyranoside (IPTG) to a concentration of ~0.07 g/L of culture and then incubated for another 3 hours. The induction with IPTG caused the azurin gene to be aggressively translated and transcribed from the pET9a plasmid.

Cells were pelleted via centrifugation and then lysed through osmotic shock. The first step in shocking the cells was suspension of the cell pellet at 37°C in a sucrose solution consisting of 20% (w/v) sucrose, 1 mM EDTA and 39 mM Tris. After subsequent centrifugation, the resulting pellets were resuspended in purified H_2O at 4°C for ~10 minutes causing the cells to swell, breaking the cell wall. Because the azurin preprotein gene includes code for a 19 amino acid leader sequence that sends the finished protein to the periplasm, Az-PHM is released into solution after cell wall lysis leaving behind intact plasma membranes. A third round of centrifugation follows osmotic shock to separate Az-PHM from the cell lysate.

In order to further purify Az-PHM from other proteins in the periplasmic supernatant, sodium acetate at pH 4.1 was added to a final concentration of ~50 mM to precipitate the unwanted protein. After a final round of centrifugation, Az-PHM's isoelectric point of ~5.1 was utilized in cation-exchange chromatography. SP-Sepharose resin, which consists of negatively-charged sulfonate groups, was added to the supernatant. Because a pH of 4.1 was maintained during this step, the sulfonate groups on the resin bind the positively-charged Az-PHM. The resin was washed in the SP-column before increasing the pH to 6.35, a pH above its isoelectric point, to elute Az-PHM. Next, the protein was added to an anion-exchange column containing Q-Sepharose resin equilibrated to a pH of 6.35 with 50 mM ammonium acetate. At this pH, other proteins in the solution bind to the positively-charged amino groups of the resin, allowing Az-PHM to flow through in a fairly pure form. Lastly, a size-exclusion column containing Sephadex resin separated any proteins in solution by their size. Before running the column, the Az-PHM in solution was titrated with copper.

Throughout the purification, the presence and concentration of Az-PHM was determined using the unique spectroscopic properties of azurin's T1 copper site. When copper is titrated into a sample of apo azurin, each azurin active site binds a copper(II) ion tightly and electrons from the copper are covalently shared with the sulfur of Cys112. This bonding characteristic gives rise to a very intense S→Cu(II) charge transfer band at ~625 nm (3). To calculate the concentration of Az-PHM, a UV-visible spectrum of the apo form of the protein is obtained and overall protein concentration is determined using

Beer's Law, absorbance at ~280 nm and a molar absorptivity of 8440 $M^{-1}cm^{-1}$. One equivalent of copper is titrated into the measured sample and a spectrum of holo Az-PHM was obtained. Knowing that azurin's molar absorptivity is 5000 $M^{-1}cm^{-1}$ at ~625 nm, Az-PHM's concentration was determined by measuring the absorbance of the signature peak near 625 nm (15).

This spectroscopic characteristic was also used to assess the purity of the fractions from the size-exclusion column. A pure sample of Az-PHM should ideally produce a spectrum where the ratio of absorbance at 280 nm to the absorbance at 625 nm is equal to 1.8. This ratio was calculated for each fraction that eluted from the size-exclusion column. Typically, fractions ~40 to 43 gave ratios close to 1.8 and were noticeably smaller than the ratios of fractions ~20-39. This trend is visible in Figure 1.4 where fractional ratios for the first two growths of Az-PHM are shown.

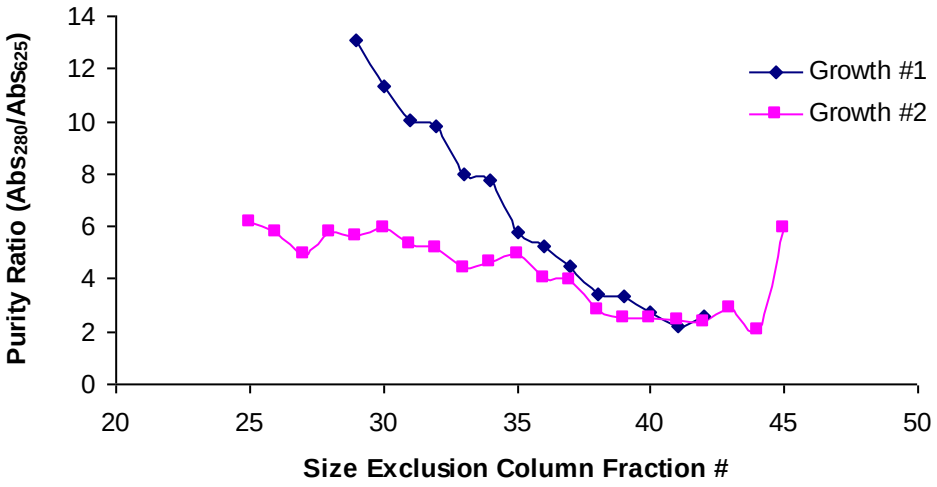

Figure 1.4. Graph showing the purity ratios of fractions containing Az-PHM from the size-exclusion column. A ratio of 1.8 indicates a pure Az-PHM sample.

Protein purity was also examined using sodium dodecyl sulfate polyacrylamide gel electrophoresis (SDS-PAGE). Small samples of Az-PHM taken before and after the size exclusion column were run down an SDS gel and analyzed for contamination by other proteins. Figure 1.5 shows a gel containing samples from two purifications. Lane 1 contains a protein ladder. Lanes 2 and 3 contain samples before running the gel-column.

Lanes 4 and 5 contain samples from fractions between ~25-39 while protein from fractions ~40-43 is found in lanes 6 and 7.

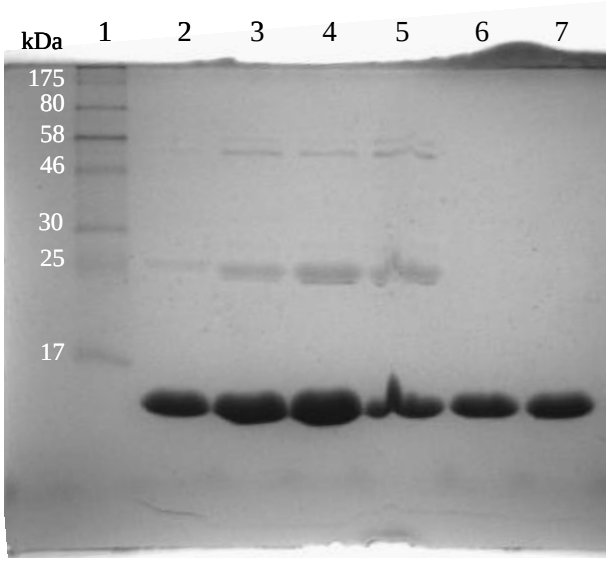

Figure 1.5. Results of SDS-PAGE using Az-PHM samples taken before and after the size-exclusion column. Lane 1 contains a protein ladder. Lanes 2 and 3 contain samples before running the gel-column for growths 1 and 2, respectively. Lanes 4 and 5 contain samples from fractions between ~25-39 while protein from fractions ~40-43 is found in lanes 6 and 7 from growths 1 and 2, respectively.

In analyzing the spectroscopic ratios and the gel from SDS-PAGE, it is apparent that the size exclusion column was successful in purifying Az-PHM from other contaminants. In analyzing the spectroscopic data, the purest protein was typically found in fractions 40-43. Though the ratios for these fractions were not 1.8, they were very close to this ideal value and suggested a nearly pure sample. Their purity was confirmed with SDS-PAGE when the resulting gel revealed single large bands which appear to be under 17 kDa in lanes 6 and 7. The extra bands present in lanes 2-5 also explain the high spectroscopic ratios calculated for fractions ~25-39. These bands near 25 kDa and 50 kDa are clearly not azurin and therefore, serve to increase the spectroscopic ratios. The ultrapure Az-PHM samples from fractions ~40-43 are ideal for crystallography and greatly increase the chances that crystals will form (18).

CHAPTER 2

Chapter 2.1 Introduction

In order to gain structural information from the Az-PHM model system, ultrapure protein samples were used to grow crystals for x-ray diffraction. Most crystallographers would agree that growing diffraction-quality protein crystals is the most time-intensive and least understood part of the crystallography process. Diffraction-quality crystals are well-ordered gelatinous solids in which protein molecules stack together in a repeating pattern. Part of the difficulty in obtaining ordered crystals is due to the irregular shape of most macromolecules. Because protein molecules lack flat edges, they don't stack well, compelling water molecules to form channels between the layers of stacked protein molecules. Water molecules facilitate interactions between protein molecules, which help the crystal nucleate and grow, however, hydrogen bonding interactions are weak which means that protein crystals are fragile and fall apart easily. Another factor that complicates stacking is the inherent chemical properties of protein molecules. Small changes in the pH of the solution cause differences in charge over the surface of the protein molecule, making it difficult to predict conditions that will cause crystallization (17).

Generally, crystallization occurs when pure, concentrated protein is placed in an environment that causes it to become supersaturated and precipitate out of solution. Supersaturation can be achieved through two different methods that are often used simultaneously, namely water loss and the use of a precipitating agent. Water loss, typically via evaporation, causes the protein in solution to become more concentrated by forcing it into a smaller volume of solution. A precipitant does a similar thing by immobilizing water, causing the protein to aggregate together in a smaller volume of solution. Most often the precipitating agent is a salt or polyethylene glycol that is either diffused in or added directly to the buffered protein solution to compete for solvation and salt out the protein. It can, however, be beneficial to use both salt and polyethylene glycol (PEG). Depending on its concentration and the makeup of the protein, salt can either salt out or salt in. Salting in describes the process of allowing the protein to more easily dissolve by raising the ionic strength of the solution. Salt can also facilitate

protein-protein interactions by shielding repulsive charges on the surface of the protein molecules (18).

After finding the exact salt and PEG concentrations coupled with the right pH and temperature that will yield crystals, two techniques called dehydration and cryoprotection can be implemented depending on the quality of the crystals and the need to protect them from ice crystallization during pinning and cryofreezing. Dehydration is a process that involves removing water molecules from a crystal that has already formed. Water is removed when crystals are equilibrated to a solution containing less water than the solution the crystals grew in. By forcing water out of the crystal in this manner, the crystal becomes more ordered. Cryoprotection, on the other hand, decreases ice formation around the crystal by providing a viscous solution to pin crystals from. Crystals are successively equilibrated against solutions of increasing glycerol. The glycerol prevents water from forming crystalline ice which would diffract with the protein crystal and cause unwanted diffraction rings ("ice rings") to appear in the diffraction pattern. The need for dehydration and cryoprotection is initially determined after screening crystals.

It is necessary to screen crystals to determine if they are well-ordered (diffraction-quality) since it is difficult to visually distinguish a good crystal from a bad crystal. Screening a protein crystal typically involves mounting it on an x-ray diffractometer and exposing it to x-ray radiation to obtain two sample diffraction images. The reflection data from the images are processed, and the resulting statistics are used to assess the quality of the crystal. These statistics include spot intensity, mosaicity, resolution, the prevalence of ice rings and the accuracy of the unit cell prediction. If the crystal is well-ordered then reflections will be intense and have a large intensity relative to background. The crystal's mosaicity, a measure of its disorder, will be low and resolution will be high, meaning reflections will be located far from the center of the image. In addition to having no ice rings, the high quality of these three statistics helps ensure that the unit cell prediction is accurate.

Chapter 2.2 Method for Crystal Growth & Crystal Box Set-up

Pure protein was used to set up crystal boxes that utilized the Hanging Drop Vapor Diffusion method. Crystallization of the protein using this method relies on the diffusion of water from the protein drop into a reservoir solution below, as depicted in Figure 2.1.

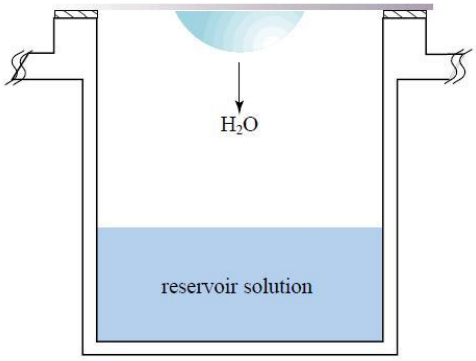

Figure 2.1. Depiction of the hanging drop vapor diffusion method, adapted from reference 19. Protein is located in the drop and becomes concentrated as water leaves the drop.

The hanging drop vapor diffusion method calls for a hanging drop that sits in a sealed environment over a reservoir solution that is typically twice as concentrated with precipitation reagents. Because the drop is in vapor equilibration with the reservoir solution, water leaves the drop in order to reach equilibrium. As water leaves, the protein located in the drop becomes more concentrated. With the right balance of salts and precipitating agents to facilitate protein-protein interactions, the protein will crystallize out of solution.

To find conditions under which Az-PHM would crystallize, primary literature was consulted (20-31). Numerous conditions were identified where azurin and variants of azurin had previously been crystallized using vapor diffusion (Table 2.1). When crystallizing Azurin on two separate occasions, Faham *et al*. used Tris buffer, lithium nitrate, polyethylene glycol (PEG)-4000 and copper chloride (22). These reagents were initially chosen to crystallize Az-PHM since a crystal structure was desired that showed a copper(II) in the weakly-binding T2 site designed on the surface of the protein.

Table 2.1. Conditions used to crystallize azurin and its variants. All conditions were found in primary literature. Special instructions regarding exact crystallization methods are not included.

Reference	Reservoir Reagents	Drop Reagents	Protein Concentration
20	0.1 M Acetate pH 5.5 3.2 M $(NH_4)_2SO_4$ 0.5 M $LiNO_3$	0.1 M Acetate pH 5.5 2.0 M $(NH_4)_2SO_4$ 0.3 M $LiNO_3$	10 mg/mL
21	3.4 M Na/KPO_4 pH 6.0	1.7 M Na/KPO_4 pH 6.0	14 mg/mL
22	0.1 M TrisHCl pH 8.0 0.1 M $LiNO_3$ 25% PEG-4000 20 mM $CuCl_2$	0.05 M TrisHCl pH 8.0 0.05 M $LiNO_3$ 12.5% PEG-4000 10 mM $CuCl_2$	10 mg/mL
23	0.1 M Tris pH 8.0 0.1 M $LiNO_3$ 30%(w/v) PEG-4000 20 mM $CuCl_2$	0.05 M Tris pH 8.0 0.05 M $LiNO_3$ 15%(w/v) PEG-4000 10 mM $CuCl_2$	15 mg/mL
24	0.1 M Imidazole pH 6.0-8.0 0.1 M $LiNO_3$ 25-38% PEG-4000/8000 6.25 mM $CuCl_2$	0.05 M Imidazole pH 6.0-8.0 0.05 M $LiNO_3$ 12.5-18% PEG-4000/8000 3.125 mM $CuCl_2$	10-15 mg/mL
25	0.1 M Imidazole pH 8.0 0.1 M $LiNO_3$ 20% PEG-8000	0.05 M Imidazole pH 8.0 0.05 M $LiNO_3$ 10% PEG-8000	13 mg/mL
26	0.1 M Imidazole pH 7.0 0.1 M $LiNO_3$ 20% PEG-4000	0.05 M Imidazole pH 7.0 0.05 M $LiNO_3$ 10% PEG-4000	15 mg/mL
27	0.1 M Imidazole pH 7.0 0.1 M $LiNO_3$ 20% PEG-4000	0.05 M Imidazole pH 7.0 0.05 M $LiNO_3$ 10% PEG-4000	15 mg/mL
28	0.1 M Citric acid pH 3.2 0.1 M $LiNO_3$ 20-24% PEG-4000	0.05 M Citric acid pH 3.2 0.05 M $LiNO_3$ 10-12% PEG-4000	15 mg/mL
29	0.1 M Imidazole pH 7.0 0.1 M $LiNO_3$ 20% PEG-4000	0.05 M Imidazole pH 7.0 0.05 M $LiNO_3$ 10% PEG-4000	15 mg/mL
30	0.22 M acetate pH 6.0 0.2 M $CaCl_2$ 25% PEG-4000		7.5-10 mg/mL
31	0.08 M Na acetate pH 6.0 0.24 M $LiNO_3$ 0.24 M $CaCl_2$ 25% PEG-8000 (or 4000)	0.04 M Na acetate pH 6.0 0.12 M $LiNO_3$ 0.12 M $CaCl_2$ 12.5% PEG-8000 (or 4000)	1 mM

Besides the reagents chosen initially, azurin was also commonly crystallized in buffers such as imidazole and acetate, other salts such as calcium chloride, copper such as copper sulfate and other precipitating agents such as PEG at molecular weights 600, 1000, 2000 and 8000 (Table 2.1). Combinations of all these reagents at various concentrations were explored using 24-well crystal boxes. The 24-well plates have four

rows (labeled A, B, C and D) with six reservoirs in each row (labeled 1, 2, 3, 4, 5 and 6). An example of the conditions used in one of the crystal box trials, called "Box #70", is presented in Table 2.2. In setting up the box, the buffer, salt, precipitant, copper and water were mixed in each of the 24 reservoirs and final concentrations of these reagents in each reservoir (denoted A1, A2, A3… through D5, D6) are indicated in parentheses in Table 2.2. Then after mixing reservoir solutions, 2 μL was taken from well A1 and mixed with 2 μL of purified Az-PHM on a coverslip. The purified Az-PHM used in crystal box set-up had concentrations between 25-35 mg/mL (or 1.8-2.5 mM). Lastly, the coverslip was sealed over the respective reservoir and the process was repeated for the remaining 23 wells.

Table 2.2. Example of crystal conditions (Box #70). All concentrations in parentheses are final concentrations in the reservoir solution. The drop above each reservoir contained 2 µL of water, 2 µL of 29.5 mg/mL Az-PHM in 50 mM imidazole pH 8.07 and 2 µL of reservoir (for drops over row A, 2 µL from A3; for drops over row B, 2 µL from A4; for drops over row C, 2 µL from A5; for drops over row D, 2 µL from A6).

	2.0 M Imidazole pH 8.02	**5.0 M $LiNO_3$**	**50% PEG-8000**	**0.1 M $CuCl_2$**	**Millipore H_2O**
A1	25 µL (0.05 M)	0 µL	260 µL (13%)	50 µL (0.005 M)	665 µL
A2	25 µL (0.05 M)	0 µL	220 µL (11%)	50 µL (0.005 M)	705 µL
A3	25 µL (0.05 M)	0 µL	180 µL (9%)	50 µL (0.005 M)	745 µL
A4	25 µL (0.05 M)	0 µL	140 µL (7%)	50 µL (0.005 M)	785 µL
A5	25 µL (0.05 M)	0 µL	100 µL (5%)	50 µL (0.005 M)	825 µL
A6	25 µL (0.05 M)	0 µL	60 µL (3%)	50 µL (0.005 M)	865 µL

	2.0 M Imidazole pH 8.02	**5.0 M $LiNO_3$**	**50% PEG-8000**	**0.1 M $CuCl_2$**	**Millipore H_2O**
B1	25 µL (0.05 M)	0 µL	260 µL (13%)	50 µL (0.005 M)	665 µL
B2	25 µL (0.05 M)	0 µL	220 µL (11%)	50 µL (0.005 M)	705 µL
B3	25 µL (0.05 M)	0 µL	180 µL (9%)	50 µL (0.005 M)	745 µL
B4	25 µL (0.05 M)	0 µL	140 µL (7%)	50 µL (0.005 M)	785 µL
B5	25 µL (0.05 M)	0 µL	100 µL (5%)	50 µL (0.005 M)	825 µL
B6	25 µL (0.05 M)	0 µL	60 µL (3%)	50 µL (0.005 M)	865 µL

	2.0 M Imidazole pH 8.02	**5.0 M $LiNO_3$**	**50% PEG-8000**	**0.1 M $CuCl_2$**	**Millipore H_2O**
C1	25 µL (0.05 M)	0 µL	260 µL (13%)	50 µL (0.005 M)	665 µL
C2	25 µL (0.05 M)	0 µL	220 µL (11%)	50 µL (0.005 M)	705 µL
C3	25 µL (0.05 M)	0 µL	180 µL (9%)	50 µL (0.005 M)	745 µL
C4	25 µL (0.05 M)	0 µL	140 µL (7%)	50 µL (0.005 M)	785 µL
C5	25 µL (0.05 M)	0 µL	100 µL (5%)	50 µL (0.005 M)	825 µL
C6	25 µL (0.05 M)	0 µL	60 µL (3%)	50 µL (0.005 M)	865 µL

	2.0 M Imidazole pH 8.02	**5.0 M $LiNO_3$**	**50% PEG-8000**	**0.1 M $CuCl_2$**	**Millipore H_2O**
D1	25 µL (0.05 M)	0 µL	260 µL (13%)	50 µL (0.005 M)	665 µL
D2	25 µL (0.05 M)	0 µL	220 µL (11%)	50 µL (0.005 M)	705 µL
D3	25 µL (0.05 M)	0 µL	180 µL (9%)	50 µL (0.005 M)	745 µL
D4	25 µL (0.05 M)	0 µL	140 µL (7%)	50 µL (0.005 M)	785 µL
D5	25 µL (0.05 M)	0 µL	100 µL (5%)	50 µL (0.005 M)	825 µL
D6	25 µL (0.05 M)	0 µL	60 µL (3%)	50 µL (0.005 M)	865 µL

Chapter 2.3 Dehydration and Cryoprotection of Crystals

Crystal boxes were stored at room temperature or at 4°C in a walk-in cold room. The boxes were checked daily over the span of days and weeks. Crystals often appeared within 24 hours, with typical growth times requiring 3-7 days. After crystals appeared to stop growing, some crystals were selectively removed from the drops to be dehydrated and cryoprotected following methods adapted from Heras *et al*. (32). To perform the dehydration, crystals were transferred into new reservoir solutions containing the exact conditions they were grown under with two exceptions: 1) the amount of PEG was increased by one-third and 2) glycerol was added to give a final 10% (v/v) reservoir solution. For example, if crystals from well A4 of Box #70 needed to be dehydrated, a dehydration reservoir would be set up with conditions described in Table 2.3. Typically dehydration was carried out at 4°C in which case the original box and the dehydration reservoir would first equilibrate to 4°C for 2 hours. The transfer of crystals was also completed at 4°C by quickly moving them from their original drop to a new coverslip with a 5 μL drop of solution from the dehydration reservoir. The drop was then sealed over the dehydration reservoir to equilibrate for approximately 12 hours at 4°C.

Table 2.3. Dehdyration conditions for crystals from Box #70, well A4.

	2.0 M Imidazole pH 8.02	**Glycerol**	**50% PEG-8000**	**0.1 M $CuCl_2$**	**Millipore H_2O**
A4	25 μL (0.05 M)	100 μL	186 μL (9.3%)	50 μL (0.005 M)	639 μL

After dehydration, the crystals were cryoprotected in a similar way. For each well of crystals being dehydrated, three reservoirs of cryoprotection solution were set up. Cryoprotection conditions are identical to dehydration conditions with one exception: the amount of total glycerol in each of the reservoirs increased successively from 15 to 20 to 25%. For example, if the dehydrated crystals from well A4 of Box #70 needed cryoprotection, three reservoirs of solution would be set up using the reagents shown in Table 2.4. After setting up the wells, they equilibrated at 4°C for 2 hours.

Table 2.4. Cryoprotection conditions for crystals from Box #70, well A4.

	2.0 M Imidazole pH 8.02	**Glycerol**	**50% PEG-8000**	**0.1 M $CuCl_2$**	**Millipore H_2O**
15%	25 µL (0.05 M)	150 µL	186 µL (9.3%)	50 µL (0.005 M)	589 µL
20%	25 µL (0.05 M)	200 µL	186 µL (9.3%)	50 µL (0.005 M)	539 µL
25%	25 µL (0.05 M)	250 µL	186 µL (9.3%)	50 µL (0.005 M)	489 µL

Using the same technique described for dehydration, crystals were first transferred from the dehydration drop into the cryoprotection drop containing 15% glycerol. After equilibrating for only 10 minutes, the crystals were next transferred to the drop containing 20% glycerol. The process was then repeated for the third and final 25% glycerol drop. After a final 10 minutes of equilibration, the crystals were immediately pinned and frozen in liquid nitrogen. Pinning the Az-PHM protein crystals involved looping the crystals with a nylon cryoloop and quickly plunging them into a dewar brimming with liquid nitrogen. The instantaneous freezing process was important because freezing crystals in a dewar that was not filled could result in a more gradual cooling of the crystal as it moves through cool, foggy air. Slower freezing is known to result in more crystalline ice forming on the outside of the crystal, prevent nice glass formation of the cryoprotection solvent and lastly, create non-uniformity within the crystal. After pinning and cryofreezing, crystals were stored in a liquid nitrogen dewar until they were screened for quality.

Chapter 2.4 Method for Screening and Predicting a Unit Cell

The quality of the Az-PHM protein crystals was assessed by obtaining their diffraction images. Crystals were carefully mounted in a Rigaku R-Axis Rapid II Diffractometer and maintained at a temperature of -150°C with a nitrogen generator and helium compressor system. The crystals were exposed to copper K_α radiation (λ = 1.541870) at a voltage of 50 kV and current of 40 mA. These x-rays were transmitted by a flat graphite monochromator to a 0.3 mm collimator with special capillary optics. Two diffraction images were collected 90° apart, with a 0.5° oscillation width and 5-minute exposure times. The resulting images were processed with Rigaku's CrystalClear 2.1 software in the macromolecular processing mode. Using the built-in d*TREK processing

suite, the software determined the crystal's unit cell and used it to predict the location of the reflections on the two images. The steps for processing the reflection data using CrystalClear 2.1 are outlined in the rest of this section.

Before the crystal was exposed to radiation, certain software parameters were set regarding the crystal and the type of x-ray radiation being used. In the Setup window (Figure 2.2) are six tabs: Main, Crystal1, Crystal2, Detector, X-Ray Source and Notes. The parameters that were typically used are shown in the Figures. Under the Main tab (Figure 2.2), values were typically entered for *Temperature*. In the Crystal1 tab (Figure 2.3), *Size* (*X (mm)*, *Y (mm)*, *Z (mm)*), *Color*, *Mount*, and *Morphology* were recorded. In the Crystal2 tab (Figure 2.4), *Space group* (always Unknown) and the *Molecular formula* of Az-PHM ($C_{610}H_{959}N_{165}O_{191}S_{10}Cu_3$) were entered. (Three copper atoms were entered because Az-PHM was titrated with one copper and two or three additional copper atoms were anticipated to bind to the protein molecule since the crystal was grown in solution containing free copper.) The Detector tab (Figure 2.5) contained information that the instrument automatically records. The X-Ray Source tab (Figure 2.6) required *Optics Type*, *collimation type*, *Voltage (kV)*, *Current (mA)*, *Element* and *Source type* to be specified. Finally, any other details about the crystal or its diffraction were recorded under the Notes section. Many of the parameters entered in the Setup window are used in data processing and also appear in the CIF file generated after the structure is solved.

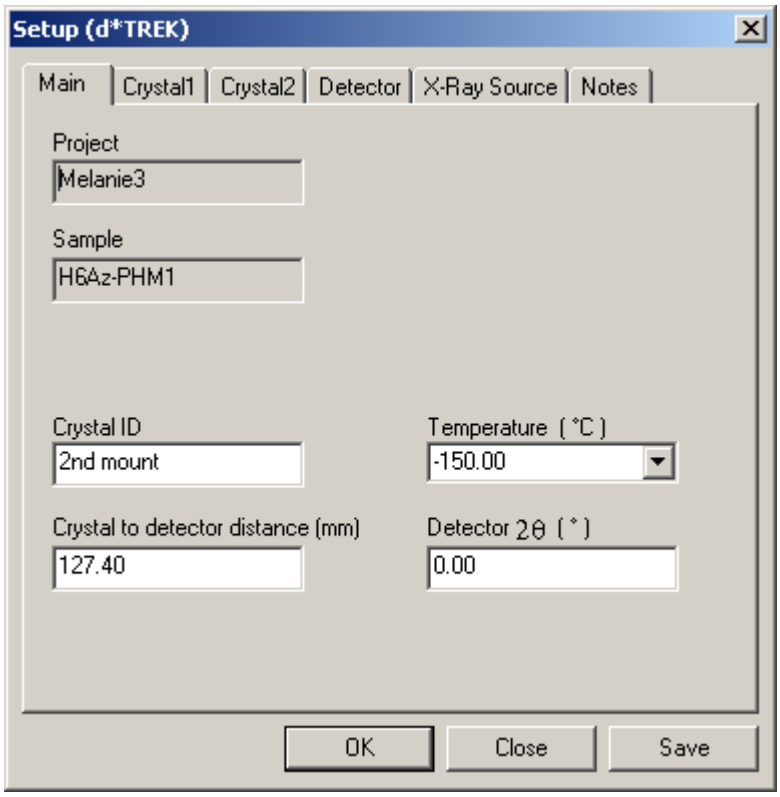

*Figure 2.2. d*TREK Setup dialog box in CrystalClear 2.1 showing the Main tab where Temperature and Crystal ID were entered. All other parameters are default.*

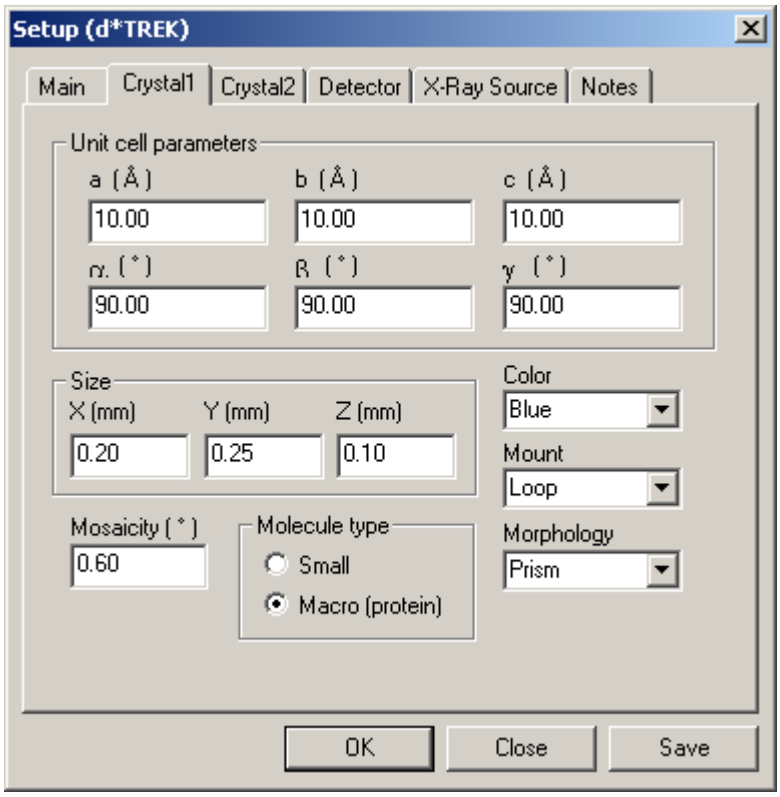

*Figure 2.3. d*TREK Setup dialog box in CrystalClear 2.1 showing the Crystal1 tab where Size, Color, Mount and Morphology were entered. All other parameters are default.*

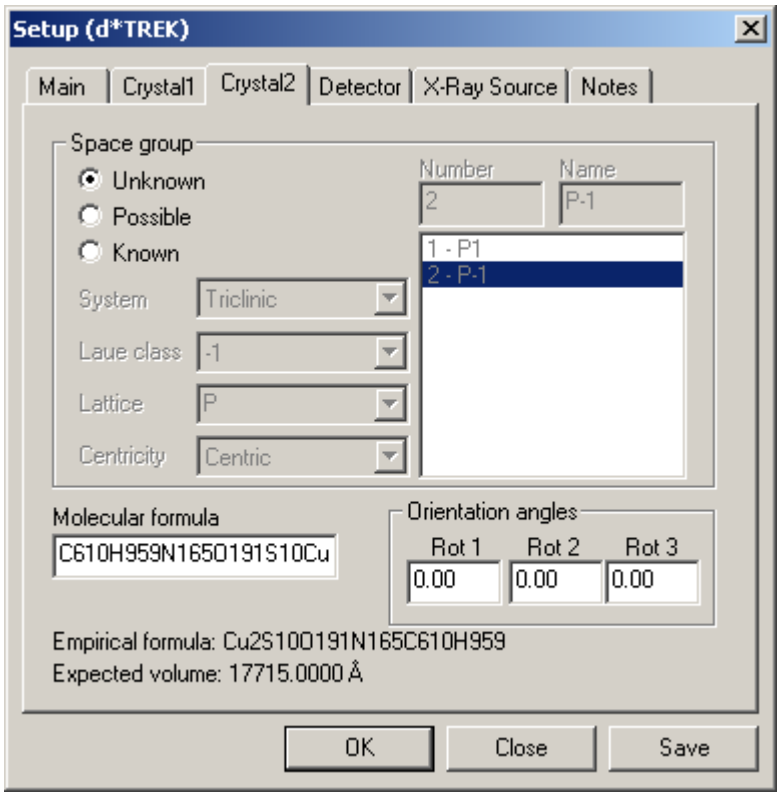

*Figure 2.4. d*TREK Setup dialog box in CrystalClear 2.1 showing the Crystal2 tab where Space group and Molecular formula were entered. All other parameters are default.*

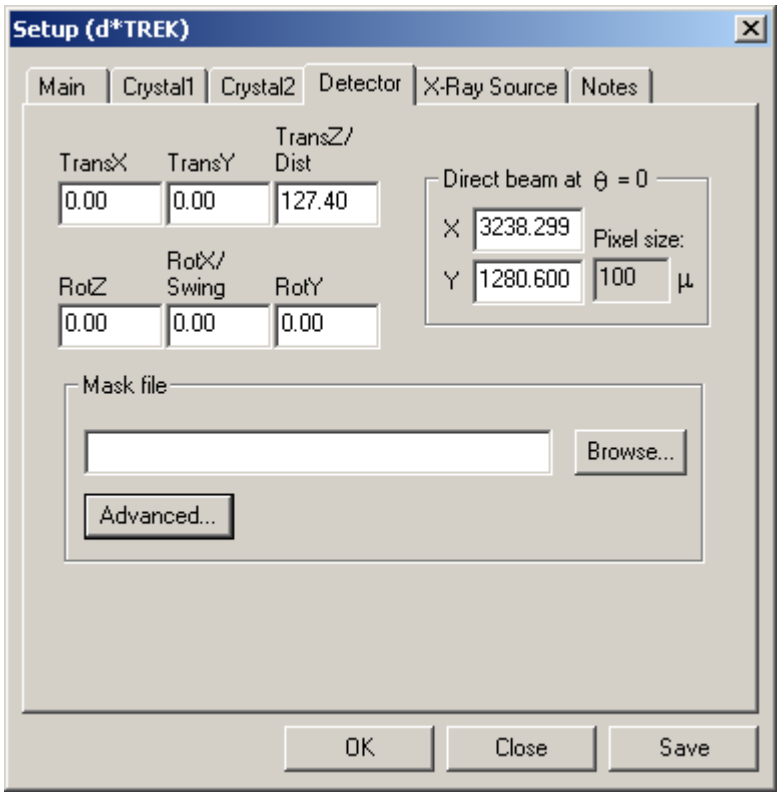

*Figure 2.5. d*TREK Setup dialog box in CrystalClear 2.1 showing the Detector tab where no parameters were entered. All parameters are default.*

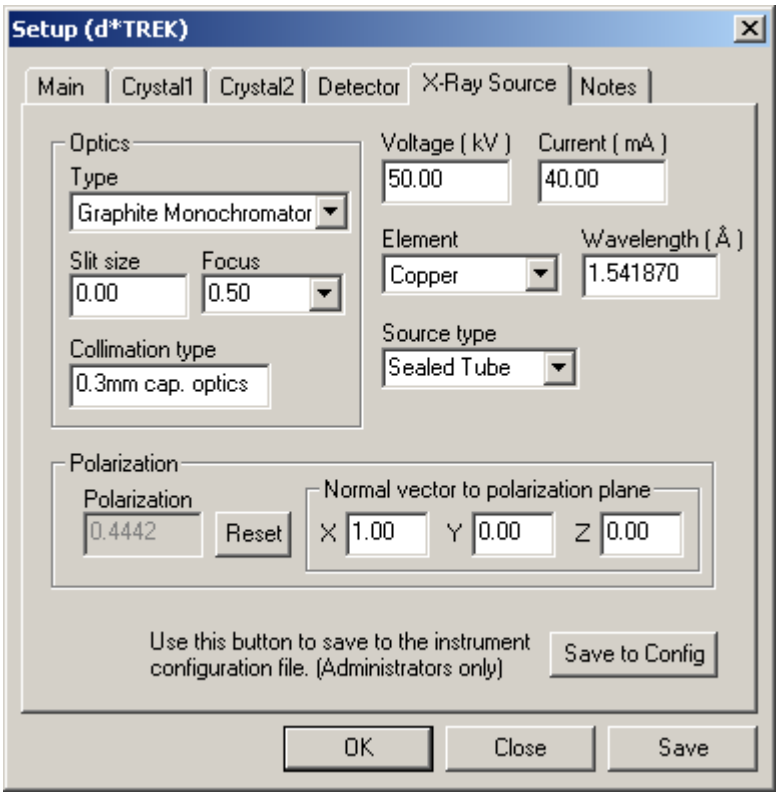

*Figure 2.6. d*TREK Setup dialog box in CrystalClear 2.1 showing the X-Ray Source tab where Optics Type, collimation type, Voltage (kV), Current (mA), Element, and Source type were entered. All other parameters are default.*

Once all Setup parameters were entered and the crystal was centered in the x-ray beam, the crystal was exposed to copper X-ray radiation and two diffraction images were collected. An example of two typical screen images is shown in Figure 2.7. The two image files each contain their own header that records any experimental settings such as beam location, image dimensions, exposure time, and oscillation width.

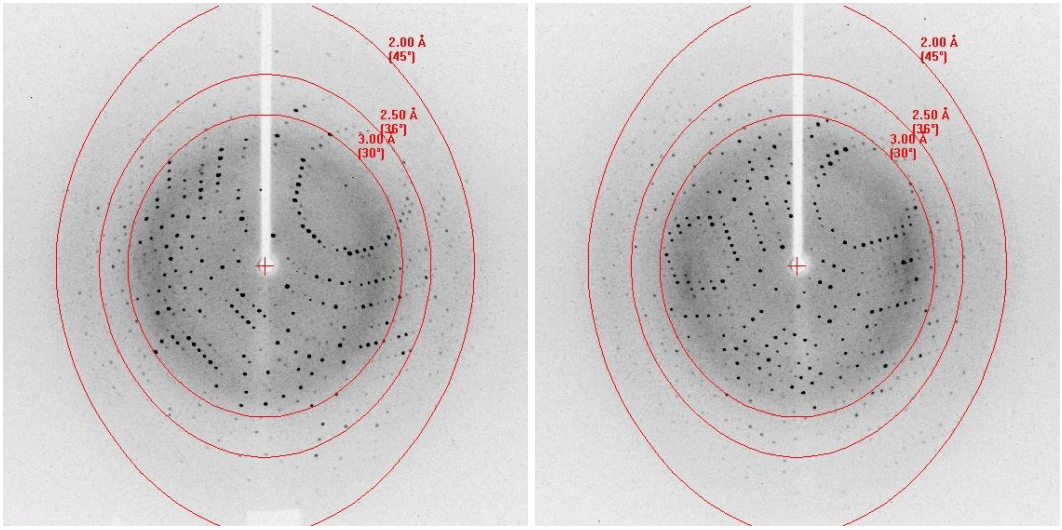

Figure 2.7. Typical screen images that are 0.5° in oscillation width. These images were taken 90° apart.

The first step in determining the unit cell involves locating reflections on the two screened images. All reflection peaks have an associated intensity relative to average background noise. The ratio of intensity to the standard deviation of average background noise (denoted I/Sigma, I/SigI or I/σI in CrystalClear) is one parameter used in finding reflections, seen in Figure 2.8. The default I/Sigma value is 5.00 which was typically used but can be raised or lowered as needed. This value is significant because any reflections having an I/Sigma value below the designated cutoff are not considered spots and therefore, not included in the reflection list that the software passes on to indexing (33). Many protein crystallographers use I/Sigma values of 2 or 3 for clean diffraction images. For images with many spots including twins or noise, it may be best to use I/Sigma values of 10 to be sure that only the strongest spots are used in unit cell determination.

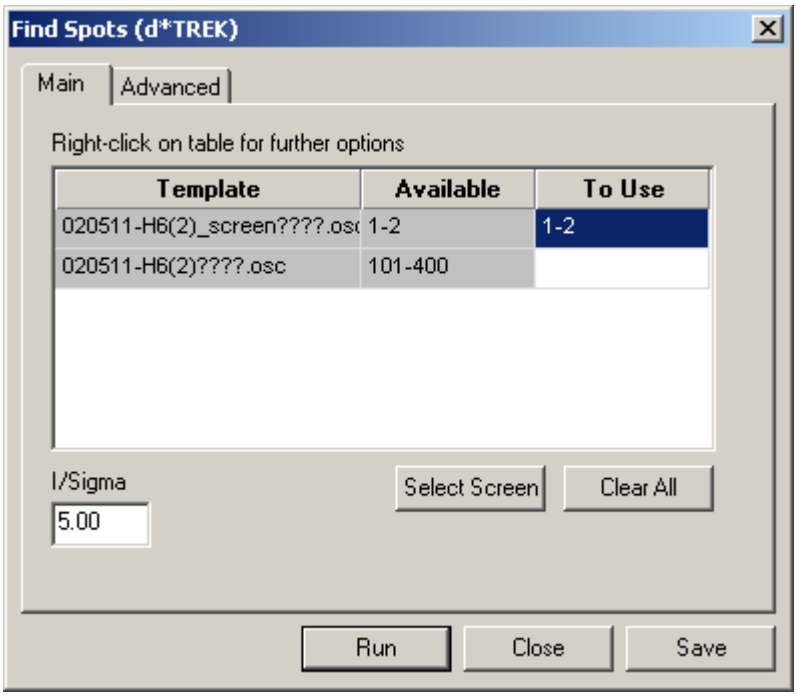

*Figure 2.8. The Main tab of the d*TREK Find Spots dialog box in CrystalClear 2.1. The dialog box pictured is an example of typical parameters used when screening a crystal.*

Other advanced settings associated with finding spots can also be changed depending on the size and intensity of the reflections produced during screening. These settings shown in Figure 2.9 were always used when finding spots.

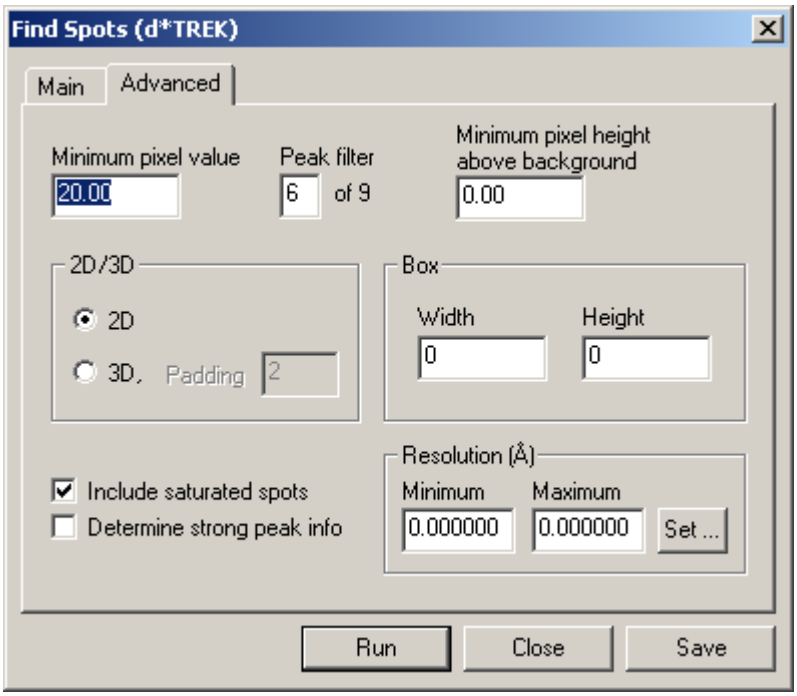

*Figure 2.9. The Advanced tab of the d*TREK Find Spots dialog box in CrystalClear 2.1. This dialog box shows default parameters that are typically used when screening a crystal.*

Once reflections have been located, a list of spot locations is passed on to the indexing stage where a unit cell, space group, orientation and Bravais lattice type are determined for the crystal being screened. The Index spot function in CrystalClear 2.1, shown in Figure 2.10, was used for this purpose. The *Unknown* option under space group was always selected so that the software was not biased in predicting any particular unit cell. A *Maximum* resolution may be specified which only allows spots out to a certain resolution to be included in indexing. The *User chooses solution* option was always selected because this instructs the software to show a list of possible unit cells after indexing is complete (33).

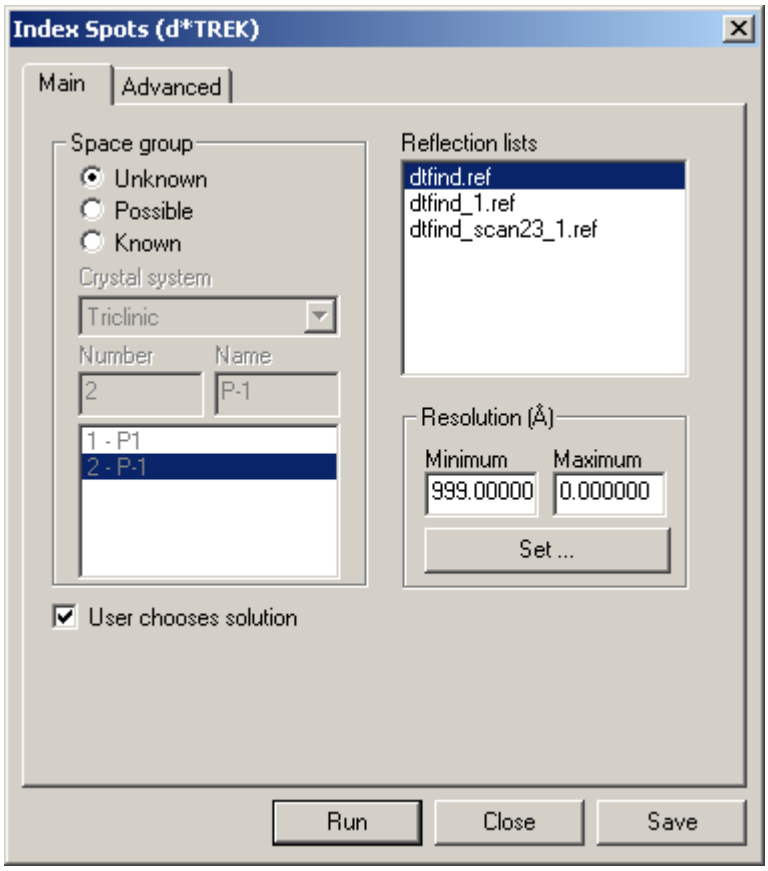

*Figure 2.10. The Main tab of the d*TREK Index Spots dialog box in CrystalClear 2.1. Space group, reflection lists, and resolution limits can be specified for indexing.*

Parameters on the Advanced tab shown in Figure 2.11 are default and were rarely changed because indexing is especially robust in d*TREK (33). *Max cell length* was not changed to anything other than 0 because doing so tended to limit the number of resulting solutions listed. Decreasing the *Max residual* also resulted in fewer unit cell options to choose from when indexing was complete. By changing *I/SigI*, reflections that do not exceed that cutoff value were excluded from indexing. The *Deice* option was selected so that reflections appearing where ice rings normally show diffraction were not used in indexing. Lastly, it was common for the *Beam check* to remain deselected, but indexing results are not negatively impacted opting to check the beam. When the beam was checked, a radius of 25 was searched for a valid radius of 20. If no better beam location was detected, the software used the location listed in the image headers.

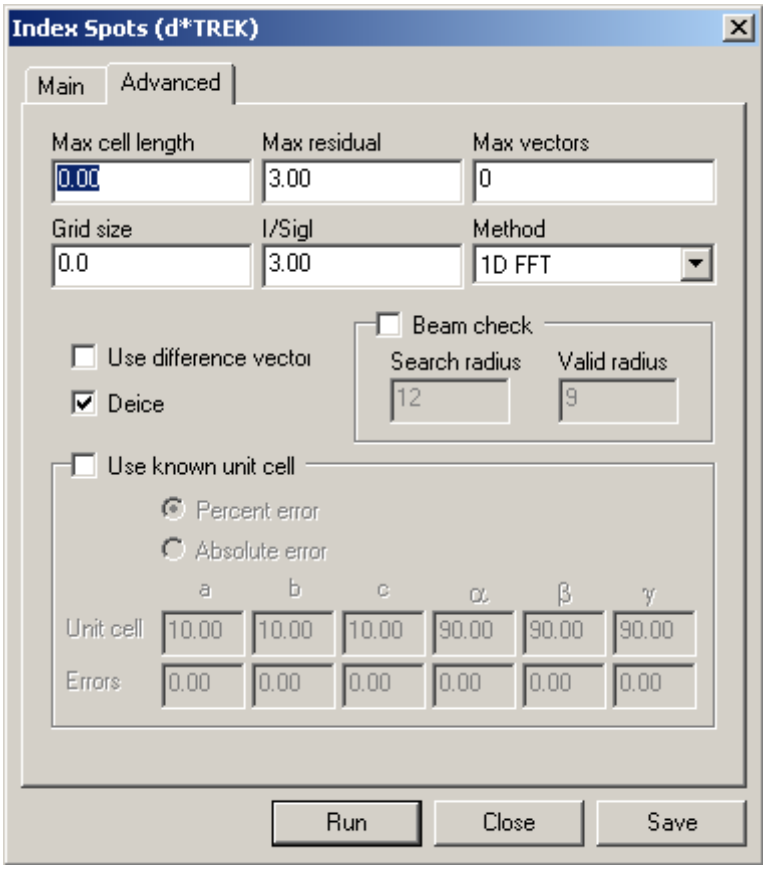

*Figure 2.11. The Advanced tab of the d*TREK Index Spots dialog box in CrystalClear 2.1. The default parameters displayed were always used when screening a crystal.*

Because the *User chooses solution* option was selected, a window displaying several unit cells opened after indexing was complete, as seen in Figure 2.12. Solutions were listed in order of symmetry, the most symmetrical unit cell appearing first on the list. The software highlighted the most probable solution and orientation. Occasionally, the unit cell that the software deemed the most probable solution was not the correct cell. A unit cell that had a *Least Sq* (least square residual) value of 2.5 or greater was not typically a valid cell (33).

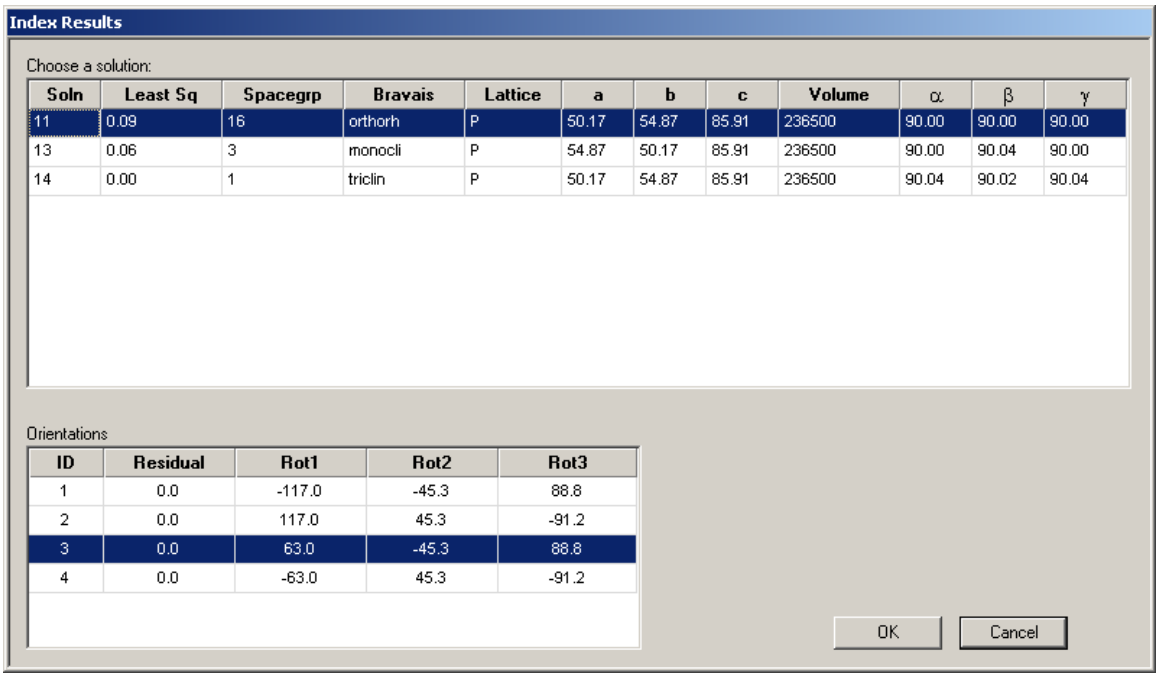

Figure 2.12. Sample Index Results where solutions are listed in order of symmetry. The highlighted solution and orientation are results that the software deems most probable.

Once a unit cell solution and orientation matrix were selected, refinement of these values as well as detector and source positions was performed. The refinement reduced differences found between the observed reflection locations and the locations that were calculated using the indexing solutions. The refinement software (Figure 2.13) was always set to *Refine on Images* rather than refining the reflection list generated after finding spots. The same screen images used to find spots (like those in Figure 2.7) were used in refinement. The option to constrain the unit cell according to symmetry was always selected to prevent the software from changing the symmetry of the cell when refining its dimensions. The refinement *Macro Most* was used because it was recommended by Rigaku. This macro has designated parameters such that resolution *Min* and *Max* are set to 0.00, $I/\sigma(I)$ to 5.00, and *Cycles* to 100. It also has designated rejection limits of 0.5 for *X(mm)* and *Y(mm)* and 1.0 for *Rot.(deg)* (33). The *Macro All* can be used as it allows certain rotation and translation values between the detector and source to be refined, however, this refinement is not essential since only two screen images are used (34).

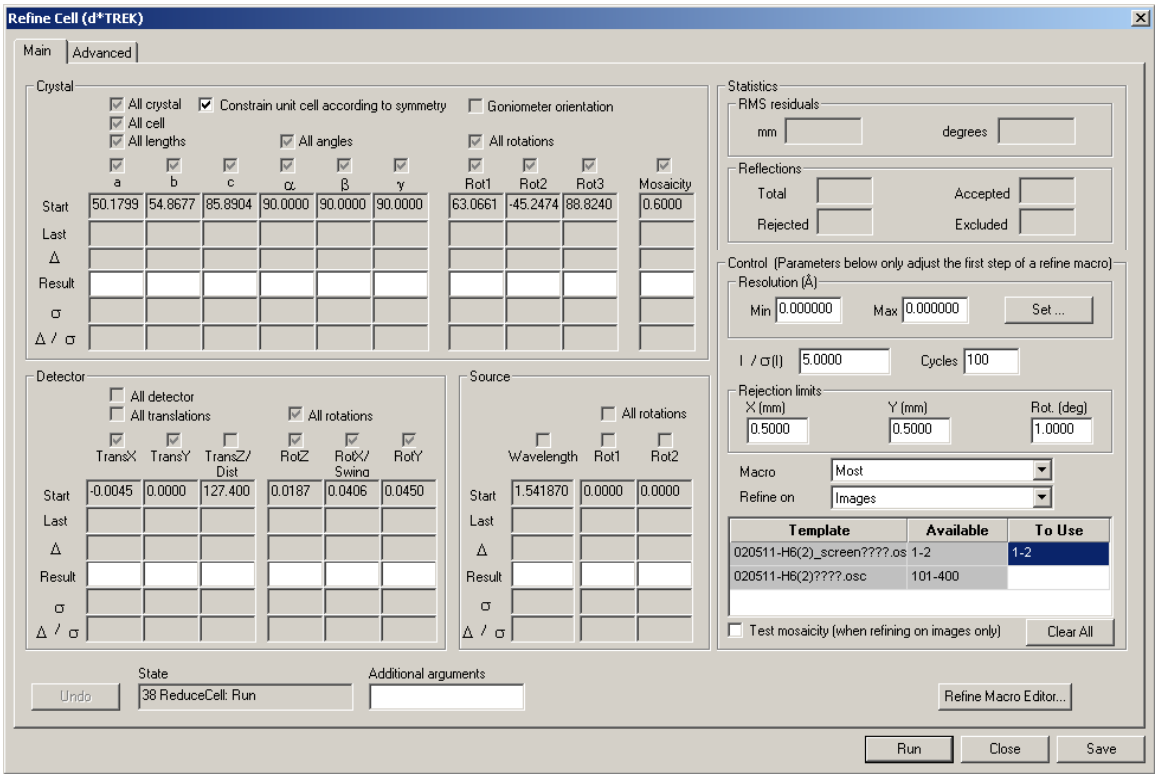

*Figure 2.13. The Main tab of the d*TREK Refine Cell window in CrystalClear 2.1. The parameters shown are default with the exception of Refine on Images where both screen images are used.*

There are few advanced refinement parameters, none of which were changed from what is shown in Figure 2.14. The *Global refinement* option was not used since it has been disabled in this software version. *Wide slice refinement* is defaulted at none because the screen images taken do not qualify as wide slice since they are smaller than three degrees (33).

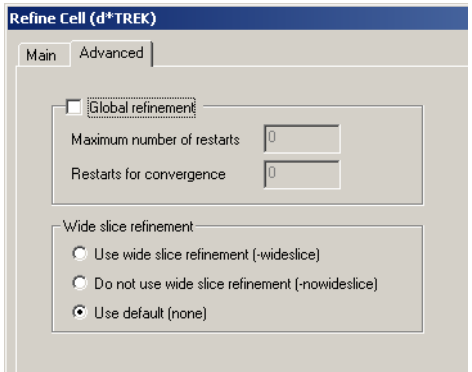

*Figure 2.14. Default parameters on the Advanced tab of the d*TREK Refine Cell window in CrystalClear 2.1.*

Refinement commenced by hitting *Run*. As multiple rounds of refinement took place, the mosaicity and the ratio of rejected reflections out of total reflections were monitored. When these values did not change appreciably, refinement was considered complete. This typically took three to five runs of refinement. Because the software refined on images, it was possible to graphically see specific reflections that were rejected on the screen images (surrounded by a red circle). With the newly refined unit cell dimensions and positions for the detector and source, calculated reflections could then be predicted and subsequently displayed on the screen images.

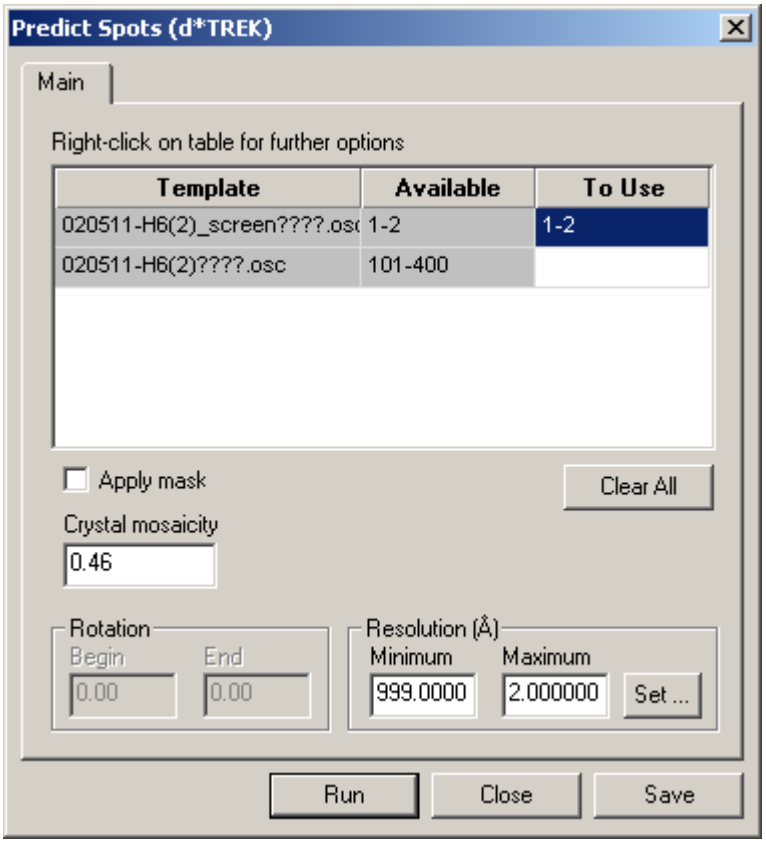

*Figure 2.15. The Main tab of the d*TREK Predict Spots window in CrystalClear 2.1. A Maximum resolution of 2.0 Å was often used for screen images.*

The last stage of screening was calculating predicted reflection positions and comparing them to the actual, observed locations. As demonstrated in Figure 2.15, screen images 1-2 were used and the *Crystal mosaicity* value was automatically carried over from refinement. A *Maximum* resolution was usually entered depending on how well the crystal diffracted. A value of 2.00 was routinely used since many crystals that

were screened did not have spots beyond 2.0 Å. If spots were visible beyond 2.0, the resolution maximum was lowered appropriately.

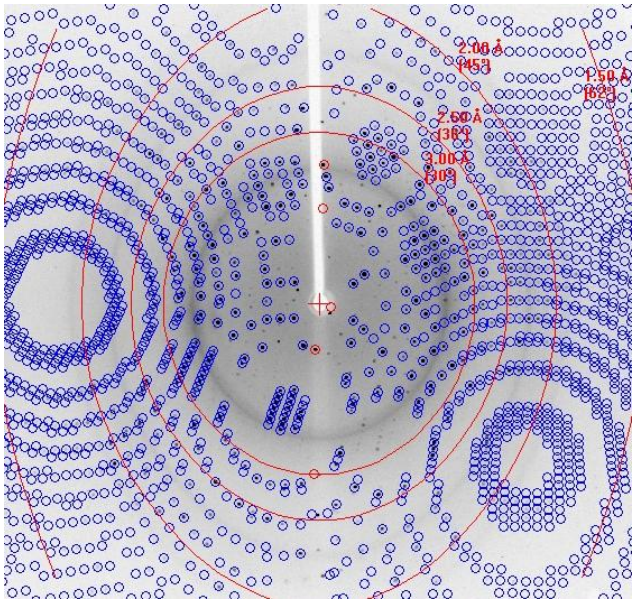

Figure 2.16. Sample prediction results. Mosaicity and refined unit cell parameters are deemed correct due to the accurate predictions for almost all reflections.

Calculated reflections are based on the unit cell and orientation matrix and visually appear on the screen images (Figure 2.16). The images were compared to the calculated reflections (blue circles) to identify the degree to which the software could predict the location of the spots on the images. If most predicted circles were centered on spots, the unit cell assigned to the crystal was deemed correct. (Not all of the spots will be predicted because some are not Bragg reflections.) The prediction also indicated whether or not the CrystalClear software accurately estimated mosaicity. An appropriate mosaicity was estimated when almost all spots were predicted. When only some of the spots were accurately predicted, the mosaicity estimation was low, while a high mosaicity estimate was indicated by many predictions that were observed at locations where no actual spot existed.

Chapter 2.5 Judging Criteria and General Results/Discussion

Predicting a unit cell accurately largely depends on the quality of several factors such as reflection intensity, resolution, crystal mosaicity and to some extent, the lack of

ice rings. These four criteria were the basis for characterizing the diffraction quality of the crystals. High-quality crystals were those that had intense reflections, resolution beyond 2.0 Å, mosaicities less than 0.60 and very minimal to no ice rings. All criteria, with the exception of ice rings, relate to the degree of order inherent in the crystal.

The ratio of reflection intensity relative to background noise is expressed as I/σ and is one criterion that determines the strength of the data. While screening crystals, it was commonly observed that large crystals gave more intense reflections upon diffraction, which is consistent with the findings of Fox & Karplus (35). Theoretically, the intensity of a given reflection is directly related to the number of x-rays that are scattered and converge at the image plate. Because a larger crystal contains more repeating units and takes up more of the beam, more x-rays will be scattered. Thus, reagent conditions were optimized to obtain large crystals for screening in order to avoid collecting weak data.

There are several ways that protein growth can be controlled to yield sizeable crystals, and within a particular buffer system, trends occur that allow for such optimization. The clearest example of reagent optimization is shown in Figure 2.17, where a similar azurin mutant (with only 1 amino acid difference from Az-PHM) was crystallized using two different molecular weights of polyethylene glycol (PEG). There is a distinct difference in size between crystals grown in PEG-4000 (columns 1, 3 and 5) and those grown in PEG-8000 (columns 2, 4 and 6). With the exception of the type of PEG used, drop conditions are identical between columns 1 & 2, between columns 3 & 4 and between columns 5 & 6. It is unmistakable that for this particular buffer system, crystals grown with PEG-8000 are larger than those grown with PEG-4000. The concentration of PEG also affects size. Moving across a pair of columns in a given row, the concentration of PEG decreases which causes a fewer number of large crystals. The number of crystals in a given well is proportional to the size of the crystals. Optimizing conditions that produced large crystals ensured that an incorrect unit cell prediction was not because of weak reflections.

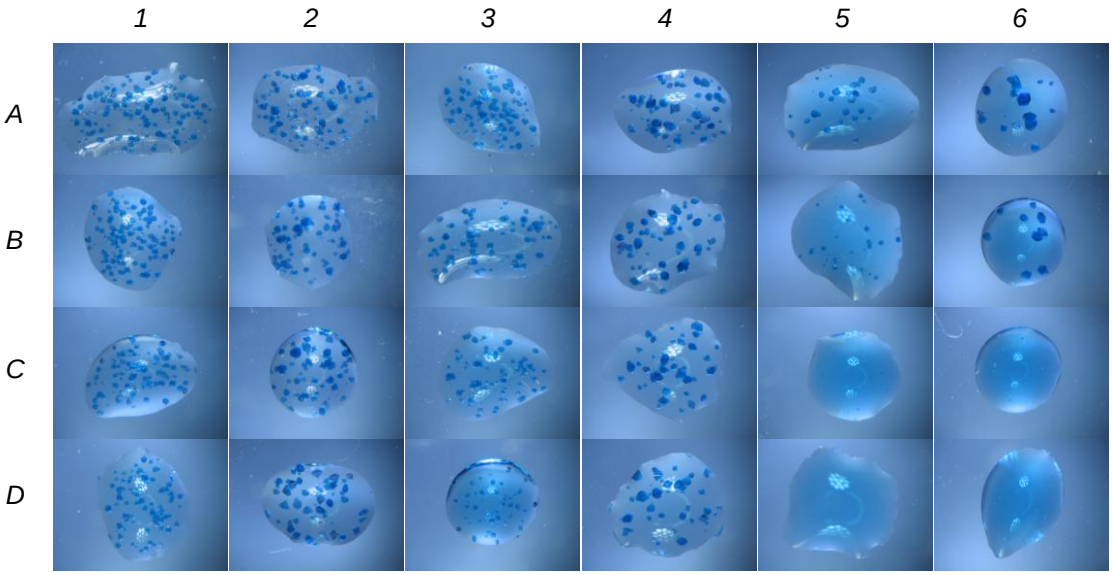

Figure 2.17. Box #58 at ~5 days of an azurin variant with 1 residue difference than Az-PHM. Conditions are identical within column pairs (1 & 2, 3 & 4, and 5 & 6) with the exception of the type of PEG used. PEG-4000 was used in columns 1, 3, and 5 whereas PEG-8000 was used in columns 2, 4 and 6. The concentration of PEG decreases across the row from left to right.

There are two probable reasons for the growth of large crystals in a solution containing a small PEG concentration. When a drop has more water, it takes longer to equilibrate with the reservoir solution below which means that saturation of the drop happens gradually. Thus, fewer nucleation sites result which correlates with the growth of larger crystals. It could also be that because there is less PEG in the drop, there is more mobile water and Az-PHM is not as concentrated. This would also result in less nucleation. In either case, once saturation is reached and nucleation begins, crystals start to grow and the concentration of protein decreases even though the volume of the drop gets smaller (35). This seems plausible because Wilson *et al*. found that as the number of crystals in a given drop decreased, their average size increased (36). Fehrer also found that when crystals grow quickly they tend to be numerous and small (37).

Consistent with these findings by Wilson and Fehrer, imidazole concentration can also be varied to optimize crystal nucleation and size. For this particular buffer, when the concentration of imidazole was decreased, nucleation and crystallization occurred within hours, resulting in many tiny crystals. The photographs in Figure 2.18 from Box #65 were taken after ~24 days. The concentration of imidazole in the drop increases from row A (5 mM) down to Row D (20 mM). With the exception of imidazole, drops within

a given column have identical reagent concentrations. It is clear that the presence of imidazole decreases the number of nucleation sites, resulting in fewer and larger crystals.

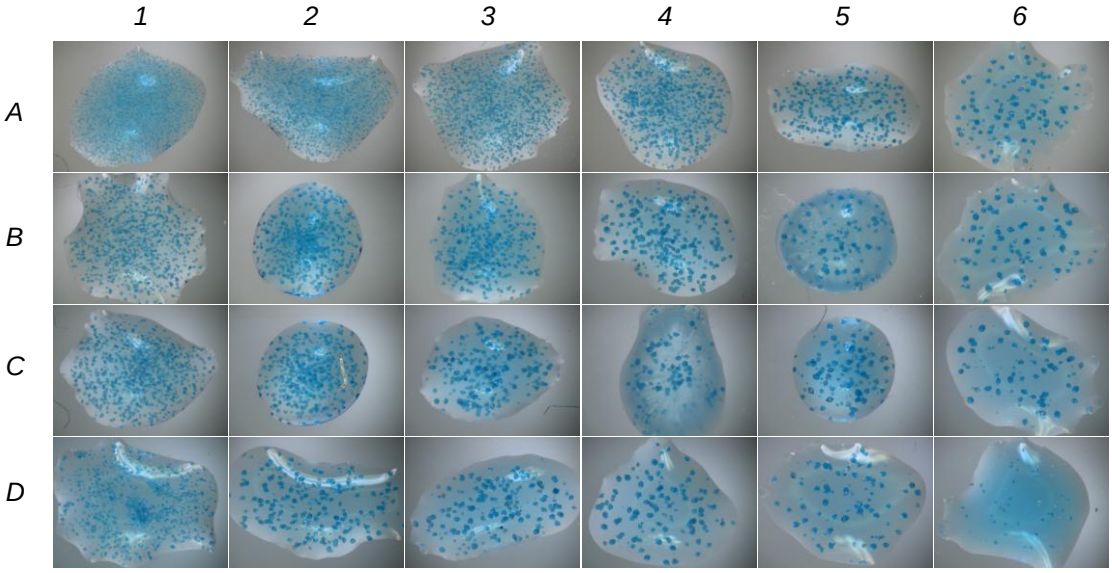

Figure 2.18. Box #65 at ~24 days of Az-PHM in imidazole at pH 8.0. Conditions are identical within columns with the exception of the amount of imidazole used. Imidazole concentration is consistent across a row but increases down a column. PEG concentration decreases across a row from left to right but is consistent down a column.

Growing and screening large crystals provides strong reflection data, however, one of the trade-offs of obtaining strong data is large mosaicity values. This is consistent with what was observed. Mosaicity, the second criterion, is a measure of the degree of overall disorder within a crystal. The root of this word, mosaic, is a great description of this concept because it suggests that although a crystal may appear to be one crystal, it is really composed of little crystals regularly referred to as mosaic blocks. Large crystals have higher mosaicities simply because there is more opportunity for disorder. More abstractly put, if mosaic blocks do not stack properly early on in crystal formation, even small disorder can be exaggerated as the crystal grows larger.

In order to combat the problem of high mosaicities in the Az-PHM crystals, two approaches were used. The first approach worked toward growing crystals more slowly, and the second called for dehydration of the crystals that had already formed. In order to cause slower crystal formation, protein drops were diluted with water, which increased the total volume of the drop. Typically, a volume of 2 μL was added to the drops, which

contained 2 μL of protein and 2 μL of the reservoir solution. Larger drops equilibrate at a slower rate and as water is lost from the drop slowly over time, the protein does not reach saturation as quickly. Diluting Az-PHM protein drops with water caused crystals to increase in size over a longer period of time, but there was no statistical drop in mosaicity. This may be because the protein drops were only diluted by 2 μL of water at the most. Increasing the volume of the drop by a greater amount may lead to even larger crystals with smaller mosaicities.

Because the first approach was largely unsuccessful, a technique called dehydration was used. In theory, dehydrating crystals after they have formed removes excess water and causes mosaic blocks within the crystal to shift to become more ordered. Mosaicity values collected from crystals with and without dehydration are shown in Table 2.5 below. The dehydrated Az-PHM crystals show a marked improvement in mosaicity values when compared to those that were not dehydrated.

Table 2.5. Mosaicity comparison of crystals from two wells with identical conditions. Crystals in well C1 were dehydrated and show much lower mosaicities than crystals from well D2 which were not dehydrated.

Box #, well #	Crystal	Dehydrated?	Mosaicity (°)
68, D2	Y13	No	-----
	Y14	No	0.55
	Y15	No	0.99
	Y16	No	0.62
69, C1	BB1	Yes	0.41
	BB2	Yes	0.48
	BB3	Yes	0.48
	BB4	Yes	0.36

The third criterion, resolution, is also directly affected by the order within a crystal. The more ordered a crystal is, the higher the resolution will be. Because high resolution reflections are located where x-rays diffracted at higher angles must converge, the impact of thermal motions and crystal disorder is greater, making these reflections less intense or non-existent. Because of this phenomenon, it is difficult to obtain high resolution data. Resolution can be improved, however, by diffracting crystals at low

temperatures to slow down thermal motions and by growing crystals with more order. Seemingly, crystals that are grown at a slower rate will be more ordered because given time, protein molecules will add to the crystal more purposefully instead of hastily.

Unfortunately, large Az-PHM crystals grown at a slower rate did not diffract to a higher resolution. The best explanation for this is that the large crystals that were grown slowly did not have improved mosaicities, and because crystal disorder has a great impact on high-resolution reflections, there were none that appeared on the diffraction pattern. However, because dehydration gave an improvement in mosaicities, there should also be an improvement in resolution, which is precisely what was observed. Diffraction patterns seen in Figure 2.19, illustrate this improvement. The patterns in these photos come from two wells with the same conditions except for PEG concentration in the drop. Crystals that were dehydrated consistently showed reflections between 2.0-2.5 Å and often times showed reflections beyond 2.0 Å, while the crystals not treated do not show diffraction between 2.0-2.5 Å.

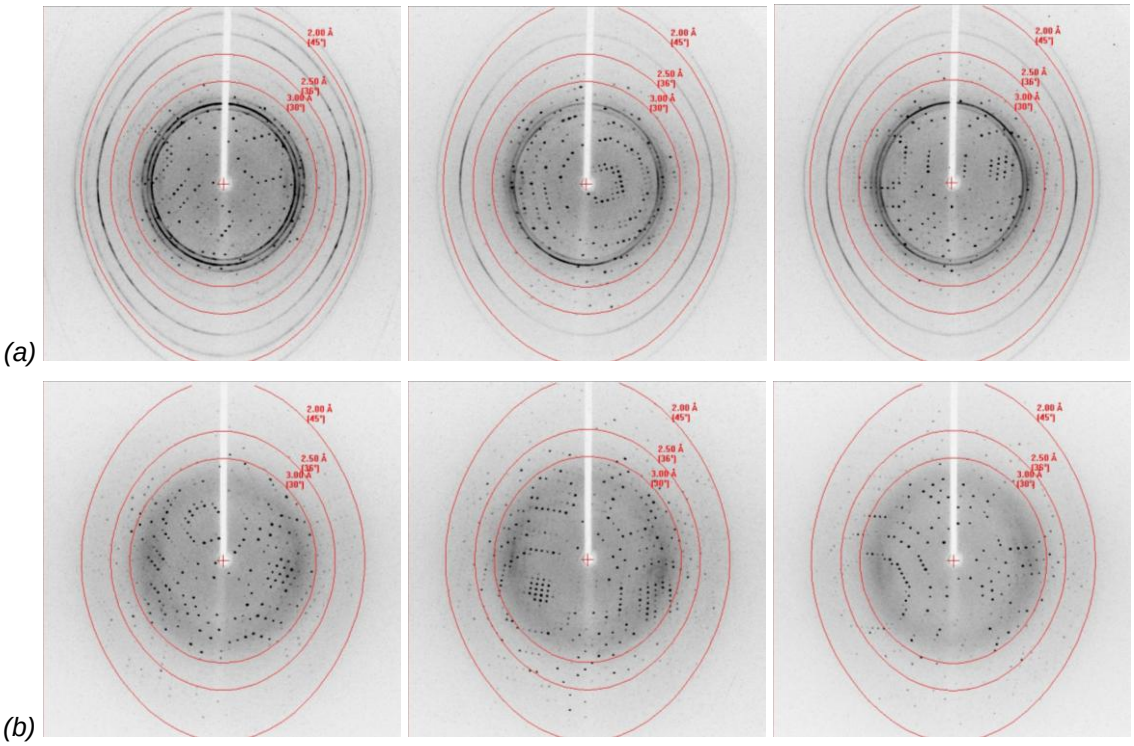

Figure 2.19. Diffraction patterns from crystals grown in (a) Box #70, well B1 and (b) Box #68, well D2. The only difference in crystallography conditions between (a) and (b) is that the drop in (a) contained 2 µL of reservoir solution with 5% PEG-8000 whereas the drop in (b) contained 7% PEG-8000.

Besides growing large crystals and using dehydration, a final technique called annealing was attempted in which a frozen crystal placed in the nitrogen stream was warmed for short time and then frozen again in the stream. This technique was mildly successful regarding resolution, but unfortunately, mosaicity values increased dramatically. The diffraction patterns in Figure 2.20 show reflections prior to annealing (left) and after annealing (right). The resolution improved from 2.0-2.5 Å, but in almost all cases, mosaicity values doubled.

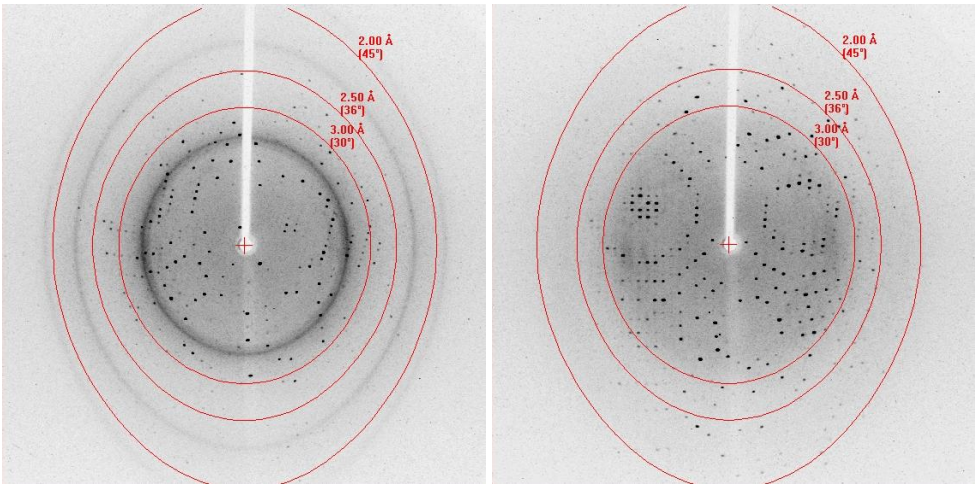

Figure 2.20. Diffraction patterns from Z9 crystal harvested from Box #67, well C1. The pattern on the left was obtained before annealing and the pattern on the right after annealing for 15 seconds.

The fourth and final criterion used to judge a crystal's quality is the presence of ice rings. Ice rings are intense rings visible on a diffraction image due to crystalline ice formation during freezing. Flash-freezing is an important last step in preparing a crystal for screening as crystalline ice can form from water vapor in the air or from liquid in the drop that is looped up during pinning. Sometimes ice rings do not affect the diffraction of the crystal itself, but they can be a hindrance in predicting the unit cell because they appear on the diffraction pattern. Though the CrystalClear software can compensate for ice rings, it is best to avoid them since the software omits all data obscured by ice rings.

To freeze a protein crystal efficiently, the pinned crystal must move from room temperature air to the liquid nitrogen at –210 °C as quickly as possible. A sharp temperature gradient was created by filling a dewar to the brim in order to provide a uniform transition between temperatures. Typically, this was sufficient to prevent water

vapor from crystallizing. However, preventing liquid in the drop from freezing was more difficult. PEG is a natural glassing agent that immobilizes water, preventing it from forming into crystalline ice. But, because many of the larger protein crystals only required small amounts of PEG to grow, the liquid in the drop often froze upon pinning and freezing crystals. To combat this problem, many different freezing methods were attempted without success, however, one technique called cryoprotection consistently worked at avoiding ice formation from liquid in the drop. At 4 °C, Az-PHM crystals were transferred between a series of three solutions each containing identical concentrations of reservoir reagents with an increase in PEG concentration and the addition of glycerol. The higher concentration of PEG and glycerol provided enough glassing agent to prevent ice formation. A visual comparison of crystals with and without cryoprotection is shown in Figure 2.21. The crystal without cryoprotection (2.21b) has liquid from the drop that was looped during pinning and froze to give crystalline ice which is evident in the crystal's corresponding screen image. The crystal with cryoprotection, however, is clear and ice rings are absent from its screen image.

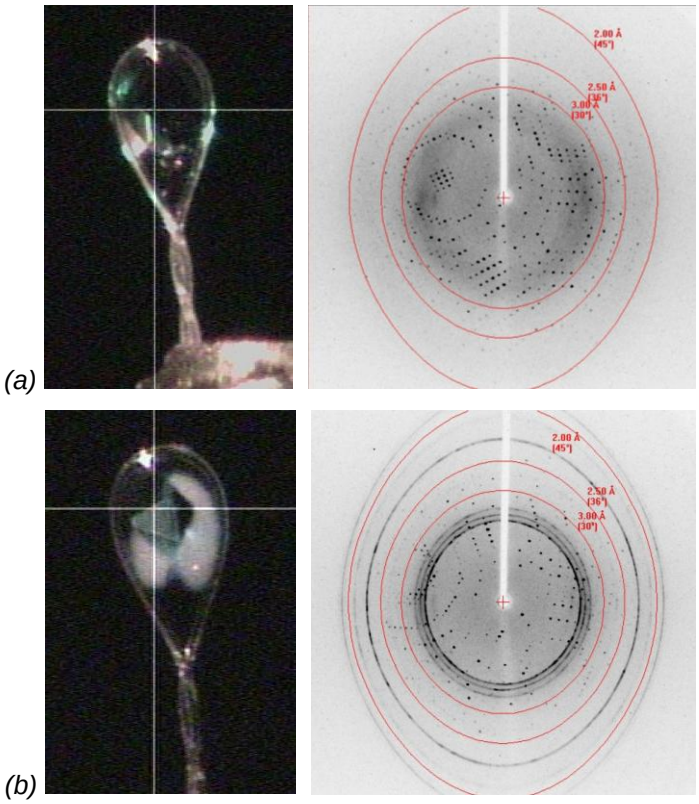

Figure 2.21. (a) Cryoprotected crystal from Box #70, well A3. (b) Crystal from Box #68, well C3 that was not cryoprotected.

After growing and screening hundreds of Az-PHM crystals, trends observed in crystal growth were used to control intensity, mosaicity, resolution and the formation of ice. Crystals were obtained that gave strong intensities, mosaicities below 0.60, and resolutions beyond 2.0 Å in the absence of ice rings by reproducibly growing large Az-PHM crystals that were subsequently dehydrated and cryoprotected. Because diffraction-quality crystals can be selectively grown, the collection of a full data set is possible wherefrom a crystal structure can be obtained.

CHAPTER 3

Chapter 3.1 Introduction

In times past, collecting diffraction data and processing it was no small task. Before the development of modern technology, data collection was a tedious process. Until approximately 50 years ago, weeks were spent collecting images, where each image was collected on a piece of photographic film that required the utmost care in alignment. For those protein crystals that were susceptible to radiation damage, a new crystal was mounted each time an exposure was captured on film. Once all of the images were collected, processing the data took weeks and even months. Reflections on each frame were individually counted and indexed by hand, and were then subsequently "measured" for intensity using a qualitative "eye estimation" scale. After reflections were indexed, complicated mathematics were carried out in order to solve the crystal structure. One two-dimensional Fourier projection took several days of steady calculation. Months and years were spent growing crystals and obtaining a single crystal structure (38).

While growing protein crystals still remains a lengthy and tedious process, great technological advances in diffraction instrumentation and software development have made it possible for crystallographers to collect data with little to no effort involved and process it in a few short hours to obtain a preliminary model. Because modern technology affords the luxury of fast data processing, it has been possible for many researchers to learn crystallography. Hence, understanding the complexities of diffraction and the process by which data is obtained, reduced and modeled is now the rate-limiting step in going from crystals to structures.

The ultimate goal of processing diffraction data is to obtain an electron density map that conveys a three-dimensional depiction of the repeating unit within the protein crystal. In essence, the map is creating by summing the waves that are diffracted from a crystal in much the same way that an image is created by a microscope when a lens collects and sums waves of visible light that have been scattered by the object. The waves diffracted from a protein crystal are called structure factors. Because structure factors are waves, they have both amplitudes and phases that must be calculated in order to create an electron density map. Structure factor amplitudes are obtained directly from

the experimental reflection intensities whereas phases must be obtained indirectly, very often through a process called molecular replacement (17).

Powerful crystallographic software programs allow amplitudes and phases to be computed with ease. Two such programs are implemented in this work, namely CrystalClear r2.1 and CCP4 6.1.3. CrystalClear, a software program created by Rigaku, contains algorithms that make data collection a fully automated process. Once diffracted reflections are obtained, CrystalClear integrates them to obtain their intensity information and then takes the experimental intensity data and predicts crystal symmetry. Next, intensities are scaled and those that are symmetry-equivalent are merged to create a list of unique reflection intensities. Later, intensities are converted to structure factor amplitudes, a process carried out by CCP4. CCP4 (Collaborative Computation Project No. 4) is free software for macromolecular crystallography that is capable of molecular replacement, refinement and even validation of a final structural model. Upon calculation of structure factor amplitudes, CCP4 performs molecular replacement, which uses atomic coordinates from a similar protein model to estimate phases. During refinement, phases from the model are coupled to their corresponding structure factor amplitudes. Finally, amplitudes and phases are input into a third program called Coot that computes the Fourier transform of the structure factors and creates an electron density map in three dimensions.

The protocol described in the rest of the chapter contains parameters that best suited the diffraction data that was collected on an Az-PHM crystal grown in Tris buffer. Data is analyzed for quality following each experimental section discussing CrystalClear and CCP4 parameters.

Chapter 3.2 Data Collection and Data Reduction in CrystalClear

Once a crystal is found that diffracts beyond 2.0 Å, has a mosaicity value less than 0.60, has intense reflections and is free of ice, a full data set can be collected. Data was collected on one such crystal, Az-PHM crystal H6, that grew in Box #26, well D6 in a 4 μL hanging drop at an initial concentration of 16.7 mg/mL in 75 mM Tris HCl pH 7.07, 25 mM lithium nitrate, 7.5% polyethylene glycol-2000 and 2.5 mM copper

chloride. The drop was equilibrated against 0.998 mL of the same reagents with double the concentration, the only exception being that the concentration of Tris HCl in the reservoir was 100 mM. The crystal was pinned and frozen without any prior dehydration or cryoprotection. Upon screening the crystal with a 5-minute exposure per frame, it diffracted to 1.5 Å with a mosaicity of 0.46°. A photo of one of the screen images is displayed in Figure 3.1 where there are intense spots visible alongside a few very faint ice rings.

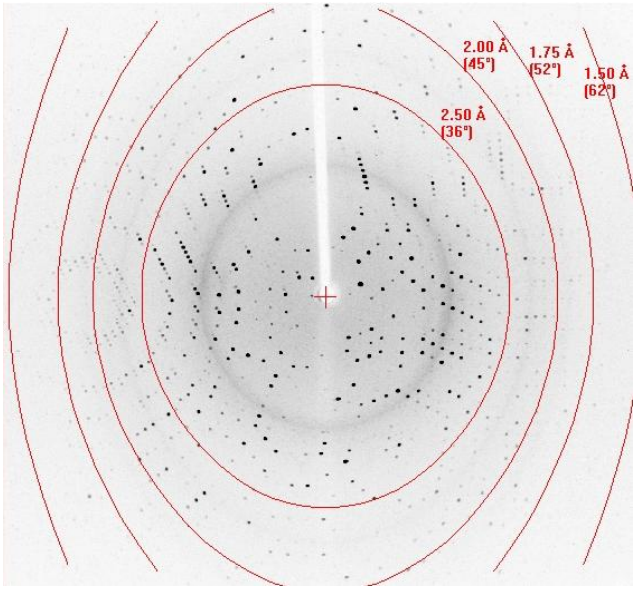

Figure 3.1. Screen image from the Az-PHM crystal H6, which was grown in Box #26, well D6 using Tris HCl buffer at pH 7.07, PEG-2000, lithium nitrate and copper chloride.

A full data set was collected on crystal H6 using a Rigaku R-Axis Rapid II Diffractometer and the d*TREK processing suite in CrystalClear r2.1. Recall that during the screening process (described in Chapter 2.4), the unit cell and crystal orientation are determined. CrystalClear uses this information along with completeness and redundancy conditions in order to identify a strategy for data collection in which the number of images that might otherwise be collected is greatly reduced, saving time and unnecessary radiation of the crystal. The *Completeness* and *Redundancy* conditions are entered by the user in the Main tab of CrystalClear's Strategy window, shown in Figure 3.2, which also allows parameters such as *Search resolution*, *Image rotation width*, and *Anomalous (I+,I–)* to be input. A resolution maximum of 1.2 Å was chosen since it was slightly

greater than the resolution where spots were found on the screen images. The image rotation width is a value that specifies the degree to which the crystal will oscillate during the exposure of one frame. Its value is varied depending on the size of the crystal's unit cell. Because protein crystals typically have large unit cells, a small oscillation range of 0.5° (anything below 3° is considered fine-slice) is commonly used to avoid reflection overlap (33). The target completeness was set to 99% with a 2% tolerance since all (or nearly all) reflections needed to generate a complete set of data (given the crystal's symmetry) should ideally be collected. These reflections are termed "unique" reflections (39). The option to collect *Anomalous (I+, I–)* was selected because it was questionable whether or not the crystal would give an anomalous signal, and since the intensities can be averaged together in later steps, there was no harm in choosing this option if it was not needed. A minimum redundancy was not specified (33).

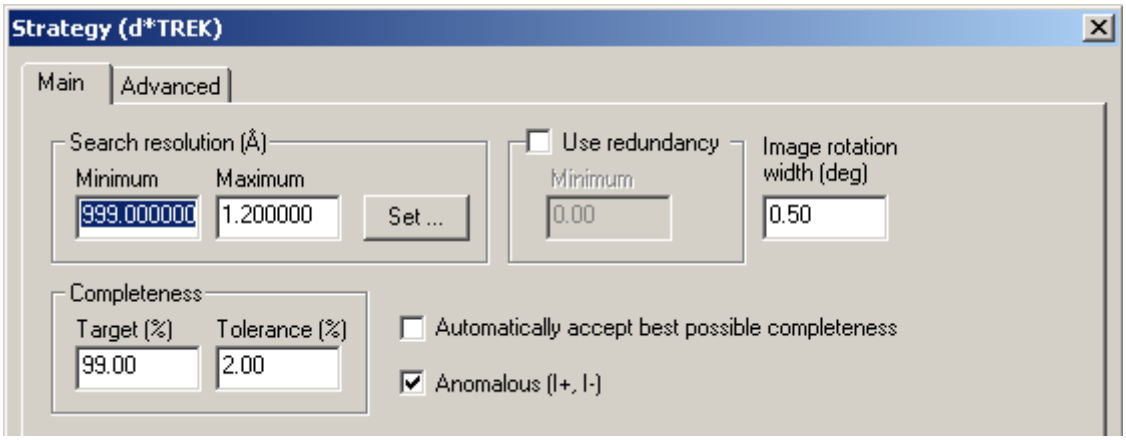

*Figure 3.2. The Main tab of the Strategy window from CrystalClear's d*TREK processing suite. Parameters specified here are those used to identify a strategy which was used to collect a full data set on Az-PHM crystal H6 from Box #26.*

There are many other strategy parameters located on the Advanced tab, shown in Figure 3.3, but these parameters do not typically require any adjustments as was the case for crystal H6. However, depending on the instrument, it may be necessary to adjust omega rotation angles which place the goniometer cradle in a position that does not interfere with diffraction. This problem was an issue when collecting data on crystal H6, but was avoided by changing the *Start* and *End Angles* in the Collect Images window which appears after the strategy is run.

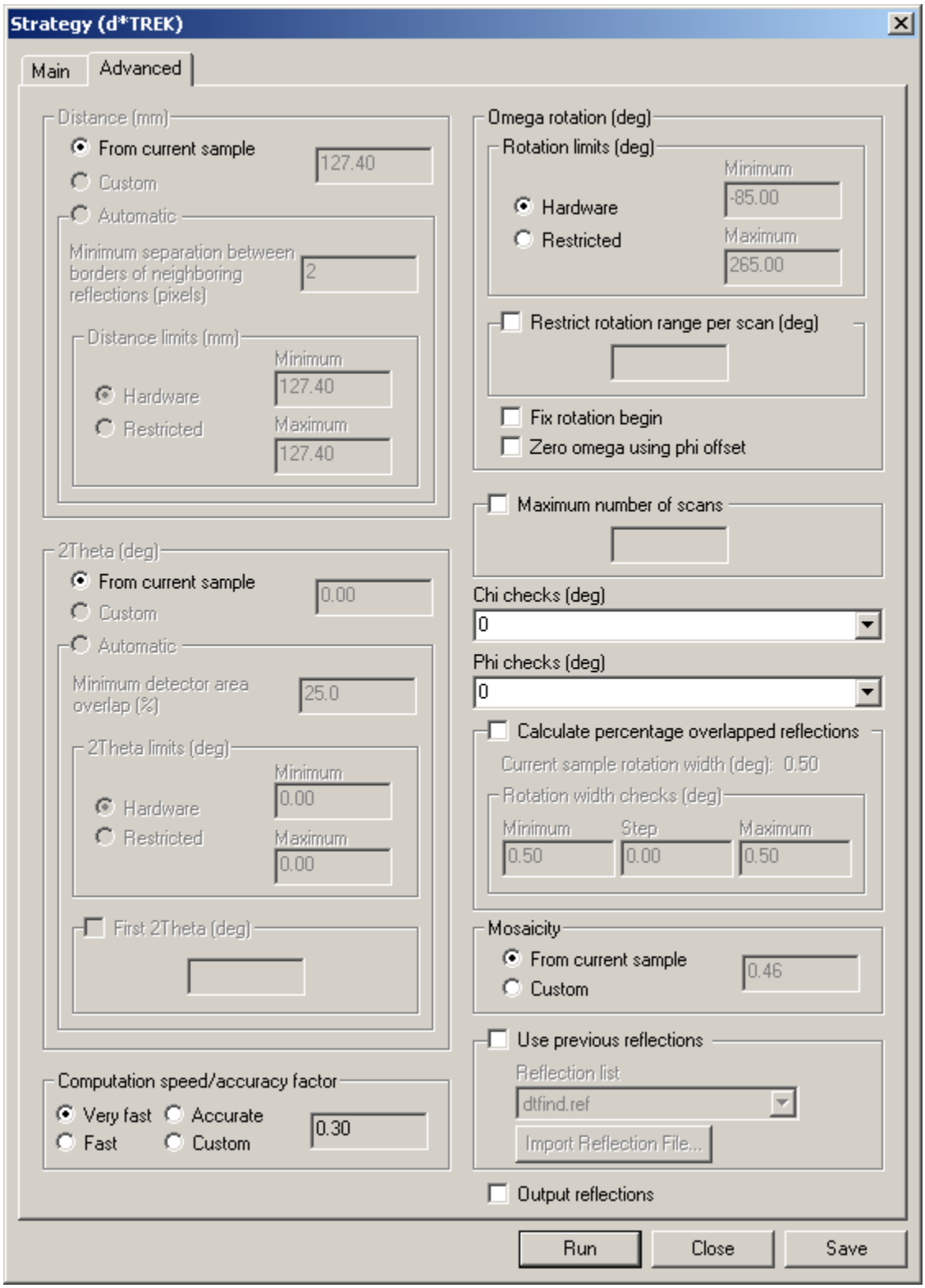

*Figure 3.3. The Advanced tab of the Srategy window while using the d*TREK processing suite in CrystalClear 2.1. All parameters designated here were used in the strategy for data collection for Az-PHM crystal H6.*

After running strategy, the algorithm calculated the percentage of data completion based on predicted reflections while considering the values specified in the Main tab. If the target percentage is reached, a schedule for data collection appears in the Collect Images window. A schedule contains detector and goniometer settings selected by the strategy algorithm along with the number of images to be collected at a specific angle. The schedule visible in Figure 3.4 shows the settings used to collect data on crystal H6. The *Start* and *End Angles* were adjusted to 5.00 and 155.00, respectively, to prevent the goniometer cradle from casting a shadow in the diffraction images, and the *Exposure Time* was increased to a total of 20 minutes per image. Because the H6 crystal was predicted to be highly symmetric (an orthorhombic unit cell), only one scan was needed to ensure all unique reflections would be collected (33).

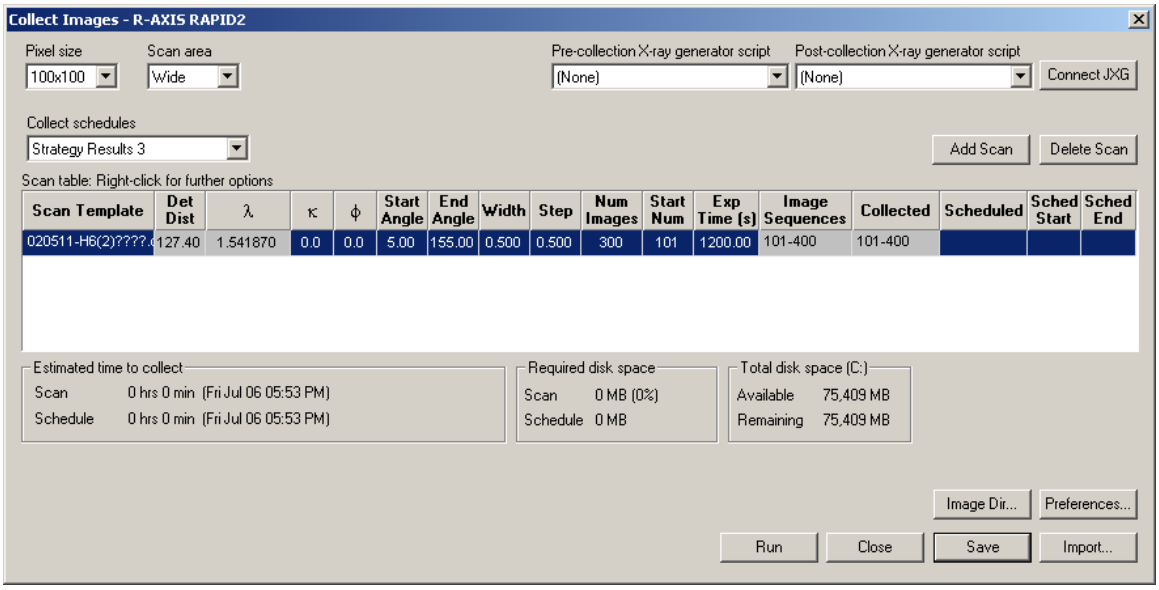

Figure 3.4. The Collect Images window in CrystalClear 2.1. The schedule shown in the figure was used to collect data on crystal H6.

Following the selection of the schedule resulting from strategy, the H6 crystal was exposed to copper K_α x-ray radiation (50 kV, 40 mA) through a 0.3 mm capillary optics collimator under a chilled stream of nitrogen gas at -150°C, and a total of 300 diffraction frames were collected. After collecting a full data set of images, the process of data reduction can begin, starting with the integration of reflections in order to obtain intensity information. However, a new unit cell was predicted before integrating. Even though

the crystal's unit cell was already determined during screening, obtaining a more accurate unit cell ensures that integration occurs in the precise location of the spot, in order to avoid integrating background noise. A more accurate unit cell that represents all reflections in the full data set was found when several parameters from the unit cell prediction protocol in Chapter 2.4 were changed, which are described below. Reflections used to determine the unit cell were selected from several images throughout the collection, including the first and last image, instead of spots from two images only. This was done so that the reflections used were an accurate representation of the entire data set (see Figure 2.8). When the reflections were indexed, the location of the beam was checked as there was more opportunity for shifting given that the full data collection took place over several days (see Figure 2.11). The "All" macro was used during refinement of the unit cell instead of the "Most" macro so that the radiation source location was refined along with the detector, crystal and goniometer. When reflections throughout space are used for indexing, everything should be refined. Finally, the number of cycles was changed from 100 to 30 and the X and Y rejection limits were adjusted to 1 (see Figure 2.13). Because CrystalClear's new refinement algorithm includes up to 5 derivative calculations per cycle (instead of 1 which was used in older versions), convergence is reached much faster and 100 cycles is not necessary (34).

After predicting a more accurate unit cell, data reduction began on the full collection of images when all reflections were measured for their intensities through integration. Prior to selecting integration parameters, a mask file was created that defined the shadow of the beam stop which prevented d*TREK from harvesting erroneous intensity information. Parameters for harvesting intensities are shown in the Main tab of the Integrate Reflections window in Figure 3.5, and several of the defaults were consciously changed. First, all images of the collection (which excludes any screen images) were used as the *Template*, and the resolution *Maximum* was set to a value just larger than the resolution on the images where spots are visible. A high maximum was entered since weak data is easily excluded during future scaling and averaging steps. Lastly, a value of 2 for the *Padding* parameter was used which is typical for fine-slice data. Because data from an individual reflection can be located on several images, this

value controls the number of images on either side of the one being integrated that are searched for a reflection's exact position. The *Images per batch*, *Box* and *Batch prefix* values used were default parameters, which are all shown in Figure 3.5 (33).

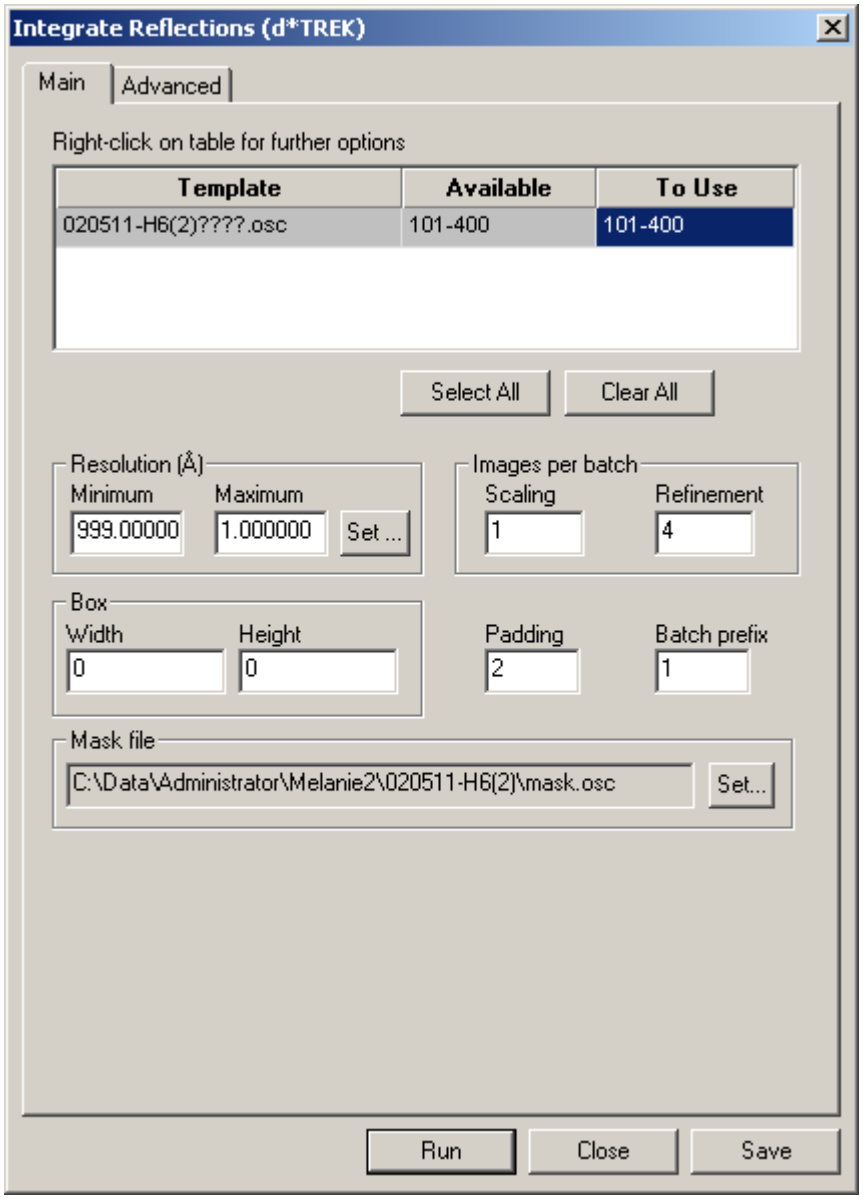

Figure 3.5. The Main tab of the Integrate Reflections window in CrystalClear 2.1 containing parameters used to integrate the diffraction data from Az-PHM crystal H6.

On the Advanced tab of the Integrate Reflections window shown in Figure 3.6, more parameters are available that offer greater flexibility when measuring intensities. Because crystal H6 is a protein crystal, it was advantageous to *Perform profile analysis*

during integration with a *Number* of 50 and *Maximum images* totaling 7. This function creates reflection profiles from well-defined reflections and uses the resulting statistics to best estimate the intensities of weak spots. The *Refinement macro* All was used when refining before integration. Before integration took place on each image, *Find reflections* and *Predict reflections* were both selected before refining using 2 refine batches each, and while finding reflections, only those pixels having an *I/sigma* of 5.00 or greater were included in spots. It is most important to find and predict spots before integration when there are multiple scans present so that any defect in goniometer position after it moves in additional scans does not affect the software's ability to locate the spots and accurately predict and integrate them. Because the prediction depends on the mosaicity value used, it was very important that the *Mosaicity model* have a value of 1 for *Multiply* and a value of 0 for *Add*. When these values were input, the software used the refined mosaicity from the unit cell prediction. For a set of well-predicted images, a high mosaicity used in the integration causes background noise to be integrated and taken for real reflection intensity. Lastly, by opting to *Check overlaps*, any reflections that overlap by a fraction greater than or equal to the value designated are excluded from integration. For H6, any spots that overlapped by $\geq 3\%$ were not harvested. The values for all other parameters not discussed that were used in integrating crystal H6 are shown in Figure 3.6 (33).

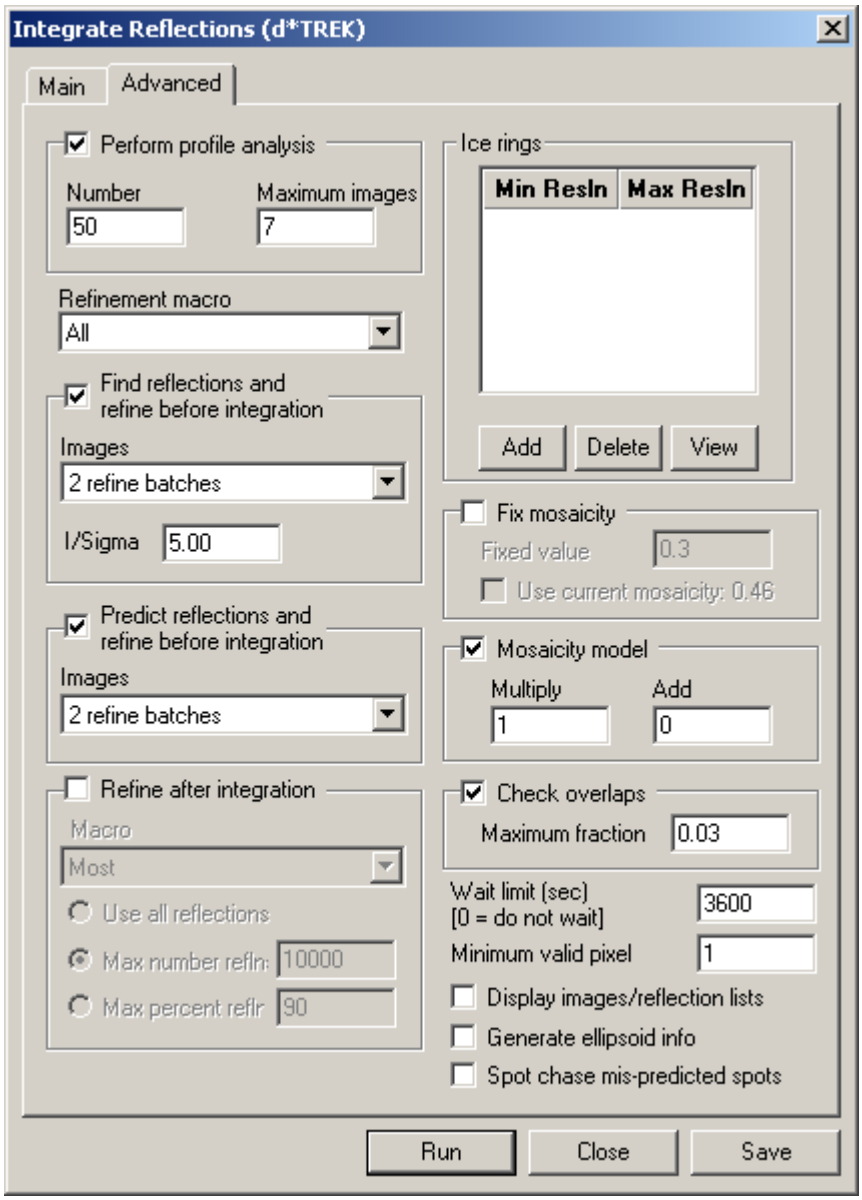

Figure 3.6. The Advanced tab of the Integrate Reflections window in CrystalClear 2.1. The parameters shown in the figure were used in integrating the data from Az-PHM crystal H6.

After the intensity data was harvested, a series of checks were employed to more accurately pinpoint the Laue class, centricity and space group that best characterize the symmetry of crystal H6. It is important to note that although these checks are vital in determining that the correct symmetry is chosen, it is not possible to be sure that the exact symmetry of the crystal has been determined until the electron density map can be viewed (39).

The first, Laue Check, is designed to use the integrated data to determine the Laue symmetry. The data are averaged for each Laue symmetry group and the resulting R_{merge} values for each group are compared. For H6, the parameters used are given in Figure 3.7. The *Reflection list* used, dtprofit.ref, contained the integrated data. Both *Average Bijvoets* and *Batch scale*, using a maximum of 50 reflections per batch, were selected. By choosing to average Bijvoet (or Friedel) pairs, any anomalous signal that is present was removed, avoiding the potential for incorrect symmetry assignment. Batch scale was selected for the same reason, even though the integrated data was all from the same crystal and the crystal was cryocooled to avoid decay. Under the *Highest Laue symmetry*, All classes were considered in determination, and under "Unit cell reduction", a *Maximum least squares residual* of 0.1 was input which limits the number of possible solutions to only those that are most likely. Lastly, *R-merge* values of 0.08 and 0.15 for *Ideal* and *Poor*, respectively, were used along with an *Incremental increase ratio maximum* of 1.5. By limiting the range of R-merge values, a shorter list of possible Laue classes is produced (33).

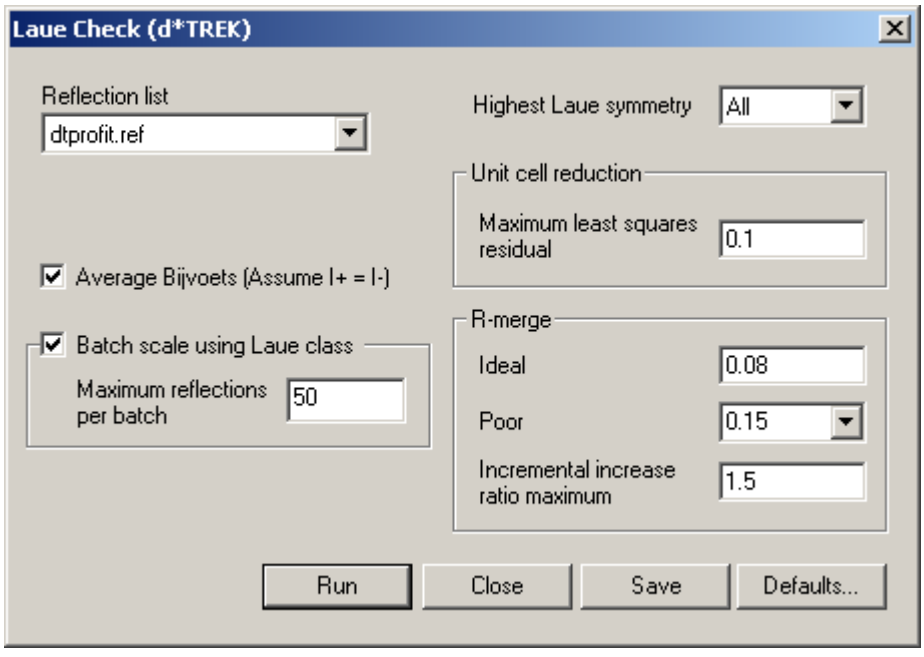

Figure 3.7. Laue Check window containing parameters used for Laue class determination for Az-PHM cyrstal H6.

The results of the Laue check for crystal H6 can be seen in Figure 3.8 where the solution highlighted in green was the recommended choice for Laue group symmetry. Each Laue group refers to a limited set of crystallographic point groups within a crystal system. Even though the unit cell dimensions already suggested an orthorhombic cell, for which there is only one possible Laue class, all possible unit cells are reconsidered using the integrated data, so that the Laue class is not biased. For crystal H6, Laue group "mmm" was suggested by the software, which is indicative of the orthorhombic crystal system. This group was recommended because it was the solution with the highest symmetry and the one with an R_{merge} value closest to the ideal of 0.08 (33).

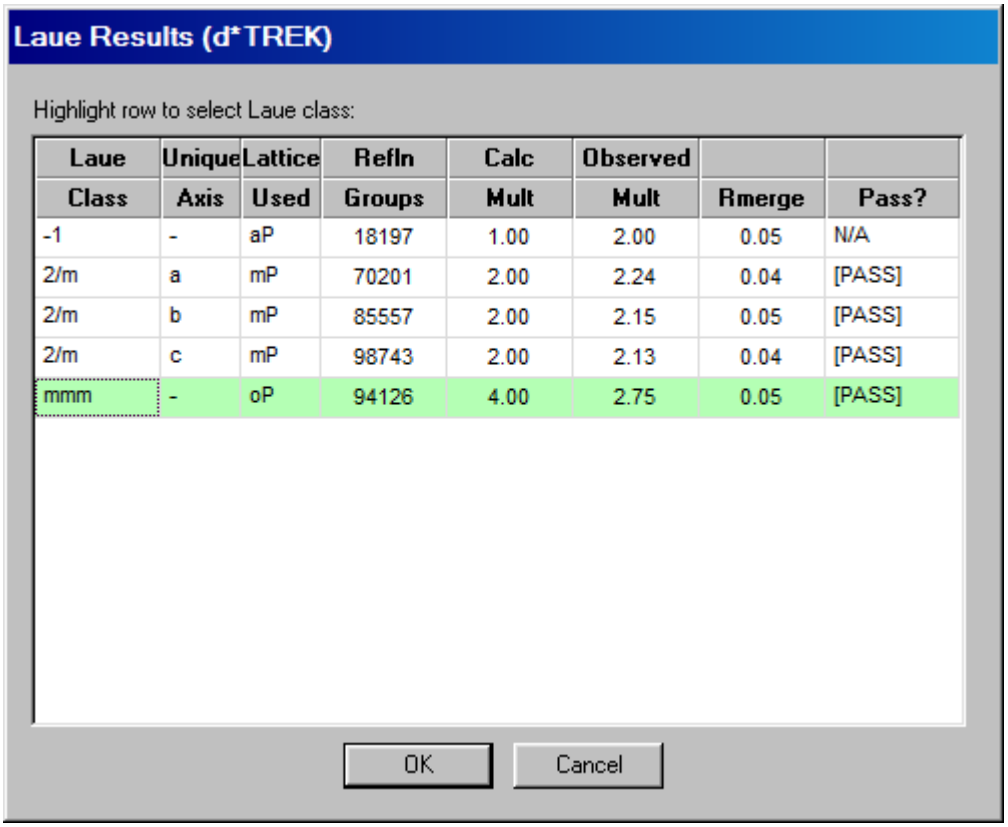

Laue Class	Unique Axis	Lattice Used	Refln Groups	Calc Mult	Observed Mult	Rmerge	Pass?
-1	-	aP	18197	1.00	2.00	0.05	N/A
2/m	a	mP	70201	2.00	2.24	0.04	[PASS]
2/m	b	mP	85557	2.00	2.15	0.05	[PASS]
2/m	c	mP	98743	2.00	2.13	0.04	[PASS]
mmm	-	oP	94126	4.00	2.75	0.05	[PASS]

Figure 3.8. Laue Results from Az-PHM crystal H6. The Laue class highlighted in green is the solution with the highest symmetry and R_{merge} closest to the ideal.

The second check uses the integrated data in dtprofit.ref to determine whether or not the space group is centric. Because all naturally-occuring protein molecules are chiral, it was not necessary to perform this check on crystal H6. Nevertheless, centricity was checked and the results can be seen in Figure 3.9.

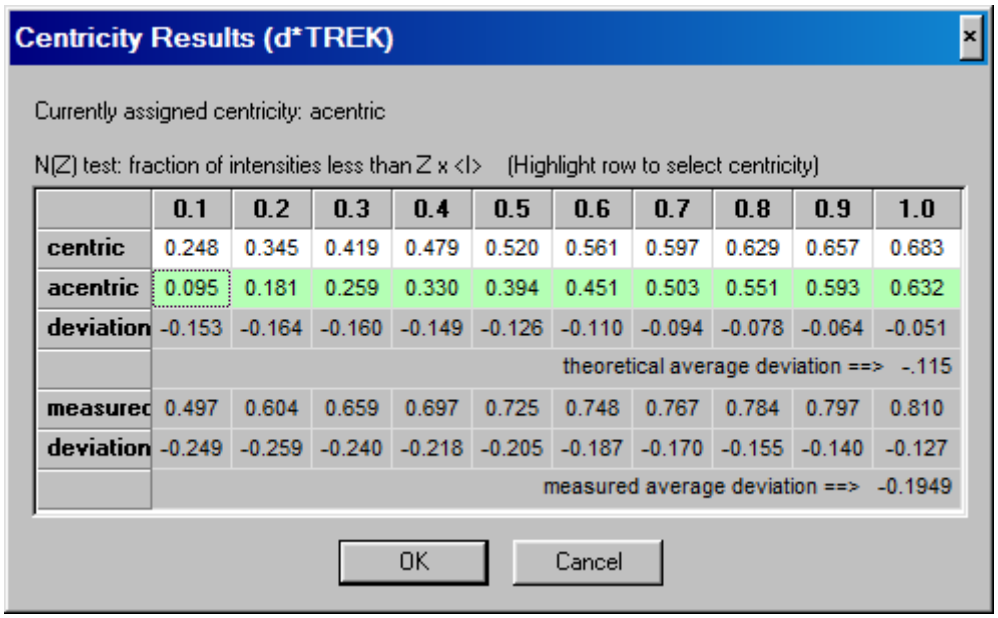

Figure 3.9. Centricity Results from Az-PHM crystal H6. The green highlighted solution is the one recommended by CrystalClear.

The third and final check determines space group by analyzing the reflection data for any systematic absences that are consistent with the laue group and centricity previously assigned. The correct determination largely depends on the I/sigma parameter entered by the user. For crystal H6, the integrated data from dtprofit.ref was used and a value of 4 was entered for *<I/Sig> tolerance*. The resulting data and suggested space group, $P2_12_12_1$, are seen in Figure 3.10. The <I/Sig> tolerance value was important in determining the correct space group since any value less than 4 would have given a different space group. For this data set, it is clear that the <I/Sig> data for h00, 0k0, and 00l reflections where h,k and l are odd is small compared to all other <I/Sig> values. These small values indicate areas where no real spots were actually located or in other words, where spots were systematically absent. Defining these locations where no spots were actually integrated allows the space group to be determined based on reflection data (33).

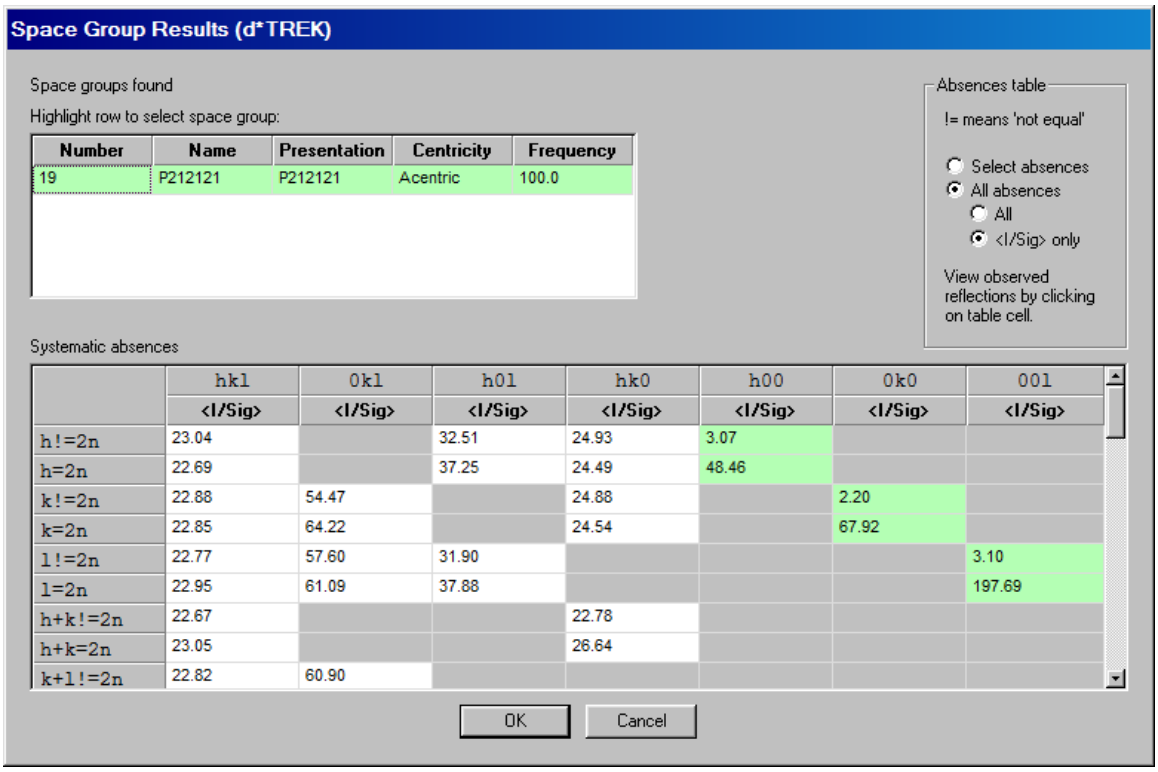

Figure 3.10. Space Group check results from Az-PHM crystal H6. The green boxes indicate systematic absences where the <I/Sig> is low.

After gathering integration data and symmetry characteristics, the final step in data reduction for crystal H6 was carried out by scaling and averaging the integrated intensity information. Integration data is scaled when there is reason to suspect that intensities from different sections of the collection differ. These differences are due to a number of factors including different exposure times, radiation damage, fluctuating source intensity and different absorption of x-rays due to varied paths through the crystal. Besides these systematic errors, random outliers should be rejected and therefore, data correction via scaling is a necessary step in data reduction. After data is scaled, d*TREK averages the intensity data and the ouput is a file that contains a list of unique reflections. For crystal H6, minimal scaling was required before reflection intensities were averaged. These collection aspects are reflected in some of the parameters used to scale and average the integrated data in dtprofit.ref, which are visible in Figure 3.11. In the scaling model section, *Batch scale* was deselected because the entire crystal was bathed in x-rays and all data was collected from the same crystal at a constant exposure rate. *B-factor* was also deselected because the crystal was cryocooled during the entire data collection,

preventing any major decay. Also in the scaling model section, *Scale I+ and I– separately* was deselected since Friedel pairs do not exist in data with a non-centrosymmetric space group like $P2_12_12_1$, and when selecting *Absorption correction*, the *REQAB* Fourier 8.3 algorithm (40) was chosen. During scaling, *reflections with I/Sigma* < 3.00 were excluded and S*ystematic absences* were rejected beforehand. Lastly, the *Resolution Maximum* was set to 1.3 Å and the *Error model* weights were determined automatically by d*TREK. All other parameters were left default as shown.

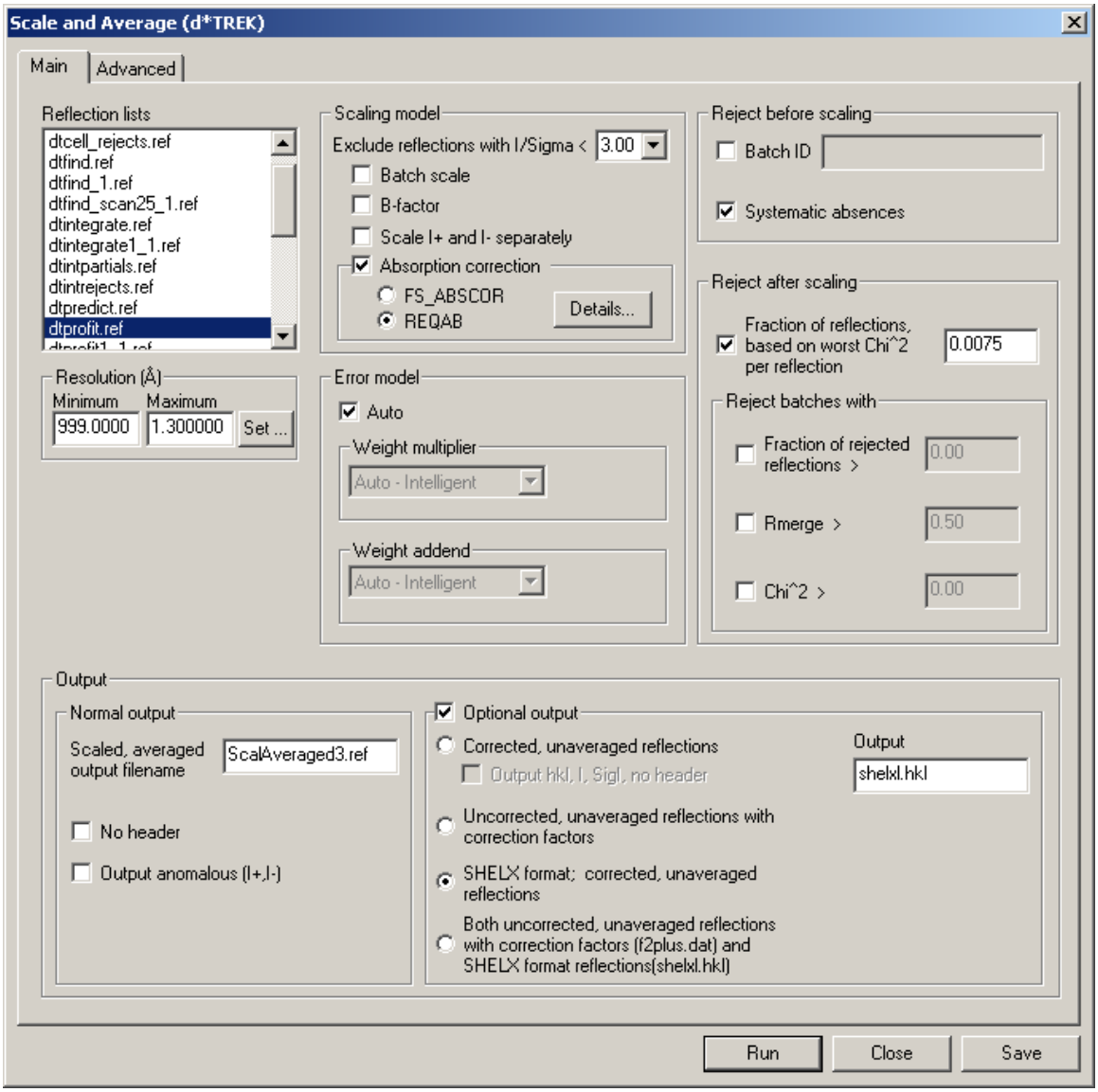

Figure 3.11. The Main tab of the Scale and Average window in CrystalClear 2.1. All parameters shown were used to scale and average integrated data from Az-PHM crystal H6.

Only a few more scale and average parameters exist in the Advanced tab for scale and average, visible in Figure 3.12. All parameters were left as default except for the *Global/per batch range argument(s)*. This value was changed to 0.002 so that the magnitude of the applied scale factors was reduced over the entire data set.

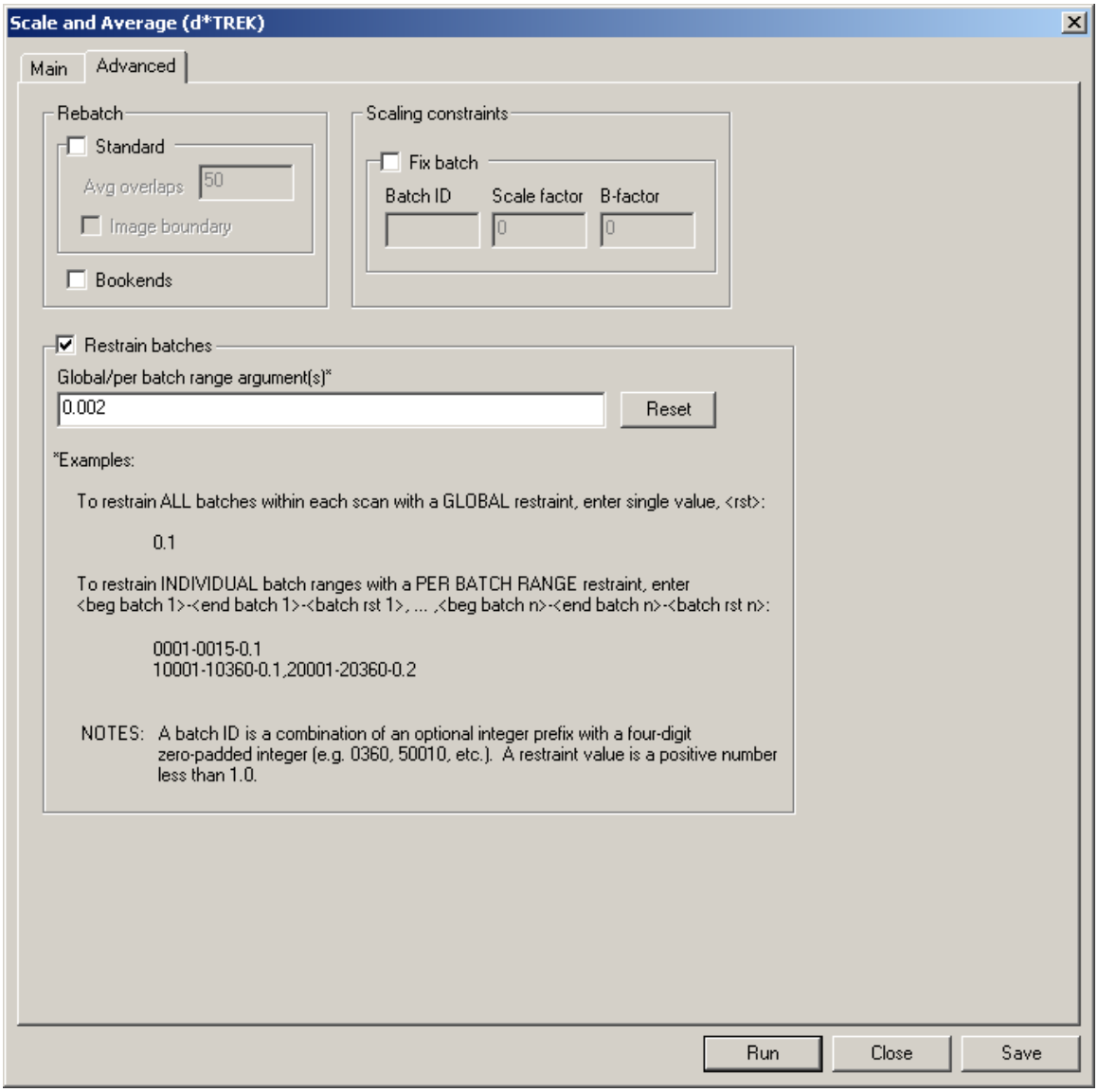

Figure 3.12. The Advanced tab of the Scale and Average window in CrystalClear 2.1. All parameters shown were used to scale and average integrated data from Az-PHM crystal H6.

After scaling and averaging the integrated reflections, statistics are generated which help assess the quality of the diffraction data. Some of the results include merging statistics, completeness, average redundancy, signal strength, resolution and final unit cell

dimensions. The resolution of the data set was limited to 1.3 Å because the average intensity of each reflection in this range had fallen to just over twice the mean standard deviation of the measurements (I/sigI = ~2.0). Hence, the results for Az-PHM crystal H6, given in Table 3.1, reflect statistics for the last resolution shell down to 1.3 Å as well as the entire data set.

Table 3.1. Data collection statistics for the reduction of reflection data from Az-PHM crystal H6 in CrystalClear 2.1. Statistics are given for the entire data set and for the last resolution shell.

	All Resolution Shells	**Last Resolution Shell**
Space Group	$P2_12_12_1$	
Unit Cell Dimensions (Å, °)	a = 50.2, b = 54.9, c = 85.9 $\alpha = \beta = \gamma = 90$	
Lattice System	Orthorhombic	
Laue Symmetry	mmm	
Mosaicity (°)	0.61	
Total number of reflections	252,950	
Number of unique reflections	52,747	
Resolution Range (Å)	28.05 – 1.30	1.35 – 1.30
Average Redundancy	4.80	2.72
Completeness (%)	89.3	70.7
R_{merge}	0.043	0.356
R_{meas}	0.047	0.437
Output <I/sigI>	15.2	2.3

Completeness is defined as the number of unique reflections measured over the total number of unique reflections possible (possible unique reflections are determined by the symmetry of the crystal) and though it is somewhat lacking at 70.7% for the last resolution shell, the presence of spots was significant enough to warrant inclusion in the data set since <I/sigI> fell to approximately 2. In Table 3.2, completeness statistics are given by resolution shells. Out of the total number of observed reflections in the last resolution shell, less than 1% of them were rejected, indicating that the spots measured in this shell should not be disregarded. However, including the last resolution shell in the data set may be frowned upon by some since shell completeness is often in the 95th

percentile (39). In hindsight, it may have been advantageous to collect the data using a lower symmetry during strategy to ensure more images were taken and that all unique reflections in this last shell were collected, which would boost completeness not only for the last shell, but also for the entire data set.

Table 3.2. Data collection statistics after the reduction of reflection data from Az-PHM crystal H6 in CrystalClear 2.1. Statistics given are completeness results for the last resolution shell, down to 1.3 Å.

Completeness results for the Last Resolution Shell	
Resolution range	1.35 – 1.30
# of observed rflns	11279
# of rejected rflns	70
Calculated unique rflns	5824
# of unique rflns	4118
# of unique rflns measured once	506
# of unique rflns measured multiple times	3612

In discussing the quality of the data in terms of intensity, it is important to remember that symmetry-equivalent reflections are often measured multiple times and should theoretically have equal intensities. R_{merge} is a statistic that conveys the quality of the intensity measurements made for symmetry-equivalent reflections. It is described as the sum of the absolute differences for all symmetry-related measurements of a particular unique reflection, where the sum of differences from every unique reflection is added together and divided by the sum of the average intensity values of all unique reflections. Though this value is typically reported in crystallographic analysis, it seems to be a poor statistic to use to determine the quality of the intensity data because it is affected by redundancy, a ratio of the total number of intensity measurements to the total number of unique reflections measured (39). If redundancy is high, then R_{merge} will also be high. The statistic R_{meas} is identical to R_{merge} but is independent of redundancy and therefore, a better measure of the quality of intensity measurements (41). The R_{meas} statistic is calculated as follows in CrystalClear,

$$R_{meas} = \frac{\sum_h \sqrt{N/(N-1)} \sum_i \left| I_{hi} - \overline{I_h} \right|}{\sum_h \sum_i \overline{I_h}},$$

where N is the number of observations for unique reflection h, I_{hi} is the i^{th} measurement for unique reflection h, and $\overline{I_h}$ is the average intensity for unique reflection h. R_{meas} for the entire data set is excellent at a value of 0.047, but R_{meas} values increase exponentially until in the outer shell, the error in intensity measurements averages more than 40% of the observed values at 0.437. This is a sensible R_{meas} value because as the diffraction angle gets larger, spots at a higher resolution are more affected by crystal disorder and tend to give more varied intensities (18). Recently, Karplus and Diederichs stated that data should be truncated before <I/sigI> reaches 2.0 and before R_{merge} or R_{meas} exceeds ~0.6 to 0.8 (42). So, even though R_{meas} is 0.437 for the outer shell, it is well below the R_{meas} cutoff and is another indication that the diffraction data in the last shell should be included in structure determination.

As previously mentioned, redundancy is a statistic describing the number of times a unique reflection is observed. When unique reflections in a data set have high redundancy (or multiplicity), it becomes easy to detect outliers. Detecting outliers accurately also depends on the correct assignment of intensities during integration, making it imperative that detector distances and beam location are properly placed (41). Because the beam location was refined and the average redundancy for most of the resolution shells is moderately high at values between 5 and 8 (see Table 3.3), the scaling and merging algorithm should have had no trouble in detecting outliers. That being said, when considering R_{merge} values no outliers were detected in the data and all frames received the same scale factor, which suggests that the data collected from crystal H6 is high-quality and that the crystal itself suffered no radiation damage during data collection to cause any significant differences in reflection intensities.

Table 3.3. Data collection statistics for the reduction of reflection data from Az-PHM crystal H6 in CrystalClear 2.1. Statistics give redundancy in resolution shells.

Resolution range	Calculated unique rflns	Percent of reflections measured N times, N = (%)						Completeness for shell (%)
		0	1	2	3	4	5-8	
28.05 – 2.80	6213	0.0	0.5	3.2	9.4	9.7	77.2	100.0
2.80 – 2.22	5987	0.2	2.1	3.0	12.3	4.4	78.0	99.8
2.22 – 1.94	5934	0.2	2.4	6.5	11.0	6.8	73.3	99.8
1.94 – 1.76	5873	1.4	2.3	8.2	12.1	13.7	62.4	98.6
1.76 – 1.64	5893	4.5	2.3	9.7	11.5	19.9	52.1	95.5
1.64 – 1.54	5860	7.2	2.1	10.9	9.9	23.8	46.1	92.8
1.54 – 1.46	5852	14.7	3.5	14.6	7.2	24.1	35.8	85.3
1.46 – 1.40	5818	23.2	3.9	23.3	6.9	25.4	17.3	93.7
1.40 – 1.35	5832	28.0	4.8	29.5	4.1	29.5	4.1	72.0
1.35 – 1.30	5824	29.3	8.7	30.8	2.7	28.5	0.0	70.7

Even in keeping the data in the last resolution shell, the statistics for the entire data set are great and promise a high-quality crystal structure. Characteristics of the diffraction, such as mosaicity, suggest that Az-PHM crystal H6 is a well-ordered crystal and the strength of the reflections throughout the data set imply that it is highly probably that the correct Laue class and space group have been chosen. Further confirmation of the excellent quality of the diffraction data will result after estimating phases during molecular replacement and viewing the electron density map.

Chapter 3.3 Intensities to Structure Factors and Molecular Replacement in CCP4

Because the data for Az-PHM crystal H6 was reduced using Rigaku's CrystalClear 2.1 software, it was introduced to the software program CCP4 6.1.3 in the form of a unique list of scaled reflection intensities. Figure 3.13 displays a small portion of the reduced intensity output data from CrystalClear. Each line of the output file includes information for a unique reflection. The location of the reflection is specified by the values for h, k and l (columns 1-3), and the averaged and scaled intensity value for each reflection is also given along with its standard deviation, which are denoted "fIntensity" and "fSigmaI", respectively (columns 4 and 5).

```
nH
nK
nL
fIntensity
fSigmaI
     0     0     4 27753.9 883.621
     0     0     6 5314.16 286.605
     0     0     8 2454.38 190.803
     0     0    10 20753.0 641.960
     0     0    12 275712.0 4416.13
     0     0    14 56.3007 18.2364
     0     0    16 50814.5 1822.22
     0     0    18 27042.6 10548.2
     0     0    20 420541.0 9527.92
```

Figure 3.13. Output file from CrystalClear 2.1 containing a portion of scaled and averaged intensity data for each unique reflection measured in the Az-PHM H6 data set.

The next step used the Import Merged Data function in CCP4 to convert these intensities from CrystalClear to structure factor amplitudes. Of all the parameters used to accomplish this task, shown in Figure 3.14, only a few needed to be modified from their initial default values. The first modification involved *converting scaled data output from d*trek into MTZ format*, a file form that CCP4 reads. Next, the *Use anomalous data* function was deselected since the integrated data, *ScalAveraged3.ref*, contains no anomalous data. To convert intensities to structure factors, the *old Truncate* algorithm was run using the *French&Wilson truncate* protocol (43). While the new structure factors would be written to the output file, *ScalAveraged3.mtz*, the option to *Keep the input intensities in the output MTZ file* was selected though this data was no longer required after conversion. Also, even though the data in ScalAveraged3.ref contains a unique list of scaled reflection intensities, it was important to choose to *Ensure unique data & add a FreeR column* to 5% of the data. By flagging a small portion of the structure factors, the data could be used in cross-validation of the model in later steps. Lastly, extra information about the crystal, data set, unit cell dimensions, protein length, space group and radiation wavelength was entered for inclusion in the final MTZ output file before running the Import Merged Data function.

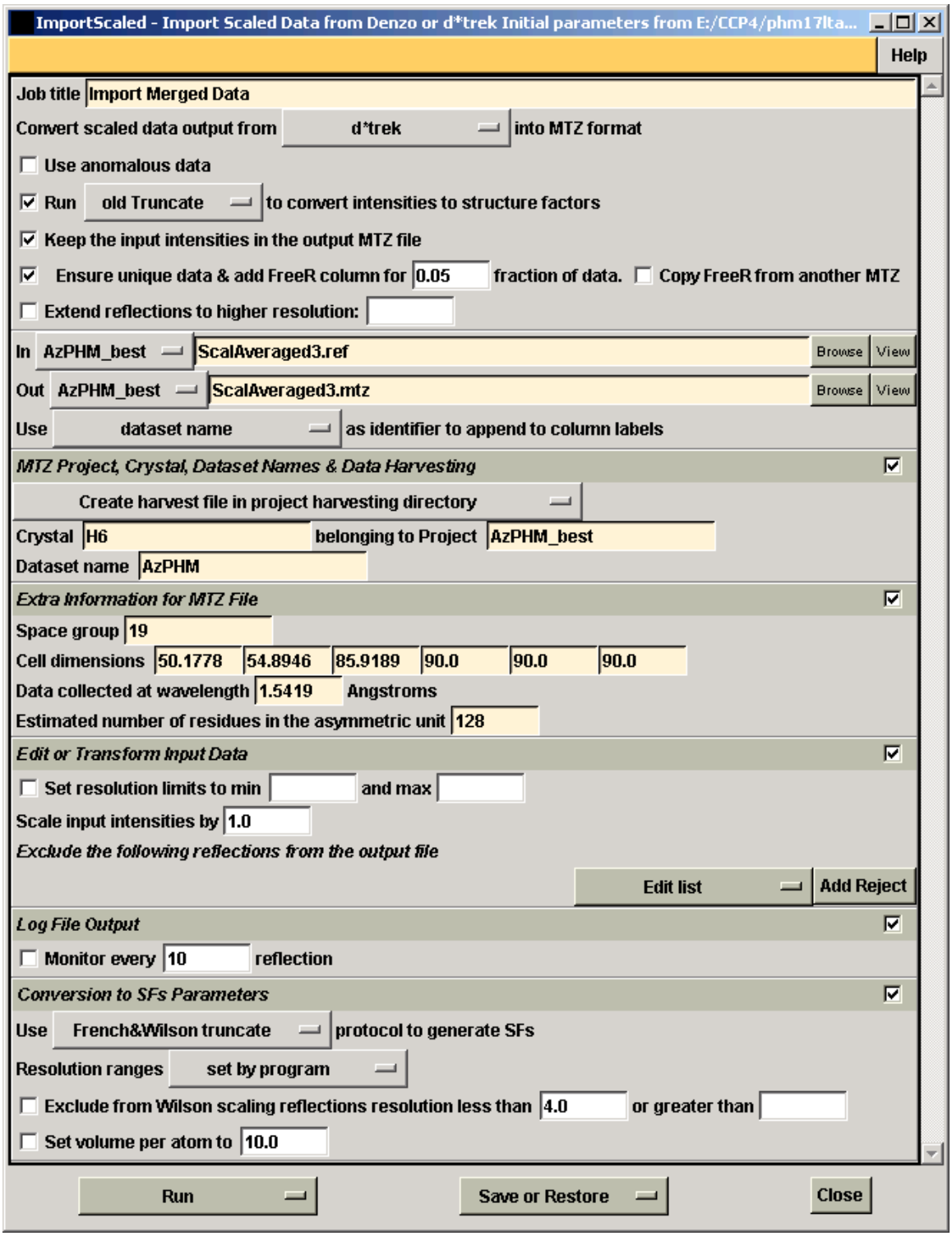

Figure 3.14. Import Merged Data parameters used in converting crystal H6's scaled and averaged intensity data into structure factors using CCP4.

A small portion of the resulting MTZ file from the Import Merged Data function is displayed in Figure 3.15. Like the output file ScalAveraged3.ref from CrystalClear, the MTZ file from CCP4 contains reflection locations h, k and l in columns 1, 2 and 3, respectively. Column 4 contains the FreeR flags that mark each reflection depending on the percentage of data withheld from model building. Structure factor amplitudes and their standard deviation are listed in columns 5 and 6, respectively, for each unique reflections from the H6 data set. Recall from Figure 3.14 that structure factor amplitudes were generated using the *French&Wilson truncate* protocol. This algorithm created by French and Wilson (43) is a complex algorithm based on Bayesian statistics that calculates a multiplier by which the data is scaled after the square root is taken. The other option in CCP4, simple square-root, is a straightforward approach that only involves taking the square root of the intensities. For this data, the *French&Wilson* protocol determined that all intensities would be multiplied by 1.569 after taking the square root. So, the structure factor amplitude located at 0, 0, 4 is 261.35 (column 5 in Figure 3.15), which was derived from its intensity of 27753.9 (column 4 in Figure 3.13) by rooting the intensity and then multiplying it by 1.569.

LIST OF REFLECTIONS

								column label
0	0	2	2.00	?	?	?	?	
0	0	4	19.00	261.35	4.17	683.64	21.77	
0	0	6	17.00	114.28	3.09	130.90	7.06	H H
0	0	8	8.00	77.57	3.04	60.46	4.70	H K
0	0	10	9.00	226.00	3.50	511.19	15.81	H L
0	0	12	11.00	823.73	6.60	6791.41	108.78	I FreeR_flag
0	0	14	18.00	11.15	2.27	1.39	0.45	F F_AzPHM
0	0	16	4.00	353.51	6.35	1251.68	44.89	Q SIGF_AzPHM
0	0	18	11.00	231.37	64.94	666.12	259.83	J IMEAN_AzPHM
0	0	20	13.00	1016.93	11.54	10358.88	234.69	Q SIGIMEAN_AzPHM

Figure 3.15. Output file from CCP4 containing structure factor amplitudes for each unique reflection measured in the Az-PHM H6 data set.

Upon obtaining structure factor amplitudes, the data was analyzed for solvent content in preparation for molecular replacement. Solvent content is related to the Matthews Coefficient, which is calculated using the cell volume and molecular weight of the crystallized protein. For H6, these parameters were entered in the Cell Content Analysis window seen in Figure 3.16. In the second line of the window, *Calculation of the Matthews coefficient* was for protein only, seeing as H6 did not contain any nucleic

acids. The input *MTZ file*, ScalAveraged3.mtz, containing the structure factor amplitudes was used and because the *Read crystal parameters from MTZ file* option was selected, *Space group*, *Cell* dimensions, and *High resolution limit* were filled in automatically. Lastly, the *Molecular weight of the protein* was 14000, *entered in Daltons*.

After running the algorithm, the Solvent Content Analysis window shows a table of results (displayed in Figure 3.16) that include the Matthews Coefficient and the corresponding solvent content in percent for a given number of molecules per asymmetric unit (Nmol/asym) along with probabilities indicating the likelihood of each solution. It is clear that there are likely 2 Az-PHM molecules in each unit cell suggested by this solution's the total probability value of 96% and solvent content of 41.83%. Solvent content in protein crystals is typically around 43% and in rare cases has been as low as 27% or as high as 65% (44).

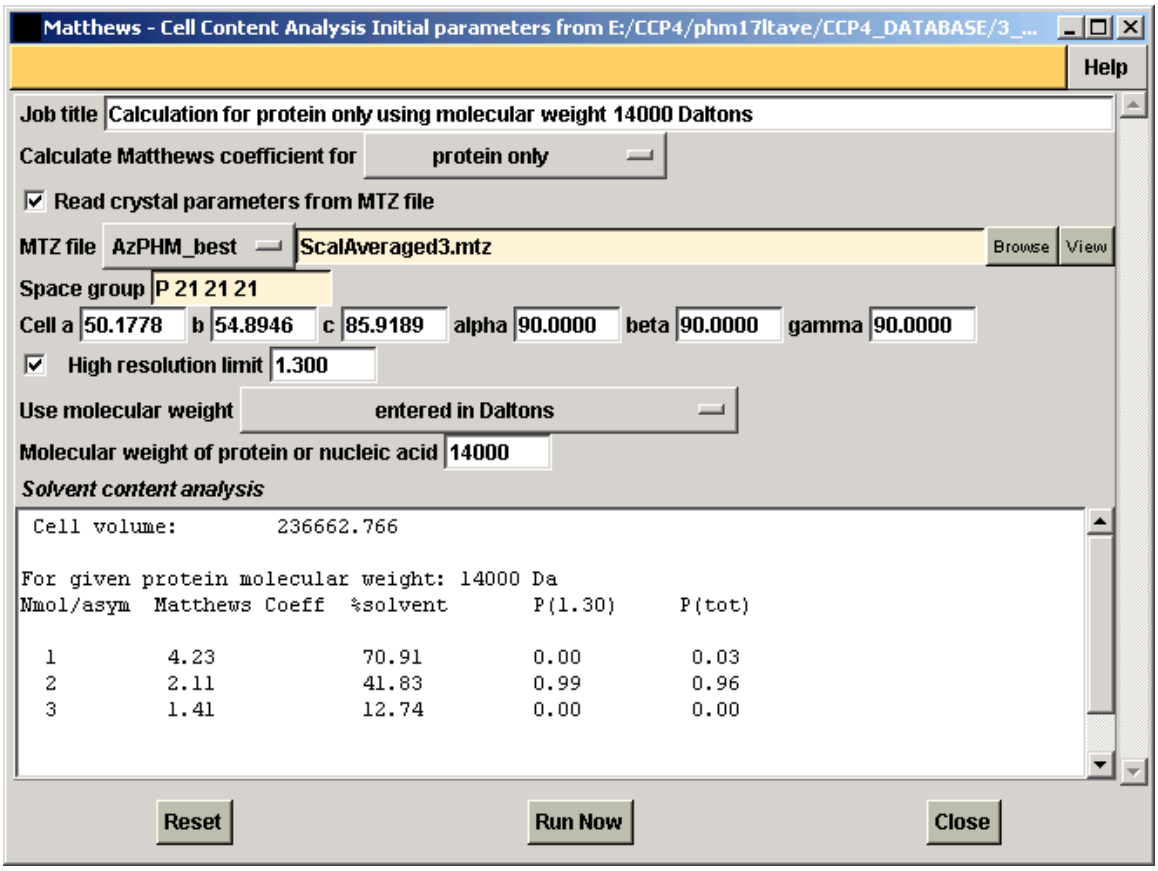

Figure 3.16. Cell Content Analysis window in CCP4 containing parameters for the calculation of the matthews coefficient for Az-PHM crystal H6.

The last step of preparation before molecular replacement involves calculation of B-factors which represent thermal disorder and the amount of smearing of electron density due to thermal motion and crystal disorder. The software algorithms BAVERAGE and WILSON accessed through the Analyse Data for MR window, shown in Figure 3.17, calculated B-values for the structure factor amplitudes in *ScalAveraged3.mtz* and for the molecular replacement model *4AZUone.pdb* in order to *Do B value analysis of the experimental data and model structure*. The model in 4AZUone.pdb is one monomer (chain A) of the structure solved by Nar *et al*. in 1991 and was deposited in the Protein Data Bank with the ID: 4AZU (16). The last parameter entered was the *Number of residues in the asymmetric unit*. This value depends on the results from the solvent content analysis performed previously. Recall that the number of molecules in the asymmetric unit was predicted to be 2. Because Az-PHM is 128 amino acids long, the number of residues in the asymmetric unit is likely 256, which is the value that was entered for this parameter.

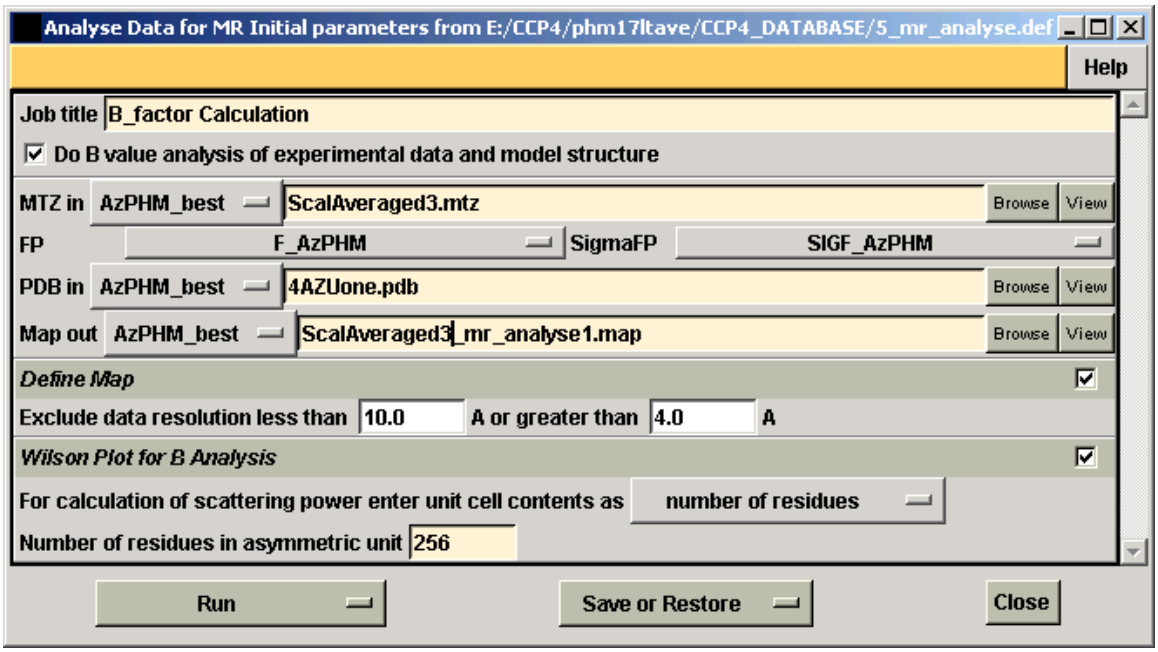

Figure 3.17. Analyse Data for MR window in CCP4 which contains all of the parameters used in calculating B-factors for the experimental structure factor data from Az-PHM crystal H6 and for the accompanying molecular replacement model.

Upon running the analysis software, there were three noteworthy values that were calculated which include B-factors for the experimental data and the molecular replacement model along with a BADD parameter. The B-factor reported for the model (4AZUone.pdb) was 16.656, and for the experimental data it was 13.655. Because the BADD parameter is simply the difference between the two B-values, it follows that its value was -3.001. A low experimental B-factor ensures that the quality of the electron density is preserved (39).

After obtaining the number of molecules per asymmetric unit and the magnitude of the BADD parameter, molecular replacement was initiated using these values. The Molrep – auto MR window in CCP4 (Figure 3.18) includes the values for all the parameters used. Molecular replacement was done *performing rotation and translation functions* to fit the *4AZUone.pdb model* to the experimental structure factor data in *ScalAveraged3.mtz*. All data out to a *maximum resolution* of 1.3 Å was used for fitting. Because Az-PHM has a 3-residue difference from native azurin, there were 3 places in the experimental data where the phases would not be estimated properly. In order to assign the correct name of these three residues to the output file 4AZUone_molrep1.pdb, the option to *Use sequence* was selected and the appropriate sequence file, *AzPHM.seq*, was entered. The file contains one chain of 4AZU's fasta sequence from the Protein Data Bank with proper modifications. All other parameters not discussed are default.

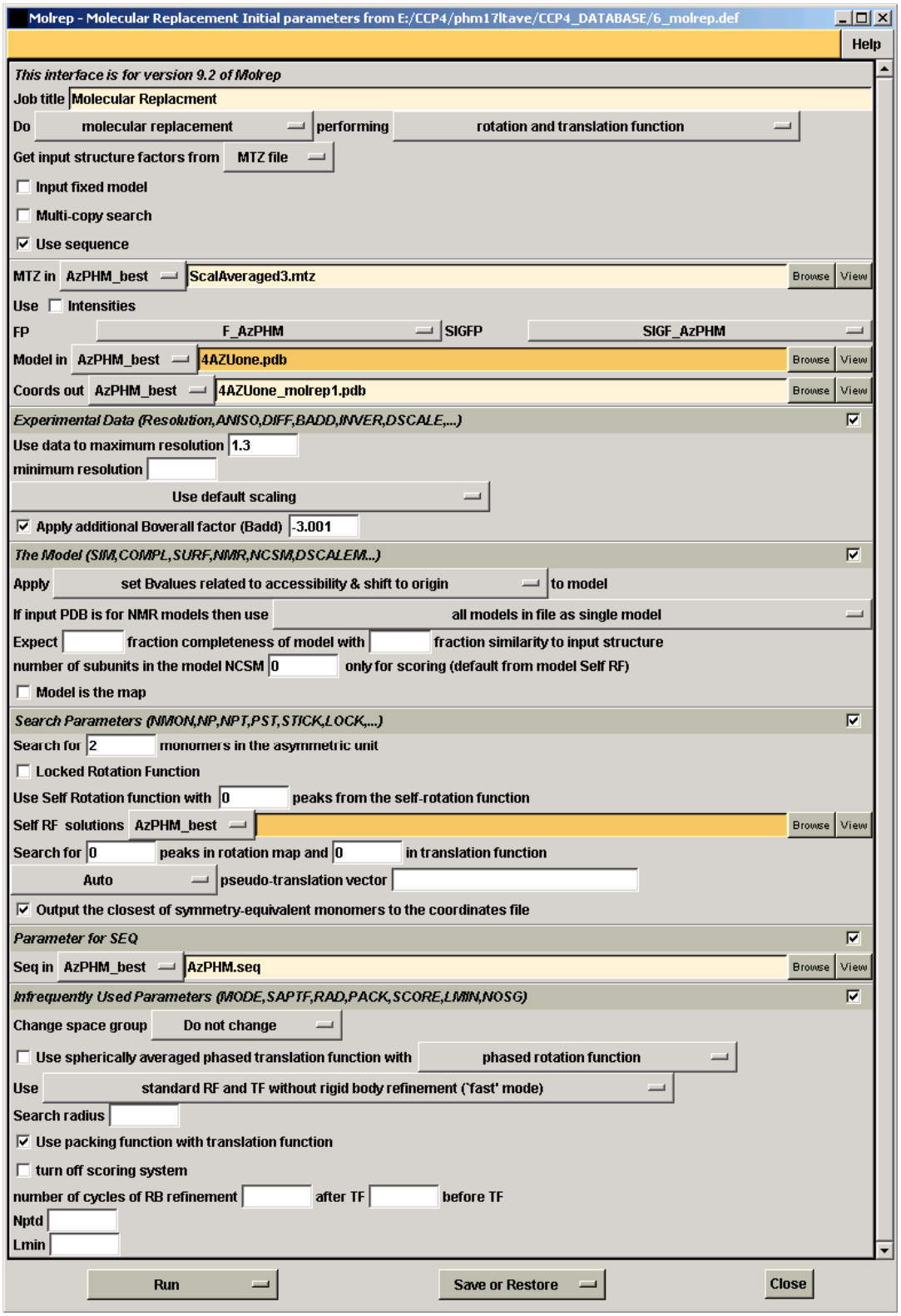

Figure 3.18. Molrep – auto MR window containing all parameters used to complete molecular replacment for the experimental data of Az-PHM crystal H6 using phase information from the 4AZU model.

Before viewing the Az-PHM model resulting from molecular replacement, the coordinates were first refined using CCP4's Refmac5 function. During refinement, the position of the atoms in the model structure is refined while accounting for geometric restraints and other restrictions specified by the presence (or absence) of input parameters. These parameters, visible in Figures 3.19 and 3.20, are numerous, so only those that were modified from their default values will be discussed. The first (shown on the second line of the refinement window) gives several options for refinement, and the type of refinement selected depends largely on the resolution of the data. It is common to use restrained refinement following molecular replacement because atoms are refined according to the electron density while using geometric restraints. Another option, unrestrained refinement, does not include geometric restraints (only used in cases of very high resolution) while rigid body refinement only refines the position of the entire asymmetric unit without refining individual atoms (used in cases of low resolution). Because the Az-PHM data is fairly high resolution and had a low thermal B-factor, *TLS & restrained refinement* was performed using *no prior phase information*. TLS, which stands for translation libration and screw-motion, is a type of refinement that takes vibrational motion into account when refining atomic positions. After the type of refinement was selected, the structure factor amplitudes (found in *ScalAveraged3.mtz*) and the Az-PHM model (found in *4AZUone_molrep1.pdb*) were entered after which names for all of the output files were automatically assigned. In the Refinement Parameters section, it was important to *Exclude data with a freer label, FreeR_flag, with a value of 0* in order to set aside 5% of the data for calculation of R_{free}, a statistical value that measures how accurately the model predicts the experimental density. This small fraction of data is also referred to as the "free" set. Looking under the Geometric Restraints section, notice that the option to *make links between all others* has "defined in file only" following it. Another option for this parameter is to select "defined in file or residues are close" and is advantageous to choose if the data are low resolution and there are certain bonds that should be maintained. Non-crystallographic Symmetry (NCS) Restraints were not used in the refinement of H6 data, even though the data suggested that it contained more than one monomer in its asymmetric unit. This is because the

resolution of the data is high, such that NCS restraints were not needed and may in fact be harmful during refinement. The only parameter modified in Figure 3.20 was the type of scaling used, which was changed from *simple* to *Babinet*. This parameter was changed in order to take bulk solvent into account. All other parameters were unchanged.

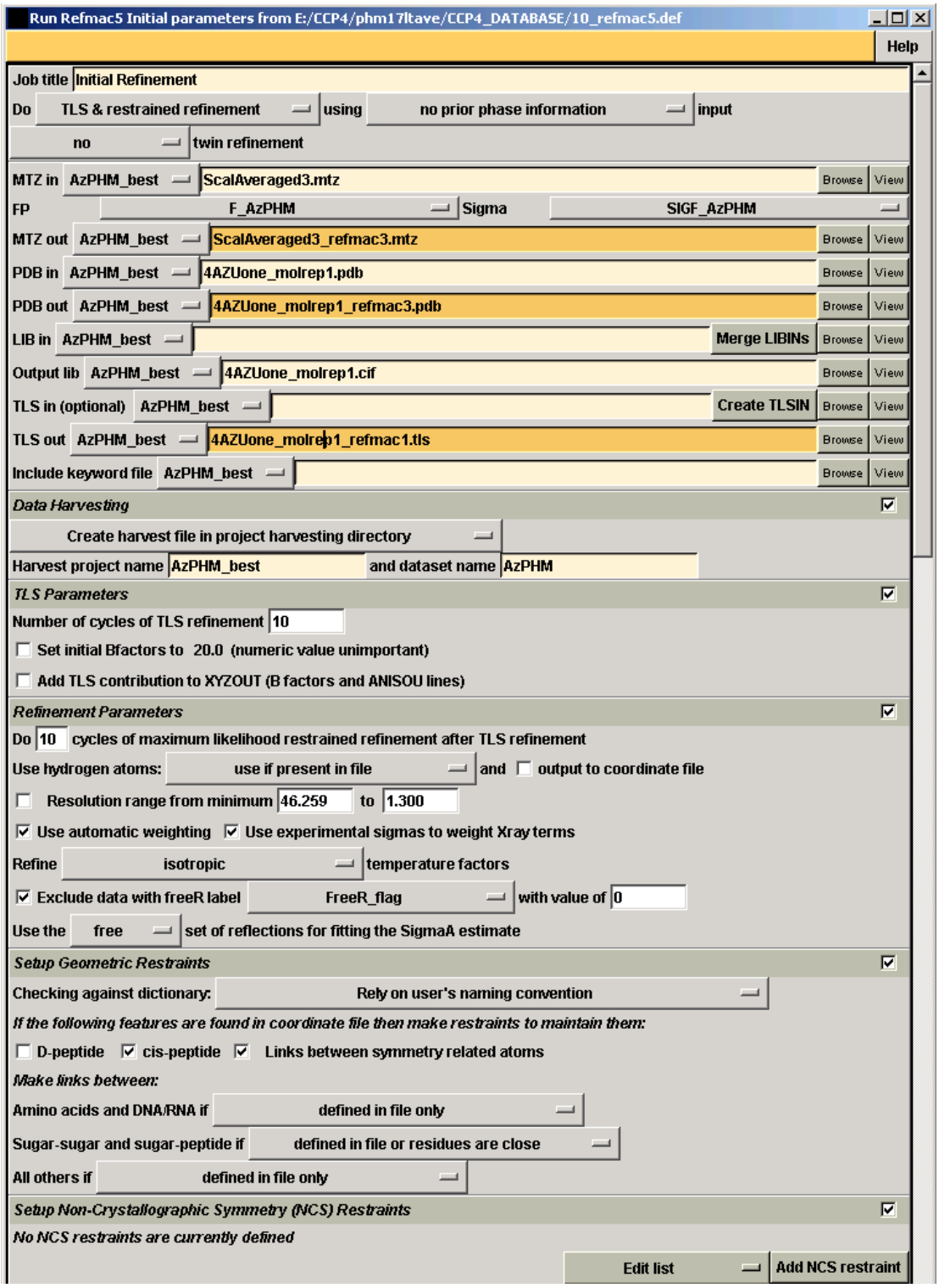

Figure 3.19. Refmac5 parameters used for running the initial round of refinement for Az-PHM crystal H6 data following molecular replacment in CCP4.

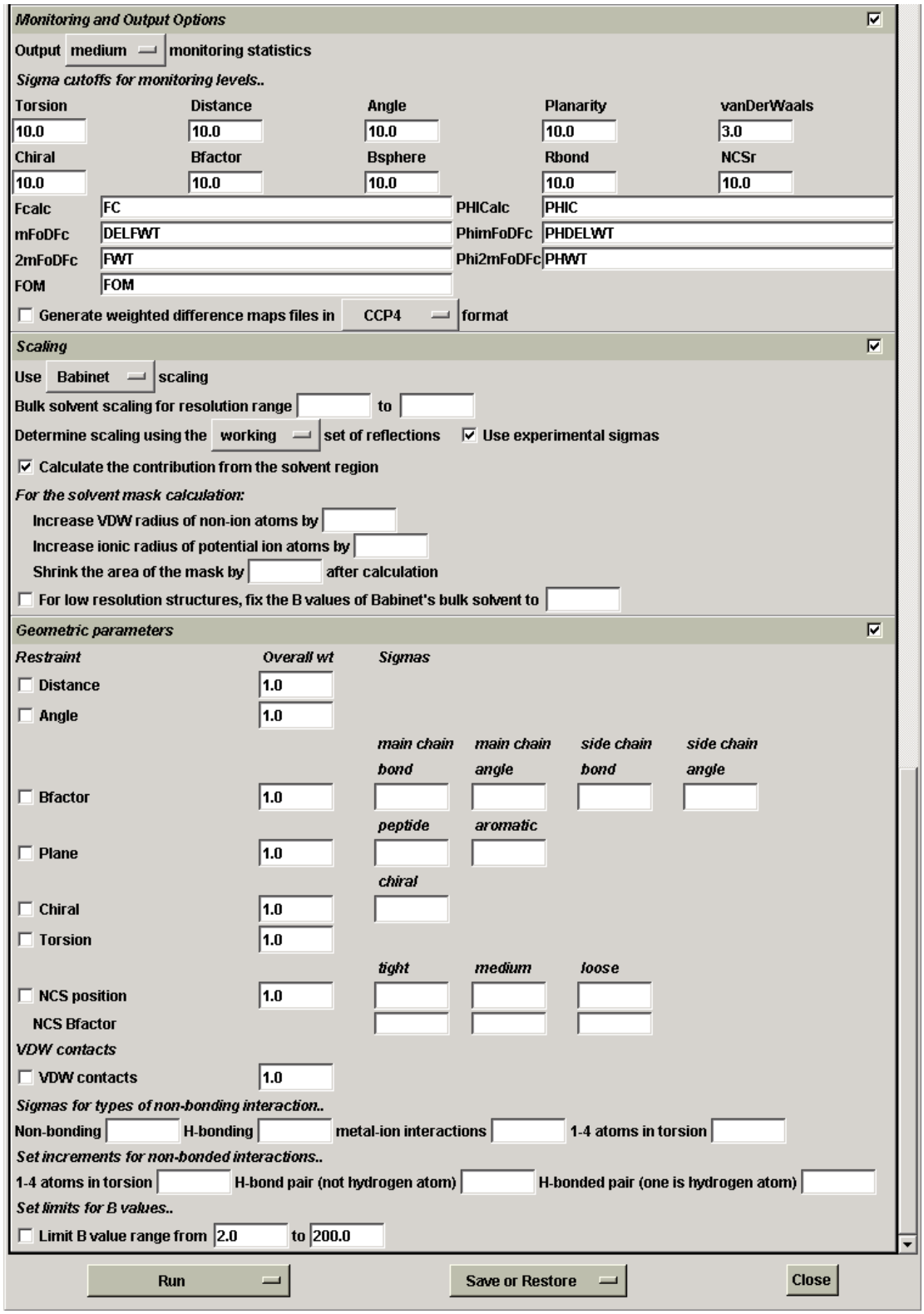

Figure 3.20. Refmac5 parameters used for running the initial round of refinement for Az-PHM crystal H6 data following molecular replacment in CCP4.

After 10 cycles of restrained refinement followed by 10 cycles of TLS refinement, R_{factor} and R_{free} are displayed. These R-values play a significant role in determining correct atomic positions in the model because they convey the accuracy of the fit of the Az-PHM model (*4AZUone_molrep1_refmac3.pdb*) to the experimental electron density map (*ScalAveraged3_refmac3.mtz*). R_{factor} is a ratio of the sum of differences between observed and calculated structure factor amplitudes to the sum of observed structure factor amplitudes (39). R_{free} is a similar unbiased statistic that uses a small portion of the reflection data (5% in this case) for "observed structure factor amplitudes" which are excluded during refinement. R_{free} was originally developed after Axel Brünger (45) noticed a bias in R_{factor} that results from using the same reflections for both model building and refinement. After the initial round of refinement for the H6 model and map, Refmac gave an R_{factor} of 32.45% and an R_{free} value of 34.55%. At present, these values are moderately-low for this stage of refinement and hold promise of a well-fitting structure.

At this stage of structure determination, confirmation of the accuracy of the results from much of the work completed in CrystalClear and CCP4 is lacking. However, by simply viewing the preliminary model and corresponding electron density map and evaluating the sheer interpretability of the map and the overall fit of the model, the success of data reduction and molecular replacement be determined. This is accomplished through the use of the macromolecular model-building program, Coot. In this software, an electron density map is created using the coupled structure factor amplitudes and phases that were written into the MTZ file during refinement carried out by Refmac. Coot also overlays the model which can be analyzed for overall fit to the map. In Figure 3.21, a photo containing the map and model leaves no doubt that the electron density surrounds the preliminary model well. This simple observation confirms a great deal: intensities were scaled and merged appropriately, structure factor amplitudes were calculated correctly and the phase estimation in molecular replacement was performed successfully.

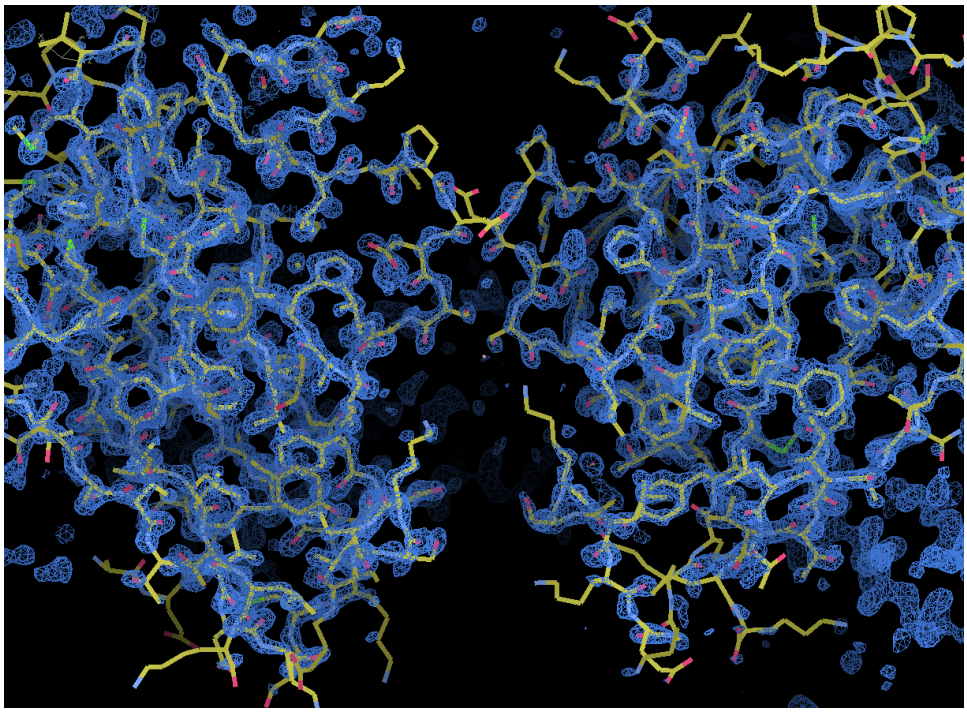

Figure 3.21. Preliminary map and model of Az-PHM resulting from molecular replacement in CCP4.

The second most noticeable feature in Figure 3.21 is the number of molecules in the asymmetric unit. Recall that the solvent content analysis predicted two molecules per unit cell which prompted the MOLREP algorithm to search for two monomers during molecular replacement. In viewing the preliminary structure, the prediction is confirmed because the experimental electron density outlines two distinct Az-PHM molecules that have opposite spatial orientations. The overall fit of the model to the map also validates the choice of Laue class and space group assigned in CrystalClear during data reduction (39).

Upon closer inspection of the structure, electron density surrounds the model equally on all sides throughout a large majority of the structure. A small detailed portion of the structure seen in Figure 3.22 illustrates this point. The high 1.3 Å resolution of the experimental data allows individual atoms in the electron density to be visible, shown most clearly by the phenylalanine residue.

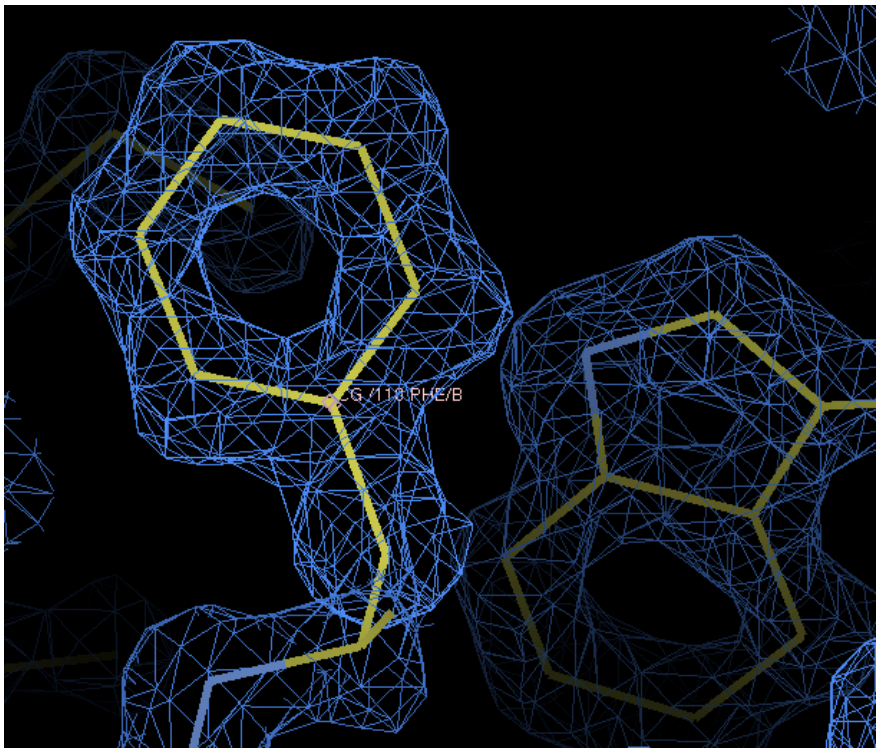

Figure 3.22. Small section of the electron density map and preliminary model from the Az-PHM crystal H6. The electron density map clearly shows individual spheres in the phenylalanine ring.

In looking at a different portion of the structure, seen in Figure 3.23, the identity of the protein is partially confirmed. In this figure, the amino acid in position 14 shows clear electron density in the shape of a histidine residue. Because a crystal structure for wild-type azurin was used for phase estimation in molecular replacement, the model contains a missing part of the histidine residue in position 14. When positions 8 and 16 were inspected, the model showed missing atoms as well. The map showed methionine and histidine density, respectively, confirming that the appropriate mutations were made when creating the Az-PHM protein.

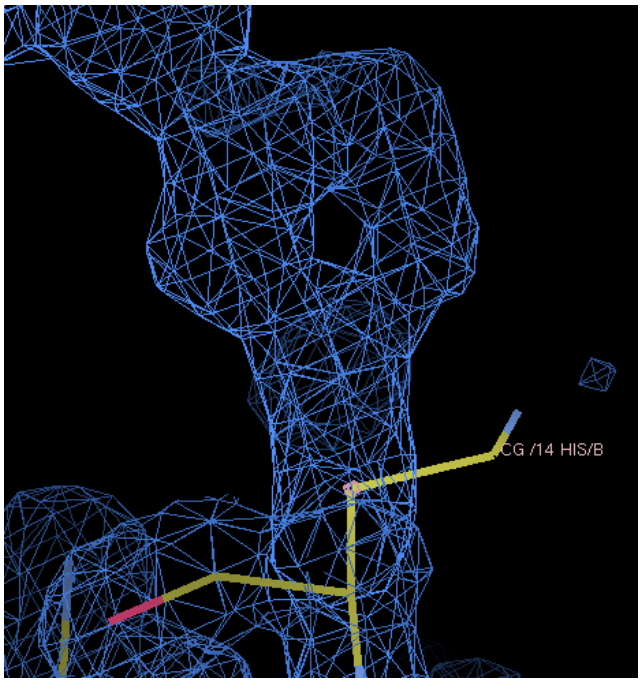

Figure 3.23. Small section of the electron density map and preliminary model from the Az-PHM crystal H6. The electron density map clearly shows electron density for a histidine residue at location 14.

The incorrectly modeled residue can be changed at these three locations within the Coot program to reveal a better model that more accurately describes the true packing of the protein molecules within the crystal. Even without the changes, the overall fit of the preliminary model to the experimentally-determined electron density supports the process and the parameters used in CrystalClear and CCP4 to collect data, reduce it and estimate phases via molecular replacement. The detailed nature of the electron density map shows the high quality of the data obtained and ultimately, the highly-ordered packing of the Az-PHM crystal that was grown.

CHAPTER 4

Chapter 4.1 Introduction

When a preliminary protein model is generated from molecular replacement and initial refinement in CCP4, it is uploaded to a molecular graphics program and compared to the electron density map. Coot (46) is one such program that allows macromolecular crystallographers to easily view their preliminary model against the experimental map and make changes to the model's amino acid sequence, residue conformations and surrounding solvent molecules. Adjustments like these create a more accurate model that better explains the experimental electron density data.

Refining a model in Coot is a tedious process that involves hours of analysis. Changes in the atomic coordinates of the model are typically guided by a difference map, which is created alongside the electron density map. A difference map consists of colored sections of density that indicate areas of positive and negative density that should be modeled and un-modeled, respectively. A crystallographer uses a difference map as an aid in deciding whether an amino acid should be moved or where a water molecule should be added. Scanning the entire difference map can be an arduous task and after a series of adjustments are made to the structure in Coot, the resulting coordinates are input into CCP4 where new coordinates and new phases are calculated upon running a re-refinement. Because the new map is slightly different than the old map, the new coordinates must again be compared to the density and adjusted further if needed. If coordinates are again changed, the model must undergo another bout of refinement in CCP4. This tedious process is known as iterative refinement.

After all residues in the model are properly positioned and iteratively refined, solvent molecules are added to the remaining electron density where appropriate. During the process of adding solvent, the model is again iteratively refined in CCP4 to monitor the effect of the changes to the model. After each round of refinement in CCP4, R-values are monitored (both R_{factor} and R_{free}). If either of the R-values increase after adjustments are made, these changes must be questioned and most-likely discarded if the experimental density does not show a marked improvement.

Changes to the model cease when the fit to the experimental density has been maximized and R-values no longer decrease. R_{factor} and R_{free} are two statistically similar values calculated by CCP4 that guide the process of model refinement by describing the fit of the protein model to the electron density map. R_{factor} is the sum of the differences in observed structure factor amplitudes (F_{obs}) to those calculated from the current model (F_{calc}) all over the sum of observed structure factor amplitudes, which is described by the equation below,

$$R_{factor} = \frac{\sum_{h} \left\| F_{obs} \right| - \left| F_{calc} \right\|}{\sum_{h} \left| F_{obs} \right|},$$

where *h* is the set of reflections that is used in creating the map, called the "working" set. This set of reflections is used to create the electron density map and is also used for monitoring the progress of refinement through the calculation of R_{factor} (39). In 1992, Axel Brünger demonstrated the bias associated with using the same set of reflections for refining and monitoring refinement and subsequently, introduced a statistic called R_{free} (45). R_{free} is also known as the "unbiased R_{factor}" because its calculation is the same as R_{factor} except that the structure factor amplitudes used are from a set of reflections that have been set aside and excluded from the electron density map. This small number of excluded reflections is also known as the "free" set (39).

In setting aside a test set of reflections that was not used to create a protein model, the true predictive power of the final structure can be evaluated. If the model makes accurate predictions of the raw experimental structure factors for the test set, then users of the model can have confidence that it is an accurate depiction of the protein in crystallized form (47). Because R_{free} is one of the only unbiased statistics that judges the model with respect to unused experimental data, it is likely the most powerful validation tool available and therefore, should be given considerable weight in terms of assessing the reliability of the refined model. The Coot software program contains many other tools that validate the model with respect to experimental data, including *Density fit analysis* and *Temperature factor variance analysis* and *NCS differences*.

Coordinate-based methods validate the model by purely assessing the model's geometry and stereochemistry without considering its fit to the experimental data. Also,

because geometry can be restrained during refinement in CCP4, many of these methods do not provide a true, independent validation of the model, but nonetheless serve to point out potential errors. However, the *Ramachandran plot* is one tool that uses phi and psi torsion angles that are not typically restrained during refinement and as such is a dependable coordinate-based validation tool. Some of the other tools for coordinate validation include side-chain analysis through the *Geometry analysis* function and torsion angle analysis using the *Peptide omega analysis* tool. Stereochemistry is analyzed through the *Incorrect Chiral Volumes* tool while the *GLN and ASN B-factor Outliers* attempts to detect incorrect placements of oxygen and nitrogen atoms in glutamine and asparagine side-chains using temperature factors.

In the sections that follow, the process of model building and refinement of the preliminary Az-PHM model will be discussed. Each of the validation tools mentioned will also be used in determining the quality of the final structure.

Chapter 4.2 Model Building and Refinement in Coot

After performing molecular replacement and initial refinement in CCP4, the Az-PHM model and structure factors were uploaded to the Coot software program where atomic coordinates were adjusted and solvent molecules were fit to un-modeled electron density. Throughout this model building process, only a few changes were made to the model before calculating new phases and thus, a new electron density map in CCP4 (i.e. running the refinement in Refmac5 again). The purpose in refining in this way was to monitor the change in R_{factor} and R_{free}. If any of the individual changes to the model did not produce a decrease in these values, the change was considered inappropriate and unsupported by the experimental data. This careful process was used throughout the Az-PHM model building and refinement process in Coot.

The first changes made to the preliminary model involved residue mutation and copper addition because these structural features were not known by the software to be a part of the Az-PHM protein, because the crystal structure used for molecular replacement only contained one amino acid chain of the wild-type azurin molecule. Copper(II) ions were added in the Type 1 and Type 2 sites of both Az-PHM molecules within the

asymmetric unit using the *Get Monomer* option in Coot, selecting copper ions with the *CU* identifier. Because histidine binds copper strongly, copper(II) ions were also added to the large spherical electron density next to both His83 residues (see Figure 4.1). So, a total of 6 copper atoms were added in the asymmetric unit. Next, electron density in the map supported the expected mutation of residues 8, 14 and 16 in chains A and B to methionine, histidine and histidine, respectively. This was accomplished using the *Mutate & Auto Fit* tool in Coot, where the correct amino acid replaced the old residue and was subsequently fit to the electron density. The new coordinates were then saved and input into CCP4 for TLS & restrained refinement along with the electron density map. The parameters used for refinement with Refmac5 were the same as those shown Figures 3.17 and 3.18 of Chapter 3.3. After refining with Refmac5 in CCP4, both R_{factor} and R_{free} dropped from 32.45% and 34.55% to 27.23% and 30.07%, respectively, indicating that the changes made were indeed warranted. However, after Refmac5 calculated new phases consistent with the newly-refined model, the resulting difference map showed negative density in portions of the copper(II) density, which was most noticeable near the copper(II) ion bound to histidine 83 in chain B (83HisB) as seen in Figure 4.1. Even though negative, red density is present which suggests that too many electrons were placed in that site, it is clear that the copper(II) ion should remain there since it makes chemical sense. There are also many other reasons why some red, negative density may appear in the map. It may be that the density is red because not every protein molecule in the crystal binds copper in this place, leaving a sphere that has less electron density than it theoretically would if all protein molecules bound copper in that space. However a better explanation, and the one that likely applies in this case, comes from paying attention to the locations of the negative density. The red blobs seem to be in a perpendicular direction to the positive, green density where solvent should be bound on either side of the copper(II) ion. In this well known phenomenon, the red density probably appeared in order to compensate for the additional electron density that is localized around the entire copper atom instead of localized around the bonds to the solvent molecules (48).

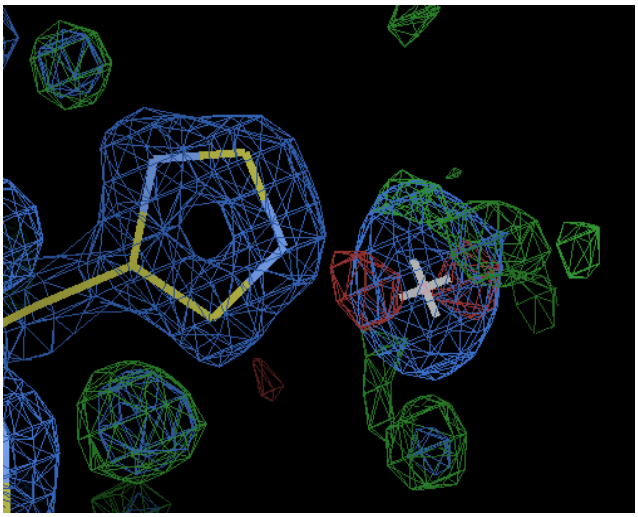

Figure 4.1. Negative, red density on a copper(II) ion next to histidine in chain B, postion 83 (83HisB). The negative density seems to be along bonds between 83HisB & copper and between copper and a blob of positive, green density.

Following copper addition and residue mutation, adjustments to individual residue atoms were made with respect to electron density fit and geometry. Residues that did not fit well in the electron density were often identified by a validation feature in Coot called *Density fit analysis*. This interactive tool displayed a color-coded bar graph (Figure 4.2) for each protein monomer, containing a bar for each amino acid residue that described its fit using a score. The score is defined as the average electron density level at the atom centers of the atoms in the residue (49). The farther the score is from 1, the higher the bar appears on the graph. For example, lysine in the 24th position in chain B (24LysB) has a moderately-high, yellow bar with a score of 0.78 (Figure 4.2) that indicates a decent, but not ideal fit to density. Amino acids such as this that had low scores were targeted and adjusted using one of three tools: *Auto Fit Rotamer*, *Rotamers*, or *Real-Space Refine Zone*. The first two options, *Auto Fit Rotamer* and *Rotamers*, fit side-chains to the density automatically or manually, respectively. *Auto Fit Rotamer* automatically chooses the best rotamer from the Molprobity Library developed by Lovell *et al*. (50) that gives the highest electron-density values at the atom centers. *Rotamers*, on the other hand, allows the best side-chain conformation to be selected manually from a generated list, sorted by frequency in the Molprobity database. Lastly, *Real-Space Refine Zone* not only refines atom centers for the highest electron density values but also considers stereochemical restraints when making adjustments to a range of atoms specified by the

user. Before making any adjustments permanent, scores regarding bonds, angles, planes, etc. are displayed that must be acceptable to the user. If desired, the user may move atoms to obtain new geometry scores, before making the adjustments permanent (49).

Figure 4.2. Interative bar graph from the Density fit analysis tool under Coot's validation options. Each bar represents an amino acid in the model and the color and height indicate its fit to the electron density map. chain A and chain B refer to two distinct Az-PHM molecules in the asymmetric unit.

Electron density fit is not the only consideration when making adjustments to atomic coordinates. When residues in a model are adjusted, each residue should fit the density but should also have an acceptable geometry. Like the density tool in Coot, *Geometry analysis* is a validation tool that describes the geometry of the model using a bar graph like the one shown in Figure 4.3. Each bar represents an amino acid in the model, the color and height of which depend on the Z-score of the amino acid in question. Z-values are calculated for bonds, angles and planes by comparing the model to dictionary conformations and are subsequently averaged together, resulting in an overall Z-score. A residue's Z-score is proportional to the height of its corresponding bar (48). For example, the lysine residue at position 24 in chain B has relatively good geometry in terms of its bonds, angles and planes since its bar is green with a moderately-low height due to a Z-score of 5.29. The caption in the graph also indicates that the angle at the 1st carbon of the side-chain (CB) in lysine is the largest contributor to the overall Z-score and should, therefore, be examined more carefully than any bonds or planes.

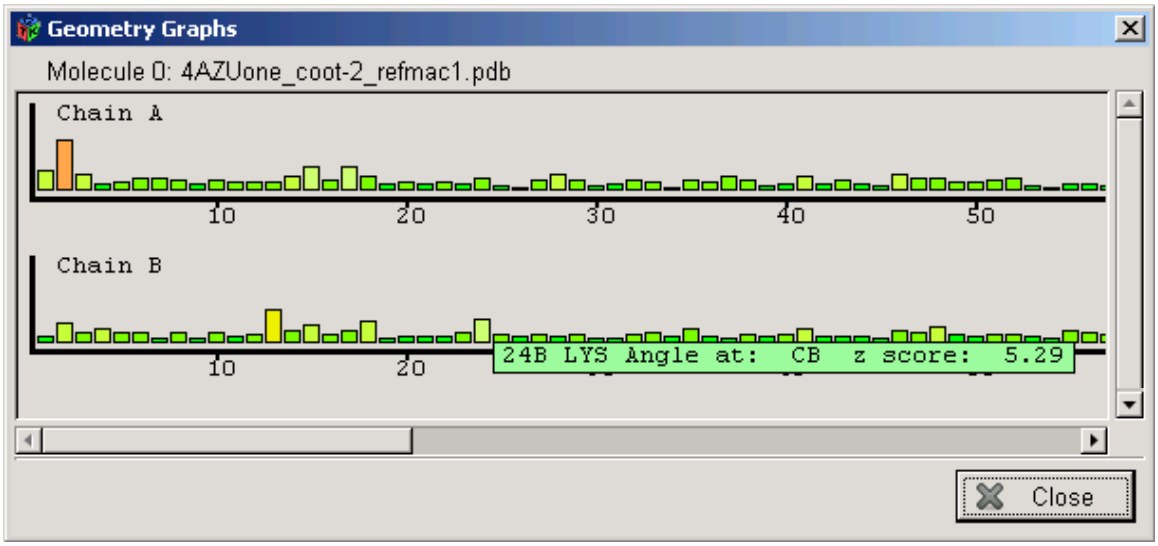

Figure 4.3. Interative bar graph from the Geometry analysis tool under Coot's validation options. Each bar represents an amino acid in the model and the color and height indicate geometry in terms of angles, bonds, and planes relative to dictionary geometries. chain A and chain B refer to two distinct Az-PHM molecules in the asymmetric unit.

There are two options for addressing geometry in Coot: *Real-Space Refine Zone* and *Regularize Zone*. *Real-Space Refine Zone*, which was previously discussed, refines coordinates while considering density and geometry whereas *Regularize Zone* refines with respect to geometry only. Normally, *Real-Space Refine Zone* was used to refine residues with high Z-scores since *Regularize Zone* frequently moved residues out of their electron density, increasing the R-values after subsequent phase recalculation.

At high resolutions, alternate or split conformations for residues can be modeled if convincing density is located. For example, in Figure 4.4a electron density shows an alternate conformation for sulfur of the methionine in the 8th residue position of chain B (8MetB) which is supported by the negative density surrounding the current position. Another method for identifying density resulting from multiple residue conformations is found in the Coot Extensions menu under Modeling: *Residues with Alt Confs*. After using this function, Coot also identified the density around 8 Met B for potential modeling. Thus, the alternate conformation for 8MetB was modeled with each side-chain occupying 50%, and the new coordinates were then refined in CCP4. Though the post-refinement solution (Figure 4.4b) shows a small amount negative density, a decrease of 0.03% and 0.05% was observed for R_{factor} and R_{free}, respectively. Considering that R_{free} is

a global indicator, it was surprising that such a small local change brought about drop of 0.05%. For this reason and because the negative density on the sulfur disappeared, the alternate coordinates for 8MetB were kept. Even though the *Residues with Alt Confs* function did not find any other density worth investigating, alternate conformations were modeled for 9 other residues, including 6AspA, 57GlnA, 61ThrA, 122LysA, 126ThrA, 4SerB, 27LysB, 34SerB, 126ThrB. Density for these conformations was identified through the use of the *Difference Map Peaks* function in Coot.

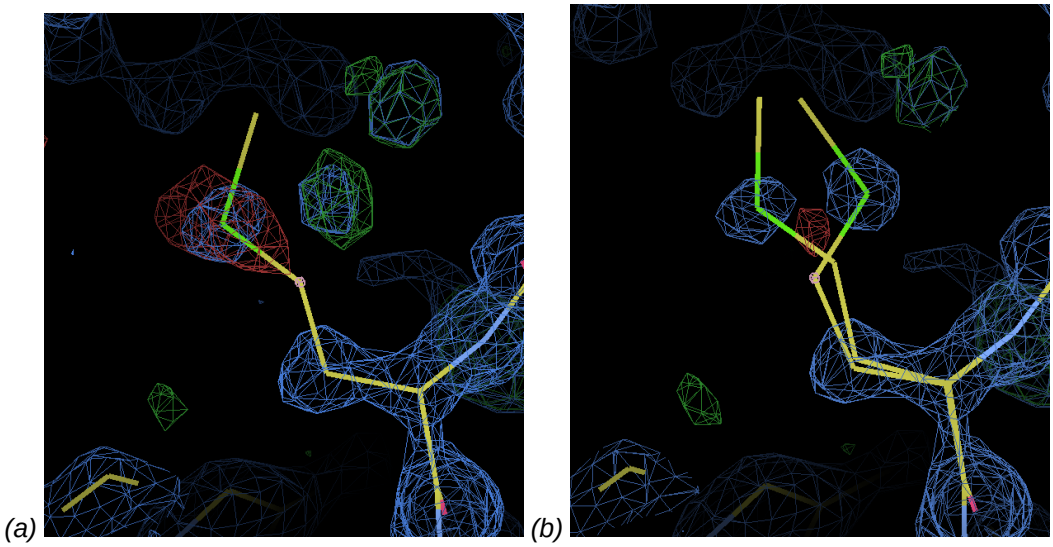

Figure 4.4. (a) Electron density around methionine 8B. This density suggests an alternate conformation should also be modelled. (b) Electron density map and model after an alternate conformation of methionine 8B was modelled.

After all individual amino acid residue adjustments were completed, the next step was to locate large volumes of empty electron density that belong to ligands and other solvent molecules. Using *Difference Map Peaks* was one way to locate these empty areas of electron density. Two other options include the *Find Ligands* function and the validation tool, *Unmodelled blobs*. Because all three functions are slightly different, all three tools were used to place any PEG, nitrate, Tris, calcium and chloride ions that might have been present in the structure. The most sophisticated option, *Find Ligands*, searches the map for a cluster of density and attempts to fit each cluster with ligand(s) specified by the user. This option was employed in the search for solvent molecules in the Az-PHM map and one Tris molecule (identifier: TRS) was located near the copper(II) ion off of 83HisA (Figure 4.5a). After Tris was found and fit to the density, it was merged to the

protein molecule, and before any refinement in CCP4, the Refmac5 parameter *Make links between: All others if* was changed to *defined in file or residues are close*. In changing this parameter, the geometry of the Tris molecule was restrained and any bonding between Tris and the copper was maintained. Following refinement in CCP4, the Tris molecule was kept because both R_{factor} and R_{free} decreased significantly for such a small change (decreased by 0.06% and 0.22%, respectively) and because the electron density map was greatly improved (Figure 4.5b).

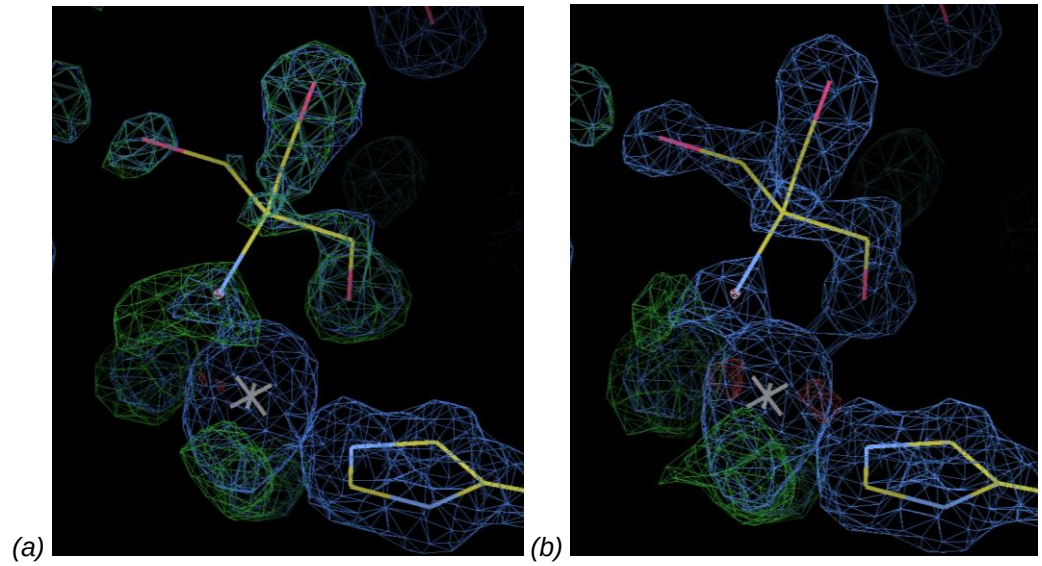

Figure 4.5. (a) Tris molecule fit to positive electron density near 83HisA in Coot. (b) Tris molecule after refinement in CCP4.

In the Az-PHM map, using the *Unmodelled blobs* tool did not reveal any un-modeled electron density, so the *Difference Map Peaks* tool was used. This tool allows the user to locate significant positive and negative peaks (blobs) of density by creating an ordered list according to peak height. Those peaks with the highest deviation from the average are listed first. Using *Difference Map Peaks*, density was located in the Az-PHM map that fit three other Tris molecules and a chloride ion. Chloride ions can be difficult to place in a model because their corresponding density is spherical which can easily be mistaken for a water molecule. The highest peak in the difference map was 21 times the standard deviation (or 21 sigmas) from the average density of the map. The second highest peak had a difference of 12 sigmas after which peak heights decreased steadily. The abnormally high peak at 21 sigmas was one indication that this density did not

belong to a water molecule. Still, both a water molecule (Figure 4.6a) and a chloride ion (Figure 4.6b) were fit in the spherical density and the new maps and resulting B-factors were consulted to determine which molecule the density belonged to. In fitting the water molecule, the new map still showed green density with a height of 7.33 sigmas, and the B-factor was 3.83. After refining the chloride ion, however, the new map showed no leftover density and chloride's B-factor was much more consistent with the rest of the model at 15.77 (recall that the average B-factor of the model is 13.655). Most importantly, though, the chloride ion was the logical choice since chemically, the density was in a pocket within the protein molecule that did not contain any other negatively charged atoms. Also, bond distances to the nearest parts of the protein molecule were between 3.05 and 3.26 Å. These distances are consistent with the chloride distances found in a halide binding protein (51) on the Protein Data Bank (PDB ID: 3SVC) which are between 3.15 and 3.34 Å. Typical hydrogen bond distances, on the other hand, are between 2.4 and 3.2 Å.

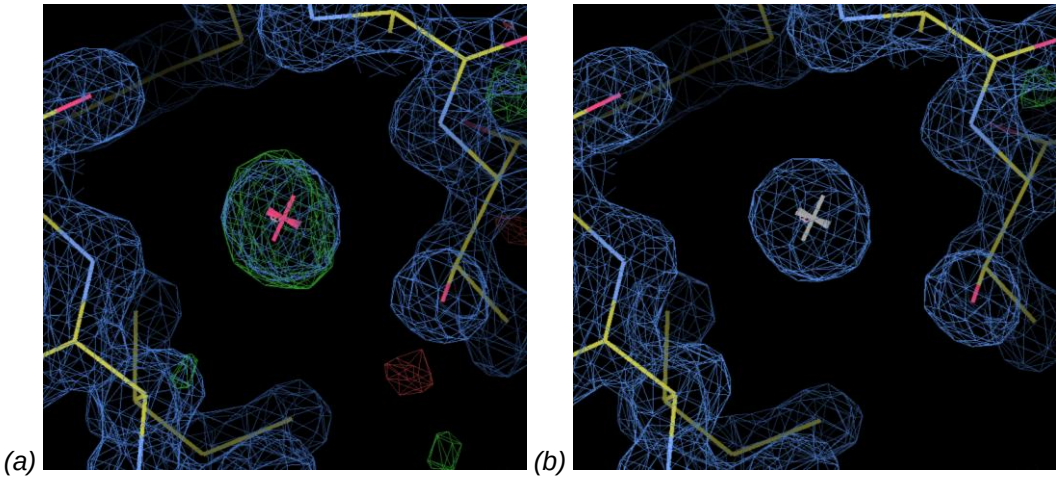

Figure 4.6. Water (a) and chloride ion (b) in a 21 sigmas difference peak. Positive electron density still exists around the water molecule after refinement in CCP4 indicating that water was not the likely reason for the observed electron density.

When all residues in the protein were adjusted and when all other ligand molecules had been added, the last task in Coot involved assigning water molecules to all other significant electron density. A common rule of thumb is that the R_{factor} should be 25% or less at this stage before adding waters. At this point the Az-PHM structure had an R_{factor} of 24.75%, and therefore, adding waters was the next step (52). There are two

ways to accomplish this task: automatically by using the *Find Waters* function in Coot or manually by assigning water molecules using the *Difference Map Peaks* tool. The *Find Waters* function has several advantages: it's a fast, systematic way to add waters and it provides some consistency across many structures in the way water molecules are added (52). However, the function is an automatic software function and could result in filled spots of electron density that do not make chemical sense. For this reason, waters were added to the Az-PHM model manually which allowed more control in the assessment of electron density blobs, where hydrogen-bonding distances could be checked and chemical knowledge could be applied. The difference map was first scanned for the highest peaks and water was assigned to those peaks that were spherical in appearance and within hydrogen bonding distance (2.4 to 3.2 Å) to polar protein atoms or other water molecules. The highest difference map peaks were determined based on their sigma values. The first shell included high peaks from 10-12 sigmas. Anywhere from 10-50 water molecules were typically assigned at a one time, after which they were merged to the structure and refined in CCP4. After refinement, the previously added water molecules were examined for fit to the new electron density map. If new electron density appeared that suggested the water was incorrectly assigned, it was removed from the structure before adding the next set of water molecules. In an ideal scenario like the one seen in Figure 4.7, a spherical blob of positive density will lie within hydrogen bonding distance of several water molecules or protein atoms.

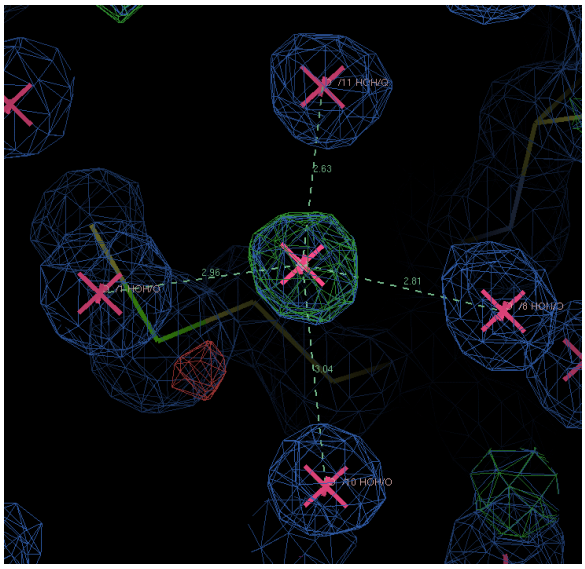

Figure 4.7. Green sphere of positive density fit with a water molecule (red cross in center). The water is ideally located within hydrogen-bonding distance of four other water molecules ~2.6-3.0 Å away.

After one "bin" of waters was added, the remaining difference map peaks were again studied. The set of electron density peaks in the next highest shell of sigmas was examined. These peaks were fitted with waters, the structure was re-refined and the waters were analyzed to confirm their chemical integrity. This process was repeated iteratively for 20 cycles until a total of 312 waters were added to the Az-PHM structure. Interestingly, after each addition of waters, the sigmas value describing the electron density for the remaining difference map peaks increased. This is a result of the way the sigma values are calculated. As more peaks are added to the model, the standard deviation (or sigma) for the total (assigned and unassigned) electron density decreases, thus the number of standard deviations (or sigmas) increases for un-modeled difference peaks even though the density of the peak remains the same.

Therefore, difficulty arose in deciding when to stop adding water molecules. When many of the significant difference peaks have been assigned, it can be difficult to determine which peaks are water molecules and which peaks are simply due to noise because the difference map starts to reveal more and more noise as their calculated sigmas begin to rise. In this case, crystallographers agree that it is best to err on the side of caution to avoid fitting noise. In determining when no more water molecules should be added, the R_{free} value was consulted since it is a global indicator of the progress of

refinement (52). As more and more bins of water molecules were added, the decrease in R_{free} became less and less substantial. When R_{free} no longer decreased, and noisy peaks became prevalent, adding water molecules ceased and one last refinement cycle was completed.

During the tedious process of adding water molecules, several unexplainable blobs of density appeared that could not be modeled by water, chloride or any of the other reagents used during crystallization. An example of one of these blobs can be seen below in Figure 4.8. Though the peanut-shaped blob did not appear to belong to PEG or nitrate, both of these molecules were used as a model (Figure 4.8a and Figure 4.8b) to fit the density. Both efforts gave decreased R-values after refinement in CCP4 but the fit was terrible, as evidenced by the negative electron density.

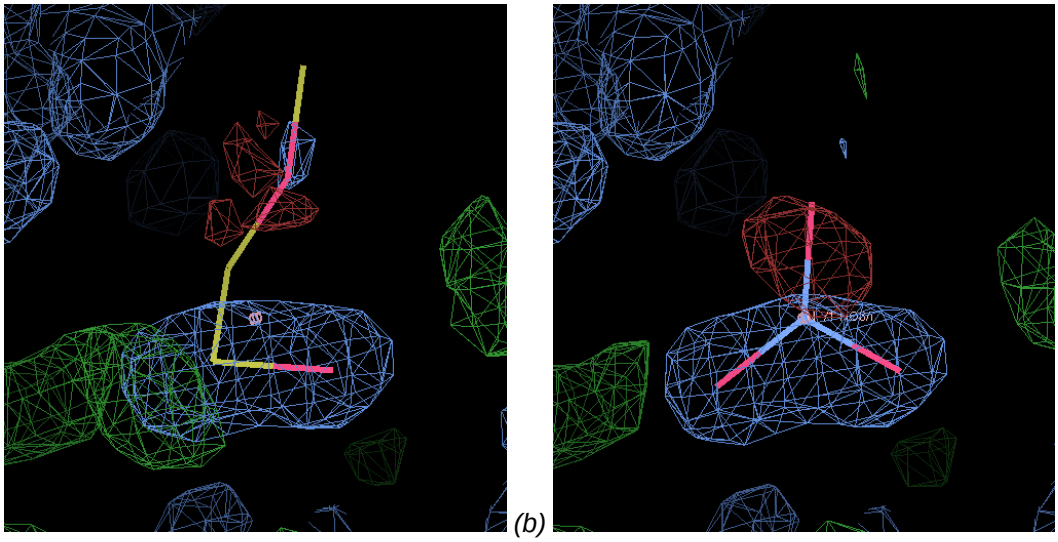

Figure 4.8. A peanut-shaped section of electron density fit with (a) a Polyethylene glycol molecule and (b) a nitrate molecule. Neither of these molecules gave a great fit.

Though modeling of this strange density and others was attempted, all efforts gave poor fits to the experimental density and even though R-values decreased in most cases, these areas could not be modeled in good conscience. This mentality ensured a conservative, yet reliable Az-PHM model where electron density was not "overfit" in an effort to push the R_{factor} down as low as possible (53). The final R_{factor} reached a value of 17.57% and R_{free} had a value of 20.70% in the final Az-PHM model. R_{factor} is expected to be lower than R_{free} because the reflections used in the calculation are not used for

refinement. However, because the diffraction data is high quality, an accurate model would yield structure factors that highly correlate with those that are not used in refinement (i.e. those that are used to calculate R_{free}), yielding similar values for R_{factor} and R_{free}. Kleywegt and Jones claim to obtain small differences in R-values of ~2% with good data sets and a difference as high as ~5-8% with poorer quality data sets and data sets with low resolution (53). The difference between R-values for the final Az-PHM model is ~3%, which suggests that the refined crystal structure adequately models the data without overfitting it.

Chapter 4.3 Validation of Final Model

X-ray crystallography is an exciting field that allows scientists to elucidate the structure of proteins and enzymes in order to better understand how structure influences function. Because inferences regarding function are made from analyzing a crystal structure, it is vital that structures are scrutinized and examined for potential errors before being made available to others. Thus, validation of the final Az-PHM model was essential to be certain that the model contained no major errors that could potentially impede the progress of other scientists who use this structure (47).

A number of structural details were examined using Coot's validation tools to ensure that a proper Az-PHM model was constructed that accurately fits the experimental electron data. In Chapter 4.2, recall that electron density and geometry were taken into account when making adjustments to the residues of the model. These tools used during refinement are validation tools that point out any outliers in the data. A representative portion of the *Density fit analysis* graph for the final model is shown in Figure 4.9. Because most of the residues show a short, green bar in the graph, the model is an excellent overall fit to the electron density map.

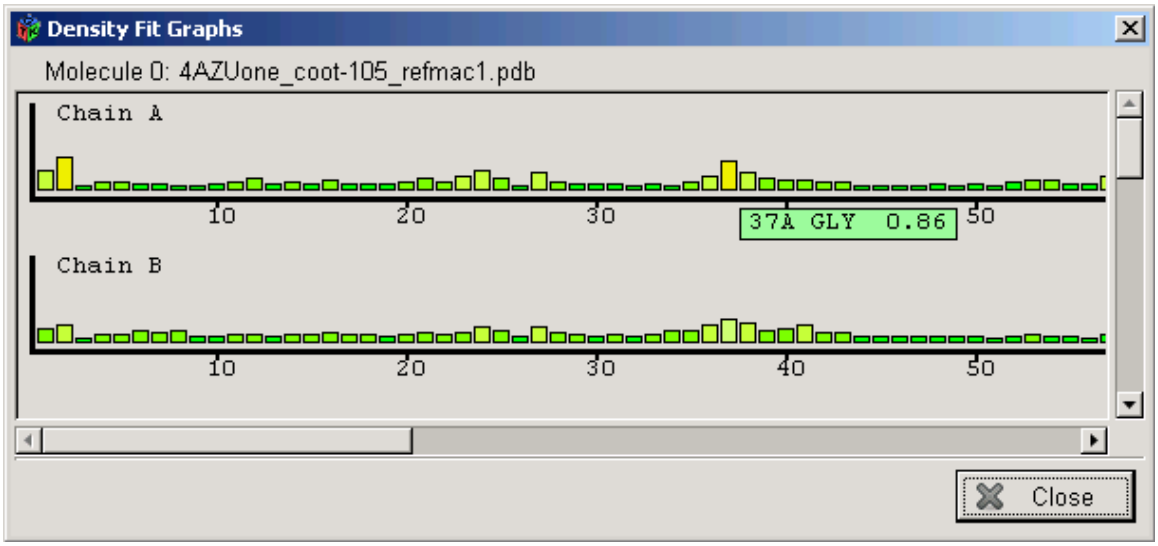

Figure 4.9. Density fit validation graph from Coot for the final model of Az-PHM. Each bar represents an amino acid in the model and the color and height indicate its fit to the electron density map. Green bars indicate excellent fit.

However, when the geometry of the model is considered (a representative portion of the graph is shown in Figure 4.10), it doesn't appear to be a very good structure. Many of the bars are yellow, orange and red, indicating moderate to poor geometry with respect to angles, bonds or planes. All of the amino acids represented by these colored bars were checked against the electron density map and 57 out of 61 residues showed excellent fit. Out of the 4 residues that did not appear to have a good fit, 2 of them gave an increase in R_{free} after modification and CCP4 refinement, and the other 2 did not show any electron density surrounding their side chains but also did not have any negative density either to suggest that their position was incorrect.

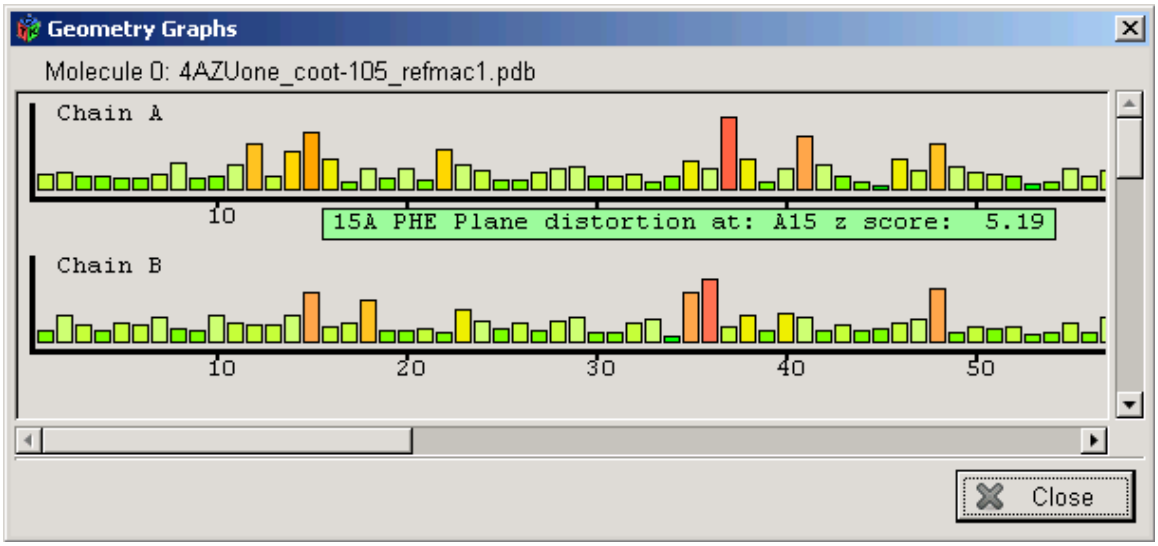

Figure 4.10. Geometry analysis validation graph from Coot for the final model of Az-PHM. Each bar represents an amino acid in the model and the color and height indicate its geometry relative to an average Z-score. Green bars indicate excellent geometry.

Though the geometry analysis appears to give moderate results, the fit of the model to the electron density is excellent. While there seem to be errors in geometry based on theoretically ideal geometries, the experimental data are at a high atomic resolution of 1.30 Å, and therefore, show exactly where atoms should be placed (with only a few exceptions due to unavailable density). To create the best model, recall that coordinates were adjusted and refined iteratively to minimize the values of R_{factor} and R_{free}. Refinement proceeded in this way because R_{free} is a powerful, unbiased statistic that provides a true validation check by evaluating the model on its ability to predict reflections from data that were not used in the creation of the model (47). Therefore, because the experimental density is clear and R-values were minimized, the residues have excellent fit and the resulting, objectionable geometries of some amino acid side-chains must be the result of inherent structural features instead of errors in the model (54). Consequently, the interactions that cause the protein to fold and crystallize in this way must outweigh any strain that results in maintaining the unusual conformations of some side-chains.

Coordinate-based validation methods, like *Geometry analysis* in Coot, are not as ideal as other methods that consider experimental data but nonetheless, can provide assurance that the model agrees with generally-known structural aspects of protein

molecules. Tools in this category are especially valuable if the criterion being used for validation was not restrained during refinement (47, 55). Because Refmac does not refine torsion angles, the model was analyzed using this criterion. The *Ramachandran Plot* function in Coot graphs each amino acid using its torsion angles, phi and psi. Because many of the combinations of phi and psi angles produce steric clashing (56), residues should theoretically only be located on a small portion of the plot. For Az-PHM, the residues in the diagram all fall in preferred or allowed regions (Figure 4.11). The Ramachandran diagram in Coot is interactive in that the "type" of residue selected determines the area of preferred (pink) and allowed (yellow) regions. For example, 44MetA, represented by a blue square with black outline is not a glycine (glycines are indicated by blue triangles) or a proline (prolines are indicated by a blue square with green outline) amino acid and therefore shows the preferred and allowed regions illustrated in Figure 4.11. Of this type of residues, only five (2.07%) fall in "allowed" regions while the rest have "preferred" phi and psi combinations. All proline and glycine residues also fall in "preferred" regions. No amino acids are "outliers". The five amino acids that do fall in allowed regions include 10AsnA, 10AsnB, 44MetA, 44MetB, and 38AsnB. In viewing these residues in Coot, the electron density map is sharp and confirms their present positions. Emsley *et al*. describe a high quality Ramachandran plot as one having less than 1% outliers and where most residues fall in preferred regions (48). Thus, the Ramachandran plot for Az-PHM indicates that the coordinates result in a high-quality structure.

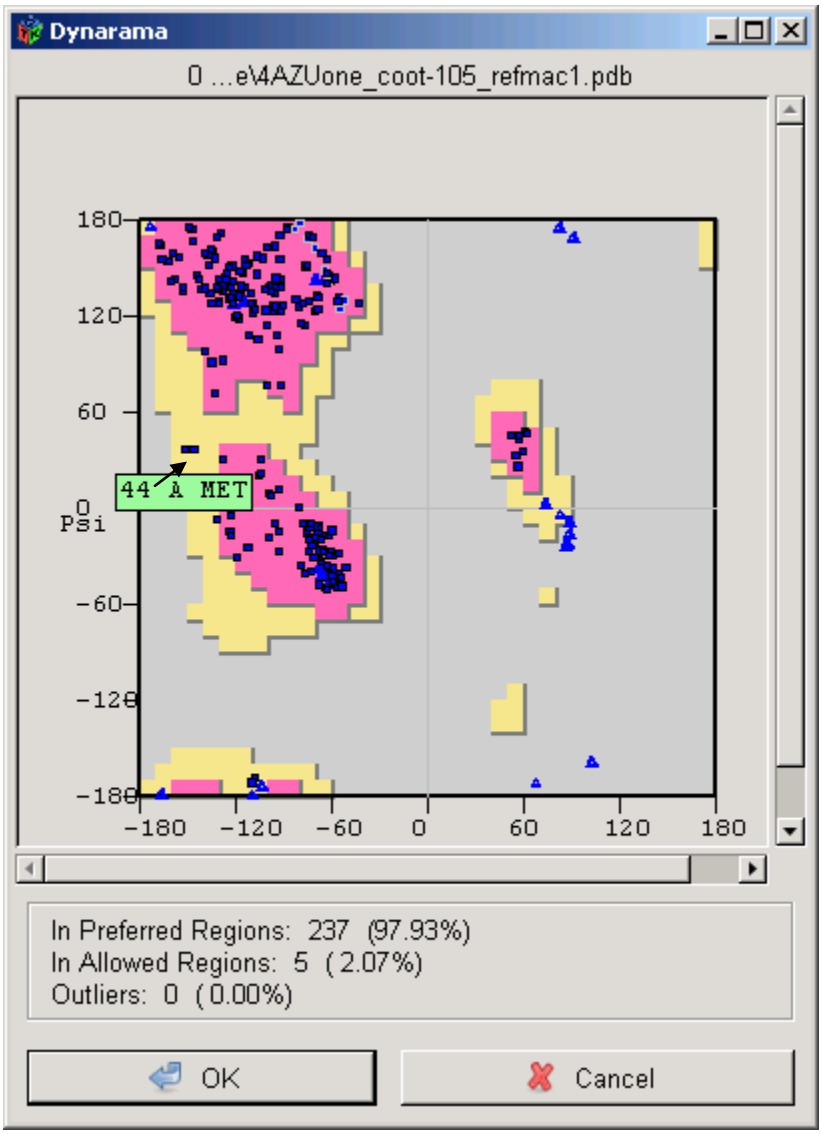

Figure 4.11. Ramachandran Diagram for all residues with preferred and allowed regions indicated for those that are not glycine or proline. The regions in pink are preferred and those in yellow are allowed regions.

The third coordinate-based validation tool used, *Peptide omega analysis*, also examines torsion angles. This function examines the third torsion angle, omega, by creating a bar graph where each bar represents an amino acid. The height and color of a bar is determined by the omega angle's deviation from ~180°. Because omega measures the angle of the peptide linkage, it is expected to be slightly less than 180° due to its partial double-bond character. Kleywegt suggests that residues that have omega angles outside the range of 180° ± 20 should be treated with caution in structures with low resolution (55). A representative portion of the omega graphs for the Az-PHM model is

shown in Figure 4.12. All residues in the model have omega angles in the accepted range with exception of 14HisA and 37GlyA. It seems that both of these residues are in the middle of sharp turns in the backbone, which explains why they are outside of the typical range. Plus, at high resolution, the density clearly indicates that these residues have been modeled clearly, which means that the abnormal omega angles are structural features of the model.

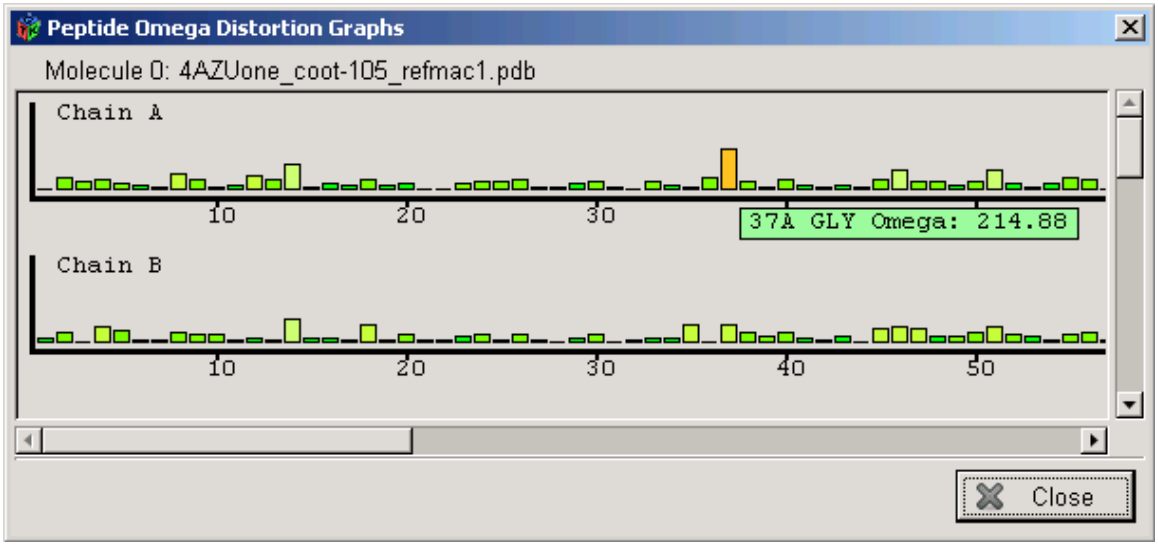

Figure 4.12. Peptide omega analysis graph for the final model of Az-PHM. Short green bars indicate residues that have acceptable omega angles. chain A and chain B refer to two distinct Az-PHM molecules in the asymmetric unit

The fourth coordinate-based method involves analysis of the amino acid side chain geometry through the use of conformation likelihoods. Residues in the Az-PHM model were compared with the Molprobity rotamer probability distribution (50) developed by Lovell and colleagues (48). The *Rotamer analysis* tool in Coot displays a bar graph containing probabilities for every amino acid in the model. The probability values express the likelihood of each amino acid's conformation, as seen in Figure 4.13 for 18AsnB. What is interesting about this particular residue is that it perfectly fits the electron density which is demonstrated in Figure 4.14. So, even though the probability of the rotamer conformation for 18B is only 0.02%, the side-chain exists in this conformation when the protein is in crystalline form. Other residues that give similar probabilities include 70LysB, 122LysA and 122LysB and two of these amino acids show defined density around the atoms of the residues. The lysine residue in chain A does not

show convincing density for its atomic coordinates, however, it does not show negative density either.

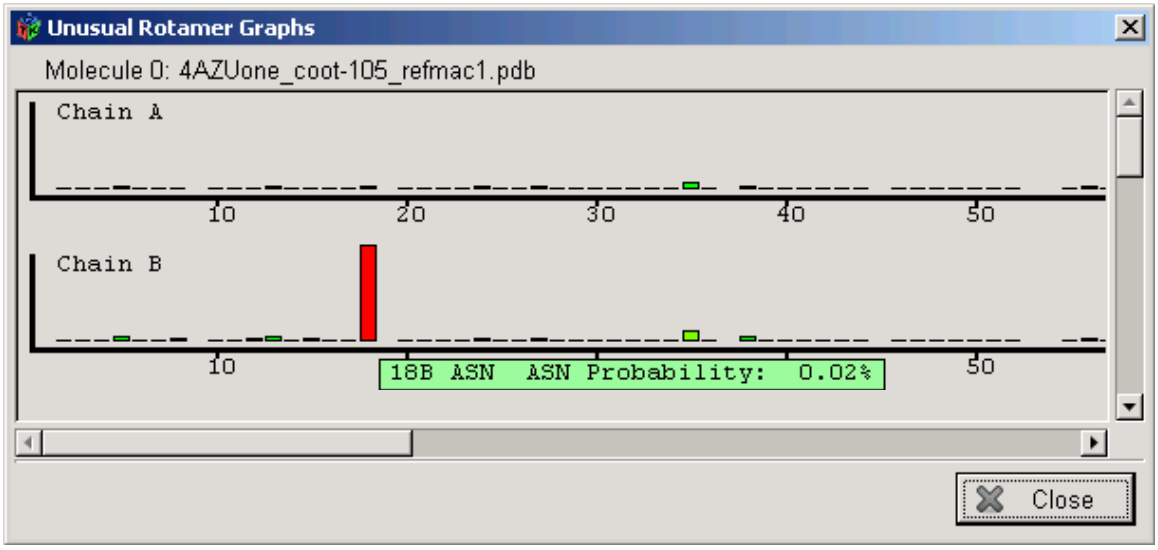

Figure 4.13. Rotamer analysis graphs created in Coot for the final Az-PHM model. Bars are inversely proprotional to probability.

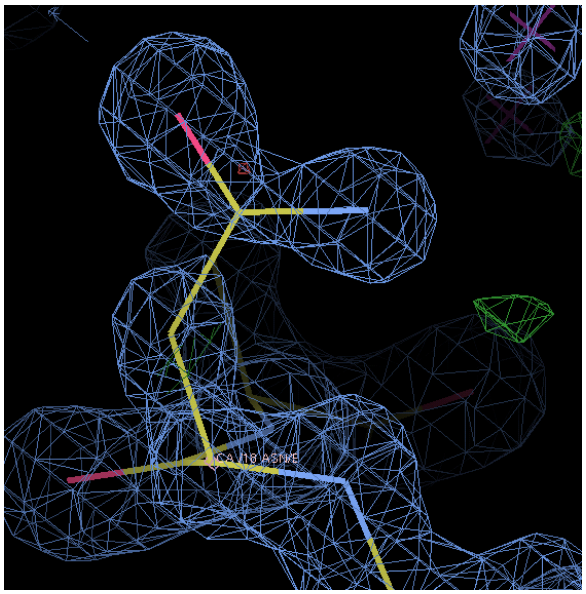

Figure 4.14. Final electron density and structure for the asparagine residue at 18 in chain B in the Az-PHM model. Though the rotamer probability suggested this conformation was 0.02% likely, the electron density shows strong evidence that suggests 18AsnB crystallized this way.

The fifth coordinate-based validation method compares the geometry of each residue in chain A against the same residue of chain B in Coot's *NCS Differences*

function. Because NCS restraints were not used during refinement in CCP4, this function identifies areas with potential error that are worth investigating. The differences in atomic positions between residues are displayed in a bar graph containing r.m.s. deviations (48) after one chain has been translated and superimposed onto another (55). For Az-PHM, a portion of the *NCS Difference* results is shown in Figure 4.15. All residues showing yellow, orange or red bars (r.m.s ~1 or greater) were checked and out of the 12 pairs showing significant differences in atomic position (1, 69, 104, 105, 106, 126 and 127), all but 5 pairs showed electron density to indicate that they were appropriately modeled and that the differences were not errors. For the 5 pairs of residues where differences could not be confirmed by electron density (13, 85, 103, 107 and 128), only 2 showed negative density for the side-chain positions (107 and 128). However, 107GlnA was moved several times to try to the experimental density better and each time, the R_{free} value increased, suggesting that this difference may be a structural feature instead of an error. The other 3 pairs (2 lysine pairs and 1 methionine pair) where atomic positions could not be confirmed did not have clear density to verify their position. In the lysine pairs, electron density was unavailable and for 13MetB, green density in the difference map suggested an alternate conformation should be modeled but could not be because a water molecule with a higher difference peak was too close. Interestingly, most of the pairs showing large differences came from two exterior areas containing turns in the backbone.

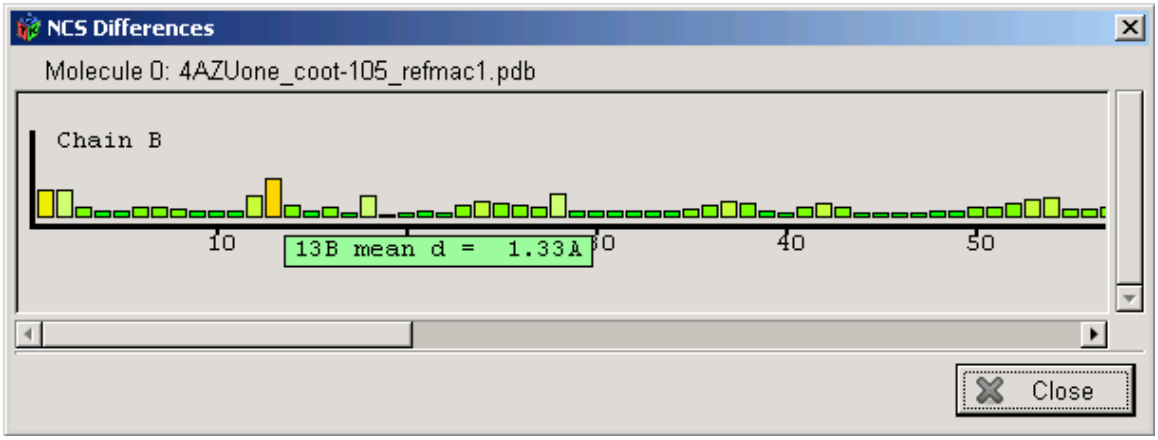

Figure 4.15. Portion of the NCS Differences graph for the final Az-PHM model. Bar height is proportional to the r.m.s. deviations between residue pairs in chains A and B.

The sixth and final tool used in validation of the Az-PHM coordinates described atomic positions in terms of temperature factors. The results of this *Temperature factor variance analysis* function in Coot, a portion of which is visible in Figure 4.16, show high average B-factors for residues in the Az-PHM model that are lengthy and solvent-exposed. Approximately ~70% of these residues are lysine and glutamate amino acids.

Figure 4.16. Results of the Temperature factor variance analysis performed on the final Az-PHM model in Coot.

Lastly, two simple tests for chirality and atom location were conducted in Coot. The test for chirality searched for *Incorrect Chiral Volumes* that would indicate the presence of erroneous D-amino acids and the test for *glutamine/asparagine outliers* attempted to detect incorrectly placed oxygen and nitrogen atoms in glutamine and asparagine side-chains using B-factor analysis. Coot found no incorrect chiral volumes and no glutamine/asparagine outliers. Interestingly, oxygen and nitrogen atoms on a couple of residues were exchanged and the test was conducted again, but did not yield different results, which indicates that this test is not sensitive even with atomic resolution data since the switch went undetected.

Results of all of the validation tools in Coot were examined to assess the quality of the final Az-PHM model and prepare it for submission to the Protein Data Bank (48). After all of the validation tests were completed, the final structure was found to be a good model of the experimental data since it scored well on every test (53). Even though a few

outliers were found when each validation was used, the atomic resolution and quality of the data collected suggest that most if not all of the flagged coordinates were structural features instead of errors. Users of this structure can have confidence that the model is a highly supported illustration of the crystallized Az-PHM protein.

CHAPTER 5

Chapter 5.1 Analysis of Final Az-PHM Crystal Structure

After successfully obtaining an accurate crystal structure, the Az-PHM model was analyzed. The overall structure, shown in Figure 5.1, is a dimer wherein the two Az-PHM molecules are pointed toward each other. A solvent filled channel spans the space between the two molecules. Two of the structure's six copper(II) ions are also located between the two structures. Histidine 83A and 83B each bind a copper in the solvent gap along with Tris molecules. The other four coppers are located in the Type 1 and Type 2 copper active sites.

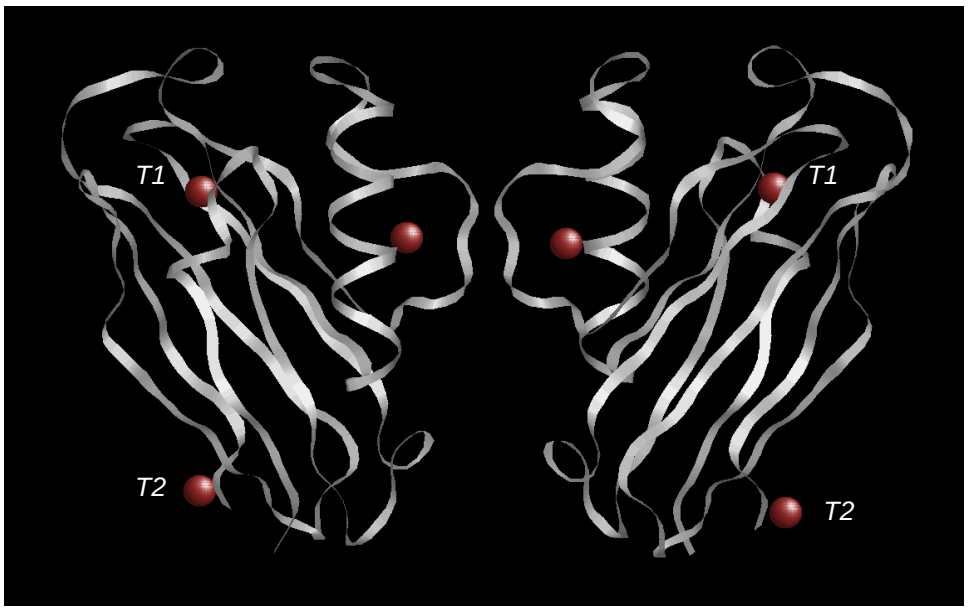

Figure 5.1. Dimerized Az-PHM molecules in the final crystal structure. Copper(II) atoms are shown as marroon spheres. Copper sites are denoted for each monomer.

Upon initial investigation of the final model, it appears that the presence of a third set of copper(II) ions and the dimerized nature of the structure alter perceptions of the Az-PHM variant. It was created as a monomer to bind coppers at the T1 and T2 sites. The two copper ions bound to histidine residues 83A and 83B are located in the center of the final model in Figure 5.1 and are somewhat unique when examining other wild-type azurin structures. The copper ions are separated by a distance of 11.9 Å and are largely solvent-exposed. The other aspect of the final crystal structure that was not anticipated is

dimerization. If it exists in solution, dimerization may affect future physiological studies. In this structure, Az-PHM monomers dimerize due to interactions at the T2 site where one monomer binds the T2 copper ion at His14 and His16, as designed, and the neighboring monomer also interacts with the T2 copper center through Ala1. Several structures of wild-type azurin show copper(II) bound to Ala1 so at high concentrations, it seems probable for Az-PHM dimerization at this residue to occur. However, if dimerization did occur even to a small extent in solution, it follows that EPR studies would show three distinct copper ions, one at the T1 site, one at the T2 site (bound by His14 and 16) and one dimerized copper (bound by His14, His16 and Ala1). Berry *et al*. show that at concentrations of 1 mM, Az-PHM samples only show two types of copper ions at the T1 and T2 sites. Even when excess copper was added to the samples, it did not bind to the protein. A third signal consistent with free copper in solution was observed (15). This EPR data also suggests that the copper(II) ions bound to His83A and 83B do not exist in solution. If they did, the third signal would be consistent with a bound copper instead of free copper(II). Therefore, the third copper ion bound to His83 and the dimerization appear to be artifacts of crystallography rather than structural features.

In creating the biosynthetic Az-PHM model to mimic PHM, it is important that its crystal structure be examined for its structural similarity to the native enzyme's active sites. Recall that PHM has two copper binding sites, one of which is bound by three histidine residues and functions in electron transfer while the other is bound by two histidines and a methionine and functions in catalysis. Since mechanistic studies suggest that an electron is passed from the T1 copper ion to the T2 copper site where catalysis occurs (9), these two copper sites must be analyzed in the Az-PHM model.

The T1 copper site in the Az-PHM model is native to azurin and therefore, should have bonding distances similar to those found in the native protein. In the final Az-PHM structure, the T1 copper shown in Figure 5.2 coordinates two histidine residues and one cysteine residue in a trigonal planar fashion. Bond distances from copper to His46, His117 and Cys112 are ~2.00-2.03 Å, 2.02-2.04 Å and 2.18-2.19 Å, respectively (range limits given for all Az-PHM distances express actual distances from both monomers). In

the wild-type azurin crystal structure, the distance from copper to His46 is 1.99-2.13 Å, from copper to His117 is 1.96-2.11 Å and from copper to Cys112 is 2.17-2.27 Å (ranges given for wild-type azurin cover actual measured distances from all four monomers in the 4AZU crystal structure). The axial ligands that coordinate the T1 center in Az-PHM, Met121 and Gly45, have copper bond distances of 3.27-3.34 Å and 2.61-2.68 Å, respectively in Az-PHM, and similarly, the native distances are 3.05-3.21 Å and 2.84-3.03 Å, respectively.

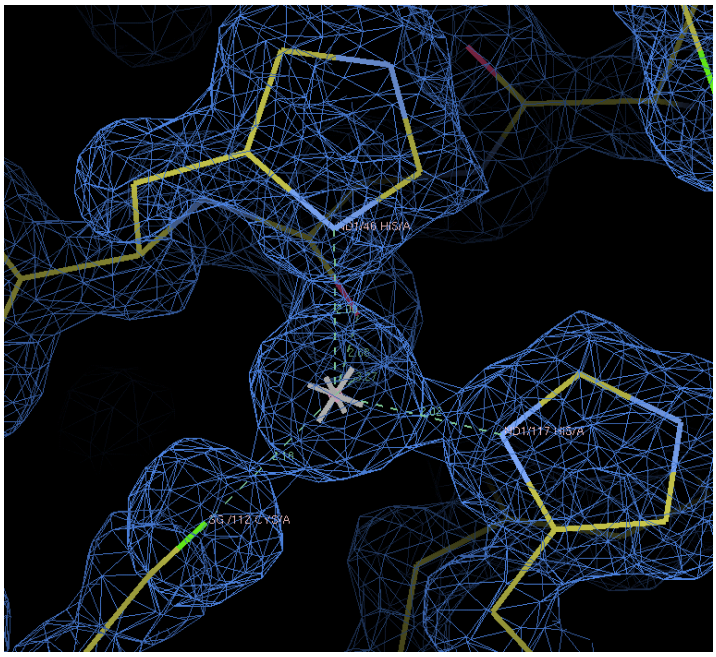

Figure 5.2. Type 1 copper active site in the final Az-PHM crystal structure. The ligands shown include His46, His117 and Cys112 which all coordinate the copper(II) ion in a trigonal planar fashion.

The Az-PHM model was crystallized in order to compare its designed T2 copper site to the native system's catalytic site. Because the azurin scaffold already contained a T1 copper site, only three residues were mutated to incorporate a second copper binding site into the protein. Residues 14 and 16 were mutated to histidines and residue 8 was mutated to a methionine. When viewing the T2 site shown in Figure 5.3, the Az-PHM structure reveals coordination of the copper(II) ion by His14, His16 and Ala1. Unfortunately, the geometry around the T2 copper was compromised due to the way the protein crystallized such that the third ligand, Ala1, is from an Az-PHM molecule in the neighboring asymmetric unit. In the Az-PHM crystal structure, the geometry of the site is

square pyramidal. The His14, His16, Ala1(O), and Ala1(N) distances are 1.97-1.98, 2.07-2.10, 2.04-2.10, and 2.05-2.20 Å, respectively. (Range limits signify actual distances measured for both T2 sites in the asymmetric unit.) All of these atoms lie in a plane with copper while a water molecule binds perpendicular to the plane to create a pyramid. Copper lies a mere ~0.1 Å out of a least-squares plane created by all four residue ligands. The water molecule is positioned above the plane with a distance to the copper(II) ion of 2.42-2.48 Å.

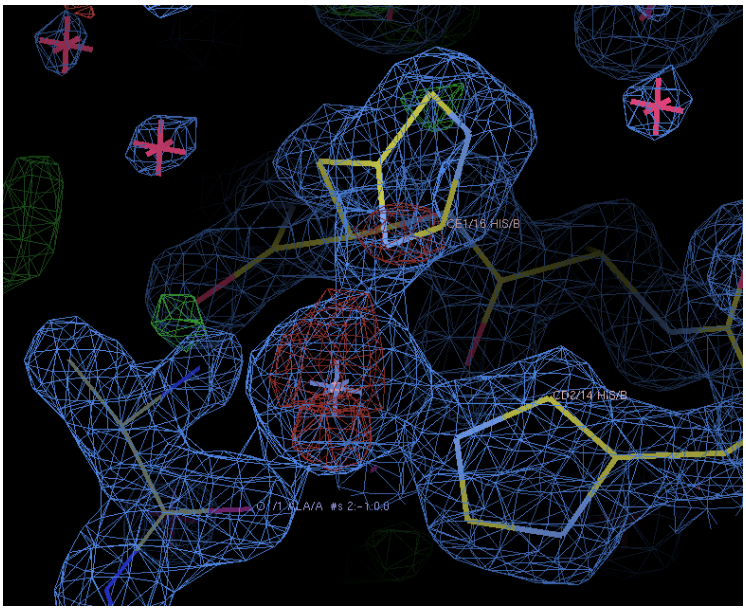

Figure 5.3. Type 2 copper active site in the final Az-PHM crystal structure. The copper(II) ion is bound by His14, His16 and an Ala1 residue from a neighboring Az-PHM molecule.

Because Met8, His14 and His16 were mutated in azurin to create the T2 copper site in Az-PHM, it is necessary to examine the final crystal structure against native azurin in order to determine the effects of the mutations on protein folding. Figure 5.4 shows the overlay of wild-type azurin (PDB ID: 4AZU) in blue and one monomer of the final Az-PHM structure in red. No gross differences exist between the backbones of the structures, which suggests that the three mutations that were made do not affect the ability of the protein to fold properly. Each monomer contains beta-sheet secondary structure with a Greek key motif as well as a looped section containing alpha helices. This also supports the conclusions that many researchers have made concerning the

stability of azurin in the presence of many mutations (13, 14). The only significant difference between the two structures appears at Ala1, where this residue binds the copper ion that bridges two azurin molecules.

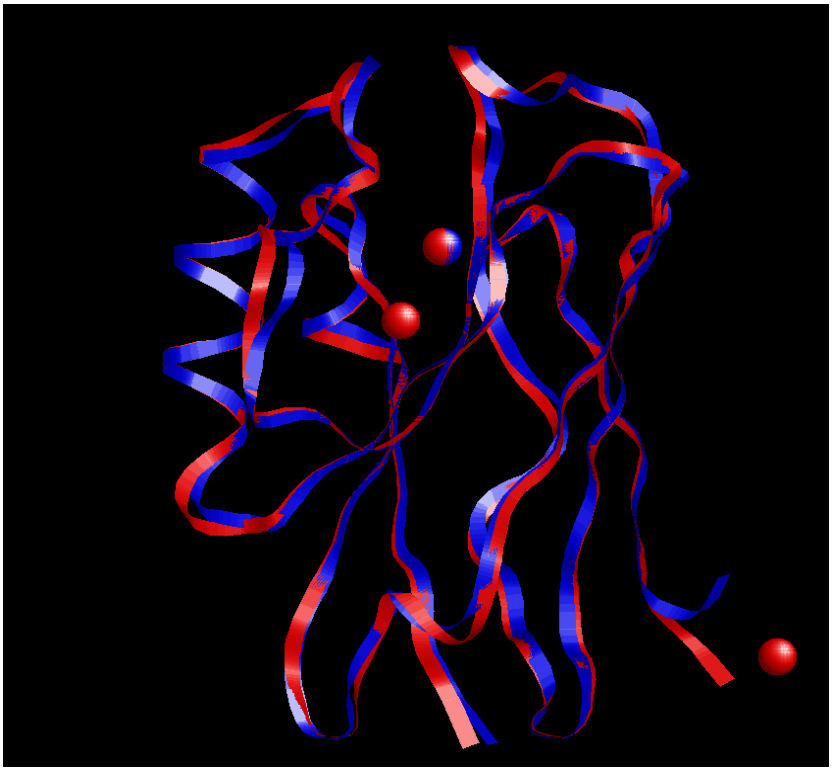

Figure 5.4. Overlay of one monomer of the 4AZU wild-type azurin crystal structure and the final structure of the Az-PHM model. Azurin is in blue and Az-PHM is colored red.

Analysis of the copper binding sites and the overall shape of Az-PHM indicate that the mutations to azurin were successful and the T1 copper center was not disturbed. The T1 and T2 coppers in the model are ~14 Å apart which is just slightly larger than the distance of 11.3 Å found in the native PHM crystal structure (7). The coordination mode of the T2 site appears to be an artifact of protein packing such that crystallizing Az-PHM in a different way may lead to a T2 site that is not dimerized with another azurin molecule and therefore, give a better idea of the structure of the protein in solution. With the knowledge gleaned from structural analysis thus far, Az-PHM seems to model the native PHM protein well.

Chapter 5.2 Conclusions and Future directions

To study the mammalian enzyme PHM, a biosynthetic model was created using azurin. The resulting Az-PHM model was successfully purified from *E. coli* cells though lysis with osmotic shock and precipitation, followed by three chromatography columns. The purity of the sample was evaluated using spectroscopic methods and confirmed using SDS-PAGE. Crystals of Az-PHM were successfully grown and crystal properties were tuned using different reagents at various concentrations to achieve the best possible intensity, resolution and mosaicity. One of the diffraction-quality crystals was irradiated with copper K_α x-rays to collect a full set of high-resolution images. CrystalClear software from Rigaku was used to assess the symmetry of the crystal and harvest intensity data from the diffraction images. Using the CCP4 software and a process called molecular replacement, the phase-problem was solved and preliminary phases were assigned to the intensity data. After rounds of refinement using Coot, a final crystal structure was produced at 1.3 Å resolution with an R_{factor} of 17.57% and an R_{free} value of 20.78%.

The model's overall structure and its copper active sites were compared to wild-type azurin and native PHM. Structurally, the model seems to mimic PHM for several reasons. First, the Type 1 copper site geometry in Az-PHM was untouched and should therefore function in electron transfer in the same way that PHM's Cu_H site does. Second, the designed site incorporated into azurin binds a copper(II) ion, though the binding in this crystal structure is not ideal since dimerization with another protein molecule occurs. Third, the 14 Å distance between the copper sites in the model is comparable to the native Cu-Cu distance of 11.3 Å in PHM, and finally, the mutations made to create the model did not cause the protein to misfold.

Even though the Type 2 copper site bridged to another molecule in the crystal lattice, the crystal structure has high resolution and will be deposited into the Protein Data Bank. Copper-ligand bond distances for the Type 1 copper site were very consistent between monomers (much more so than those in 4AZU) and thus, may be more accurate. The Type 2 site, though it does not hold all of the information hoped for, does bind a copper and seems distorted merely due to the way the protein molecules dimerized and

packed together during crystallization. Thus, attempts to obtain a diffraction-quality Az-PHM crystal under different conditions will be pursued in the future in order to elucidate the geometry of the designed Type 2 copper site as it exists in solution

REFERENCES

1. Bertini, Gray, Stiefel, Valentine. *Biological Inorganic Chemistry, Structure & Reactivity*. 2007. University Science Books, Sausalito, CA.
2. Underwood, E.J. *Trace elements in human health and animal nutrition*. 1977. New York, NY: Academic Press.
3. Adman, E.T. (1991). Copper Protein Structures. In *Advances in Protein Chemistry* (Vol. 42) (pp. 145-192). San Diego, CA: Academic Press.
4. Holm, R.H, Kennepohl, P. & Solomon, E.I. Structural and functional aspects of metal sites in biology. *Chemical Reviews*, **96**, 2239-2314 (1996).
5. Solomon, E.I., Baldwin, M.J. & Lowery, M.D. Electronic structures of active sites in copper proteins: Contributions to reactivity. *Chemical Reviews*, **92**, 521-542 (1992).
6. Lu, Y., Berry, S.M. & Pfister, T.D. Engineering novel metalloproteins: Design of metal-binding sites into native protein scaffolds. *Chemical Reviews*, **101**, 3047-3080 (2001).
7. Prigge, S.T., Kolhekar, A.S., Eipper, B.A., Mains, R.E. & Amzel, L.M. Amidation of bioactive peptides: the structure of peptidylglycine alpha-hydroxylating monooxygenase. *Science*, **278**, 1300-1305 (1997).
8. Murthy, A.S., Mains, R.E. & Eipper, B.A. Purification and characterization of peptidylglycine alpha-amidating monooxygenase from bovine neurointermediate pituitary. *Journal of Bioinorganic Chemistry*, **261**, 1815-1822 (1986).
9. Klinman, J.P. The Copper-enzyme family of dopamine β-monooxygenase: Resolving the chemical pathway for substrate hydroxylation. *Journal of Biological Chemistry*, **281**, 3013-3016 (2006).
10. Adman, E.T., Stenkamp, R.E., Sieker, L.C. & Jensen, L.H. A crystallographic model for azurin at 3 Å resolution. *Journal of Molecular Biology*, **123**, 35-47 (1978).
11. van de Kamp, M., Silvestrini, M.C., Brunori, M., Van Beeumen, J. Jali, F.C. & Canters, G.W. Involvement of the hydrophobic patch of azurin in the electron-transfer reactions with cytochrome c_{551} and nitrite reductase. *European Journal of Biochemistry*, **194**, 109-118 (1990).
12. Murphy, L.M. Dodd, F.E., Yousafzai, F.K., Eady, R.R. & Hasnain, S.S. Electron donation between copper containing nitrite reductases and cupredoxins: The nature of protein-protein interaction in complex formation. *Journal of Molecular Biology*, **315**, 859-871 (2002).
13. Cioni, P., de Wall, E., Canters, G.W. & Strambini, G.B. Effects of cavity-forming mutations on the internal dynamics of azurin. *Biophysical Journal*, **86**, 1149-1159 (2004).
14. Okvist M., Bonander, N., Sandberg, A., Karlsson, B.G., Krengel, U., Xue, Y. & Sjölin, L. Crystal structure of the double azurin mutant Cys3Ser/Ser100Pro from Pseudomonas aeruginosa at 1.8 Å resolution: its folding-unfolding energy and unfolding kinetics. *Biochimida et Biophysica Acta*, **1596**, 336-345 (2002).
15. Berry, S.M., Mayers, J.R. & Zehm, N.A. Models of noncoupled dinuclear copper centers in azurin. *Journal of Biological Inorganic Chemistry*, **14**, 143-149 (2009).
16. Nar, H.; Messerschmidt, A., Huber, R.; van de Kamp, M.; Canters, G.W. Crystal structure analysis of oxidized Pseudomonas aeruginosa at pH 5.5 and pH 9.0. A pH-

induced conformational transition involves a peptide bond flip. *Journal of Molecular Biology*, **221**, 765-772 (1991).
17. Allewell, N.M., & Trikha, J. (1995). Chapter 8: Diffraction Methods. In J.A. Glasel & M.P. Deutscher (Eds.), *Introduction to Biophysical Methods for Protein and Nucleic Acid Research* (pp. 381-390). San Diego, CA: Academic Press.
18. Drenth, J., & Mesters, J. (2007). Chapter 1: Crystallizing a Protein. In Principles of Protein X-ray Crystallography (pp. 1-20). New York, NY: Springer.
19. Hampton Research; Aliso Viejo, CA. Technical Notes in Crystallization Catalog, **17 (**2009).
20. Nar, H., Messerschmidt, A., Huber, R., van de Kamp, M. & Canters, G.W. Crystal structure of *Pseudomonas aeruginosa* apo-azurin at 1.85 Å resolution. *FEBS Letters*, **306**, 119-124 (1992).
21. Hammann, C., van Pouderoyen, G., Nar, H., Rüth, F.X.G., Messerschmidt, A., Humber, R., den Blaauwen, T. & Canters, G.W. Crystal structures of modified apo-His117Gly and apo-His46Gly mutants of *Pseudomonas aeruginosa* azurin. *Journal of Molecular Biology*, **266**, 357-366 (1997).
22. Faham, S., Mizoguchi, T.J., Adman, E.T., Gray, H.B., Richards, J.H. & Rees, D.C. Role of the active-site cysteine of *Pseudomonas aeruginosa* azurin. Crystal structure analysis of the CuII(Cys112Asp) protein. *Journal of Biological Inorganic Chemistry*, **2**, 464-469 (1997).
23. Faham, S., Day, M.W., Connick, W.B., Crane, B.R., Di Bilio, A.J., Schaefer, W.P., Rees, D.C. & Gray, H.B. Structures of ruthenium-modified *Pseudomonas aeruginosa* azurin and $[Ru(2,20\text{-bipyridine})_2(imidazole)_2]SO_4 \cdot 10H_2O$. *Acta Crystallograpica*, D**55**, 379-385 (1999).
24. Crane, B.R., Di Bilio, A.J., Winkler, J.R. & Gray, H. B. Electron tunneling in single crystals of *Pseudomonas aeruginosa* azurins. *Journal of the American Chemical Society*, **123**, 11623-11631 (2001).
25. Di Bilio, A.J., Crane, B.R., Wehbi, W.A., Kiser, C.N., Abu-Omar, M.M., Carlos, R.M., Richards, J.H., Winkler, J.R. & Gray, H.B. Properties of photogenerated tryptophan and tyrosyl tadicals in structurally characterized proteins containing rhenium(I) tricarbonyl diimines. *Journal of the American Chemical Society*, **123**, 3181-3182 (2001).
26. Miller, J.E., Gradinaru, C., Crane, B.R., Di Bilio, A.J., Wehbi, W.A., Un, S., Winkler, J.R. & Gray, H.B. Spectroscopy and reactivity of a photogenerated tryptophan radical in a structurally defined protein environment. *Journal of the American Chemical Society*, **125**, 14220-14221 (2003).
27. Blanco-Rodriguez, A.M., Busby, M., Gradinaru, C., Crane, B.R., Di Bilio, A.J., Matousek, P., Towrie, M., Leigh, B.S., Richards, J.H., Vlcek, A. Jr. & Gray, H.B. Excited-state dynamics of structurally characterized $[Re^{I}(CO)_3(phen)(HisX)]^+$ (X = 83, 109) *Pseudomonas aeruginosa* azurins in aqueous solution. *Journal of the American Chemical Society*, **128**, 4365-4370 (2006).
28. Shih, C., Museth, A.K., Abrahamsson, M., Blanco-Rodriguez, A.M., Di Bilio, A.J., Sudhamsu, J., Crane, B.R., Ronayne, K.L., Towrie, M., Vlcˇek, A. Jr., Richards, J.H., Winkler, J.R. & Gray, H.B. Tryptophan-accelerated electron flow through proteins. *Science*, **320**, 1760-1762 (2008).

29. Gradinaru, C. & Crane, B.R. Comparison of intra- vs intermolecular long-range electron transfer in crystals of ruthenium-modified azurin. *Journal of Physical Chemistry B*, **110**, 20073-20076 (2006).
30. Tsai, L.C., Sjolin, L., Langer, V., Pascher, T. & Nar, H. Structure of the azurin mutant Phe114Ala from *Pseudomonas aeruginosa* at 2.6 Å resolution. *Acta Crystallographica*, D**51**, 168-176 (1995).
31. Marshall, N.M., Garner, D.K., Wilson, T.D., Gao, Y.G., Robinson, H., Nilges, M.J. & Lu, Y. Rationally tuning the reduction potential of a single cupredoxin beyond the natural range. *Nature (London, U. K.)*, **462**, 113-116 (2009).
32. Heras, B., Edeling, M.A., Byriel, K.A., Jones, A., Raina, S. & Martin, J.L. Dehydration converts DsbG crystal diffraction from low to high resolution. *Structure*, **11**, 139-145 (2003).
33. Rigaku Corporation. (2009). *CrystalClear User Manual*. The Woodlands, TX.
34. Pflugrath, J. "An insider's guide to CrystalClear and d*TREK: Improve your results with these new features and tips." http://www.rigaku.com/webinars (2011).
35. Fox, K.M. and Karplus, A.P. Crystallization of old yellow enzyme illustrates an effective strategy for increasing protein crystal size. *Journal of Molecular Biology*, **243**, 502-507 (1993).
36. Wilson, L.J. Bray, T.L. and Suddath, F.L. Crystallization of proteins by dynamic control of evaporation. *Journal of Crystal Growth*, **110**, 142-147 (1991).
37. Fehrer, G. Mechanisms of nucleation and growth of protein crystals. *Journal Crystal Growth*, **76**, 545-546 (1986).
38. Matthews, B.W. (2003). Chapter 1: Transformations in Structural Biology: A Personal View. In C.W. Carter Jr. & R.M. Sweet (Eds.), *Methods in Enzymology (Vol. 368)* (pp. 3-11). Elselvier Inc.
39. Blow, D.M. (2002). *Outline of Crystallography for Biologists*. New York, NY: Oxford University Press.
40. Jacobson, R. (1998). *REQAB* Private communication to the Rigaku Corporation, Tokyo, Japan.
41. Evans, P. Scaling and assessment of data quality. *Acta Crystallographica*, D**62**, 72-82 (2006).
42. Karplus, P.A. & Diederichs, K. Linking Crystallographic Model and Data Quality. *Science*, **336**, 1030-1033 (2012).
43. French, S. & Wilson, K. On the treatment of negative intensity observations. *Acta Crystallographica*. A**34**, 517-525 (1978).
44. Matthews, B.W. Solvent content of protein crystals. *Journal of Molecular Biology*, **33**, 491-497 (1968).
45. Brünger, A.T. Free R value: a novel statistical quantity for assessing the accuracy of crystal structures. *Nature*, **355**, 472-475 (1992).
46. Emsley, P. & Cowtan, K. Coot: model-building tools for molecular graphics. *Acta Crystallographica*, D**60**, 2126-2132 (2004).
47. Kleywegt, G.J. On vital aid: the why, what and how of validation. *Acta Crystallographica*, D**65**, 134-139 (2009).
48. Emsley, P., Lohkamp, B., Scott, W.G., & Cowtan, K. Features and development of Coot. *Acta Crystallographica*, D**66**, 486-501 (2010).

49. Emsley, P. The Coot User Manual. http://www.biop.ox.ac.uk/coot/doc/coot.html
50. Lovell, S.C., Word, J.M., Richardson, J.S. & Richardson, D.C. The penultimate rotamer library. *Proteins*, **40**, 389-408 (2000).
51. Wang, W., Grimley, J.S., Augustine, G.J., Beese, L.S. & Hellinga, H.W. Engineered medium-affinity halide-binding protein derived from YFP: chloride complex. *PDB ID: 3SVC*.
52. Badger, J. (1997). Chapter 17: Modeling and Refinement of Water Molecules and Disordered Solvent. In C.W. Carter Jr. & R.M. Sweet (Eds.), *Methods in Enzymology (Vol. 277)* (pp. 344-352). San Diego, CA: Academic Press.
53. Kleywegt, G.J. & Jones, T.A. (1997). Chapter 11: Model Building and Refinement Practice. In C.W. Carter Jr. & R.M. Sweet (Eds.), *Methods in Enzymology (Vol. 277)* (pp. 208-230). San Diego, CA: Academic Press.
54. Jones, T.A., Kleywegt, G.J. & Brünger, A.T. Correspondence: Storing diffraction data. *Nature (London)*, **383** 18-19 (1996).
55. Kleywegt, G.J. Validation of protein crystal structures. *Acta Crystallographica*, D**56**, 249-265 (2000).
56. Ramakrishnan, C. & Ramachandran, G.N. Stereochemical criteria for polypeptide and protein chain conformations II: Allowed conformation for a pair of peptide units. *Biophysical Journal*, **5**, 909-933 (1965).

APPENDIX

Information concerning a structure's coordinates, geometry, r.m.s. deviations and refinement details are found in its coordinate file. The coordinate file for the final Az-PHM structure is given below.

```
HEADER    ELECTRON TRANSPORT(C                23-JUN-93   4AZU
COMPND    CONFORMATIONAL TRANSITION INVOLVES A PE
REMARK   3
REMARK   3 REFINEMENT.
REMARK   3   PROGRAM     : REFMAC 5.5.0109
REMARK   3   AUTHORS     : MURSHUDOV,VAGIN,DODSON
REMARK   3
REMARK   3    REFINEMENT TARGET : MAXIMUM LIKELIHOOD
REMARK   3
REMARK   3  DATA USED IN REFINEMENT.
REMARK   3   RESOLUTION RANGE HIGH (ANGSTROMS) :   1.30
REMARK   3   RESOLUTION RANGE LOW  (ANGSTROMS) :  28.05
REMARK   3   DATA CUTOFF          (SIGMA(F)) : NONE
REMARK   3   COMPLETENESS FOR RANGE       (%) :  89.23
REMARK   3   NUMBER OF REFLECTIONS          :   50049
REMARK   3
REMARK   3  FIT TO DATA USED IN REFINEMENT.
REMARK   3   CROSS-VALIDATION METHOD        : THROUGHOUT
REMARK   3   FREE R VALUE TEST SET SELECTION  : RANDOM
REMARK   3   R VALUE     (WORKING + TEST SET) : 0.17730
REMARK   3   R VALUE          (WORKING SET) :  0.17572
REMARK   3   FREE R VALUE                   :  0.20704
REMARK   3   FREE R VALUE TEST SET SIZE   (%) :  5.1
REMARK   3   FREE R VALUE TEST SET COUNT      :  2672
REMARK   3
REMARK   3  FIT IN THE HIGHEST RESOLUTION BIN.
REMARK   3   TOTAL NUMBER OF BINS USED         :     20
REMARK   3   BIN RESOLUTION RANGE HIGH         :   1.300
REMARK   3   BIN RESOLUTION RANGE LOW          :   1.334
REMARK   3   REFLECTION IN BIN     (WORKING SET) :    2868
REMARK   3   BIN COMPLETENESS (WORKING+TEST) (%) :   70.86
REMARK   3   BIN R VALUE          (WORKING SET) :   0.262
REMARK   3   BIN FREE R VALUE SET COUNT        :     167
REMARK   3   BIN FREE R VALUE                  :   0.301
REMARK   3
REMARK   3  NUMBER OF NON-HYDROGEN ATOMS USED IN REFINEMENT.
REMARK   3   ALL ATOMS             :    2349
REMARK   3
REMARK   3  B VALUES.
REMARK   3   FROM WILSON PLOT          (A**2) : NULL
REMARK   3   MEAN B VALUE      (OVERALL, A**2) :  14.138
REMARK   3   OVERALL ANISOTROPIC B VALUE.
REMARK   3    B11 (A**2) :    0.00
REMARK   3    B22 (A**2) :    0.00
REMARK   3    B33 (A**2) :    0.00
```

REMARK 3 B12 (A**2) : 0.00
REMARK 3 B13 (A**2) : 0.00
REMARK 3 B23 (A**2) : 0.00
REMARK 3
REMARK 3 ESTIMATED OVERALL COORDINATE ERROR.
REMARK 3 ESU BASED ON R VALUE (A): 0.058
REMARK 3 ESU BASED ON FREE R VALUE (A): 0.062
REMARK 3 ESU BASED ON MAXIMUM LIKELIHOOD (A): 0.037
REMARK 3 ESU FOR B VALUES BASED ON MAXIMUM LIKELIHOOD (A**2): 1.672
REMARK 3
REMARK 3 CORRELATION COEFFICIENTS.
REMARK 3 CORRELATION COEFFICIENT FO-FC : 0.967
REMARK 3 CORRELATION COEFFICIENT FO-FC FREE : 0.951
REMARK 3
REMARK 3 RMS DEVIATIONS FROM IDEAL VALUES COUNT RMS WEIGHT
REMARK 3 BOND LENGTHS REFINED ATOMS (A): 2076 ; 0.027 ; 0.021
REMARK 3 BOND ANGLES REFINED ATOMS (DEGREES): 2815 ; 2.213 ; 1.962
REMARK 3 TORSION ANGLES, PERIOD 1 (DEGREES): 274 ; 7.027 ; 5.000
REMARK 3 TORSION ANGLES, PERIOD 2 (DEGREES): 84 ;39.420 ;25.952
REMARK 3 TORSION ANGLES, PERIOD 3 (DEGREES): 373 ;13.156 ;15.000
REMARK 3 TORSION ANGLES, PERIOD 4 (DEGREES): 2 ;14.198 ;15.000
REMARK 3 CHIRAL-CENTER RESTRAINTS (A**3): 315 ; 0.167 ; 0.200
REMARK 3 GENERAL PLANES REFINED ATOMS (A): 1522 ; 0.014 ; 0.021
REMARK 3
REMARK 3 ISOTROPIC THERMAL FACTOR RESTRAINTS. COUNT RMS WEIGHT
REMARK 3 MAIN-CHAIN BOND REFINED ATOMS (A**2): 1312 ; 1.329 ; 1.500
REMARK 3 MAIN-CHAIN ANGLE REFINED ATOMS (A**2): 2125 ; 2.042 ; 2.000
REMARK 3 SIDE-CHAIN BOND REFINED ATOMS (A**2): 764 ; 2.875 ; 3.000
REMARK 3 SIDE-CHAIN ANGLE REFINED ATOMS (A**2): 680 ; 4.252 ; 4.500
REMARK 3
REMARK 3 NCS RESTRAINTS STATISTICS
REMARK 3 NUMBER OF NCS GROUPS : NULL
REMARK 3
REMARK 3 TWIN DETAILS
REMARK 3 NUMBER OF TWIN DOMAINS : NULL
REMARK 3
REMARK 3
REMARK 3 TLS DETAILS
REMARK 3 NUMBER OF TLS GROUPS : 2
REMARK 3 ATOM RECORD CONTAINS RESIDUAL B FACTORS ONLY
REMARK 3
REMARK 3 TLS GROUP : 1
REMARK 3 NUMBER OF COMPONENTS GROUP : 1
REMARK 3 COMPONENTS C SSSEQI TO C SSSEQI
REMARK 3 RESIDUE RANGE : A -10 A 9999
REMARK 3 ORIGIN FOR THE GROUP (A): -10.4640 10.3031 -20.6267
REMARK 3 T TENSOR
REMARK 3 T11: 0.0035 T22: 0.0322
REMARK 3 T33: 0.0189 T12: -0.0002
REMARK 3 T13: 0.0017 T23: 0.0029
REMARK 3 L TENSOR
REMARK 3 L11: 0.5667 L22: 1.2055
REMARK 3 L33: 1.0449 L12: 0.1447
REMARK 3 L13: -0.2101 L23: -0.2559
REMARK 3 S TENSOR

```
REMARK   3     S11:   0.0070 S12:  -0.0142 S13:  -0.0031
REMARK   3     S21:  -0.0472 S22:  -0.0132 S23:   0.0543
REMARK   3     S31:   0.0280 S32:  -0.0559 S33:   0.0062
REMARK   3
REMARK   3  TLS GROUP :     2
REMARK   3   NUMBER OF COMPONENTS GROUP :    1
REMARK   3   COMPONENTS       C SSSEQI   TO  C SSSEQI
REMARK   3   RESIDUE RANGE :   B   -10       B  9999
REMARK   3   ORIGIN FOR THE GROUP (A): -27.2598  28.9550  -1.1153
REMARK   3   T TENSOR
REMARK   3     T11:   0.0462 T22:   0.0064
REMARK   3     T33:   0.0053 T12:  -0.0149
REMARK   3     T13:   0.0021 T23:   0.0007
REMARK   3   L TENSOR
REMARK   3     L11:   0.8751 L22:   0.6344
REMARK   3     L33:   1.1725 L12:   0.0514
REMARK   3     L13:   0.6096 L23:   0.3847
REMARK   3   S TENSOR
REMARK   3     S11:  -0.0539 S12:   0.0009 S13:  -0.0239
REMARK   3     S21:  -0.1557 S22:   0.0468 S23:   0.0002
REMARK   3     S31:  -0.0760 S32:   0.0062 S33:   0.0071
REMARK   3
REMARK   3
REMARK   3  BULK SOLVENT MODELLING.
REMARK   3   METHOD USED : BABINET MODEL WITH MASK
REMARK   3   PARAMETERS FOR MASK CALCULATION
REMARK   3   VDW PROBE RADIUS   :  1.40
REMARK   3   ION PROBE RADIUS   :  0.80
REMARK   3   SHRINKAGE RADIUS   :  0.80
REMARK   3
REMARK   3  OTHER REFINEMENT REMARKS:
REMARK   3  HYDROGENS HAVE BEEN ADDED IN THE RIDING POSITIONS
REMARK   3  U VALUES      : RESIDUAL ONLY
REMARK   3
SSBOND   1 CYS A    3    CYS A   26
SSBOND   2 CYS B    3    CYS B   26
LINKR        NE2 HIS A  83            CU    CU F   1            HIS-CU
LINKR        N   ALA A   1            CU    CU J   1            ALA-CU
LINKR        O   ALA A   1            CU    CU J   1            ALA-CU1
LINKR        ND1 HIS A  46            CU    CU C   1            HIS-CU1
LINKR        SG  CYS A 112            CU    CU C   1            CYS-CU
LINKR        ND1 HIS A 117            CU    CU C   1            HIS-CU1
LINKR        N   ALA B   1            CU    CU G   1            ALA-CU
LINKR        O   ALA B   1            CU    CU G   1            ALA-CU1
LINKR        NE2 HIS B  83            CU    CU I   1            HIS-CU
LINKR        ND1 HIS B  46            CU    CU D   1            HIS-CU1
LINKR        SG  CYS B 112            CU    CU D   1            CYS-CU
LINKR        ND1 HIS B 117            CU    CU D   1            HIS-CU1
LINKR       CU    CU F   1            O3  TRS E   1           CU-TRS
LINKR       CU    CU F   1            N   TRS E   1           CU-TRS1
LINKR       CU    CU I   1            N   TRS H   1           CU-TRS1
LINKR       CU    CU F   1            C2  TRS g   1           CU-TRS2
LINKR       CU    CU F   1            O2  TRS g   1           CU-TRS3
LINKR       CU    CU F   1            O1  TRS g   1           CU-TRS4
CRYST1   50.178   54.895   85.919  90.00  90.00  90.00 P 21 21 21
```

```
SCALE1      0.019929  0.000000  0.000000        0.00000
SCALE2      0.000000  0.018217  0.000000        0.00000
SCALE3      0.000000  0.000000  0.011639        0.00000
ATOM      1  N   ALA A   1     -14.633  -9.476  -8.661  1.00 19.02      AA   N
ATOM      2  CA  ALA A   1     -15.132  -8.162  -9.248  1.00 17.94      AA   C
ATOM      3  CB  ALA A   1     -15.499  -7.147  -8.125  1.00 18.09      AA   C
ATOM      4  C   ALA A   1     -14.136  -7.558 -10.161  1.00 17.21      AA   C
ATOM      5  O   ALA A   1     -12.938  -7.781  -9.952  1.00 17.41      AA   O
ATOM      6  N   GLU A   2     -14.619  -6.849 -11.165  1.00 14.78      AA   N
ATOM      7  CA  GLU A   2     -13.763  -6.185 -12.139  1.00 17.35      AA   C
ATOM      8  CB  GLU A   2     -13.605  -6.963 -13.471  1.00 20.52      AA   C
ATOM      9  CG  GLU A   2     -13.237  -8.476 -13.363  1.00 24.46      AA   C
ATOM     10  CD  GLU A   2     -11.874  -8.793 -12.718  1.00 35.77      AA   C
ATOM     11  OE1 GLU A   2     -10.977  -7.898 -12.714  1.00 41.25      AA   O
ATOM     12  OE2 GLU A   2     -11.701  -9.942 -12.225  1.00 34.43      AA   O
ATOM     13  C   GLU A   2     -14.168  -4.745 -12.426  1.00 17.02      AA   C
ATOM     14  O   GLU A   2     -14.531  -4.389 -13.562  1.00 21.18      AA   O
ATOM     15  N   CYS A   3     -13.924  -3.885 -11.463  1.00 11.30      AA   N
ATOM     16  CA  CYS A   3     -14.452  -2.484 -11.522  1.00 10.97      AA   C
ATOM     17  CB  CYS A   3     -15.109  -2.131 -10.174  1.00 10.00      AA   C
ATOM     18  SG  CYS A   3     -16.539  -3.238  -9.819  1.00 10.95      AA   S
ATOM     19  C   CYS A   3     -13.372  -1.467 -11.875  1.00 10.61      AA   C
ATOM     20  O   CYS A   3     -13.411  -0.334 -11.480  1.00 10.61      AA   O
ATOM     21  N   SER A   4     -12.408  -1.946 -12.663  1.00 10.81      AA   N
ATOM     22  CA  SER A   4     -11.409  -1.026 -13.163  1.00 11.31      AA   C
ATOM     23  CB  SER A   4     -10.271  -1.036 -12.202  1.00 12.35      AA   C
ATOM     24  OG  SER A   4      -9.565  -2.265 -12.277  1.00 15.23      AA   O
ATOM     25  C   SER A   4     -10.908  -1.387 -14.520  1.00 12.94      AA   C
ATOM     26  O   SER A   4     -11.143  -2.538 -15.007  1.00 13.32      AA   O
ATOM     27  N   VAL A   5     -10.196  -0.477 -15.180  1.00 10.03      AA   N
ATOM     28  CA  VAL A   5      -9.515  -0.782 -16.426  1.00 10.47      AA   C
ATOM     29  CB  VAL A   5     -10.409  -0.448 -17.628  1.00 12.05      AA   C
ATOM     30  CG1 VAL A   5     -10.766   1.087 -17.714  1.00 12.84      AA   C
ATOM     31  CG2 VAL A   5      -9.847  -1.010 -18.917  1.00 17.27      AA   C
ATOM     32  C   VAL A   5      -8.228  -0.010 -16.467  1.00 10.01      AA   C
ATOM     33  O   VAL A   5      -8.126   1.115 -15.931  1.00 10.86      AA   O
ATOM     34  N   ASP A   6      -7.210  -0.614 -17.057  1.00  9.44      AA   N
ATOM     35  CA AASP A   6      -5.903   0.070 -17.300  0.50  8.89      AA   C
ATOM     36  CA BASP A   6      -5.886   0.037 -17.300  0.50  9.40      AA   C
ATOM     37  CB AASP A   6      -4.729  -0.869 -17.056  0.50  8.64      AA   C
ATOM     38  CB BASP A   6      -4.756  -0.972 -17.114  0.50  9.33      AA   C
ATOM     39  CG AASP A   6      -4.673  -1.425 -15.620  0.50  9.57      AA   C
ATOM     40  CG BASP A   6      -4.476  -1.327 -15.644  0.50 12.98      AA   C
ATOM     41  OD1AASP A   6      -5.328  -0.879 -14.735  0.50  9.04      AA   O
ATOM     42  OD1BASP A   6      -4.212  -0.417 -14.878  0.50  9.96      AA   O
ATOM     43  OD2AASP A   6      -3.907  -2.440 -15.419  0.50 12.73      AA   O
ATOM     44  OD2BASP A   6      -4.371  -2.541 -15.280  0.50 17.94      AA   O
ATOM     45  C   ASP A   6      -5.831   0.511 -18.748  1.00  9.51      AA   C
ATOM     46  O   ASP A   6      -6.126  -0.288 -19.639  1.00 11.28      AA   O
ATOM     47  N   ILE A   7      -5.545   1.760 -18.933  1.00  8.82      AA   N
ATOM     48  CA  ILE A   7      -5.528   2.351 -20.273  1.00  9.22      AA   C
ATOM     49  CB  ILE A   7      -6.559   3.536 -20.323  1.00 10.25      AA   C
ATOM     50  CG1 ILE A   7      -7.992   3.039 -20.077  1.00 11.65      AA   C
ATOM     51  CD1 ILE A   7      -8.485   2.072 -21.193  1.00 15.31      AA   C
ATOM     52  CG2 ILE A   7      -6.481   4.259 -21.713  1.00 12.08      AA   C
```

```
ATOM     53  C   ILE A   7     -4.128   2.938 -20.511  1.00  9.24      AA   C
ATOM     54  O   ILE A   7     -3.539   3.504 -19.543  1.00  9.25      AA   O
ATOM     55  N   MET A   8     -3.617   2.808 -21.737  1.00  8.38      AA   N
ATOM     56  CA  MET A   8     -2.265   3.382 -22.086  1.00  8.90      AA   C
ATOM     57  CB  MET A   8     -1.356   2.243 -22.602  1.00  8.74      AA   C
ATOM     58  CG  MET A   8     -0.914   1.275 -21.476  1.00 10.75      AA   C
ATOM     59  SD  MET A   8     -0.165  -0.212 -22.186  1.00 12.05      AA   S
ATOM     60  CE  MET A   8     -1.737  -1.051 -22.541  1.00 13.37      AA   C
ATOM     61  C   MET A   8     -2.462   4.339 -23.261  1.00  9.25      AA   C
ATOM     62  O   MET A   8     -3.188   3.932 -24.205  1.00  9.48      AA   O
ATOM     63  N   GLY A   9     -1.803   5.487 -23.203  1.00  7.90      AA   N
ATOM     64  CA  GLY A   9     -1.708   6.324 -24.424  1.00  8.65      AA   C
ATOM     65  C   GLY A   9     -0.230   6.496 -24.710  1.00  8.65      AA   C
ATOM     66  O   GLY A   9      0.568   6.796 -23.826  1.00  9.37      AA   O
ATOM     67  N   ASN A  10      0.150   6.191 -25.928  1.00  9.92      AA   N
ATOM     68  CA  ASN A  10      1.573   6.142 -26.251  1.00  8.91      AA   C
ATOM     69  CB  ASN A  10      1.910   4.741 -26.801  1.00 11.13      AA   C
ATOM     70  CG  ASN A  10      1.277   4.484 -28.131  1.00 11.35      AA   C
ATOM     71  OD1 ASN A  10      0.832   5.388 -28.835  1.00 11.46      AA   O
ATOM     72  ND2 ASN A  10      1.272   3.226 -28.542  1.00 12.42      AA   N
ATOM     73  C   ASN A  10      2.012   7.327 -27.128  1.00 10.80      AA   C
ATOM     74  O   ASN A  10      1.271   8.307 -27.350  1.00 10.17      AA   O
ATOM     75  N   ASP A  11      3.228   7.241 -27.668  1.00 11.00      AA   N
ATOM     76  CA  ASP A  11      3.775   8.334 -28.499  1.00  9.31      AA   C
ATOM     77  CB  ASP A  11      5.306   8.253 -28.596  1.00 13.14      AA   C
ATOM     78  CG  ASP A  11      6.013   8.769 -27.359  1.00 13.84      AA   C
ATOM     79  OD1 ASP A  11      5.469   9.368 -26.398  1.00 14.47      AA   O
ATOM     80  OD2 ASP A  11      7.257   8.486 -27.283  1.00 17.89      AA   O
ATOM     81  C   ASP A  11      3.267   8.307 -29.913  1.00 11.44      AA   C
ATOM     82  O   ASP A  11      3.595   9.277 -30.664  1.00 12.98      AA   O
ATOM     83  N   GLN A  12      2.382   7.346 -30.272  1.00 10.46      AA   N
ATOM     84  CA  GLN A  12      1.761   7.292 -31.623  1.00 12.35      AA   C
ATOM     85  CB  GLN A  12      1.829   5.899 -32.301  1.00 12.98      AA   C
ATOM     86  CG  GLN A  12      3.103   5.162 -32.061  1.00 18.78      AA   C
ATOM     87  CD  GLN A  12      4.212   5.971 -32.465  1.00 15.60      AA   C
ATOM     88  OE1 GLN A  12      4.179   6.578 -33.620  1.00 18.21      AA   O
ATOM     89  NE2 GLN A  12      5.302   6.007 -31.615  1.00 20.59      AA   N
ATOM     90  C   GLN A  12      0.360   7.736 -31.530  1.00 11.43      AA   C
ATOM     91  O   GLN A  12     -0.389   7.459 -32.394  1.00 13.22      AA   O
ATOM     92  N   MET A  13      0.039   8.478 -30.473  1.00 11.20      AA   N
ATOM     93  CA  MET A  13     -1.260   9.182 -30.390  1.00 12.18      AA   C
ATOM     94  CB  MET A  13     -1.442  10.217 -31.540  1.00 11.56      AA   C
ATOM     95  CG  MET A  13     -2.478  11.280 -31.145  1.00 11.60      AA   C
ATOM     96  SD  MET A  13     -2.812  12.425 -32.480  1.00 14.34      AA   S
ATOM     97  CE  MET A  13     -4.021  11.488 -33.432  1.00 17.08      AA   C
ATOM     98  C   MET A  13     -2.368   8.103 -30.447  1.00 11.56      AA   C
ATOM     99  O   MET A  13     -3.347   8.255 -31.127  1.00 12.72      AA   O
ATOM    100  N   HIS A  14     -2.239   7.028 -29.638  1.00 10.92      AA   N
ATOM    101  CA  HIS A  14     -3.130   5.853 -29.720  1.00 11.19      AA   C
ATOM    102  CB  HIS A  14     -2.306   4.753 -30.454  1.00 12.09      AA   C
ATOM    103  CG  HIS A  14     -2.984   3.412 -30.508  1.00 10.92      AA   C
ATOM    104  ND1 HIS A  14     -4.089   3.126 -31.308  1.00 14.18      AA   N
ATOM    105  CE1 HIS A  14     -4.396   1.831 -31.191  1.00 10.41      AA   C
ATOM    106  NE2 HIS A  14     -3.502   1.251 -30.385  1.00  8.12      AA   N
ATOM    107  CD2 HIS A  14     -2.630   2.236 -29.932  1.00 10.16      AA   C
```

```
ATOM    108  C   HIS A  14     -3.398   5.351 -28.291  1.00 10.85      AA   C
ATOM    109  O   HIS A  14     -2.453   5.288 -27.449  1.00 10.61      AA   O
ATOM    110  N   PHE A  15     -4.664   5.019 -28.021  1.00  9.42      AA   N
ATOM    111  CA  PHE A  15     -5.036   4.130 -26.921  1.00  7.61      AA   C
ATOM    112  CB  PHE A  15     -6.431   4.529 -26.363  1.00  9.65      AA   C
ATOM    113  CG  PHE A  15     -6.546   5.857 -25.611  1.00  8.76      AA   C
ATOM    114  CD1 PHE A  15     -5.671   6.181 -24.542  1.00  9.75      AA   C
ATOM    115  CE1 PHE A  15     -5.885   7.389 -23.765  1.00 11.12      AA   C
ATOM    116  CZ  PHE A  15     -6.983   8.216 -24.023  1.00 11.04      AA   C
ATOM    117  CE2 PHE A  15     -7.788   7.894 -25.111  1.00 11.58      AA   C
ATOM    118  CD2 PHE A  15     -7.598   6.713 -25.858  1.00 10.06      AA   C
ATOM    119  C   PHE A  15     -5.261   2.758 -27.464  1.00 10.18      AA   C
ATOM    120  O   PHE A  15     -5.905   2.612 -28.524  1.00 10.88      AA   O
ATOM    121  N   HIS A  16     -4.771   1.721 -26.739  1.00  9.74      AA   N
ATOM    122  CA  HIS A  16     -5.025   0.397 -27.259  1.00 11.19      AA   C
ATOM    123  CB  HIS A  16     -4.058  -0.666 -26.660  1.00 12.48      AA   C
ATOM    124  CG  HIS A  16     -2.606  -0.391 -26.970  1.00 11.17      AA   C
ATOM    125  ND1 HIS A  16     -2.076  -0.427 -28.248  1.00 11.61      AA   N
ATOM    126  CE1 HIS A  16     -0.768  -0.130 -28.211  1.00 11.53      AA   C
ATOM    127  NE2 HIS A  16     -0.469   0.191 -26.962  1.00 12.97      AA   N
ATOM    128  CD2 HIS A  16     -1.574  -0.014 -26.161  1.00 13.81      AA   C
ATOM    129  C   HIS A  16     -6.472  -0.078 -27.138  1.00 13.30      AA   C
ATOM    130  O   HIS A  16     -7.017  -0.857 -28.027  1.00 15.93      AA   O
ATOM    131  N   THR A  17     -7.154   0.524 -26.187  1.00  8.81      AA   N
ATOM    132  CA  THR A  17     -8.517   0.164 -25.841  1.00 10.01      AA   C
ATOM    133  CB  THR A  17     -8.768   0.478 -24.358  1.00 10.24      AA   C
ATOM    134  OG1 THR A  17     -7.949  -0.411 -23.563  1.00 12.83      AA   O
ATOM    135  CG2 THR A  17    -10.213   0.299 -23.985  1.00 12.49      AA   C
ATOM    136  C   THR A  17     -9.492   1.033 -26.685  1.00 10.67      AA   C
ATOM    137  O   THR A  17     -9.373   2.249 -26.746  1.00 10.41      AA   O
ATOM    138  N   ASN A  18    -10.412   0.351 -27.375  1.00  9.41      AA   N
ATOM    139  CA  ASN A  18    -11.456   1.053 -28.158  1.00 10.47      AA   C
ATOM    140  CB  ASN A  18    -11.647   0.356 -29.534  1.00  9.79      AA   C
ATOM    141  CG  ASN A  18    -12.073  -1.134 -29.407  1.00 12.97      AA   C
ATOM    142  OD1 ASN A  18    -11.310  -1.985 -28.884  1.00 11.16      AA   O
ATOM    143  ND2 ASN A  18    -13.213  -1.512 -30.015  1.00 10.31      AA   N
ATOM    144  C   ASN A  18    -12.814   1.158 -27.447  1.00  9.36      AA   C
ATOM    145  O   ASN A  18    -13.590   2.042 -27.864  1.00 10.44      AA   O
ATOM    146  N   ALA A  19    -13.048   0.346 -26.453  1.00  9.14      AA   N
ATOM    147  CA  ALA A  19    -14.414   0.272 -25.852  1.00  8.31      AA   C
ATOM    148  CB  ALA A  19    -15.322  -0.626 -26.633  1.00  9.28      AA   C
ATOM    149  C   ALA A  19    -14.250  -0.174 -24.433  1.00  9.36      AA   C
ATOM    150  O   ALA A  19    -13.526  -1.115 -24.178  1.00 11.51      AA   O
ATOM    151  N   ILE A  20    -14.952   0.478 -23.533  1.00  9.94      AA   N
ATOM    152  CA  ILE A  20    -14.980   0.143 -22.092  1.00 10.77      AA   C
ATOM    153  CB  ILE A  20    -14.495   1.322 -21.271  1.00 10.67      AA   C
ATOM    154  CG1 ILE A  20    -13.011   1.587 -21.602  1.00  9.87      AA   C
ATOM    155  CD1 ILE A  20    -12.461   2.946 -21.012  1.00 13.55      AA   C
ATOM    156  CG2 ILE A  20    -14.732   1.025 -19.737  1.00 11.57      AA   C
ATOM    157  C   ILE A  20    -16.417  -0.209 -21.758  1.00 10.47      AA   C
ATOM    158  O   ILE A  20    -17.346   0.544 -22.105  1.00 11.86      AA   O
ATOM    159  N   THR A  21    -16.567  -1.308 -21.023  1.00 11.58      AA   N
ATOM    160  CA  THR A  21    -17.910  -1.711 -20.531  1.00 13.46      AA   C
ATOM    161  CB  THR A  21    -18.180  -3.151 -20.910  1.00 15.19      AA   C
ATOM    162  OG1 THR A  21    -18.242  -3.225 -22.349  1.00 17.57      AA   O
```

```
ATOM   163  CG2 THR A  21     -19.488  -3.654 -20.289  1.00 15.26     AA   C
ATOM   164  C   THR A  21     -17.833  -1.680 -18.996  1.00 13.88     AA   C
ATOM   165  O   THR A  21     -16.982  -2.381 -18.398  1.00 16.67     AA   O
ATOM   166  N   VAL A  22     -18.662  -0.823 -18.377  1.00 10.28     AA   N
ATOM   167  CA  VAL A  22     -18.691  -0.688 -16.887  1.00 10.41     AA   C
ATOM   168  CB  VAL A  22     -19.015   0.705 -16.480  1.00 10.02     AA   C
ATOM   169  CG1 VAL A  22     -19.113   0.779 -14.912  1.00 12.93     AA   C
ATOM   170  CG2 VAL A  22     -17.845   1.704 -17.056  1.00 12.74     AA   C
ATOM   171  C   VAL A  22     -19.775  -1.666 -16.371  1.00 10.68     AA   C
ATOM   172  O   VAL A  22     -20.946  -1.568 -16.852  1.00 12.04     AA   O
ATOM   173  N   ASP A  23     -19.412  -2.582 -15.481  1.00 11.13     AA   N
ATOM   174  CA  ASP A  23     -20.385  -3.580 -14.916  1.00 13.43     AA   C
ATOM   175  CB  ASP A  23     -19.567  -4.682 -14.197  1.00 15.01     AA   C
ATOM   176  CG  ASP A  23     -20.392  -5.755 -13.556  1.00 21.17     AA   C
ATOM   177  OD1 ASP A  23     -21.614  -5.577 -13.280  1.00 24.78     AA   O
ATOM   178  OD2 ASP A  23     -19.715  -6.793 -13.346  1.00 29.18     AA   O
ATOM   179  C   ASP A  23     -21.336  -2.790 -13.973  1.00 11.96     AA   C
ATOM   180  O   ASP A  23     -20.846  -2.116 -13.049  1.00 11.65     AA   O
ATOM   181  N   LYS A  24     -22.662  -2.839 -14.198  1.00 14.49     AA   N
ATOM   182  CA  LYS A  24     -23.565  -1.998 -13.383  1.00 15.75     AA   C
ATOM   183  CB  LYS A  24     -25.010  -1.917 -13.951  1.00 17.45     AA   C
ATOM   184  CG  LYS A  24     -25.633  -3.231 -14.190  1.00 17.66     AA   C
ATOM   185  CD  LYS A  24     -27.033  -3.048 -14.792  1.00 20.41     AA   C
ATOM   186  CE  LYS A  24     -27.731  -4.375 -14.961  1.00 18.91     AA   C
ATOM   187  NZ  LYS A  24     -26.787  -5.466 -15.518  1.00 21.24     AA   N
ATOM   188  C   LYS A  24     -23.618  -2.452 -11.907  1.00 14.86     AA   C
ATOM   189  O   LYS A  24     -24.167  -1.715 -11.018  1.00 15.50     AA   O
ATOM   190  N   SER A  25     -23.066  -3.622 -11.615  1.00 12.95     AA   N
ATOM   191  CA  SER A  25     -22.942  -4.045 -10.230  1.00 14.87     AA   C
ATOM   192  CB  SER A  25     -22.767  -5.565 -10.188  1.00 14.89     AA   C
ATOM   193  OG  SER A  25     -21.507  -5.927 -10.572  1.00 16.79     AA   O
ATOM   194  C   SER A  25     -21.817  -3.321  -9.500  1.00 12.12     AA   C
ATOM   195  O   SER A  25     -21.756  -3.321  -8.240  1.00 13.48     AA   O
ATOM   196  N   CYS A  26     -20.910  -2.681 -10.229  1.00 12.29     AA   N
ATOM   197  CA  CYS A  26     -19.872  -1.849  -9.580  1.00 10.69     AA   C
ATOM   198  CB  CYS A  26     -18.815  -1.425 -10.623  1.00  9.78     AA   C
ATOM   199  SG  CYS A  26     -17.895  -2.794 -11.296  1.00 12.00     AA   S
ATOM   200  C   CYS A  26     -20.453  -0.607  -8.975  1.00 10.46     AA   C
ATOM   201  O   CYS A  26     -21.173   0.099  -9.626  1.00 13.78     AA   O
ATOM   202  N   LYS A  27     -20.110  -0.279  -7.728  1.00  9.23     AA   N
ATOM   203  CA  LYS A  27     -20.474   1.026  -7.106  1.00 10.83     AA   C
ATOM   204  CB  LYS A  27     -20.326   0.981  -5.574  1.00 11.53     AA   C
ATOM   205  CG  LYS A  27     -21.357   0.090  -4.880  1.00 21.53     AA   C
ATOM   206  CD  LYS A  27     -22.828   0.591  -4.986  1.00 28.18     AA   C
ATOM   207  CE  LYS A  27     -23.776  -0.405  -4.229  1.00 29.85     AA   C
ATOM   208  NZ  LYS A  27     -23.131  -1.808  -4.318  1.00 30.84     AA   N
ATOM   209  C   LYS A  27     -19.655   2.172  -7.670  1.00  9.71     AA   C
ATOM   210  O   LYS A  27     -20.150   3.265  -7.922  1.00 10.17     AA   O
ATOM   211  N   GLN A  28     -18.392   1.890  -7.893  1.00  9.61     AA   N
ATOM   212  CA  GLN A  28     -17.428   2.907  -8.427  1.00  8.56     AA   C
ATOM   213  CB  GLN A  28     -16.522   3.400  -7.345  1.00 10.04     AA   C
ATOM   214  CG  GLN A  28     -17.355   4.170  -6.286  1.00 11.30     AA   C
ATOM   215  CD  GLN A  28     -16.453   5.075  -5.491  1.00 17.23     AA   C
ATOM   216  OE1 GLN A  28     -15.561   4.601  -4.782  1.00 17.87     AA   O
ATOM   217  NE2 GLN A  28     -16.645   6.397  -5.627  1.00 21.61     AA   N
```

```
ATOM    218  C   GLN A  28     -16.594   2.218  -9.492  1.00  9.27      AA   C
ATOM    219  O   GLN A  28     -16.478   0.941  -9.483  1.00 10.75      AA   O
ATOM    220  N   PHE A  29     -16.127   2.988 -10.426  1.00  8.27      AA   N
ATOM    221  CA  PHE A  29     -15.269   2.466 -11.511  1.00  8.63      AA   C
ATOM    222  CB  PHE A  29     -16.006   2.580 -12.816  1.00 11.26      AA   C
ATOM    223  CG  PHE A  29     -15.382   1.856 -13.937  1.00  9.97      AA   C
ATOM    224  CD1 PHE A  29     -15.413   0.460 -14.038  1.00  8.09      AA   C
ATOM    225  CE1 PHE A  29     -14.786  -0.220 -15.136  1.00 12.25      AA   C
ATOM    226  CZ  PHE A  29     -14.108   0.512 -16.084  1.00  9.12      AA   C
ATOM    227  CE2 PHE A  29     -13.984   1.880 -15.957  1.00  9.79      AA   C
ATOM    228  CD2 PHE A  29     -14.667   2.569 -14.892  1.00  9.92      AA   C
ATOM    229  C   PHE A  29     -14.018   3.292 -11.543  1.00  9.00      AA   C
ATOM    230  O   PHE A  29     -14.026   4.485 -11.299  1.00  9.00      AA   O
ATOM    231  N   THR A  30     -12.914   2.604 -11.792  1.00  8.32      AA   N
ATOM    232  CA  THR A  30     -11.566   3.237 -11.753  1.00  8.44      AA   C
ATOM    233  CB  THR A  30     -10.714   2.623 -10.674  1.00  9.14      AA   C
ATOM    234  OG1 THR A  30     -11.384   2.764  -9.396  1.00 11.09      AA   O
ATOM    235  CG2 THR A  30      -9.316   3.270 -10.568  1.00 10.54      AA   C
ATOM    236  C   THR A  30     -10.875   2.993 -13.076  1.00  9.15      AA   C
ATOM    237  O   THR A  30     -10.751   1.889 -13.610  1.00  9.05      AA   O
ATOM    238  N   VAL A  31     -10.335   4.103 -13.628  1.00  9.02      AA   N
ATOM    239  CA  VAL A  31      -9.495   4.070 -14.817  1.00  8.63      AA   C
ATOM    240  CB  VAL A  31      -9.966   5.086 -15.912  1.00 10.15      AA   C
ATOM    241  CG1 VAL A  31      -8.966   5.216 -17.069  1.00 13.06      AA   C
ATOM    242  CG2 VAL A  31     -11.390   4.700 -16.333  1.00 12.07      AA   C
ATOM    243  C   VAL A  31      -8.092   4.395 -14.354  1.00  8.77      AA   C
ATOM    244  O   VAL A  31      -7.822   5.473 -13.766  1.00  9.13      AA   O
ATOM    245  N   ASN A  32      -7.129   3.524 -14.721  1.00  8.46      AA   N
ATOM    246  CA  ASN A  32      -5.718   3.716 -14.375  1.00  8.57      AA   C
ATOM    247  CB  ASN A  32      -5.144   2.467 -13.722  1.00  7.88      AA   C
ATOM    248  CG  ASN A  32      -5.987   2.085 -12.501  1.00  7.87      AA   C
ATOM    249  OD1 ASN A  32      -6.030   2.804 -11.490  1.00  9.53      AA   O
ATOM    250  ND2 ASN A  32      -6.576   0.902 -12.580  1.00 10.21      AA   N
ATOM    251  C   ASN A  32      -5.025   4.011 -15.721  1.00  8.78      AA   C
ATOM    252  O   ASN A  32      -4.769   3.088 -16.513  1.00  9.14      AA   O
ATOM    253  N   LEU A  33      -4.623   5.280 -15.914  1.00  7.98      AA   N
ATOM    254  CA  LEU A  33      -3.966   5.696 -17.158  1.00  8.67      AA   C
ATOM    255  CB  LEU A  33      -4.423   7.098 -17.508  1.00  9.68      AA   C
ATOM    256  CG  LEU A  33      -3.940   7.717 -18.803  1.00  9.52      AA   C
ATOM    257  CD1 LEU A  33      -4.412   6.952 -20.033  1.00 12.48      AA   C
ATOM    258  CD2 LEU A  33      -4.316   9.167 -18.922  1.00 10.70      AA   C
ATOM    259  C   LEU A  33      -2.472   5.729 -17.019  1.00  8.45      AA   C
ATOM    260  O   LEU A  33      -1.950   6.175 -16.012  1.00  9.07      AA   O
ATOM    261  N   SER A  34      -1.754   5.271 -18.044  1.00  7.84      AA   N
ATOM    262  CA  SER A  34      -0.286   5.367 -18.108  1.00  9.06      AA   C
ATOM    263  CB  SER A  34       0.417   4.036 -17.707  1.00  9.06      AA   C
ATOM    264  OG  SER A  34       0.127   3.059 -18.686  1.00 10.25      AA   O
ATOM    265  C   SER A  34       0.132   5.857 -19.464  1.00 10.21      AA   C
ATOM    266  O   SER A  34      -0.677   5.860 -20.424  1.00 10.53      AA   O
ATOM    267  N   HIS A  35       1.380   6.357 -19.472  1.00 10.92      AA   N
ATOM    268  CA  HIS A  35       1.922   6.955 -20.733  1.00 10.47      AA   C
ATOM    269  CB  HIS A  35       2.097   8.453 -20.564  1.00 11.96      AA   C
ATOM    270  CG  HIS A  35       2.454   9.150 -21.849  1.00 11.40      AA   C
ATOM    271  ND1 HIS A  35       3.351   8.655 -22.814  1.00 12.57      AA   N
ATOM    272  CE1 HIS A  35       3.410   9.530 -23.826  1.00 11.20      AA   C
```

```
ATOM    273  NE2 HIS A  35       2.622  10.576 -23.530  1.00 10.28      AA   N
ATOM    274  CD2 HIS A  35       1.988  10.333 -22.311  1.00  9.41      AA   C
ATOM    275  C   HIS A  35       3.260   6.279 -20.958  1.00 12.00      AA   C
ATOM    276  O   HIS A  35       4.306   6.766 -20.502  1.00 15.23      AA   O
ATOM    277  N   PRO A  36       3.287   5.187 -21.721  1.00 10.94      AA   N
ATOM    278  CA  PRO A  36       4.566   4.509 -22.018  1.00 14.36      AA   C
ATOM    279  CB  PRO A  36       4.115   3.137 -22.509  1.00 17.31      AA   C
ATOM    280  CG  PRO A  36       2.762   3.270 -22.989  1.00 17.68      AA   C
ATOM    281  CD  PRO A  36       2.138   4.349 -22.115  1.00 12.48      AA   C
ATOM    282  C   PRO A  36       5.228   5.289 -23.124  1.00 17.18      AA   C
ATOM    283  O   PRO A  36       4.600   6.256 -23.658  1.00 20.62      AA   O
ATOM    284  N   GLY A  37       6.443   4.839 -23.501  1.00 19.22      AA   N
ATOM    285  CA  GLY A  37       7.159   5.820 -24.449  1.00 22.44      AA   C
ATOM    286  C   GLY A  37       7.623   7.224 -23.874  1.00 22.56      AA   C
ATOM    287  O   GLY A  37       7.527   7.494 -22.649  1.00 22.71      AA   O
ATOM    288  N   ASN A  38       8.082   8.137 -24.734  1.00 16.77      AA   N
ATOM    289  CA  ASN A  38       9.150   9.003 -24.274  1.00 15.33      AA   C
ATOM    290  CB  ASN A  38      10.449   8.715 -25.040  1.00 14.98      AA   C
ATOM    291  CG  ASN A  38      10.885   7.242 -24.968  1.00 22.39      AA   C
ATOM    292  OD1 ASN A  38      11.218   6.642 -26.005  1.00 33.69      AA   O
ATOM    293  ND2 ASN A  38      10.915   6.662 -23.757  1.00 27.41      AA   N
ATOM    294  C   ASN A  38       8.955  10.497 -24.297  1.00 14.63      AA   C
ATOM    295  O   ASN A  38       9.801  11.219 -23.786  1.00 15.81      AA   O
ATOM    296  N   LEU A  39       7.819  10.967 -24.828  1.00 13.03      AA   N
ATOM    297  CA  LEU A  39       7.634  12.425 -25.006  1.00 13.24      AA   C
ATOM    298  CB  LEU A  39       6.869  12.739 -26.299  1.00 14.89      AA   C
ATOM    299  CG  LEU A  39       7.618  12.316 -27.551  1.00 12.62      AA   C
ATOM    300  CD1 LEU A  39       6.643  12.409 -28.721  1.00 18.12      AA   C
ATOM    301  CD2 LEU A  39       8.735  13.315 -27.821  1.00 16.41      AA   C
ATOM    302  C   LEU A  39       6.943  13.079 -23.788  1.00  9.47      AA   C
ATOM    303  O   LEU A  39       6.030  12.479 -23.201  1.00 12.60      AA   O
ATOM    304  N   PRO A  40       7.350  14.284 -23.458  1.00 11.73      AA   N
ATOM    305  CA  PRO A  40       6.769  14.959 -22.313  1.00 11.74      AA   C
ATOM    306  CB  PRO A  40       7.709  16.108 -22.059  1.00 15.39      AA   C
ATOM    307  CG  PRO A  40       8.241  16.407 -23.310  1.00 14.79      AA   C
ATOM    308  CD  PRO A  40       8.375  15.119 -24.086  1.00 13.78      AA   C
ATOM    309  C   PRO A  40       5.312  15.510 -22.591  1.00 12.24      AA   C
ATOM    310  O   PRO A  40       4.864  15.572 -23.772  1.00 10.79      AA   O
ATOM    311  N   LYS A  41       4.637  15.923 -21.526  1.00 10.03      AA   N
ATOM    312  CA  LYS A  41       3.255  16.275 -21.600  1.00 10.77      AA   C
ATOM    313  CB  LYS A  41       2.570  16.352 -20.241  1.00 14.89      AA   C
ATOM    314  CG  LYS A  41       2.861  17.479 -19.474  1.00 17.49      AA   C
ATOM    315  CD  LYS A  41       1.947  17.387 -18.195  1.00 18.06      AA   C
ATOM    316  CE  LYS A  41       2.534  18.330 -17.264  1.00 16.95      AA   C
ATOM    317  NZ  LYS A  41       1.872  18.344 -15.929  1.00 13.11      AA   N
ATOM    318  C   LYS A  41       3.006  17.491 -22.448  1.00 10.88      AA   C
ATOM    319  O   LYS A  41       1.908  17.621 -22.958  1.00 10.38      AA   O
ATOM    320  N   ASN A  42       3.986  18.398 -22.564  1.00  9.40      AA   N
ATOM    321  CA  ASN A  42       3.705  19.614 -23.333  1.00 11.34      AA   C
ATOM    322  CB  ASN A  42       4.567  20.848 -22.925  1.00 12.46      AA   C
ATOM    323  CG  ASN A  42       5.983  20.677 -23.154  1.00 16.90      AA   C
ATOM    324  OD1 ASN A  42       6.443  19.674 -23.618  1.00 14.70      AA   O
ATOM    325  ND2 ASN A  42       6.738  21.744 -22.801  1.00 20.08      AA   N
ATOM    326  C   ASN A  42       3.689  19.365 -24.842  1.00  9.80      AA   C
ATOM    327  O   ASN A  42       3.207  20.250 -25.598  1.00 11.29      AA   O
```

```
ATOM    328  N   VAL A  43      4.136  18.220 -25.307  1.00 10.48      AA   N
ATOM    329  CA  VAL A  43      4.116  17.890 -26.750  1.00 10.84      AA   C
ATOM    330  CB  VAL A  43      5.470  17.890 -27.459  1.00  9.82      AA   C
ATOM    331  CG1 VAL A  43      6.162  19.296 -27.369  1.00 12.44      AA   C
ATOM    332  CG2 VAL A  43      6.317  16.763 -26.921  1.00 11.23      AA   C
ATOM    333  C   VAL A  43      3.359  16.588 -27.072  1.00  8.37      AA   C
ATOM    334  O   VAL A  43      3.063  16.300 -28.201  1.00  9.76      AA   O
ATOM    335  N   MET A  44      3.095  15.798 -26.023  1.00  9.30      AA   N
ATOM    336  CA  MET A  44      2.431  14.509 -26.234  1.00  9.57      AA   C
ATOM    337  CB  MET A  44      3.428  13.383 -26.658  1.00 10.78      AA   C
ATOM    338  CG  MET A  44      2.843  12.100 -27.175  1.00 13.29      AA   C
ATOM    339  SD  MET A  44      1.642  12.219 -28.526  1.00 11.99      AA   S
ATOM    340  CE  MET A  44      2.732  12.697 -29.870  1.00 12.13      AA   C
ATOM    341  C   MET A  44      1.634  14.122 -24.987  1.00  9.73      AA   C
ATOM    342  O   MET A  44      1.556  12.935 -24.604  1.00 11.12      AA   O
ATOM    343  N   GLY A  45      1.043  15.123 -24.349  1.00  9.07      AA   N
ATOM    344  CA  GLY A  45      0.231  14.870 -23.186  1.00  9.38      AA   C
ATOM    345  C   GLY A  45     -1.009  14.036 -23.509  1.00  8.83      AA   C
ATOM    346  O   GLY A  45     -1.633  14.200 -24.577  1.00  9.39      AA   O
ATOM    347  N   HIS A  46     -1.385  13.166 -22.538  1.00  7.59      AA   N
ATOM    348  CA  HIS A  46     -2.658  12.464 -22.646  1.00  8.18      AA   C
ATOM    349  CB  HIS A  46     -2.468  10.941 -22.983  1.00  9.72      AA   C
ATOM    350  CG  HIS A  46     -1.684  10.677 -24.227  1.00  7.90      AA   C
ATOM    351  ND1 HIS A  46     -1.949  11.275 -25.466  1.00  8.83      AA   N
ATOM    352  CE1 HIS A  46     -1.086  10.769 -26.356  1.00  9.73      AA   C
ATOM    353  NE2 HIS A  46     -0.316   9.870 -25.754  1.00  9.82      AA   N
ATOM    354  CD2 HIS A  46     -0.670   9.799 -24.410  1.00  9.87      AA   C
ATOM    355  C   HIS A  46     -3.439  12.569 -21.371  1.00  9.04      AA   C
ATOM    356  O   HIS A  46     -2.872  12.492 -20.256  1.00  9.64      AA   O
ATOM    357  N   ASN A  47     -4.745  12.687 -21.516  1.00  8.45      AA   N
ATOM    358  CA  ASN A  47     -5.638  12.450 -20.416  1.00  8.32      AA   C
ATOM    359  CB  ASN A  47     -6.225  13.800 -19.889  1.00  9.57      AA   C
ATOM    360  CG  ASN A  47     -6.919  14.648 -20.957  1.00  9.54      AA   C
ATOM    361  OD1 ASN A  47     -7.191  14.175 -22.043  1.00  9.34      AA   O
ATOM    362  ND2 ASN A  47     -7.206  15.939 -20.657  1.00 10.37      AA   N
ATOM    363  C   ASN A  47     -6.716  11.486 -20.862  1.00  9.54      AA   C
ATOM    364  O   ASN A  47     -6.811  11.030 -22.032  1.00  9.29      AA   O
ATOM    365  N   TRP A  48     -7.531  11.043 -19.903  1.00  9.05      AA   N
ATOM    366  CA  TRP A  48     -8.713  10.214 -20.208  1.00  8.25      AA   C
ATOM    367  CB  TRP A  48     -8.561   8.870 -19.480  1.00  8.60      AA   C
ATOM    368  CG  TRP A  48     -9.708   7.904 -19.795  1.00  8.47      AA   C
ATOM    369  CD1 TRP A  48     -9.749   6.946 -20.755  1.00  8.28      AA   C
ATOM    370  NE1 TRP A  48    -10.959   6.230 -20.714  1.00  9.07      AA   N
ATOM    371  CE2 TRP A  48    -11.705   6.746 -19.662  1.00  8.04      AA   C
ATOM    372  CD2 TRP A  48    -10.981   7.809 -19.082  1.00  9.16      AA   C
ATOM    373  CE3 TRP A  48    -11.512   8.463 -17.935  1.00 10.25      AA   C
ATOM    374  CZ3 TRP A  48    -12.790   8.092 -17.520  1.00  8.59      AA   C
ATOM    375  CH2 TRP A  48    -13.446   7.077 -18.146  1.00 10.13      AA   C
ATOM    376  CZ2 TRP A  48    -12.973   6.432 -19.234  1.00  8.99      AA   C
ATOM    377  C   TRP A  48     -9.906  11.005 -19.663  1.00  8.65      AA   C
ATOM    378  O   TRP A  48     -9.944  11.318 -18.439  1.00  9.23      AA   O
ATOM    379  N   VAL A  49    -10.813  11.370 -20.553  1.00  9.20      AA   N
ATOM    380  CA  VAL A  49    -11.929  12.254 -20.213  1.00  9.01      AA   C
ATOM    381  CB  VAL A  49    -11.734  13.620 -20.994  1.00  9.05      AA   C
ATOM    382  CG1 VAL A  49    -12.912  14.642 -20.642  1.00 10.87      AA   C
```

```
ATOM    383  CG2 VAL A  49     -10.391  14.247 -20.571  1.00 10.08      AA   C
ATOM    384  C   VAL A  49     -13.201  11.570 -20.661  1.00  8.46      AA   C
ATOM    385  O   VAL A  49     -13.221  11.023 -21.799  1.00  9.17      AA   O
ATOM    386  N   LEU A  50     -14.283  11.625 -19.841  1.00  8.53      AA   N
ATOM    387  CA  LEU A  50     -15.535  10.954 -20.157  1.00  9.13      AA   C
ATOM    388  CB  LEU A  50     -15.825  10.008 -18.983  1.00 10.01      AA   C
ATOM    389  CG  LEU A  50     -17.131   9.144 -19.128  1.00  9.71      AA   C
ATOM    390  CD1 LEU A  50     -17.060   8.202 -20.241  1.00 12.74      AA   C
ATOM    391  CD2 LEU A  50     -17.335   8.367 -17.821  1.00 11.39      AA   C
ATOM    392  C   LEU A  50     -16.631  11.973 -20.253  1.00  9.86      AA   C
ATOM    393  O   LEU A  50     -16.749  12.824 -19.365  1.00  9.49      AA   O
ATOM    394  N   SER A  51     -17.424  11.864 -21.300  1.00  8.28      AA   N
ATOM    395  CA  SER A  51     -18.647  12.712 -21.420  1.00  7.55      AA   C
ATOM    396  CB  SER A  51     -18.367  14.037 -22.204  1.00  9.61      AA   C
ATOM    397  OG  SER A  51     -18.109  13.800 -23.594  1.00  9.96      AA   O
ATOM    398  C   SER A  51     -19.680  11.896 -22.149  1.00  8.69      AA   C
ATOM    399  O   SER A  51     -19.393  10.828 -22.727  1.00  9.29      AA   O
ATOM    400  N   THR A  52     -20.887  12.451 -22.259  1.00  8.90      AA   N
ATOM    401  CA  THR A  52     -21.832  11.910 -23.256  1.00 10.68      AA   C
ATOM    402  CB  THR A  52     -23.200  12.538 -23.209  1.00  9.81      AA   C
ATOM    403  OG1 THR A  52     -23.043  13.915 -23.540  1.00 11.55      AA   O
ATOM    404  CG2 THR A  52     -23.822  12.345 -21.817  1.00 10.60      AA   C
ATOM    405  C   THR A  52     -21.276  12.093 -24.684  1.00 11.09      AA   C
ATOM    406  O   THR A  52     -20.430  12.962 -24.909  1.00 11.23      AA   O
ATOM    407  N   ALA A  53     -21.728  11.270 -25.612  1.00 11.12      AA   N
ATOM    408  CA  ALA A  53     -21.321  11.478 -26.999  1.00 13.00      AA   C
ATOM    409  CB  ALA A  53     -21.967  10.365 -27.883  1.00 15.58      AA   C
ATOM    410  C   ALA A  53     -21.760  12.859 -27.494  1.00 12.44      AA   C
ATOM    411  O   ALA A  53     -21.022  13.501 -28.240  1.00 13.56      AA   O
ATOM    412  N   ALA A  54     -22.940  13.322 -27.088  1.00 11.86      AA   N
ATOM    413  CA  ALA A  54     -23.364  14.635 -27.498  1.00 11.31      AA   C
ATOM    414  CB  ALA A  54     -24.781  14.931 -26.968  1.00 12.74      AA   C
ATOM    415  C   ALA A  54     -22.471  15.777 -27.079  1.00 10.03      AA   C
ATOM    416  O   ALA A  54     -22.343  16.789 -27.807  1.00 13.10      AA   O
ATOM    417  N   ASP A  55     -21.782  15.595 -25.948  1.00  9.66      AA   N
ATOM    418  CA  ASP A  55     -20.935  16.700 -25.386  1.00  9.50      AA   C
ATOM    419  CB  ASP A  55     -20.976  16.672 -23.899  1.00  9.37      AA   C
ATOM    420  CG  ASP A  55     -22.262  17.266 -23.316  1.00 11.67      AA   C
ATOM    421  OD1 ASP A  55     -22.857  18.121 -24.053  1.00 14.34      AA   O
ATOM    422  OD2 ASP A  55     -22.616  16.905 -22.170  1.00 11.74      AA   O
ATOM    423  C   ASP A  55     -19.439  16.628 -25.849  1.00  9.73      AA   C
ATOM    424  O   ASP A  55     -18.716  17.556 -25.545  1.00 10.86      AA   O
ATOM    425  N   MET A  56     -19.008  15.491 -26.418  1.00  9.18      AA   N
ATOM    426  CA  MET A  56     -17.574  15.274 -26.674  1.00  9.56      AA   C
ATOM    427  CB  MET A  56     -17.326  13.955 -27.384  1.00 11.57      AA   C
ATOM    428  CG  MET A  56     -15.880  13.822 -27.821  1.00 10.70      AA   C
ATOM    429  SD  MET A  56     -15.561  12.215 -28.600  1.00 12.60      AA   S
ATOM    430  CE  MET A  56     -13.857  12.584 -29.120  1.00 14.76      AA   C
ATOM    431  C   MET A  56     -16.992  16.401 -27.508  1.00 10.50      AA   C
ATOM    432  O   MET A  56     -15.912  16.927 -27.139  1.00  9.41      AA   O
ATOM    433  N   GLN A  57     -17.608  16.809 -28.620  1.00 10.32      AA   N
ATOM    434  CA AGLN A  57     -16.933  17.805 -29.470  0.50 10.79      AA   C
ATOM    435  CA BGLN A  57     -16.946  17.752 -29.479  0.50 10.35      AA   C
ATOM    436  CB AGLN A  57     -17.639  18.084 -30.807  0.50 12.75      AA   C
ATOM    437  CB BGLN A  57     -17.723  17.861 -30.809  0.50 12.00      AA   C
```

```
ATOM    438  CG AGLN A  57     -16.822  19.043 -31.735  0.50 13.64      AA   C
ATOM    439  CG BGLN A  57     -17.689  16.617 -31.812  0.50  9.06      AA   C
ATOM    440  CD AGLN A  57     -15.457  18.422 -32.119  0.50 19.29      AA   C
ATOM    441  CD BGLN A  57     -18.585  16.835 -33.053  0.50 14.60      AA   C
ATOM    442  OE1AGLN A  57     -15.437  17.504 -32.944  0.50 22.26      AA   O
ATOM    443  OE1BGLN A  57     -19.805  16.818 -32.952  0.50 17.99      AA   O
ATOM    444  NE2AGLN A  57     -14.321  18.909 -31.538  0.50 15.50      AA   N
ATOM    445  NE2BGLN A  57     -17.960  17.061 -34.223  0.50 14.10      AA   N
ATOM    446  C   GLN A  57     -16.737  19.093 -28.751  1.00  9.55      AA   C
ATOM    447  O   GLN A  57     -15.679  19.714 -28.890  1.00 10.26      AA   O
ATOM    448  N   GLY A  58     -17.756  19.547 -28.012  1.00  9.61      AA   N
ATOM    449  CA  GLY A  58     -17.601  20.822 -27.284  1.00 10.64      AA   C
ATOM    450  C   GLY A  58     -16.565  20.713 -26.169  1.00  9.95      AA   C
ATOM    451  O   GLY A  58     -15.801  21.621 -25.982  1.00  9.96      AA   O
ATOM    452  N   VAL A  59     -16.473  19.589 -25.455  1.00  9.61      AA   N
ATOM    453  CA  VAL A  59     -15.432  19.428 -24.437  1.00  9.50      AA   C
ATOM    454  CB  VAL A  59     -15.609  18.069 -23.679  1.00  8.96      AA   C
ATOM    455  CG1 VAL A  59     -14.372  17.814 -22.757  1.00  9.93      AA   C
ATOM    456  CG2 VAL A  59     -16.889  18.096 -22.871  1.00  8.66      AA   C
ATOM    457  C   VAL A  59     -14.021  19.484 -25.099  1.00  8.50      AA   C
ATOM    458  O   VAL A  59     -13.098  20.155 -24.588  1.00 10.72      AA   O
ATOM    459  N   VAL A  60     -13.843  18.827 -26.256  1.00  8.41      AA   N
ATOM    460  CA  VAL A  60     -12.555  18.824 -26.966  1.00  9.02      AA   C
ATOM    461  CB  VAL A  60     -12.617  17.829 -28.101  1.00  9.38      AA   C
ATOM    462  CG1 VAL A  60     -11.404  18.042 -29.075  1.00 11.19      AA   C
ATOM    463  CG2 VAL A  60     -12.651  16.447 -27.570  1.00 12.07      AA   C
ATOM    464  C   VAL A  60     -12.185  20.236 -27.454  1.00  8.91      AA   C
ATOM    465  O   VAL A  60     -11.087  20.743 -27.223  1.00  9.13      AA   O
ATOM    466  N   THR A  61     -13.107  20.929 -28.110  1.00 10.58      AA   N
ATOM    467  CA ATHR A  61     -12.894  22.295 -28.669  0.50 10.27      AA   C
ATOM    468  CA BTHR A  61     -12.758  22.228 -28.699  0.50 11.06      AA   C
ATOM    469  CB ATHR A  61     -14.154  22.799 -29.379  0.50  9.43      AA   C
ATOM    470  CB BTHR A  61     -13.748  22.615 -29.811  0.50 11.57      AA   C
ATOM    471  OG1ATHR A  61     -14.353  21.990 -30.525  0.50 11.01      AA   O
ATOM    472  OG1BTHR A  61     -15.059  22.579 -29.285  0.50 13.23      AA   O
ATOM    473  CG2ATHR A  61     -13.988  24.297 -29.772  0.50 10.46      AA   C
ATOM    474  CG2BTHR A  61     -13.654  21.642 -30.940  0.50  8.90      AA   C
ATOM    475  C   THR A  61     -12.546  23.283 -27.571  1.00 11.38      AA   C
ATOM    476  O   THR A  61     -11.609  24.079 -27.648  1.00 10.57      AA   O
ATOM    477  N   ASP A  62     -13.398  23.266 -26.548  1.00  9.41      AA   N
ATOM    478  CA  ASP A  62     -13.218  24.198 -25.449  1.00  9.36      AA   C
ATOM    479  CB  ASP A  62     -14.444  24.306 -24.509  1.00  8.64      AA   C
ATOM    480  CG  ASP A  62     -15.635  24.888 -25.165  1.00 11.73      AA   C
ATOM    481  OD1 ASP A  62     -15.580  25.625 -26.185  1.00 12.79      AA   O
ATOM    482  OD2 ASP A  62     -16.728  24.647 -24.613  1.00 11.41      AA   O
ATOM    483  C   ASP A  62     -11.934  23.881 -24.657  1.00  9.28      AA   C
ATOM    484  O   ASP A  62     -11.236  24.797 -24.172  1.00 10.11      AA   O
ATOM    485  N   GLY A  63     -11.615  22.589 -24.578  1.00 10.23      AA   N
ATOM    486  CA  GLY A  63     -10.413  22.129 -23.897  1.00  9.84      AA   C
ATOM    487  C   GLY A  63      -9.181  22.714 -24.597  1.00  9.50      AA   C
ATOM    488  O   GLY A  63      -8.195  23.246 -23.973  1.00 10.30      AA   O
ATOM    489  N   MET A  64      -9.159  22.630 -25.935  1.00 10.84      AA   N
ATOM    490  CA  MET A  64      -8.004  23.169 -26.737  1.00 12.57      AA   C
ATOM    491  CB  MET A  64      -8.197  22.973 -28.235  1.00 13.39      AA   C
ATOM    492  CG  MET A  64      -7.097  23.730 -28.918  1.00 14.27      AA   C
```

```
ATOM    493  SD  MET A  64      -6.780  23.121 -30.517  1.00 21.17      AA   S
ATOM    494  CE  MET A  64      -8.146  23.139 -31.305  1.00 13.17      AA   C
ATOM    495  C   MET A  64      -7.843  24.642 -26.436  1.00 11.92      AA   C
ATOM    496  O   MET A  64      -6.727  25.095 -26.218  1.00 12.86      AA   O
ATOM    497  N   ALA A  65      -8.932  25.376 -26.440  1.00  9.79      AA   N
ATOM    498  CA  ALA A  65      -8.880  26.821 -26.265  1.00 11.59      AA   C
ATOM    499  CB  ALA A  65     -10.250  27.477 -26.539  1.00 11.76      AA   C
ATOM    500  C   ALA A  65      -8.431  27.196 -24.858  1.00 11.10      AA   C
ATOM    501  O   ALA A  65      -7.803  28.221 -24.692  1.00 13.09      AA   O
ATOM    502  N   SER A  66      -8.725  26.389 -23.859  1.00 10.38      AA   N
ATOM    503  CA  SER A  66      -8.238  26.646 -22.476  1.00 11.41      AA   C
ATOM    504  CB  SER A  66      -8.976  25.762 -21.506  1.00 10.82      AA   C
ATOM    505  OG  SER A  66     -10.325  26.256 -21.456  1.00 17.70      AA   O
ATOM    506  C   SER A  66      -6.738  26.468 -22.323  1.00 10.55      AA   C
ATOM    507  O   SER A  66      -6.115  27.127 -21.476  1.00 11.87      AA   O
ATOM    508  N   GLY A  67      -6.151  25.570 -23.108  1.00  9.35      AA   N
ATOM    509  CA  GLY A  67      -4.695  25.426 -23.103  1.00 10.07      AA   C
ATOM    510  C   GLY A  67      -4.110  24.581 -21.998  1.00  8.65      AA   C
ATOM    511  O   GLY A  67      -4.804  24.042 -21.125  1.00 10.39      AA   O
ATOM    512  N   LEU A  68      -2.804  24.408 -22.079  1.00  8.85      AA   N
ATOM    513  CA  LEU A  68      -2.064  23.628 -21.067  1.00 11.15      AA   C
ATOM    514  CB  LEU A  68      -0.585  23.451 -21.558  1.00 10.95      AA   C
ATOM    515  CG  LEU A  68       0.337  22.630 -20.627  1.00  9.98      AA   C
ATOM    516  CD1 LEU A  68      -0.218  21.189 -20.456  1.00 13.46      AA   C
ATOM    517  CD2 LEU A  68       1.781  22.632 -21.214  1.00 13.67      AA   C
ATOM    518  C   LEU A  68      -2.162  24.180 -19.647  1.00 10.09      AA   C
ATOM    519  O   LEU A  68      -2.141  23.359 -18.706  1.00 13.24      AA   O
ATOM    520  N   ASP A  69      -2.378  25.479 -19.499  1.00 10.75      AA   N
ATOM    521  CA  ASP A  69      -2.567  26.053 -18.170  1.00 11.98      AA   C
ATOM    522  CB  ASP A  69      -2.908  27.531 -18.320  1.00 12.29      AA   C
ATOM    523  CG  ASP A  69      -3.018  28.280 -17.009  1.00 15.20      AA   C
ATOM    524  OD1 ASP A  69      -2.044  28.423 -16.248  1.00 13.08      AA   O
ATOM    525  OD2 ASP A  69      -4.058  28.879 -16.679  1.00 15.04      AA   O
ATOM    526  C   ASP A  69      -3.705  25.359 -17.446  1.00 12.74      AA   C
ATOM    527  O   ASP A  69      -3.706  25.266 -16.230  1.00 13.92      AA   O
ATOM    528  N   LYS A  70      -4.688  24.820 -18.189  1.00 11.72      AA   N
ATOM    529  CA  LYS A  70      -5.913  24.141 -17.616  1.00 10.32      AA   C
ATOM    530  CB  LYS A  70      -7.120  24.812 -18.235  1.00 12.24      AA   C
ATOM    531  CG  LYS A  70      -7.152  26.318 -18.052  1.00 13.26      AA   C
ATOM    532  CD  LYS A  70      -7.029  26.731 -16.600  1.00 14.94      AA   C
ATOM    533  CE  LYS A  70      -7.441  28.242 -16.467  1.00 16.14      AA   C
ATOM    534  NZ  LYS A  70      -6.574  29.256 -17.288  1.00 12.36      AA   N
ATOM    535  C   LYS A  70      -5.884  22.648 -17.917  1.00 12.11      AA   C
ATOM    536  O   LYS A  70      -6.965  21.976 -17.833  1.00 12.27      AA   O
ATOM    537  N   ASP A  71      -4.760  22.038 -18.313  1.00 11.91      AA   N
ATOM    538  CA  ASP A  71      -4.718  20.645 -18.735  1.00 12.13      AA   C
ATOM    539  CB  ASP A  71      -4.981  19.651 -17.540  1.00 14.93      AA   C
ATOM    540  CG  ASP A  71      -3.704  19.204 -16.765  1.00 15.10      AA   C
ATOM    541  OD1 ASP A  71      -2.663  19.715 -17.080  1.00 16.74      AA   O
ATOM    542  OD2 ASP A  71      -3.965  18.328 -15.888  1.00 19.09      AA   O
ATOM    543  C   ASP A  71      -5.705  20.361 -19.858  1.00 11.37      AA   C
ATOM    544  O   ASP A  71      -6.224  19.242 -20.006  1.00 11.45      AA   O
ATOM    545  N   TYR A  72      -5.922  21.350 -20.700  1.00  9.40      AA   N
ATOM    546  CA  TYR A  72      -6.778  21.166 -21.882  1.00  8.92      AA   C
ATOM    547  CB  TYR A  72      -6.141  20.224 -22.925  1.00  9.70      AA   C
```

```
ATOM    548  CG  TYR A  72      -4.883  20.871 -23.507  1.00  8.62      AA   C
ATOM    549  CD1 TYR A  72      -4.930  21.950 -24.361  1.00  8.59      AA   C
ATOM    550  CE1 TYR A  72      -3.800  22.547 -24.897  1.00  9.77      AA   C
ATOM    551  CZ  TYR A  72      -2.570  21.930 -24.682  1.00 11.55      AA   C
ATOM    552  OH  TYR A  72      -1.412  22.463 -25.303  1.00 11.11      AA   O
ATOM    553  CE2 TYR A  72      -2.453  20.840 -23.873  1.00 11.97      AA   C
ATOM    554  CD2 TYR A  72      -3.572  20.274 -23.270  1.00 10.15      AA   C
ATOM    555  C   TYR A  72      -8.180  20.751 -21.540  1.00  9.05      AA   C
ATOM    556  O   TYR A  72      -8.855  20.042 -22.292  1.00  9.09      AA   O
ATOM    557  N   LEU A  73      -8.711  21.275 -20.418  1.00  8.36      AA   N
ATOM    558  CA  LEU A  73     -10.130  21.179 -20.103  1.00  9.84      AA   C
ATOM    559  CB  LEU A  73     -10.382  20.204 -18.900  1.00 10.55      AA   C
ATOM    560  CG  LEU A  73     -10.242  18.741 -19.304  1.00 13.67      AA   C
ATOM    561  CD1 LEU A  73     -10.391  17.911 -17.997  1.00 16.02      AA   C
ATOM    562  CD2 LEU A  73     -11.279  18.316 -20.314  1.00 12.63      AA   C
ATOM    563  C   LEU A  73     -10.643  22.536 -19.726  1.00  9.37      AA   C
ATOM    564  O   LEU A  73     -10.016  23.233 -18.871  1.00 11.06      AA   O
ATOM    565  N   LYS A  74     -11.734  22.974 -20.322  1.00  9.85      AA   N
ATOM    566  CA  LYS A  74     -12.367  24.243 -19.853  1.00  9.46      AA   C
ATOM    567  CB  LYS A  74     -13.654  24.459 -20.666  1.00 12.26      AA   C
ATOM    568  CG  LYS A  74     -14.304  25.837 -20.309  1.00 11.48      AA   C
ATOM    569  CD  LYS A  74     -15.661  26.015 -20.998  1.00 17.75      AA   C
ATOM    570  CE  LYS A  74     -16.675  25.040 -20.501  1.00 18.93      AA   C
ATOM    571  NZ  LYS A  74     -18.161  25.576 -20.594  1.00 20.94      AA   N
ATOM    572  C   LYS A  74     -12.681  24.161 -18.356  1.00 10.00      AA   C
ATOM    573  O   LYS A  74     -13.236  23.172 -17.914  1.00 11.27      AA   O
ATOM    574  N   PRO A  75     -12.311  25.208 -17.586  1.00 12.22      AA   N
ATOM    575  CA  PRO A  75     -12.664  25.137 -16.163  1.00 14.07      AA   C
ATOM    576  CB  PRO A  75     -12.115  26.435 -15.576  1.00 14.84      AA   C
ATOM    577  CG  PRO A  75     -10.918  26.793 -16.546  1.00 15.79      AA   C
ATOM    578  CD  PRO A  75     -11.457  26.317 -17.942  1.00 11.75      AA   C
ATOM    579  C   PRO A  75     -14.188  25.137 -15.986  1.00 12.73      AA   C
ATOM    580  O   PRO A  75     -14.954  25.686 -16.816  1.00 11.68      AA   O
ATOM    581  N   ASP A  76     -14.582  24.452 -14.923  1.00 12.94      AA   N
ATOM    582  CA  ASP A  76     -16.010  24.387 -14.567  1.00 16.53      AA   C
ATOM    583  CB  ASP A  76     -16.583  25.782 -14.214  1.00 16.75      AA   C
ATOM    584  CG  ASP A  76     -16.369  26.181 -12.799  1.00 27.06      AA   C
ATOM    585  OD1 ASP A  76     -15.436  25.641 -12.149  1.00 31.54      AA   O
ATOM    586  OD2 ASP A  76     -17.211  27.026 -12.356  1.00 31.94      AA   O
ATOM    587  C   ASP A  76     -16.844  23.840 -15.711  1.00 14.23      AA   C
ATOM    588  O   ASP A  76     -17.922  24.394 -16.087  1.00 15.77      AA   O
ATOM    589  N   ASP A  77     -16.327  22.773 -16.333  1.00 13.08      AA   N
ATOM    590  CA  ASP A  77     -17.059  22.162 -17.453  1.00 11.42      AA   C
ATOM    591  CB  ASP A  77     -16.074  21.659 -18.502  1.00 12.05      AA   C
ATOM    592  CG  ASP A  77     -16.780  21.318 -19.767  1.00 10.72      AA   C
ATOM    593  OD1 ASP A  77     -18.018  21.125 -19.765  1.00 11.51      AA   O
ATOM    594  OD2 ASP A  77     -16.145  21.253 -20.843  1.00 12.18      AA   O
ATOM    595  C   ASP A  77     -17.919  21.041 -16.908  1.00 11.77      AA   C
ATOM    596  O   ASP A  77     -17.436  19.922 -16.663  1.00 12.27      AA   O
ATOM    597  N   SER A  78     -19.202  21.363 -16.714  1.00 11.61      AA   N
ATOM    598  CA  SER A  78     -20.146  20.357 -16.166  1.00 13.11      AA   C
ATOM    599  CB  SER A  78     -21.517  20.976 -15.876  1.00 14.96      AA   C
ATOM    600  OG  SER A  78     -22.030  21.653 -17.034  1.00 19.53      AA   O
ATOM    601  C   SER A  78     -20.352  19.146 -17.091  1.00 13.24      AA   C
ATOM    602  O   SER A  78     -20.900  18.084 -16.654  1.00 14.89      AA   O
```

```
ATOM    603  N   ARG A  79     -19.976  19.270 -18.363  1.00  9.94      AA   N
ATOM    604  CA  ARG A  79     -20.141  18.148 -19.283  1.00 10.97      AA   C
ATOM    605  CB  ARG A  79     -19.930  18.650 -20.710  1.00 10.07      AA   C
ATOM    606  CG  ARG A  79     -20.904  19.726 -21.102  1.00 10.12      AA   C
ATOM    607  CD  ARG A  79     -20.519  20.294 -22.463  1.00 12.52      AA   C
ATOM    608  NE  ARG A  79     -19.216  20.980 -22.350  1.00 11.29      AA   N
ATOM    609  CZ  ARG A  79     -18.741  21.811 -23.243  1.00 10.10      AA   C
ATOM    610  NH1 ARG A  79     -19.402  22.016 -24.409  1.00 11.56      AA   N
ATOM    611  NH2 ARG A  79     -17.554  22.356 -23.085  1.00 11.22      AA   N
ATOM    612  C   ARG A  79     -19.174  17.004 -18.986  1.00 10.26      AA   C
ATOM    613  O   ARG A  79     -19.336  15.878 -19.513  1.00 12.07      AA   O
ATOM    614  N   VAL A  80     -18.073  17.332 -18.328  1.00  9.25      AA   N
ATOM    615  CA  VAL A  80     -17.078  16.258 -18.013  1.00 10.37      AA   C
ATOM    616  CB  VAL A  80     -15.679  16.892 -17.670  1.00 10.11      AA   C
ATOM    617  CG1 VAL A  80     -14.712  15.800 -17.261  1.00 11.06      AA   C
ATOM    618  CG2 VAL A  80     -15.116  17.672 -18.934  1.00 12.14      AA   C
ATOM    619  C   VAL A  80     -17.586  15.395 -16.825  1.00 12.27      AA   C
ATOM    620  O   VAL A  80     -17.744  15.883 -15.706  1.00 11.18      AA   O
ATOM    621  N   ILE A  81     -17.860  14.135 -17.112  1.00  9.83      AA   N
ATOM    622  CA  ILE A  81     -18.385  13.243 -16.095  1.00 10.15      AA   C
ATOM    623  CB  ILE A  81     -19.019  12.064 -16.748  1.00 11.04      AA   C
ATOM    624  CG1 ILE A  81     -20.219  12.530 -17.560  1.00 10.97      AA   C
ATOM    625  CD1 ILE A  81     -20.813  11.372 -18.475  1.00 15.01      AA   C
ATOM    626  CG2 ILE A  81     -19.448  11.020 -15.646  1.00 10.19      AA   C
ATOM    627  C   ILE A  81     -17.242  12.795 -15.158  1.00 10.36      AA   C
ATOM    628  O   ILE A  81     -17.402  12.726 -13.952  1.00 11.88      AA   O
ATOM    629  N   ALA A  82     -16.057  12.496 -15.717  1.00  8.86      AA   N
ATOM    630  CA  ALA A  82     -14.879  12.145 -14.931  1.00  9.74      AA   C
ATOM    631  CB  ALA A  82     -14.946  10.652 -14.596  1.00 11.00      AA   C
ATOM    632  C   ALA A  82     -13.685  12.391 -15.825  1.00  9.79      AA   C
ATOM    633  O   ALA A  82     -13.765  12.356 -17.077  1.00  9.61      AA   O
ATOM    634  N   HIS A  83     -12.501  12.544 -15.237  1.00  9.46      AA   N
ATOM    635  CA  HIS A  83     -11.287  12.730 -16.034  1.00  8.72      AA   C
ATOM    636  CB  HIS A  83     -11.188  14.159 -16.595  1.00  9.83      AA   C
ATOM    637  CG  HIS A  83     -11.102  15.202 -15.538  1.00  9.67      AA   C
ATOM    638  ND1 HIS A  83      -9.904  15.746 -15.107  1.00 11.00      AA   N
ATOM    639  CE1 HIS A  83     -10.176  16.585 -14.107  1.00 11.89      AA   C
ATOM    640  NE2 HIS A  83     -11.481  16.630 -13.894  1.00 12.53      AA   N
ATOM    641  CD2 HIS A  83     -12.071  15.768 -14.798  1.00 11.77      AA   C
ATOM    642  C   HIS A  83     -10.076  12.454 -15.154  1.00  9.24      AA   C
ATOM    643  O   HIS A  83     -10.107  12.706 -13.915  1.00 10.06      AA   O
ATOM    644  N   THR A  84      -8.971  12.064 -15.778  1.00  9.98      AA   N
ATOM    645  CA  THR A  84      -7.661  12.066 -15.130  1.00 10.31      AA   C
ATOM    646  CB  THR A  84      -6.693  11.008 -15.830  1.00 10.71      AA   C
ATOM    647  OG1 THR A  84      -6.448  11.399 -17.172  1.00 10.05      AA   O
ATOM    648  CG2 THR A  84      -7.268   9.611 -15.843  1.00 11.67      AA   C
ATOM    649  C   THR A  84      -7.065  13.428 -15.326  1.00 10.82      AA   C
ATOM    650  O   THR A  84      -7.581  14.277 -16.086  1.00 11.39      AA   O
ATOM    651  N   LYS A  85      -5.903  13.639 -14.718  1.00 10.24      AA   N
ATOM    652  CA  LYS A  85      -5.045  14.777 -15.105  1.00 11.70      AA   C
ATOM    653  CB  LYS A  85      -4.008  15.108 -14.027  1.00 13.10      AA   C
ATOM    654  CG  LYS A  85      -2.968  14.162 -13.977  1.00 14.24      AA   C
ATOM    655  CD  LYS A  85      -1.983  14.543 -12.771  1.00 19.10      AA   C
ATOM    656  CE  LYS A  85      -0.758  13.621 -12.783  1.00 21.05      AA   C
ATOM    657  NZ  LYS A  85       0.175  13.697 -11.583  1.00 23.44      AA   N
```

```
ATOM    658  C   LYS A  85     -4.370  14.469 -16.469  1.00  9.71      AA   C
ATOM    659  O   LYS A  85     -4.351  13.309 -16.975  1.00  9.39      AA   O
ATOM    660  N   LEU A  86     -3.716  15.499 -17.016  1.00 10.11      AA   N
ATOM    661  CA  LEU A  86     -2.875  15.290 -18.210  1.00  9.24      AA   C
ATOM    662  CB  LEU A  86     -2.732  16.672 -18.944  1.00 10.67      AA   C
ATOM    663  CG  LEU A  86     -2.127  16.588 -20.357  1.00  9.93      AA   C
ATOM    664  CD1 LEU A  86     -3.167  16.137 -21.310  1.00 10.60      AA   C
ATOM    665  CD2 LEU A  86     -1.519  17.991 -20.744  1.00 12.37      AA   C
ATOM    666  C   LEU A  86     -1.520  14.774 -17.817  1.00 10.79      AA   C
ATOM    667  O   LEU A  86     -0.903  15.260 -16.870  1.00 10.50      AA   O
ATOM    668  N   ILE A  87     -1.083  13.711 -18.475  1.00  9.60      AA   N
ATOM    669  CA  ILE A  87      0.186  13.069 -18.138  1.00 10.26      AA   C
ATOM    670  CB  ILE A  87      0.019  11.665 -17.491  1.00 10.10      AA   C
ATOM    671  CG1 ILE A  87     -0.568  10.687 -18.495  1.00 10.51      AA   C
ATOM    672  CD1 ILE A  87     -0.626   9.214 -17.958  1.00 12.63      AA   C
ATOM    673  CG2 ILE A  87     -0.699  11.765 -16.111  1.00 11.84      AA   C
ATOM    674  C   ILE A  87      1.137  13.022 -19.355  1.00  9.51      AA   C
ATOM    675  O   ILE A  87      0.685  12.948 -20.514  1.00 10.07      AA   O
ATOM    676  N   GLY A  88      2.443  13.035 -19.051  1.00  9.46      AA   N
ATOM    677  CA  GLY A  88      3.509  12.815 -20.042  1.00 10.03      AA   C
ATOM    678  C   GLY A  88      4.181  11.462 -19.808  1.00 10.23      AA   C
ATOM    679  O   GLY A  88      3.790  10.660 -18.976  1.00 11.06      AA   O
ATOM    680  N   SER A  89      5.169  11.212 -20.651  1.00 12.14      AA   N
ATOM    681  CA  SER A  89      5.976   9.983 -20.602  1.00 15.13      AA   C
ATOM    682  CB  SER A  89      7.289  10.267 -21.421  1.00 18.21      AA   C
ATOM    683  OG  SER A  89      8.365   9.506 -20.966  1.00 21.43      AA   O
ATOM    684  C   SER A  89      6.368   9.604 -19.171  1.00 12.17      AA   C
ATOM    685  O   SER A  89      6.853  10.397 -18.399  1.00 13.10      AA   O
ATOM    686  N   GLY A  90      6.062   8.351 -18.859  1.00 10.68      AA   N
ATOM    687  CA  GLY A  90      6.522   7.812 -17.576  1.00 11.31      AA   C
ATOM    688  C   GLY A  90      5.629   8.167 -16.399  1.00 11.22      AA   C
ATOM    689  O   GLY A  90      5.827   7.640 -15.279  1.00 15.28      AA   O
ATOM    690  N   GLU A  91      4.580   8.976 -16.612  1.00 11.30      AA   N
ATOM    691  CA  GLU A  91      3.649   9.322 -15.532  1.00  9.23      AA   C
ATOM    692  CB  GLU A  91      3.204  10.788 -15.602  1.00 10.09      AA   C
ATOM    693  CG  GLU A  91      4.375  11.730 -15.435  1.00 12.53      AA   C
ATOM    694  CD  GLU A  91      4.059  13.202 -15.575  1.00 18.23      AA   C
ATOM    695  OE1 GLU A  91      3.229  13.581 -16.351  1.00 16.69      AA   O
ATOM    696  OE2 GLU A  91      4.708  14.078 -14.910  1.00 22.86      AA   O
ATOM    697  C   GLU A  91      2.443   8.400 -15.579  1.00  9.43      AA   C
ATOM    698  O   GLU A  91      2.190   7.671 -16.545  1.00 10.71      AA   O
ATOM    699  N   LYS A  92      1.725   8.409 -14.451  1.00 10.62      AA   N
ATOM    700  CA  LYS A  92      0.434   7.642 -14.315  1.00 10.41      AA   C
ATOM    701  CB  LYS A  92      0.708   6.414 -13.448  1.00 12.09      AA   C
ATOM    702  CG  LYS A  92      1.640   5.456 -14.034  1.00 14.55      AA   C
ATOM    703  CD  LYS A  92      1.748   4.289 -13.086  1.00 14.34      AA   C
ATOM    704  CE  LYS A  92      2.853   3.286 -13.509  1.00 23.10      AA   C
ATOM    705  NZ  LYS A  92      3.802   3.522 -14.660  1.00 25.05      AA   N
ATOM    706  C   LYS A  92     -0.546   8.513 -13.577  1.00 10.67      AA   C
ATOM    707  O   LYS A  92     -0.168   9.410 -12.812  1.00 12.25      AA   O
ATOM    708  N   ASP A  93     -1.833   8.201 -13.763  1.00 10.12      AA   N
ATOM    709  CA  ASP A  93     -2.867   8.818 -12.926  1.00  9.64      AA   C
ATOM    710  CB  ASP A  93     -3.256  10.199 -13.486  1.00 10.24      AA   C
ATOM    711  CG  ASP A  93     -4.056  11.031 -12.476  1.00 12.08      AA   C
ATOM    712  OD1 ASP A  93     -3.672  11.077 -11.261  1.00 13.44      AA   O
```

```
ATOM    713  OD2 ASP A  93      -5.056  11.616 -12.884  1.00 12.07      AA   O
ATOM    714  C   ASP A  93      -4.090   7.935 -12.960  1.00  8.75      AA   C
ATOM    715  O   ASP A  93      -4.414   7.348 -14.005  1.00 10.48      AA   O
ATOM    716  N   SER A  94      -4.765   7.835 -11.840  1.00  9.30      AA   N
ATOM    717  CA  SER A  94      -6.013   7.041 -11.745  1.00  8.68      AA   C
ATOM    718  CB  SER A  94      -5.940   6.074 -10.589  1.00  8.91      AA   C
ATOM    719  OG  SER A  94      -4.952   5.105 -10.868  1.00 10.20      AA   O
ATOM    720  C   SER A  94      -7.155   8.007 -11.441  1.00 10.19      AA   C
ATOM    721  O   SER A  94      -7.032   8.981 -10.680  1.00 12.13      AA   O
ATOM    722  N   VAL A  95      -8.314   7.678 -11.974  1.00  9.34      AA   N
ATOM    723  CA  VAL A  95      -9.559   8.376 -11.599  1.00  9.86      AA   C
ATOM    724  CB  VAL A  95     -10.103   9.337 -12.764  1.00 10.08      AA   C
ATOM    725  CG1 VAL A  95     -10.370   8.633 -14.050  1.00 12.87      AA   C
ATOM    726  CG2 VAL A  95     -11.370  10.059 -12.281  1.00 12.58      AA   C
ATOM    727  C   VAL A  95     -10.617   7.344 -11.199  1.00  9.00      AA   C
ATOM    728  O   VAL A  95     -10.807   6.381 -11.924  1.00 10.38      AA   O
ATOM    729  N   THR A  96     -11.315   7.614 -10.094  1.00  8.85      AA   N
ATOM    730  CA  THR A  96     -12.405   6.786  -9.642  1.00  9.18      AA   C
ATOM    731  CB  THR A  96     -12.163   6.291  -8.249  1.00 10.61      AA   C
ATOM    732  OG1 THR A  96     -11.137   5.307  -8.370  1.00  9.34      AA   O
ATOM    733  CG2 THR A  96     -13.410   5.598  -7.640  1.00 10.96      AA   C
ATOM    734  C   THR A  96     -13.680   7.669  -9.691  1.00 10.07      AA   C
ATOM    735  O   THR A  96     -13.674   8.859  -9.274  1.00 10.79      AA   O
ATOM    736  N   PHE A  97     -14.760   7.095 -10.207  1.00  8.97      AA   N
ATOM    737  CA  PHE A  97     -16.050   7.809 -10.214  1.00 10.08      AA   C
ATOM    738  CB  PHE A  97     -16.305   8.520 -11.562  1.00 11.37      AA   C
ATOM    739  CG  PHE A  97     -16.385   7.647 -12.710  1.00 10.20      AA   C
ATOM    740  CD1 PHE A  97     -15.213   7.267 -13.473  1.00 11.31      AA   C
ATOM    741  CE1 PHE A  97     -15.274   6.426 -14.593  1.00 11.76      AA   C
ATOM    742  CZ  PHE A  97     -16.487   5.971 -14.999  1.00 12.68      AA   C
ATOM    743  CE2 PHE A  97     -17.710   6.323 -14.219  1.00 12.99      AA   C
ATOM    744  CD2 PHE A  97     -17.648   7.169 -13.139  1.00 11.53      AA   C
ATOM    745  C   PHE A  97     -17.186   6.908  -9.828  1.00  9.84      AA   C
ATOM    746  O   PHE A  97     -17.098   5.701  -9.984  1.00 10.65      AA   O
ATOM    747  N   ASP A  98     -18.272   7.525  -9.385  1.00  9.32      AA   N
ATOM    748  CA  ASP A  98     -19.489   6.786  -9.019  1.00 10.28      AA   C
ATOM    749  CB  ASP A  98     -20.430   7.698  -8.226  1.00 12.16      AA   C
ATOM    750  CG  ASP A  98     -19.912   8.093  -6.893  1.00 16.37      AA   C
ATOM    751  OD1 ASP A  98     -19.120   7.399  -6.229  1.00 16.78      AA   O
ATOM    752  OD2 ASP A  98     -20.478   9.090  -6.375  1.00 20.90      AA   O
ATOM    753  C   ASP A  98     -20.227   6.301 -10.257  1.00 10.03      AA   C
ATOM    754  O   ASP A  98     -20.510   7.118 -11.169  1.00  9.52      AA   O
ATOM    755  N   VAL A  99     -20.568   4.997 -10.264  1.00  9.78      AA   N
ATOM    756  CA  VAL A  99     -21.265   4.428 -11.374  1.00 11.32      AA   C
ATOM    757  CB  VAL A  99     -21.229   2.901 -11.241  1.00 10.09      AA   C
ATOM    758  CG1 VAL A  99     -22.130   2.192 -12.312  1.00 15.20      AA   C
ATOM    759  CG2 VAL A  99     -19.785   2.402 -11.480  1.00 12.93      AA   C
ATOM    760  C   VAL A  99     -22.690   4.994 -11.473  1.00 11.27      AA   C
ATOM    761  O   VAL A  99     -23.268   5.006 -12.571  1.00 10.66      AA   O
ATOM    762  N   SER A 100     -23.202   5.575 -10.355  1.00  9.97      AA   N
ATOM    763  CA  SER A 100     -24.518   6.289 -10.413  1.00 10.77      AA   C
ATOM    764  CB  SER A 100     -24.889   6.723  -9.005  1.00 12.56      AA   C
ATOM    765  OG  SER A 100     -23.933   7.608  -8.459  1.00 14.49      AA   O
ATOM    766  C   SER A 100     -24.451   7.470 -11.377  1.00 10.51      AA   C
ATOM    767  O   SER A 100     -25.523   8.024 -11.755  1.00 10.96      AA   O
```

```
ATOM    768  N   LYS A 101     -23.251   7.929 -11.759  1.00 10.79      AA   N
ATOM    769  CA  LYS A 101     -23.201   8.981 -12.756  1.00 11.81      AA   C
ATOM    770  CB  LYS A 101     -21.843   9.690 -12.790  1.00 14.35      AA   C
ATOM    771  CG  LYS A 101     -21.615  10.538 -11.509  1.00 14.32      AA   C
ATOM    772  CD  LYS A 101     -20.293  11.270 -11.527  1.00 21.28      AA   C
ATOM    773  CE  LYS A 101     -20.282  12.363 -10.396  1.00 25.41      AA   C
ATOM    774  NZ  LYS A 101     -20.548  11.709  -9.053  1.00 35.15      AA   N
ATOM    775  C   LYS A 101     -23.638   8.554 -14.144  1.00 13.02      AA   C
ATOM    776  O   LYS A 101     -23.810   9.465 -15.007  1.00 15.22      AA   O
ATOM    777  N   LEU A 102     -23.703   7.245 -14.425  1.00 10.62      AA   N
ATOM    778  CA  LEU A 102     -23.969   6.719 -15.745  1.00  8.80      AA   C
ATOM    779  CB  LEU A 102     -23.040   5.555 -16.030  1.00  9.64      AA   C
ATOM    780  CG  LEU A 102     -21.545   5.944 -15.946  1.00 10.40      AA   C
ATOM    781  CD1 LEU A 102     -20.667   4.684 -16.242  1.00 13.20      AA   C
ATOM    782  CD2 LEU A 102     -21.200   7.154 -16.865  1.00 13.14      AA   C
ATOM    783  C   LEU A 102     -25.396   6.156 -15.741  1.00 11.28      AA   C
ATOM    784  O   LEU A 102     -25.917   5.689 -14.699  1.00 12.32      AA   O
ATOM    785  N   LYS A 103     -25.993   6.054 -16.945  1.00 10.61      AA   N
ATOM    786  CA  LYS A 103     -27.312   5.428 -17.123  1.00 12.16      AA   C
ATOM    787  CB  LYS A 103     -28.249   6.585 -17.590  1.00 13.79      AA   C
ATOM    788  CG  LYS A 103     -29.744   6.393 -17.788  1.00 21.48      AA   C
ATOM    789  CD  LYS A 103     -30.265   7.851 -18.133  1.00 26.31      AA   C
ATOM    790  CE  LYS A 103     -31.753   7.944 -18.493  1.00 31.11      AA   C
ATOM    791  NZ  LYS A 103     -32.687   7.642 -17.336  1.00 33.89      AA   N
ATOM    792  C   LYS A 103     -27.185   4.364 -18.207  1.00 13.04      AA   C
ATOM    793  O   LYS A 103     -26.477   4.566 -19.202  1.00 13.19      AA   O
ATOM    794  N   GLU A 104     -27.907   3.234 -18.069  1.00 12.62      AA   N
ATOM    795  CA  GLU A 104     -28.010   2.299 -19.211  1.00 15.57      AA   C
ATOM    796  CB  GLU A 104     -28.888   1.120 -18.878  1.00 11.89      AA   C
ATOM    797  CG  GLU A 104     -28.166   0.220 -17.950  1.00 16.05      AA   C
ATOM    798  CD  GLU A 104     -28.816  -1.138 -17.879  1.00 18.04      AA   C
ATOM    799  OE1 GLU A 104     -28.767  -1.922 -18.896  1.00 22.62      AA   O
ATOM    800  OE2 GLU A 104     -29.336  -1.421 -16.803  1.00 18.45      AA   O
ATOM    801  C   GLU A 104     -28.690   2.969 -20.380  1.00 16.29      AA   C
ATOM    802  O   GLU A 104     -29.542   3.825 -20.174  1.00 17.17      AA   O
ATOM    803  N   GLY A 105     -28.284   2.641 -21.597  1.00 18.05      AA   N
ATOM    804  CA  GLY A 105     -28.944   3.187 -22.775  1.00 21.63      AA   C
ATOM    805  C   GLY A 105     -28.375   4.526 -23.245  1.00 23.80      AA   C
ATOM    806  O   GLY A 105     -28.546   4.868 -24.425  1.00 25.04      AA   O
ATOM    807  N   GLU A 106     -27.701   5.271 -22.345  1.00 21.93      AA   N
ATOM    808  CA  GLU A 106     -26.984   6.495 -22.730  1.00 21.33      AA   C
ATOM    809  CB  GLU A 106     -26.809   7.471 -21.546  1.00 21.42      AA   C
ATOM    810  CG  GLU A 106     -26.024   8.818 -21.848  1.00 21.58      AA   C
ATOM    811  CD  GLU A 106     -26.669   9.776 -22.861  1.00 26.42      AA   C
ATOM    812  OE1 GLU A 106     -27.367  10.723 -22.395  1.00 27.89      AA   O
ATOM    813  OE2 GLU A 106     -26.488   9.596 -24.116  1.00 24.30      AA   O
ATOM    814  C   GLU A 106     -25.705   6.085 -23.419  1.00 20.39      AA   C
ATOM    815  O   GLU A 106     -25.105   4.991 -23.166  1.00 21.12      AA   O
ATOM    816  N   GLN A 107     -25.277   6.970 -24.312  1.00 16.79      AA   N
ATOM    817  CA  GLN A 107     -24.014   6.702 -25.035  1.00 16.63      AA   C
ATOM    818  CB  GLN A 107     -24.144   6.792 -26.546  1.00 17.36      AA   C
ATOM    819  CG  GLN A 107     -25.252   5.840 -27.157  1.00 22.40      AA   C
ATOM    820  CD  GLN A 107     -25.582   6.249 -28.606  1.00 35.06      AA   C
ATOM    821  OE1 GLN A 107     -25.672   7.456 -28.934  1.00 38.85      AA   O
ATOM    822  NE2 GLN A 107     -25.758   5.254 -29.473  1.00 34.17      AA   N
```

ATOM 823 C GLN A 107 -22.924 7.648 -24.582 1.00 14.12 AA C
ATOM 824 O GLN A 107 -23.202 8.887 -24.563 1.00 14.95 AA O
ATOM 825 N TYR A 108 -21.813 7.043 -24.083 1.00 14.27 AA N
ATOM 826 CA TYR A 108 -20.719 7.835 -23.628 1.00 9.78 AA C
ATOM 827 CB TYR A 108 -20.345 7.451 -22.171 1.00 10.45 AA C
ATOM 828 CG TYR A 108 -21.505 7.555 -21.221 1.00 9.47 AA C
ATOM 829 CD1 TYR A 108 -21.887 8.787 -20.761 1.00 9.42 AA C
ATOM 830 CE1 TYR A 108 -23.016 8.978 -19.942 1.00 10.93 AA C
ATOM 831 CZ TYR A 108 -23.761 7.849 -19.619 1.00 9.33 AA C
ATOM 832 OH TYR A 108 -24.889 7.995 -18.791 1.00 9.56 AA O
ATOM 833 CE2 TYR A 108 -23.397 6.603 -20.097 1.00 9.21 AA C
ATOM 834 CD2 TYR A 108 -22.294 6.446 -20.855 1.00 10.00 AA C
ATOM 835 C TYR A 108 -19.489 7.598 -24.521 1.00 9.07 AA C
ATOM 836 O TYR A 108 -19.304 6.571 -25.183 1.00 10.05 AA O
ATOM 837 N MET A 109 -18.624 8.621 -24.512 1.00 8.19 AA N
ATOM 838 CA MET A 109 -17.294 8.540 -25.195 1.00 8.63 AA C
ATOM 839 CB MET A 109 -17.225 9.562 -26.334 1.00 10.30 AA C
ATOM 840 CG MET A 109 -18.235 9.324 -27.508 1.00 11.08 AA C
ATOM 841 SD MET A 109 -17.922 7.800 -28.427 1.00 11.83 AA S
ATOM 842 CE MET A 109 -16.415 8.247 -29.207 1.00 13.65 AA C
ATOM 843 C MET A 109 -16.254 8.884 -24.221 1.00 7.60 AA C
ATOM 844 O MET A 109 -16.449 9.777 -23.380 1.00 9.86 AA O
ATOM 845 N PHE A 110 -15.098 8.185 -24.314 1.00 7.73 AA N
ATOM 846 CA PHE A 110 -13.918 8.634 -23.625 1.00 9.46 AA C
ATOM 847 CB PHE A 110 -13.312 7.474 -22.746 1.00 8.44 AA C
ATOM 848 CG PHE A 110 -12.741 6.319 -23.501 1.00 8.03 AA C
ATOM 849 CD1 PHE A 110 -11.425 6.326 -23.972 1.00 8.84 AA C
ATOM 850 CE1 PHE A 110 -10.827 5.251 -24.669 1.00 10.04 AA C
ATOM 851 CZ PHE A 110 -11.625 4.151 -24.962 1.00 9.21 AA C
ATOM 852 CE2 PHE A 110 -12.951 4.107 -24.548 1.00 9.93 AA C
ATOM 853 CD2 PHE A 110 -13.493 5.210 -23.818 1.00 8.34 AA C
ATOM 854 C PHE A 110 -12.895 9.095 -24.653 1.00 7.92 AA C
ATOM 855 O PHE A 110 -12.923 8.634 -25.846 1.00 8.71 AA O
ATOM 856 N PHE A 111 -12.040 10.004 -24.258 1.00 7.84 AA N
ATOM 857 CA PHE A 111 -11.123 10.633 -25.248 1.00 8.68 AA C
ATOM 858 CB PHE A 111 -11.912 11.564 -26.204 1.00 9.45 AA C
ATOM 859 CG PHE A 111 -12.893 12.470 -25.492 1.00 8.44 AA C
ATOM 860 CD1 PHE A 111 -14.206 12.052 -25.215 1.00 8.62 AA C
ATOM 861 CE1 PHE A 111 -15.066 12.843 -24.534 1.00 8.54 AA C
ATOM 862 CZ PHE A 111 -14.680 14.080 -24.057 1.00 8.13 AA C
ATOM 863 CE2 PHE A 111 -13.447 14.550 -24.305 1.00 8.74 AA C
ATOM 864 CD2 PHE A 111 -12.528 13.725 -25.024 1.00 8.18 AA C
ATOM 865 C PHE A 111 -10.045 11.403 -24.515 1.00 8.32 AA C
ATOM 866 O PHE A 111 -10.146 11.706 -23.321 1.00 8.58 AA O
ATOM 867 N CYS A 112 -8.999 11.722 -25.247 1.00 8.37 AA N
ATOM 868 CA CYS A 112 -7.935 12.667 -24.850 1.00 9.06 AA C
ATOM 869 CB CYS A 112 -6.571 12.148 -25.377 1.00 9.23 AA C
ATOM 870 SG CYS A 112 -5.221 13.275 -24.941 1.00 9.32 AA S
ATOM 871 C CYS A 112 -8.252 14.059 -25.432 1.00 7.72 AA C
ATOM 872 O CYS A 112 -8.580 14.134 -26.622 1.00 9.36 AA O
ATOM 873 N THR A 113 -8.110 15.100 -24.609 1.00 7.83 AA N
ATOM 874 CA THR A 113 -8.303 16.454 -25.107 1.00 8.70 AA C
ATOM 875 CB THR A 113 -9.154 17.295 -24.118 1.00 7.73 AA C
ATOM 876 OG1 THR A 113 -8.430 17.432 -22.909 1.00 8.57 AA O
ATOM 877 CG2 THR A 113 -10.445 16.652 -23.818 1.00 8.83 AA C

```
ATOM    878  C   THR A 113      -7.064  17.228 -25.451  1.00  7.20      AA   C
ATOM    879  O   THR A 113      -7.146  18.406 -25.793  1.00  9.30      AA   O
ATOM    880  N   PHE A 114      -5.901  16.571 -25.452  1.00  8.23      AA   N
ATOM    881  CA  PHE A 114      -4.694  17.292 -25.916  1.00  8.51      AA   C
ATOM    882  CB  PHE A 114      -3.443  16.385 -25.792  1.00  8.02      AA   C
ATOM    883  CG  PHE A 114      -2.162  17.117 -26.060  1.00  9.31      AA   C
ATOM    884  CD1 PHE A 114      -1.750  17.359 -27.371  1.00  9.64      AA   C
ATOM    885  CE1 PHE A 114      -0.568  18.060 -27.644  1.00 11.07      AA   C
ATOM    886  CZ  PHE A 114       0.145  18.576 -26.543  1.00 11.47      AA   C
ATOM    887  CE2 PHE A 114      -0.263  18.363 -25.228  1.00  9.06      AA   C
ATOM    888  CD2 PHE A 114      -1.432  17.681 -25.004  1.00  9.36      AA   C
ATOM    889  C   PHE A 114      -4.967  17.693 -27.413  1.00  9.12      AA   C
ATOM    890  O   PHE A 114      -5.506  16.847 -28.134  1.00  8.70      AA   O
ATOM    891  N   PRO A 115      -4.549  18.882 -27.898  1.00  7.88      AA   N
ATOM    892  CA  PRO A 115      -4.902  19.297 -29.262  1.00  8.50      AA   C
ATOM    893  CB  PRO A 115      -4.096  20.568 -29.435  1.00  8.46      AA   C
ATOM    894  CG  PRO A 115      -3.970  21.141 -27.991  1.00 10.13      AA   C
ATOM    895  CD  PRO A 115      -3.938  19.954 -27.083  1.00  8.41      AA   C
ATOM    896  C   PRO A 115      -4.555  18.222 -30.290  1.00  7.60      AA   C
ATOM    897  O   PRO A 115      -3.426  17.737 -30.353  1.00  8.02      AA   O
ATOM    898  N   GLY A 116      -5.554  17.923 -31.126  1.00  7.94      AA   N
ATOM    899  CA  GLY A 116      -5.373  16.935 -32.221  1.00  8.82      AA   C
ATOM    900  C   GLY A 116      -5.604  15.509 -31.856  1.00  7.47      AA   C
ATOM    901  O   GLY A 116      -5.870  14.716 -32.725  1.00  9.98      AA   O
ATOM    902  N   HIS A 117      -5.484  15.167 -30.605  1.00  7.99      AA   N
ATOM    903  CA  HIS A 117      -5.432  13.755 -30.241  1.00  8.60      AA   C
ATOM    904  CB  HIS A 117      -4.874  13.517 -28.817  1.00  9.26      AA   C
ATOM    905  CG  HIS A 117      -3.435  13.902 -28.685  1.00  8.77      AA   C
ATOM    906  ND1 HIS A 117      -2.707  13.503 -27.592  1.00  7.21      AA   N
ATOM    907  CE1 HIS A 117      -1.450  13.898 -27.800  1.00  7.59      AA   C
ATOM    908  NE2 HIS A 117      -1.314  14.496 -28.976  1.00  8.66      AA   N
ATOM    909  CD2 HIS A 117      -2.577  14.503 -29.549  1.00  8.80      AA   C
ATOM    910  C   HIS A 117      -6.712  13.007 -30.379  1.00  8.21      AA   C
ATOM    911  O   HIS A 117      -6.680  11.791 -30.706  1.00 10.15      AA   O
ATOM    912  N   SER A 118      -7.840  13.669 -30.193  1.00  8.17      AA   N
ATOM    913  CA  SER A 118      -9.125  12.922 -30.220  1.00  8.77      AA   C
ATOM    914  CB  SER A 118     -10.273  13.851 -29.780  1.00 10.59      AA   C
ATOM    915  OG  SER A 118     -10.546  14.871 -30.704  1.00 12.27      AA   O
ATOM    916  C   SER A 118      -9.415  12.409 -31.648  1.00 10.16      AA   C
ATOM    917  O   SER A 118     -10.354  11.599 -31.832  1.00 11.22      AA   O
ATOM    918  N   ALA A 119      -8.714  12.825 -32.698  1.00  8.35      AA   N
ATOM    919  CA  ALA A 119      -8.863  12.207 -34.013  1.00 10.31      AA   C
ATOM    920  CB  ALA A 119      -7.821  12.792 -35.071  1.00 11.07      AA   C
ATOM    921  C   ALA A 119      -8.726  10.726 -33.933  1.00 10.44      AA   C
ATOM    922  O   ALA A 119      -9.389  10.006 -34.710  1.00 11.79      AA   O
ATOM    923  N   LEU A 120      -7.825  10.234 -33.073  1.00  8.71      AA   N
ATOM    924  CA  LEU A 120      -7.605   8.808 -32.847  1.00  9.94      AA   C
ATOM    925  CB  LEU A 120      -6.187   8.318 -33.285  1.00 13.06      AA   C
ATOM    926  CG  LEU A 120      -6.018   8.297 -34.820  1.00 17.49      AA   C
ATOM    927  CD1 LEU A 120      -4.616   7.907 -35.150  1.00 19.16      AA   C
ATOM    928  CD2 LEU A 120      -7.021   7.328 -35.502  1.00 16.93      AA   C
ATOM    929  C   LEU A 120      -7.857   8.356 -31.453  1.00  9.27      AA   C
ATOM    930  O   LEU A 120      -8.280   7.242 -31.278  1.00  9.45      AA   O
ATOM    931  N   MET A 121      -7.644   9.213 -30.490  1.00  8.26      AA   N
ATOM    932  CA  MET A 121      -7.654   8.783 -29.055  1.00  8.56      AA   C
```

ATOM 933 CB MET A 121 -6.637 9.598 -28.286 1.00 8.37 AA C
ATOM 934 CG MET A 121 -5.228 9.261 -28.776 1.00 10.95 AA C
ATOM 935 SD MET A 121 -3.921 9.991 -27.741 1.00 9.56 AA S
ATOM 936 CE MET A 121 -3.871 8.772 -26.423 1.00 9.54 AA C
ATOM 937 C MET A 121 -9.071 8.970 -28.524 1.00 9.21 AA C
ATOM 938 O MET A 121 -9.357 9.957 -27.840 1.00 9.45 AA O
ATOM 939 N LYS A 122 -9.956 8.042 -28.883 1.00 8.44 AA N
ATOM 940 CA ALYS A 122 -11.331 8.090 -28.394 0.50 8.33 AA C
ATOM 941 CA BLYS A 122 -11.355 8.091 -28.422 0.50 8.40 AA C
ATOM 942 CB ALYS A 122 -12.168 9.089 -29.233 0.50 9.70 AA C
ATOM 943 CB BLYS A 122 -12.240 9.025 -29.304 0.50 9.91 AA C
ATOM 944 CG ALYS A 122 -12.593 8.575 -30.618 0.50 9.83 AA C
ATOM 945 CG BLYS A 122 -12.387 8.598 -30.774 0.50 10.30 AA C
ATOM 946 CD ALYS A 122 -11.459 8.468 -31.645 0.50 8.54 AA C
ATOM 947 CD BLYS A 122 -13.204 9.608 -31.518 0.50 14.15 AA C
ATOM 948 CE ALYS A 122 -12.073 8.228 -33.052 0.50 13.27 AA C
ATOM 949 CE BLYS A 122 -12.707 9.853 -32.977 0.50 15.12 AA C
ATOM 950 NZ ALYS A 122 -10.967 7.687 -33.945 0.50 10.86 AA N
ATOM 951 NZ BLYS A 122 -12.790 11.380 -33.152 0.50 19.31 AA N
ATOM 952 C LYS A 122 -11.899 6.679 -28.481 1.00 8.74 AA C
ATOM 953 O LYS A 122 -11.398 5.826 -29.241 1.00 9.21 AA O
ATOM 954 N GLY A 123 -12.988 6.447 -27.756 1.00 8.61 AA N
ATOM 955 CA GLY A 123 -13.700 5.147 -27.836 1.00 7.60 AA C
ATOM 956 C GLY A 123 -14.950 5.246 -27.047 1.00 8.04 AA C
ATOM 957 O GLY A 123 -15.299 6.325 -26.546 1.00 8.70 AA O
ATOM 958 N THR A 124 -15.733 4.153 -27.103 1.00 8.39 AA N
ATOM 959 CA THR A 124 -17.059 4.189 -26.450 1.00 8.66 AA C
ATOM 960 CB THR A 124 -18.072 3.300 -27.227 1.00 7.93 AA C
ATOM 961 OG1 THR A 124 -17.533 1.964 -27.285 1.00 7.96 AA O
ATOM 962 CG2 THR A 124 -18.162 3.828 -28.625 1.00 7.31 AA C
ATOM 963 C THR A 124 -16.943 3.657 -25.012 1.00 8.22 AA C
ATOM 964 O THR A 124 -16.070 2.866 -24.656 1.00 8.84 AA O
ATOM 965 N LEU A 125 -17.929 4.125 -24.209 1.00 9.24 AA N
ATOM 966 CA LEU A 125 -18.058 3.560 -22.850 1.00 10.34 AA C
ATOM 967 CB LEU A 125 -17.486 4.474 -21.751 1.00 9.09 AA C
ATOM 968 CG LEU A 125 -17.573 3.863 -20.317 1.00 8.31 AA C
ATOM 969 CD1 LEU A 125 -16.399 4.330 -19.484 1.00 10.53 AA C
ATOM 970 CD2 LEU A 125 -18.926 4.393 -19.638 1.00 9.06 AA C
ATOM 971 C LEU A 125 -19.575 3.311 -22.619 1.00 9.13 AA C
ATOM 972 O LEU A 125 -20.399 4.142 -22.969 1.00 10.51 AA O
ATOM 973 N THR A 126 -19.896 2.152 -22.101 1.00 10.04 AA N
ATOM 974 CA ATHR A 126 -21.290 1.789 -21.875 0.50 10.57 AA C
ATOM 975 CA BTHR A 126 -21.296 1.831 -21.855 0.50 10.65 AA C
ATOM 976 CB ATHR A 126 -21.823 0.817 -22.987 0.50 11.84 AA C
ATOM 977 CB BTHR A 126 -21.844 0.943 -23.012 0.50 12.54 AA C
ATOM 978 OG1ATHR A 126 -21.601 -0.550 -22.636 0.50 17.39 AA O
ATOM 979 OG1BTHR A 126 -23.239 0.606 -22.834 0.50 14.19 AA O
ATOM 980 CG2ATHR A 126 -21.170 1.137 -24.367 0.50 10.02 AA C
ATOM 981 CG2BTHR A 126 -20.980 -0.270 -23.189 0.50 13.03 AA C
ATOM 982 C THR A 126 -21.459 1.138 -20.526 1.00 13.09 AA C
ATOM 983 O THR A 126 -20.561 0.363 -20.110 1.00 12.75 AA O
ATOM 984 N LEU A 127 -22.616 1.405 -19.886 1.00 12.72 AA N
ATOM 985 CA LEU A 127 -22.949 0.754 -18.620 1.00 14.49 AA C
ATOM 986 CB LEU A 127 -23.769 1.744 -17.796 1.00 15.69 AA C
ATOM 987 CG LEU A 127 -24.284 1.281 -16.442 1.00 13.62 AA C

```
ATOM    988  CD1 LEU A 127     -23.053   0.974 -15.606  1.00 15.17      AA   C
ATOM    989  CD2 LEU A 127     -25.209   2.306 -15.824  1.00 14.24      AA   C
ATOM    990  C   LEU A 127     -23.850  -0.423 -18.973  1.00 15.12      AA   C
ATOM    991  O   LEU A 127     -24.858  -0.205 -19.699  1.00 15.50      AA   O
ATOM    992  N   LYS A 128     -23.434  -1.620 -18.566  1.00 14.46      AA   N
ATOM    993  CA  LYS A 128     -24.309  -2.774 -18.771  1.00 17.12      AA   C
ATOM    994  CB  LYS A 128     -23.879  -3.522 -20.022  1.00 18.04      AA   C
ATOM    995  CG  LYS A 128     -22.755  -4.463 -19.843  1.00 23.54      AA   C
ATOM    996  CD  LYS A 128     -23.104  -5.761 -20.637  1.00 28.32      AA   C
ATOM    997  CE  LYS A 128     -22.045  -6.899 -20.574  1.00 29.21      AA   C
ATOM    998  NZ  LYS A 128     -22.475  -8.053 -21.465  1.00 36.07      AA   N
ATOM    999  C   LYS A 128     -24.364  -3.740 -17.597  1.00 17.14      AA   C
ATOM   1000  O   LYS A 128     -23.490  -3.717 -16.741  1.00 18.73      AA   O
ATOM   1001  OXT LYS A 128     -25.305  -4.608 -17.550  1.00 17.50      AA   O
ATOM   1002  N   ALA B   1     -47.066  24.741 -13.022  1.00 13.47      BA   N
ATOM   1003  CA  ALA B   1     -45.902  24.219 -12.243  1.00 11.73      BA   C
ATOM   1004  CB  ALA B   1     -44.820  23.692 -13.204  1.00 15.51      BA   C
ATOM   1005  C   ALA B   1     -45.340  25.235 -11.304  1.00 12.42      BA   C
ATOM   1006  O   ALA B   1     -45.667  26.430 -11.437  1.00 13.52      BA   O
ATOM   1007  N   GLU B   2     -44.646  24.838 -10.286  1.00 12.12      BA   N
ATOM   1008  CA  GLU B   2     -44.004  25.767  -9.353  1.00 12.95      BA   C
ATOM   1009  CB  GLU B   2     -44.799  25.880  -8.046  1.00 16.05      BA   C
ATOM   1010  CG  GLU B   2     -46.127  26.719  -8.097  1.00 21.36      BA   C
ATOM   1011  CD  GLU B   2     -45.955  28.257  -8.399  1.00 27.46      BA   C
ATOM   1012  OE1 GLU B   2     -44.812  28.800  -8.565  1.00 26.74      BA   O
ATOM   1013  OE2 GLU B   2     -47.026  28.914  -8.476  1.00 33.29      BA   O
ATOM   1014  C   GLU B   2     -42.643  25.148  -9.066  1.00 13.18      BA   C
ATOM   1015  O   GLU B   2     -42.557  24.176  -8.288  1.00 15.26      BA   O
ATOM   1016  N   CYS B   3     -41.621  25.628  -9.747  1.00 12.02      BA   N
ATOM   1017  CA  CYS B   3     -40.290  25.084  -9.758  1.00  8.85      BA   C
ATOM   1018  CB  CYS B   3     -40.034  24.468 -11.132  1.00  8.99      BA   C
ATOM   1019  SG  CYS B   3     -41.080  23.027 -11.407  1.00 11.35      BA   S
ATOM   1020  C   CYS B   3     -39.283  26.180  -9.448  1.00 11.50      BA   C
ATOM   1021  O   CYS B   3     -38.100  25.984  -9.817  1.00 10.46      BA   O
ATOM   1022  N   SER B   4     -39.666  27.200  -8.648  1.00 11.47      BA   N
ATOM   1023  CA ASER B   4     -38.651  28.151  -8.178  0.50 11.27      BA   C
ATOM   1024  CA BSER B   4     -38.776  28.332  -8.267  0.50  9.68      BA   C
ATOM   1025  CB ASER B   4     -38.618  29.276  -9.163  0.50 11.38      BA   C
ATOM   1026  CB BSER B   4     -39.094  29.593  -9.100  0.50  7.57      BA   C
ATOM   1027  OG ASER B   4     -39.820  29.946  -9.054  0.50 15.63      BA   O
ATOM   1028  OG BSER B   4     -38.941  29.385 -10.521  0.50  7.47      BA   O
ATOM   1029  C   SER B   4     -38.996  28.670  -6.796  1.00 11.99      BA   C
ATOM   1030  O   SER B   4     -40.089  28.373  -6.263  1.00 14.09      BA   O
ATOM   1031  N   VAL B   5     -38.052  29.344  -6.159  1.00 11.12      BA   N
ATOM   1032  CA  VAL B   5     -38.220  29.974  -4.859  1.00 10.66      BA   C
ATOM   1033  CB  VAL B   5     -37.804  29.019  -3.777  1.00 13.58      BA   C
ATOM   1034  CG1 VAL B   5     -36.282  28.733  -3.728  1.00 14.71      BA   C
ATOM   1035  CG2 VAL B   5     -38.301  29.594  -2.468  1.00 15.81      BA   C
ATOM   1036  C   VAL B   5     -37.424  31.281  -4.880  1.00 12.49      BA   C
ATOM   1037  O   VAL B   5     -36.391  31.358  -5.527  1.00 13.18      BA   O
ATOM   1038  N   ASP B   6     -37.948  32.319  -4.228  1.00 12.87      BA   N
ATOM   1039  CA  ASP B   6     -37.256  33.585  -3.945  1.00 13.04      BA   C
ATOM   1040  CB  ASP B   6     -38.189  34.744  -4.143  1.00 15.20      BA   C
ATOM   1041  CG  ASP B   6     -38.758  34.731  -5.573  1.00 20.37      BA   C
ATOM   1042  OD1 ASP B   6     -38.015  34.875  -6.552  1.00 21.50      BA   O
```

ATOM 1043 OD2 ASP B 6 -39.956 34.447 -5.686 1.00 22.74 BA O
ATOM 1044 C ASP B 6 -36.683 33.535 -2.560 1.00 15.23 BA C
ATOM 1045 O ASP B 6 -37.421 33.250 -1.587 1.00 16.65 BA O
ATOM 1046 N ILE B 7 -35.376 33.812 -2.497 1.00 12.76 BA N
ATOM 1047 CA ILE B 7 -34.625 33.860 -1.217 1.00 13.48 BA C
ATOM 1048 CB ILE B 7 -33.503 32.870 -1.258 1.00 13.45 BA C
ATOM 1049 CG1 ILE B 7 -33.986 31.417 -1.402 1.00 15.65 BA C
ATOM 1050 CD1 ILE B 7 -34.858 30.876 -0.233 1.00 18.97 BA C
ATOM 1051 CG2 ILE B 7 -32.726 32.951 0.132 1.00 16.52 BA C
ATOM 1052 C ILE B 7 -34.047 35.277 -1.148 1.00 12.83 BA C
ATOM 1053 O ILE B 7 -33.432 35.790 -2.087 1.00 13.06 BA O
ATOM 1054 N MET B 8 -34.190 35.891 0.036 1.00 13.40 BA N
ATOM 1055 CA AMET B 8 -33.590 37.213 0.252 0.50 12.71 BA C
ATOM 1056 CA BMET B 8 -33.677 37.264 0.308 0.50 13.31 BA C
ATOM 1057 CB AMET B 8 -34.675 38.292 0.333 0.50 13.65 BA C
ATOM 1058 CB BMET B 8 -34.816 38.273 0.664 0.50 14.60 BA C
ATOM 1059 CG AMET B 8 -35.494 38.375 -0.964 0.50 15.17 BA C
ATOM 1060 CG BMET B 8 -35.710 38.745 -0.476 0.50 16.74 BA C
ATOM 1061 SD AMET B 8 -37.249 38.891 -0.844 0.50 19.13 BA S
ATOM 1062 SD BMET B 8 -36.699 37.358 -1.133 0.50 15.35 BA S
ATOM 1063 CE AMET B 8 -37.666 38.843 -2.601 0.50 19.36 BA C
ATOM 1064 CE BMET B 8 -37.961 38.114 -2.137 0.50 13.60 BA C
ATOM 1065 C MET B 8 -32.777 37.197 1.541 1.00 11.47 BA C
ATOM 1066 O MET B 8 -33.270 36.716 2.573 1.00 14.29 BA O
ATOM 1067 N GLY B 9 -31.560 37.722 1.407 1.00 12.39 BA N
ATOM 1068 CA GLY B 9 -30.633 37.878 2.567 1.00 12.60 BA C
ATOM 1069 C GLY B 9 -30.426 39.349 2.771 1.00 12.96 BA C
ATOM 1070 O GLY B 9 -30.076 40.046 1.825 1.00 12.55 BA O
ATOM 1071 N ASN B 10 -30.608 39.782 4.031 1.00 11.75 BA N
ATOM 1072 CA ASN B 10 -30.589 41.253 4.290 1.00 12.30 BA C
ATOM 1073 CB ASN B 10 -31.876 41.677 5.049 1.00 12.40 BA C
ATOM 1074 CG ASN B 10 -31.983 41.064 6.482 1.00 12.93 BA C
ATOM 1075 OD1 ASN B 10 -31.036 40.545 7.052 1.00 11.25 BA O
ATOM 1076 ND2 ASN B 10 -33.187 41.091 7.051 1.00 14.57 BA N
ATOM 1077 C ASN B 10 -29.340 41.671 5.068 1.00 11.37 BA C
ATOM 1078 O ASN B 10 -28.404 40.799 5.282 1.00 11.61 BA O
ATOM 1079 N ASP B 11 -29.214 42.917 5.555 1.00 9.81 BA N
ATOM 1080 CA ASP B 11 -28.001 43.387 6.149 1.00 10.03 BA C
ATOM 1081 CB ASP B 11 -28.004 44.912 6.245 1.00 11.30 BA C
ATOM 1082 CG ASP B 11 -27.688 45.630 4.954 1.00 11.56 BA C
ATOM 1083 OD1 ASP B 11 -27.233 45.057 3.949 1.00 14.08 BA O
ATOM 1084 OD2 ASP B 11 -28.020 46.843 4.977 1.00 13.78 BA O
ATOM 1085 C ASP B 11 -27.857 42.864 7.553 1.00 10.69 BA C
ATOM 1086 O ASP B 11 -26.830 43.119 8.212 1.00 13.75 BA O
ATOM 1087 N GLN B 12 -28.890 42.257 8.086 1.00 10.05 BA N
ATOM 1088 CA GLN B 12 -28.898 41.650 9.439 1.00 11.41 BA C
ATOM 1089 CB GLN B 12 -30.273 41.818 10.139 1.00 12.78 BA C
ATOM 1090 CG GLN B 12 -30.597 43.299 10.612 1.00 11.20 BA C
ATOM 1091 CD GLN B 12 -30.774 44.248 9.480 1.00 14.02 BA C
ATOM 1092 OE1 GLN B 12 -31.530 43.982 8.538 1.00 15.38 BA O
ATOM 1093 NE2 GLN B 12 -30.143 45.376 9.578 1.00 14.98 BA N
ATOM 1094 C GLN B 12 -28.536 40.151 9.396 1.00 11.15 BA C
ATOM 1095 O GLN B 12 -28.657 39.415 10.379 1.00 13.29 BA O
ATOM 1096 N MET B 13 -28.052 39.678 8.268 1.00 9.80 BA N
ATOM 1097 CA MET B 13 -27.594 38.281 8.149 1.00 10.96 BA C

```
ATOM   1098  CB  MET B  13     -26.328  37.954   8.922  1.00 14.82     BA   C
ATOM   1099  CG  MET B  13     -25.127  38.630   8.287  1.00 15.75     BA   C
ATOM   1100  SD  MET B  13     -23.980  39.247   9.499  1.00 15.28     BA   S
ATOM   1101  CE  MET B  13     -24.970  40.531  10.261  1.00 16.47     BA   C
ATOM   1102  C   MET B  13     -28.725  37.336   8.396  1.00 12.78     BA   C
ATOM   1103  O   MET B  13     -28.576  36.293   9.125  1.00 12.40     BA   O
ATOM   1104  N   HIS B  14     -29.842  37.625   7.758  1.00 11.08     BA   N
ATOM   1105  CA  HIS B  14     -31.069  36.818   7.921  1.00 13.01     BA   C
ATOM   1106  CB  HIS B  14     -32.114  37.646   8.724  1.00 13.49     BA   C
ATOM   1107  CG  HIS B  14     -33.458  37.031   8.866  1.00 13.46     BA   C
ATOM   1108  ND1 HIS B  14     -33.722  36.014   9.773  1.00 15.76     BA   N
ATOM   1109  CE1 HIS B  14     -34.998  35.671   9.697  1.00 14.92     BA   C
ATOM   1110  NE2 HIS B  14     -35.604  36.471   8.829  1.00 14.74     BA   N
ATOM   1111  CD2 HIS B  14     -34.661  37.339   8.308  1.00 12.46     BA   C
ATOM   1112  C   HIS B  14     -31.620  36.466   6.577  1.00 12.33     BA   C
ATOM   1113  O   HIS B  14     -31.725  37.331   5.690  1.00 12.36     BA   O
ATOM   1114  N   PHE B  15     -31.863  35.175   6.366  1.00 11.74     BA   N
ATOM   1115  CA  PHE B  15     -32.765  34.755   5.305  1.00 12.67     BA   C
ATOM   1116  CB  PHE B  15     -32.395  33.327   4.778  1.00 11.86     BA   C
ATOM   1117  CG  PHE B  15     -31.100  33.242   3.936  1.00 11.84     BA   C
ATOM   1118  CD1 PHE B  15     -30.868  34.074   2.821  1.00 12.45     BA   C
ATOM   1119  CE1 PHE B  15     -29.742  33.863   2.032  1.00 11.94     BA   C
ATOM   1120  CZ  PHE B  15     -28.823  32.808   2.362  1.00 11.38     BA   C
ATOM   1121  CE2 PHE B  15     -29.030  31.966   3.386  1.00 10.71     BA   C
ATOM   1122  CD2 PHE B  15     -30.206  32.188   4.186  1.00 12.35     BA   C
ATOM   1123  C   PHE B  15     -34.182  34.637   5.909  1.00 10.92     BA   C
ATOM   1124  O   PHE B  15     -34.351  34.048   6.993  1.00 13.33     BA   O
ATOM   1125  N   HIS B  16     -35.231  35.082   5.231  1.00 11.62     BA   N
ATOM   1126  CA  HIS B  16     -36.586  34.903   5.774  1.00 13.03     BA   C
ATOM   1127  CB  HIS B  16     -37.594  35.874   5.117  1.00 13.84     BA   C
ATOM   1128  CG  HIS B  16     -37.378  37.301   5.466  1.00 12.99     BA   C
ATOM   1129  ND1 HIS B  16     -37.418  37.754   6.746  1.00 12.45     BA   N
ATOM   1130  CE1 HIS B  16     -37.216  39.074   6.756  1.00 15.42     BA   C
ATOM   1131  NE2 HIS B  16     -37.054  39.457   5.502  1.00 16.20     BA   N
ATOM   1132  CD2 HIS B  16     -37.151  38.379   4.683  1.00 17.91     BA   C
ATOM   1133  C   HIS B  16     -37.044  33.429   5.663  1.00 14.67     BA   C
ATOM   1134  O   HIS B  16     -37.935  32.944   6.459  1.00 16.84     BA   O
ATOM   1135  N   THR B  17     -36.420  32.689   4.761  1.00 13.54     BA   N
ATOM   1136  CA  THR B  17     -36.778  31.267   4.483  1.00 14.97     BA   C
ATOM   1137  CB  THR B  17     -36.515  30.976   3.021  1.00 14.07     BA   C
ATOM   1138  OG1 THR B  17     -37.362  31.801   2.298  1.00 18.78     BA   O
ATOM   1139  CG2 THR B  17     -36.741  29.518   2.594  1.00 16.93     BA   C
ATOM   1140  C   THR B  17     -35.903  30.323   5.250  1.00 13.39     BA   C
ATOM   1141  O   THR B  17     -34.675  30.400   5.192  1.00 14.30     BA   O
ATOM   1142  N   ASN B  18     -36.544  29.409   6.009  1.00 13.68     BA   N
ATOM   1143  CA  ASN B  18     -35.832  28.423   6.783  1.00 14.78     BA   C
ATOM   1144  CB  ASN B  18     -36.613  28.204   8.138  1.00 14.20     BA   C
ATOM   1145  CG  ASN B  18     -38.076  27.598   7.950  1.00 17.33     BA   C
ATOM   1146  OD1 ASN B  18     -38.488  26.538   8.582  1.00 16.28     BA   O
ATOM   1147  ND2 ASN B  18     -38.935  28.384   7.229  1.00 14.51     BA   N
ATOM   1148  C   ASN B  18     -35.636  27.079   6.030  1.00 12.84     BA   C
ATOM   1149  O   ASN B  18     -34.753  26.242   6.406  1.00 12.30     BA   O
ATOM   1150  N   ALA B  19     -36.533  26.792   5.101  1.00 11.18     BA   N
ATOM   1151  CA  ALA B  19     -36.674  25.474   4.560  1.00 11.39     BA   C
ATOM   1152  CB  ALA B  19     -37.596  24.587   5.454  1.00 13.31     BA   C
```

```
ATOM   1153  C   ALA B  19     -37.244  25.634   3.154  1.00 10.60      BA   C
ATOM   1154  O   ALA B  19     -38.195  26.346   2.946  1.00 13.04      BA   O
ATOM   1155  N   ILE B  20     -36.714  24.855   2.234  1.00 11.94      BA   N
ATOM   1156  CA  ILE B  20     -37.170  24.845   0.819  1.00 10.62      BA   C
ATOM   1157  CB  ILE B  20     -35.977  25.260  -0.140  1.00 11.47      BA   C
ATOM   1158  CG1 ILE B  20     -35.564  26.709   0.143  1.00 11.80      BA   C
ATOM   1159  CD1 ILE B  20     -34.207  27.100  -0.450  1.00 13.13      BA   C
ATOM   1160  CG2 ILE B  20     -36.316  25.027  -1.605  1.00 13.29      BA   C
ATOM   1161  C   ILE B  20     -37.575  23.429   0.482  1.00 10.50      BA   C
ATOM   1162  O   ILE B  20     -36.833  22.462   0.686  1.00 12.90      BA   O
ATOM   1163  N   THR B  21     -38.755  23.319  -0.117  1.00 10.86      BA   N
ATOM   1164  CA  THR B  21     -39.186  21.997  -0.627  1.00 12.54      BA   C
ATOM   1165  CB  THR B  21     -40.624  21.724  -0.147  1.00 14.08      BA   C
ATOM   1166  OG1 THR B  21     -40.632  21.725   1.287  1.00 15.54      BA   O
ATOM   1167  CG2 THR B  21     -41.112  20.358  -0.754  1.00 14.86      BA   C
ATOM   1168  C   THR B  21     -39.180  22.068  -2.118  1.00 12.93      BA   C
ATOM   1169  O   THR B  21     -39.861  22.946  -2.707  1.00 16.96      BA   O
ATOM   1170  N   VAL B  22     -38.539  21.142  -2.763  1.00 11.09      BA   N
ATOM   1171  CA  VAL B  22     -38.487  21.069  -4.220  1.00 11.84      BA   C
ATOM   1172  CB  VAL B  22     -37.051  20.700  -4.642  1.00 11.47      BA   C
ATOM   1173  CG1 VAL B  22     -36.979  20.467  -6.163  1.00 12.80      BA   C
ATOM   1174  CG2 VAL B  22     -36.049  21.787  -4.142  1.00 12.72      BA   C
ATOM   1175  C   VAL B  22     -39.468  20.012  -4.684  1.00 12.38      BA   C
ATOM   1176  O   VAL B  22     -39.362  18.840  -4.239  1.00 13.38      BA   O
ATOM   1177  N   ASP B  23     -40.393  20.381  -5.543  1.00 12.05      BA   N
ATOM   1178  CA  ASP B  23     -41.354  19.442  -6.079  1.00 10.10      BA   C
ATOM   1179  CB  ASP B  23     -42.493  20.295  -6.780  1.00 14.03      BA   C
ATOM   1180  CG  ASP B  23     -43.488  19.482  -7.551  1.00 14.81      BA   C
ATOM   1181  OD1 ASP B  23     -43.324  18.278  -7.765  1.00 15.42      BA   O
ATOM   1182  OD2 ASP B  23     -44.539  20.099  -7.863  1.00 18.09      BA   O
ATOM   1183  C   ASP B  23     -40.559  18.511  -6.979  1.00 12.26      BA   C
ATOM   1184  O   ASP B  23     -39.985  18.944  -8.026  1.00 12.77      BA   O
ATOM   1185  N   LYS B  24     -40.683  17.200  -6.667  1.00 12.71      BA   N
ATOM   1186  CA  LYS B  24     -39.866  16.251  -7.407  1.00 15.03      BA   C
ATOM   1187  CB  LYS B  24     -39.801  14.887  -6.679  1.00 14.87      BA   C
ATOM   1188  CG  LYS B  24     -41.176  14.194  -6.756  1.00 14.68      BA   C
ATOM   1189  CD  LYS B  24     -41.181  12.930  -5.820  1.00 14.75      BA   C
ATOM   1190  CE  LYS B  24     -42.515  12.214  -5.753  1.00 12.15      BA   C
ATOM   1191  NZ  LYS B  24     -43.029  11.871  -7.128  1.00 13.60      BA   N
ATOM   1192  C   LYS B  24     -40.325  16.083  -8.866  1.00 14.27      BA   C
ATOM   1193  O   LYS B  24     -39.650  15.420  -9.645  1.00 15.60      BA   O
ATOM   1194  N   SER B  25     -41.506  16.601  -9.248  1.00 13.17      BA   N
ATOM   1195  CA  SER B  25     -41.880  16.582 -10.679  1.00 12.14      BA   C
ATOM   1196  CB  SER B  25     -43.371  16.724 -10.838  1.00 14.12      BA   C
ATOM   1197  OG  SER B  25     -43.814  17.967 -10.483  1.00 15.12      BA   O
ATOM   1198  C   SER B  25     -41.156  17.635 -11.537  1.00 12.40      BA   C
ATOM   1199  O   SER B  25     -41.314  17.647 -12.764  1.00 15.21      BA   O
ATOM   1200  N   CYS B  26     -40.525  18.603 -10.874  1.00 11.03      BA   N
ATOM   1201  CA  CYS B  26     -39.754  19.632 -11.603  1.00 13.09      BA   C
ATOM   1202  CB  CYS B  26     -39.343  20.783 -10.608  1.00 12.47      BA   C
ATOM   1203  SG  CYS B  26     -40.633  21.707  -9.935  1.00 11.92      BA   S
ATOM   1204  C   CYS B  26     -38.511  18.996 -12.236  1.00 11.21      BA   C
ATOM   1205  O   CYS B  26     -37.803  18.280 -11.592  1.00 15.18      BA   O
ATOM   1206  N   LYS B  27     -38.283  19.285 -13.492  1.00 11.00      BA   N
ATOM   1207  CA ALYS B  27     -37.036  18.821 -14.123  0.50 10.76      BA   C
```

```
ATOM   1208  CA BLYS B  27     -37.038  18.822 -14.112  0.50 10.58     BA   C
ATOM   1209  CB ALYS B  27     -37.120  18.927 -15.637  0.50 12.25     BA   C
ATOM   1210  CB BLYS B  27     -37.155  18.922 -15.615  0.50 12.02     BA   C
ATOM   1211  CG ALYS B  27     -38.215  18.104 -16.322  0.50 13.24     BA   C
ATOM   1212  CG BLYS B  27     -35.895  18.538 -16.361  0.50 11.94     BA   C
ATOM   1213  CD ALYS B  27     -38.328  16.671 -15.833  0.50 17.25     BA   C
ATOM   1214  CD BLYS B  27     -36.112  18.729 -17.815  0.50 18.60     BA   C
ATOM   1215  CE ALYS B  27     -39.109  15.806 -16.856  0.50 19.87     BA   C
ATOM   1216  CE BLYS B  27     -34.939  19.390 -18.441  0.50 18.78     BA   C
ATOM   1217  NZ ALYS B  27     -40.251  16.552 -17.591  0.50 20.27     BA   N
ATOM   1218  NZ BLYS B  27     -35.383  19.829 -19.752  0.50 21.39     BA   N
ATOM   1219  C   LYS B  27    -35.838  19.640 -13.595  1.00 11.40     BA   C
ATOM   1220  O   LYS B  27    -34.747  19.097 -13.369  1.00 11.14     BA   O
ATOM   1221  N   GLN B  28    -36.073  20.934 -13.438  1.00 10.25     BA   N
ATOM   1222  CA  GLN B  28    -35.060  21.836 -12.913  1.00  9.52     BA   C
ATOM   1223  CB  GLN B  28    -34.395  22.704 -14.007  1.00 10.40     BA   C
ATOM   1224  CG  GLN B  28    -33.761  21.920 -15.229  1.00 13.06     BA   C
ATOM   1225  CD  GLN B  28    -33.087  22.831 -16.155  1.00 17.00     BA   C
ATOM   1226  OE1 GLN B  28    -31.846  22.914 -16.176  1.00 24.03     BA   O
ATOM   1227  NE2 GLN B  28    -33.854  23.525 -16.924  1.00 21.87     BA   N
ATOM   1228  C   GLN B  28    -35.677  22.707 -11.863  1.00  9.89     BA   C
ATOM   1229  O   GLN B  28    -36.917  22.968 -11.931  1.00 12.18     BA   O
ATOM   1230  N   PHE B  29    -34.859  23.238 -10.943  1.00 10.40     BA   N
ATOM   1231  CA  PHE B  29    -35.347  24.110  -9.844  1.00  9.61     BA   C
ATOM   1232  CB  PHE B  29    -35.231  23.376  -8.502  1.00 12.00     BA   C
ATOM   1233  CG  PHE B  29    -35.823  24.136  -7.408  1.00 11.97     BA   C
ATOM   1234  CD1 PHE B  29    -37.201  24.104  -7.184  1.00 12.56     BA   C
ATOM   1235  CE1 PHE B  29    -37.779  24.859  -6.100  1.00 12.77     BA   C
ATOM   1236  CZ  PHE B  29    -36.999  25.552  -5.275  1.00 13.23     BA   C
ATOM   1237  CE2 PHE B  29    -35.633  25.566  -5.450  1.00 14.44     BA   C
ATOM   1238  CD2 PHE B  29    -35.017  24.848  -6.511  1.00 13.37     BA   C
ATOM   1239  C   PHE B  29    -34.523  25.363  -9.880  1.00  9.40     BA   C
ATOM   1240  O   PHE B  29    -33.305  25.314 -10.118  1.00  9.79     BA   O
ATOM   1241  N   THR B  30    -35.167  26.483  -9.673  1.00  9.49     BA   N
ATOM   1242  CA  THR B  30    -34.502  27.817  -9.763  1.00  9.74     BA   C
ATOM   1243  CB  THR B  30    -35.208  28.653 -10.891  1.00  8.97     BA   C
ATOM   1244  OG1 THR B  30    -35.084  27.942 -12.126  1.00 10.85     BA   O
ATOM   1245  CG2 THR B  30    -34.509  30.025 -11.046  1.00 11.21     BA   C
ATOM   1246  C   THR B  30    -34.642  28.562  -8.446  1.00 10.21     BA   C
ATOM   1247  O   THR B  30    -35.742  28.712  -7.908  1.00 11.19     BA   O
ATOM   1248  N   VAL B  31    -33.489  29.020  -7.942  1.00 10.10     BA   N
ATOM   1249  CA  VAL B  31    -33.438  29.864  -6.765  1.00 11.34     BA   C
ATOM   1250  CB  VAL B  31    -32.359  29.333  -5.802  1.00 11.68     BA   C
ATOM   1251  CG1 VAL B  31    -32.166  30.353  -4.629  1.00 14.55     BA   C
ATOM   1252  CG2 VAL B  31    -32.727  27.958  -5.246  1.00 14.60     BA   C
ATOM   1253  C   VAL B  31    -33.066  31.257  -7.212  1.00 10.79     BA   C
ATOM   1254  O   VAL B  31    -32.071  31.490  -7.904  1.00 11.57     BA   O
ATOM   1255  N   ASN B  32    -33.948  32.215  -6.826  1.00 11.33     BA   N
ATOM   1256  CA  ASN B  32    -33.785  33.656  -7.174  1.00 11.05     BA   C
ATOM   1257  CB  ASN B  32    -35.129  34.227  -7.747  1.00 12.26     BA   C
ATOM   1258  CG  ASN B  32    -35.593  33.428  -8.915  1.00 13.41     BA   C
ATOM   1259  OD1 ASN B  32    -34.859  33.345  -9.906  1.00 12.11     BA   O
ATOM   1260  ND2 ASN B  32    -36.786  32.878  -8.850  1.00 15.08     BA   N
ATOM   1261  C   ASN B  32    -33.345  34.367  -5.886  1.00 10.80     BA   C
ATOM   1262  O   ASN B  32    -34.184  34.505  -4.999  1.00 11.62     BA   O
```

```
ATOM   1263  N   LEU B  33    -32.044  34.732  -5.820  1.00 11.41     BA   N
ATOM   1264  CA  LEU B  33     -31.487  35.397  -4.577  1.00 10.97     BA   C
ATOM   1265  CB  LEU B  33     -30.047  34.913  -4.386  1.00 11.56     BA   C
ATOM   1266  CG  LEU B  33     -29.419  35.503  -3.105  1.00 11.79     BA   C
ATOM   1267  CD1 LEU B  33     -30.169  35.065  -1.806  1.00 13.41     BA   C
ATOM   1268  CD2 LEU B  33     -27.980  35.115  -3.190  1.00 12.76     BA   C
ATOM   1269  C   LEU B  33     -31.524  36.902  -4.800  1.00 12.61     BA   C
ATOM   1270  O   LEU B  33     -31.099  37.408  -5.873  1.00 13.48     BA   O
ATOM   1271  N   SER B  34     -31.913  37.604  -3.749  1.00 13.27     BA   N
ATOM   1272  CA ASER B  34     -31.670  39.043  -3.771  0.50 13.45     BA   C
ATOM   1273  CA BSER B  34     -31.953  39.072  -3.688  0.50 14.34     BA   C
ATOM   1274  CB ASER B  34     -32.926  39.808  -4.140  0.50 13.19     BA   C
ATOM   1275  CB BSER B  34     -33.417  39.583  -3.594  0.50 14.87     BA   C
ATOM   1276  OG ASER B  34     -33.946  39.480  -3.201  0.50 11.42     BA   O
ATOM   1277  OG BSER B  34     -34.222  39.224  -4.735  0.50 15.85     BA   O
ATOM   1278  C   SER B  34     -31.179  39.513  -2.415  1.00 14.07     BA   C
ATOM   1279  O   SER B  34     -31.146  38.755  -1.422  1.00 13.33     BA   O
ATOM   1280  N   HIS B  35     -30.708  40.772  -2.382  1.00 14.49     BA   N
ATOM   1281  CA  HIS B  35     -30.017  41.378  -1.200  1.00 12.67     BA   C
ATOM   1282  CB  HIS B  35     -28.537  41.469  -1.488  1.00 14.34     BA   C
ATOM   1283  CG  HIS B  35     -27.692  41.818  -0.294  1.00 13.00     BA   C
ATOM   1284  ND1 HIS B  35     -28.068  42.706   0.729  1.00 14.61     BA   N
ATOM   1285  CE1 HIS B  35     -27.073  42.763   1.608  1.00 13.51     BA   C
ATOM   1286  NE2 HIS B  35     -26.073  42.021   1.139  1.00 11.88     BA   N
ATOM   1287  CD2 HIS B  35     -26.487  41.326   0.032  1.00 12.52     BA   C
ATOM   1288  C   HIS B  35     -30.630  42.789  -1.028  1.00 15.14     BA   C
ATOM   1289  O   HIS B  35     -30.054  43.765  -1.477  1.00 13.57     BA   O
ATOM   1290  N   PRO B  36     -31.689  42.870  -0.215  1.00 13.91     BA   N
ATOM   1291  CA  PRO B  36     -32.199  44.146   0.328  1.00 17.00     BA   C
ATOM   1292  CB  PRO B  36     -33.311  43.667   1.245  1.00 16.47     BA   C
ATOM   1293  CG  PRO B  36     -33.676  42.445   0.782  1.00 18.82     BA   C
ATOM   1294  CD  PRO B  36     -32.514  41.788   0.272  1.00 16.69     BA   C
ATOM   1295  C   PRO B  36     -31.229  44.686   1.333  1.00 17.64     BA   C
ATOM   1296  O   PRO B  36     -30.490  43.901   1.953  1.00 18.41     BA   O
ATOM   1297  N   GLY B  37     -31.425  45.967   1.577  1.00 19.46     BA   N
ATOM   1298  CA  GLY B  37     -30.542  46.691   2.550  1.00 18.53     BA   C
ATOM   1299  C   GLY B  37     -29.570  47.505   1.727  1.00 18.40     BA   C
ATOM   1300  O   GLY B  37     -29.823  47.867   0.550  1.00 19.49     BA   O
ATOM   1301  N   ASN B  38     -28.458  47.847   2.363  1.00 15.13     BA   N
ATOM   1302  CA  ASN B  38     -27.532  48.890   1.887  1.00 15.72     BA   C
ATOM   1303  CB  ASN B  38     -27.565  50.157   2.782  1.00 17.11     BA   C
ATOM   1304  CG  ASN B  38     -28.920  50.544   3.209  1.00 24.71     BA   C
ATOM   1305  OD1 ASN B  38     -29.224  50.590   4.424  1.00 30.91     BA   O
ATOM   1306  ND2 ASN B  38     -29.744  50.881   2.236  1.00 25.87     BA   N
ATOM   1307  C   ASN B  38     -26.052  48.575   1.846  1.00 14.91     BA   C
ATOM   1308  O   ASN B  38     -25.279  49.402   1.333  1.00 14.42     BA   O
ATOM   1309  N   LEU B  39     -25.638  47.414   2.372  1.00 12.29     BA   N
ATOM   1310  CA  LEU B  39     -24.229  47.168   2.504  1.00 13.02     BA   C
ATOM   1311  CB  LEU B  39     -23.967  46.436   3.817  1.00 12.31     BA   C
ATOM   1312  CG  LEU B  39     -24.202  47.184   5.129  1.00 11.33     BA   C
ATOM   1313  CD1 LEU B  39     -23.945  46.306   6.352  1.00 12.77     BA   C
ATOM   1314  CD2 LEU B  39     -23.230  48.407   5.230  1.00 11.44     BA   C
ATOM   1315  C   LEU B  39     -23.708  46.386   1.314  1.00 12.73     BA   C
ATOM   1316  O   LEU B  39     -24.410  45.511   0.800  1.00 13.44     BA   O
ATOM   1317  N   PRO B  40     -22.460  46.697   0.880  1.00 13.62     BA   N
```

```
ATOM   1318  CA  PRO B  40     -21.926  46.088  -0.325  1.00 14.12     BA   C
ATOM   1319  CB  PRO B  40     -20.850  47.101  -0.798  1.00 15.00     BA   C
ATOM   1320  CG  PRO B  40     -20.338  47.589   0.381  1.00 13.78     BA   C
ATOM   1321  CD  PRO B  40     -21.583  47.806   1.297  1.00 13.12     BA   C
ATOM   1322  C   PRO B  40     -21.317  44.703  -0.061  1.00 13.58     BA   C
ATOM   1323  O   PRO B  40     -21.216  44.313   1.146  1.00 13.16     BA   O
ATOM   1324  N   LYS B  41     -20.916  44.019  -1.133  1.00 13.32     BA   N
ATOM   1325  CA  LYS B  41     -20.496  42.619  -1.049  1.00 13.04     BA   C
ATOM   1326  CB  LYS B  41     -20.515  41.854  -2.395  1.00 17.15     BA   C
ATOM   1327  CG  LYS B  41     -19.366  42.160  -3.275  1.00 19.69     BA   C
ATOM   1328  CD  LYS B  41     -19.553  41.307  -4.532  1.00 19.95     BA   C
ATOM   1329  CE  LYS B  41     -18.283  41.470  -5.312  1.00 22.00     BA   C
ATOM   1330  NZ  LYS B  41     -18.356  40.905  -6.701  1.00 22.08     BA   N
ATOM   1331  C   LYS B  41     -19.222  42.398  -0.231  1.00 12.78     BA   C
ATOM   1332  O   LYS B  41     -19.074  41.304   0.319  1.00 12.66     BA   O
ATOM   1333  N   ASN B  42     -18.322  43.405  -0.117  1.00 10.48     BA   N
ATOM   1334  CA  ASN B  42     -17.074  43.119   0.614  1.00 12.08     BA   C
ATOM   1335  CB  ASN B  42     -15.975  44.105   0.214  1.00 12.03     BA   C
ATOM   1336  CG  ASN B  42     -16.246  45.547   0.656  1.00 15.06     BA   C
ATOM   1337  OD1 ASN B  42     -17.334  45.907   1.116  1.00 15.57     BA   O
ATOM   1338  ND2 ASN B  42     -15.223  46.420   0.451  1.00 16.51     BA   N
ATOM   1339  C   ASN B  42     -17.236  42.958   2.108  1.00 10.98     BA   C
ATOM   1340  O   ASN B  42     -16.374  42.355   2.769  1.00 13.31     BA   O
ATOM   1341  N   VAL B  43     -18.367  43.451   2.639  1.00 11.97     BA   N
ATOM   1342  CA  VAL B  43     -18.656  43.383   4.128  1.00 11.16     BA   C
ATOM   1343  CB  VAL B  43     -18.643  44.759   4.858  1.00 11.03     BA   C
ATOM   1344  CG1 VAL B  43     -17.252  45.377   4.717  1.00 13.16     BA   C
ATOM   1345  CG2 VAL B  43     -19.583  45.762   4.153  1.00 12.68     BA   C
ATOM   1346  C   VAL B  43     -19.969  42.667   4.424  1.00 11.05     BA   C
ATOM   1347  O   VAL B  43     -20.165  42.233   5.550  1.00 11.64     BA   O
ATOM   1348  N   MET B  44     -20.841  42.510   3.403  1.00  9.87     BA   N
ATOM   1349  CA  MET B  44     -22.176  41.917   3.603  1.00 11.02     BA   C
ATOM   1350  CB  MET B  44     -23.201  42.986   3.998  1.00 12.54     BA   C
ATOM   1351  CG  MET B  44     -24.499  42.450   4.609  1.00 11.34     BA   C
ATOM   1352  SD  MET B  44     -24.391  41.310   5.941  1.00 12.97     BA   S
ATOM   1353  CE  MET B  44     -23.562  42.345   7.180  1.00 14.07     BA   C
ATOM   1354  C   MET B  44     -22.632  41.110   2.404  1.00 11.11     BA   C
ATOM   1355  O   MET B  44     -23.830  41.056   2.064  1.00 12.64     BA   O
ATOM   1356  N   GLY B  45     -21.646  40.431   1.801  1.00 10.28     BA   N
ATOM   1357  CA  GLY B  45     -21.984  39.611   0.601  1.00 10.39     BA   C
ATOM   1358  C   GLY B  45     -22.810  38.416   1.034  1.00 10.71     BA   C
ATOM   1359  O   GLY B  45     -22.581  37.828   2.153  1.00 10.83     BA   O
ATOM   1360  N   HIS B  46     -23.785  38.053   0.196  1.00 11.01     BA   N
ATOM   1361  CA  HIS B  46     -24.494  36.789   0.367  1.00 10.19     BA   C
ATOM   1362  CB  HIS B  46     -25.968  36.994   0.759  1.00 10.51     BA   C
ATOM   1363  CG  HIS B  46     -26.145  37.805   2.015  1.00  9.67     BA   C
ATOM   1364  ND1 HIS B  46     -25.429  37.619   3.167  1.00  9.13     BA   N
ATOM   1365  CE1 HIS B  46     -25.868  38.466   4.109  1.00  8.76     BA   C
ATOM   1366  NE2 HIS B  46     -26.837  39.199   3.588  1.00 11.40     BA   N
ATOM   1367  CD2 HIS B  46     -27.029  38.811   2.281  1.00 12.82     BA   C
ATOM   1368  C   HIS B  46     -24.457  35.959  -0.875  1.00 10.92     BA   C
ATOM   1369  O   HIS B  46     -24.604  36.511  -1.982  1.00 11.66     BA   O
ATOM   1370  N   ASN B  47     -24.423  34.661  -0.678  1.00 10.26     BA   N
ATOM   1371  CA  ASN B  47     -24.663  33.690  -1.754  1.00 10.35     BA   C
ATOM   1372  CB  ASN B  47     -23.381  33.044  -2.325  1.00 10.91     BA   C
```

```
ATOM   1373  CG  ASN B  47     -22.507  32.459  -1.317  1.00 11.47     BA   C
ATOM   1374  OD1 ASN B  47     -22.914  32.207  -0.202  1.00 10.34     BA   O
ATOM   1375  ND2 ASN B  47     -21.257  32.226  -1.704  1.00 11.47     BA   N
ATOM   1376  C   ASN B  47     -25.655  32.683  -1.193  1.00  9.26     BA   C
ATOM   1377  O   ASN B  47     -26.012  32.729  -0.001  1.00 11.03     BA   O
ATOM   1378  N   TRP B  48     -26.193  31.822  -2.064  1.00  9.66     BA   N
ATOM   1379  CA  TRP B  48     -26.960  30.643  -1.705  1.00 10.05     BA   C
ATOM   1380  CB  TRP B  48     -28.389  30.800  -2.310  1.00 11.35     BA   C
ATOM   1381  CG  TRP B  48     -29.316  29.688  -1.978  1.00 10.37     BA   C
ATOM   1382  CD1 TRP B  48     -30.181  29.672  -0.896  1.00 11.86     BA   C
ATOM   1383  NE1 TRP B  48     -30.931  28.518  -0.941  1.00 11.44     BA   N
ATOM   1384  CE2 TRP B  48     -30.489  27.748  -1.934  1.00 10.39     BA   C
ATOM   1385  CD2 TRP B  48     -29.494  28.447  -2.663  1.00 10.44     BA   C
ATOM   1386  CE3 TRP B  48     -28.939  27.861  -3.804  1.00 11.47     BA   C
ATOM   1387  CZ3 TRP B  48     -29.391  26.542  -4.164  1.00 12.22     BA   C
ATOM   1388  CH2 TRP B  48     -30.394  25.920  -3.371  1.00 11.23     BA   C
ATOM   1389  CZ2 TRP B  48     -30.944  26.492  -2.315  1.00 10.53     BA   C
ATOM   1390  C   TRP B  48     -26.224  29.474  -2.251  1.00 10.22     BA   C
ATOM   1391  O   TRP B  48     -26.000  29.373  -3.463  1.00 10.69     BA   O
ATOM   1392  N   VAL B  49     -25.831  28.570  -1.350  1.00  9.51     BA   N
ATOM   1393  CA  VAL B  49     -25.012  27.419  -1.692  1.00  9.89     BA   C
ATOM   1394  CB  VAL B  49     -23.595  27.609  -1.042  1.00  9.77     BA   C
ATOM   1395  CG1 VAL B  49     -22.663  26.441  -1.429  1.00 12.01     BA   C
ATOM   1396  CG2 VAL B  49     -22.975  28.975  -1.475  1.00 11.72     BA   C
ATOM   1397  C   VAL B  49     -25.655  26.180  -1.102  1.00  9.53     BA   C
ATOM   1398  O   VAL B  49     -26.129  26.222   0.008  1.00 10.35     BA   O
ATOM   1399  N   LEU B  50     -25.705  25.103  -1.889  1.00  9.79     BA   N
ATOM   1400  CA  LEU B  50     -26.412  23.868  -1.477  1.00  9.65     BA   C
ATOM   1401  CB  LEU B  50     -27.437  23.543  -2.585  1.00 10.45     BA   C
ATOM   1402  CG  LEU B  50     -28.372  22.364  -2.275  1.00 10.50     BA   C
ATOM   1403  CD1 LEU B  50     -29.269  22.588  -1.064  1.00 11.79     BA   C
ATOM   1404  CD2 LEU B  50     -29.178  21.940  -3.572  1.00 11.53     BA   C
ATOM   1405  C   LEU B  50     -25.398  22.738  -1.408  1.00  9.16     BA   C
ATOM   1406  O   LEU B  50     -24.579  22.515  -2.341  1.00 10.70     BA   O
ATOM   1407  N   SER B  51     -25.420  21.981  -0.324  1.00  9.31     BA   N
ATOM   1408  CA  SER B  51     -24.604  20.728  -0.185  1.00  9.52     BA   C
ATOM   1409  CB  SER B  51     -23.237  21.094   0.403  1.00  9.99     BA   C
ATOM   1410  OG  SER B  51     -23.320  21.395   1.819  1.00 10.73     BA   O
ATOM   1411  C   SER B  51     -25.322  19.733   0.693  1.00 10.09     BA   C
ATOM   1412  O   SER B  51     -26.376  20.028   1.300  1.00 10.20     BA   O
ATOM   1413  N   THR B  52     -24.731  18.542   0.804  1.00 10.24     BA   N
ATOM   1414  CA  THR B  52     -25.212  17.663   1.855  1.00  9.45     BA   C
ATOM   1415  CB  THR B  52     -24.597  16.281   1.745  1.00  8.98     BA   C
ATOM   1416  OG1 THR B  52     -23.204  16.454   1.998  1.00 11.09     BA   O
ATOM   1417  CG2 THR B  52     -24.878  15.651   0.391  1.00 10.55     BA   C
ATOM   1418  C   THR B  52     -24.876  18.290   3.226  1.00  8.95     BA   C
ATOM   1419  O   THR B  52     -24.008  19.181   3.354  1.00  9.41     BA   O
ATOM   1420  N   ALA B  53     -25.588  17.857   4.270  1.00 10.92     BA   N
ATOM   1421  CA  ALA B  53     -25.267  18.293   5.674  1.00 12.94     BA   C
ATOM   1422  CB  ALA B  53     -26.180  17.604   6.666  1.00 13.65     BA   C
ATOM   1423  C   ALA B  53     -23.822  17.983   6.031  1.00 11.99     BA   C
ATOM   1424  O   ALA B  53     -23.170  18.801   6.629  1.00 11.95     BA   O
ATOM   1425  N   ALA B  54     -23.336  16.789   5.601  1.00 11.72     BA   N
ATOM   1426  CA  ALA B  54     -21.996  16.355   5.967  1.00 12.75     BA   C
ATOM   1427  CB  ALA B  54     -21.737  14.908   5.701  1.00 12.97     BA   C
```

```
ATOM   1428  C   ALA B  54     -20.907  17.198   5.337  1.00 10.81     BA   C
ATOM   1429  O   ALA B  54     -19.819  17.374   5.887  1.00 11.17     BA   O
ATOM   1430  N   ASP B  55     -21.271  17.789   4.181  1.00 10.07     BA   N
ATOM   1431  CA  ASP B  55     -20.285  18.580   3.464  1.00 11.16     BA   C
ATOM   1432  CB  ASP B  55     -20.499  18.465   1.947  1.00 10.36     BA   C
ATOM   1433  CG  ASP B  55     -19.921  17.185   1.342  1.00 11.95     BA   C
ATOM   1434  OD1 ASP B  55     -18.999  16.571   1.977  1.00 12.95     BA   O
ATOM   1435  OD2 ASP B  55     -20.337  16.728   0.312  1.00 10.74     BA   O
ATOM   1436  C   ASP B  55     -20.338  20.087   3.757  1.00 10.52     BA   C
ATOM   1437  O   ASP B  55     -19.430  20.836   3.353  1.00 11.22     BA   O
ATOM   1438  N   MET B  56     -21.367  20.563   4.459  1.00 10.69     BA   N
ATOM   1439  CA  MET B  56     -21.540  22.024   4.636  1.00  9.66     BA   C
ATOM   1440  CB  MET B  56     -22.778  22.306   5.488  1.00  9.07     BA   C
ATOM   1441  CG  MET B  56     -22.878  23.758   5.877  1.00  9.77     BA   C
ATOM   1442  SD  MET B  56     -24.455  24.082   6.724  1.00 11.20     BA   S
ATOM   1443  CE  MET B  56     -24.117  25.764   7.260  1.00 13.34     BA   C
ATOM   1444  C   MET B  56     -20.297  22.651   5.284  1.00  9.83     BA   C
ATOM   1445  O   MET B  56     -19.785  23.665   4.855  1.00 10.20     BA   O
ATOM   1446  N   GLN B  57     -19.817  22.054   6.379  1.00 10.02     BA   N
ATOM   1447  CA  GLN B  57     -18.762  22.719   7.141  1.00 11.12     BA   C
ATOM   1448  CB  GLN B  57     -18.372  21.961   8.429  1.00 11.01     BA   C
ATOM   1449  CG  GLN B  57     -17.238  22.706   9.194  1.00 14.30     BA   C
ATOM   1450  CD  GLN B  57     -17.717  23.989   9.742  1.00 14.19     BA   C
ATOM   1451  OE1 GLN B  57     -18.726  23.995  10.528  1.00 16.83     BA   O
ATOM   1452  NE2 GLN B  57     -17.212  25.111   9.236  1.00 17.50     BA   N
ATOM   1453  C   GLN B  57     -17.491  22.888   6.298  1.00 10.51     BA   C
ATOM   1454  O   GLN B  57     -16.840  23.979   6.341  1.00 10.59     BA   O
ATOM   1455  N   GLY B  58     -17.142  21.842   5.520  1.00 10.53     BA   N
ATOM   1456  CA  GLY B  58     -15.969  21.929   4.642  1.00 11.19     BA   C
ATOM   1457  C   GLY B  58     -16.112  22.950   3.504  1.00  9.56     BA   C
ATOM   1458  O   GLY B  58     -15.185  23.686   3.192  1.00 10.93     BA   O
ATOM   1459  N   VAL B  59     -17.324  23.004   2.894  1.00  9.48     BA   N
ATOM   1460  CA  VAL B  59     -17.618  24.014   1.869  1.00 10.51     BA   C
ATOM   1461  CB  VAL B  59     -19.039  23.834   1.277  1.00 10.31     BA   C
ATOM   1462  CG1 VAL B  59     -19.439  24.945   0.346  1.00 11.12     BA   C
ATOM   1463  CG2 VAL B  59     -19.092  22.507   0.470  1.00 10.01     BA   C
ATOM   1464  C   VAL B  59     -17.436  25.418   2.485  1.00 11.29     BA   C
ATOM   1465  O   VAL B  59     -16.840  26.270   1.860  1.00 11.19     BA   O
ATOM   1466  N   VAL B  60     -17.973  25.633   3.691  1.00 10.19     BA   N
ATOM   1467  CA  VAL B  60     -17.917  26.924   4.373  1.00 10.64     BA   C
ATOM   1468  CB  VAL B  60     -18.791  26.903   5.649  1.00 10.08     BA   C
ATOM   1469  CG1 VAL B  60     -18.494  28.156   6.477  1.00 11.22     BA   C
ATOM   1470  CG2 VAL B  60     -20.269  26.894   5.194  1.00 11.45     BA   C
ATOM   1471  C   VAL B  60     -16.468  27.329   4.684  1.00  9.90     BA   C
ATOM   1472  O   VAL B  60     -16.042  28.434   4.390  1.00 10.49     BA   O
ATOM   1473  N   THR B  61     -15.743  26.405   5.286  1.00 11.02     BA   N
ATOM   1474  CA  THR B  61     -14.381  26.717   5.724  1.00 12.03     BA   C
ATOM   1475  CB  THR B  61     -13.885  25.557   6.534  1.00 13.72     BA   C
ATOM   1476  OG1 THR B  61     -14.542  25.601   7.773  1.00 15.66     BA   O
ATOM   1477  CG2 THR B  61     -12.340  25.693   6.863  1.00 15.08     BA   C
ATOM   1478  C   THR B  61     -13.486  26.924   4.504  1.00 11.64     BA   C
ATOM   1479  O   THR B  61     -12.728  27.907   4.415  1.00 13.52     BA   O
ATOM   1480  N   ASP B  62     -13.543  26.025   3.522  1.00 11.33     BA   N
ATOM   1481  CA  ASP B  62     -12.724  26.188   2.285  1.00 11.64     BA   C
ATOM   1482  CB  ASP B  62     -12.679  24.927   1.443  1.00 10.98     BA   C
```

```
ATOM   1483  CG  ASP B  62     -12.048  23.766   2.160  1.00 12.85     BA   C
ATOM   1484  OD1 ASP B  62     -11.354  23.956   3.229  1.00 16.62     BA   O
ATOM   1485  OD2 ASP B  62     -12.274  22.663   1.649  1.00 13.63     BA   O
ATOM   1486  C   ASP B  62     -13.113  27.422   1.520  1.00 11.38     BA   C
ATOM   1487  O   ASP B  62     -12.240  28.124   0.947  1.00 13.17     BA   O
ATOM   1488  N   GLY B  63     -14.423  27.751   1.525  1.00 11.62     BA   N
ATOM   1489  CA  GLY B  63     -14.891  28.933   0.834  1.00 13.29     BA   C
ATOM   1490  C   GLY B  63     -14.357  30.197   1.478  1.00 14.67     BA   C
ATOM   1491  O   GLY B  63     -13.929  31.085   0.749  1.00 13.69     BA   O
ATOM   1492  N   MET B  64     -14.329  30.251   2.818  1.00 14.73     BA   N
ATOM   1493  CA  MET B  64     -13.737  31.406   3.528  1.00 16.72     BA   C
ATOM   1494  CB  MET B  64     -13.780  31.201   5.041  1.00 18.24     BA   C
ATOM   1495  CG  MET B  64     -12.863  32.234   5.743  1.00 18.22     BA   C
ATOM   1496  SD  MET B  64     -13.040  32.168   7.569  1.00 27.19     BA   S
ATOM   1497  CE  MET B  64     -14.773  32.215   7.937  1.00 28.58     BA   C
ATOM   1498  C   MET B  64     -12.325  31.642   3.033  1.00 17.17     BA   C
ATOM   1499  O   MET B  64     -11.936  32.802   2.650  1.00 17.17     BA   O
ATOM   1500  N   ALA B  65     -11.537  30.574   2.981  1.00 16.03     BA   N
ATOM   1501  CA  ALA B  65     -10.139  30.677   2.560  1.00 17.31     BA   C
ATOM   1502  CB  ALA B  65      -9.490  29.307   2.710  1.00 16.77     BA   C
ATOM   1503  C   ALA B  65     -10.023  31.191   1.111  1.00 16.05     BA   C
ATOM   1504  O   ALA B  65      -9.023  31.822   0.743  1.00 17.31     BA   O
ATOM   1505  N   SER B  66     -10.978  30.932   0.241  1.00 15.57     BA   N
ATOM   1506  CA  SER B  66     -10.884  31.296  -1.144  1.00 16.13     BA   C
ATOM   1507  CB  SER B  66     -11.907  30.443  -1.898  1.00 16.36     BA   C
ATOM   1508  OG  SER B  66     -11.554  29.111  -1.668  1.00 24.38     BA   O
ATOM   1509  C   SER B  66     -11.066  32.782  -1.469  1.00 16.19     BA   C
ATOM   1510  O   SER B  66     -10.541  33.299  -2.461  1.00 16.13     BA   O
ATOM   1511  N   GLY B  67     -11.796  33.493  -0.625  1.00 14.55     BA   N
ATOM   1512  CA  GLY B  67     -11.912  34.948  -0.753  1.00 13.59     BA   C
ATOM   1513  C   GLY B  67     -13.027  35.461  -1.579  1.00 14.94     BA   C
ATOM   1514  O   GLY B  67     -13.651  34.784  -2.364  1.00 13.47     BA   O
ATOM   1515  N   LEU B  68     -13.169  36.827  -1.421  1.00 16.02     BA   N
ATOM   1516  CA  LEU B  68     -14.248  37.560  -2.091  1.00 15.39     BA   C
ATOM   1517  CB  LEU B  68     -14.148  39.083  -1.704  1.00 18.25     BA   C
ATOM   1518  CG  LEU B  68     -15.012  40.058  -2.447  1.00 20.47     BA   C
ATOM   1519  CD1 LEU B  68     -16.414  40.069  -1.967  1.00 25.72     BA   C
ATOM   1520  CD2 LEU B  68     -14.277  41.332  -1.968  1.00 19.64     BA   C
ATOM   1521  C   LEU B  68     -14.263  37.330  -3.642  1.00 12.87     BA   C
ATOM   1522  O   LEU B  68     -15.276  37.274  -4.301  1.00 13.59     BA   O
ATOM   1523  N   ASP B  69     -13.043  37.372  -4.194  1.00 14.84     BA   N
ATOM   1524  CA  ASP B  69     -12.927  37.347  -5.677  1.00 13.35     BA   C
ATOM   1525  CB  ASP B  69     -11.504  37.741  -6.163  1.00 11.58     BA   C
ATOM   1526  CG  ASP B  69     -11.125  39.168  -5.794  1.00 15.72     BA   C
ATOM   1527  OD1 ASP B  69     -11.993  40.009  -5.556  1.00 14.71     BA   O
ATOM   1528  OD2 ASP B  69      -9.938  39.406  -5.712  1.00 19.22     BA   O
ATOM   1529  C   ASP B  69     -13.306  35.997  -6.253  1.00 13.15     BA   C
ATOM   1530  O   ASP B  69     -13.531  35.924  -7.464  1.00 17.70     BA   O
ATOM   1531  N   LYS B  70     -13.310  34.961  -5.392  1.00 14.21     BA   N
ATOM   1532  CA  LYS B  70     -13.809  33.630  -5.794  1.00 14.36     BA   C
ATOM   1533  CB  LYS B  70     -12.866  32.514  -5.316  1.00 14.08     BA   C
ATOM   1534  CG  LYS B  70     -11.374  32.637  -5.767  1.00 19.70     BA   C
ATOM   1535  CD  LYS B  70     -11.252  32.290  -7.152  1.00 22.71     BA   C
ATOM   1536  CE  LYS B  70      -9.767  32.011  -7.523  1.00 20.00     BA   C
ATOM   1537  NZ  LYS B  70      -8.740  32.757  -6.755  1.00 28.09     BA   N
```

```
ATOM   1538  C   LYS B  70     -15.170  33.408  -5.182  1.00 14.12      BA   C
ATOM   1539  O   LYS B  70     -15.578  32.242  -5.077  1.00 13.08      BA   O
ATOM   1540  N   ASP B  71     -15.875  34.514  -4.821  1.00 14.49      BA   N
ATOM   1541  CA  ASP B  71     -17.206  34.421  -4.253  1.00 14.41      BA   C
ATOM   1542  CB  ASP B  71     -18.187  33.923  -5.299  1.00 16.35      BA   C
ATOM   1543  CG  ASP B  71     -18.696  35.041  -6.250  1.00 14.65      BA   C
ATOM   1544  OD1 ASP B  71     -18.034  36.105  -6.227  1.00 23.21      BA   O
ATOM   1545  OD2 ASP B  71     -19.537  34.715  -7.054  1.00 23.60      BA   O
ATOM   1546  C   ASP B  71     -17.291  33.533  -2.964  1.00 12.69      BA   C
ATOM   1547  O   ASP B  71     -18.347  32.909  -2.718  1.00 12.21      BA   O
ATOM   1548  N   TYR B  72     -16.191  33.436  -2.268  1.00 12.15      BA   N
ATOM   1549  CA  TYR B  72     -16.041  32.631  -1.077  1.00 11.11      BA   C
ATOM   1550  CB  TYR B  72     -16.849  33.253   0.082  1.00 11.96      BA   C
ATOM   1551  CG  TYR B  72     -16.154  34.469   0.617  1.00 10.49      BA   C
ATOM   1552  CD1 TYR B  72     -14.982  34.342   1.286  1.00 11.04      BA   C
ATOM   1553  CE1 TYR B  72     -14.296  35.496   1.834  1.00 12.38      BA   C
ATOM   1554  CZ  TYR B  72     -14.872  36.727   1.684  1.00 10.45      BA   C
ATOM   1555  OH  TYR B  72     -14.225  37.819   2.239  1.00 14.01      BA   O
ATOM   1556  CE2 TYR B  72     -16.073  36.869   0.991  1.00 13.26      BA   C
ATOM   1557  CD2 TYR B  72     -16.740  35.730   0.480  1.00 12.85      BA   C
ATOM   1558  C   TYR B  72     -16.492  31.199  -1.315  1.00 10.60      BA   C
ATOM   1559  O   TYR B  72     -17.140  30.521  -0.462  1.00 11.32      BA   O
ATOM   1560  N   LEU B  73     -16.052  30.655  -2.449  1.00 10.48      BA   N
ATOM   1561  CA  LEU B  73     -16.255  29.216  -2.752  1.00 10.92      BA   C
ATOM   1562  CB  LEU B  73     -17.319  28.975  -3.848  1.00 12.37      BA   C
ATOM   1563  CG  LEU B  73     -18.740  29.212  -3.319  1.00 14.12      BA   C
ATOM   1564  CD1 LEU B  73     -19.583  29.148  -4.587  1.00 17.32      BA   C
ATOM   1565  CD2 LEU B  73     -19.142  28.112  -2.312  1.00 14.16      BA   C
ATOM   1566  C   LEU B  73     -14.943  28.669  -3.287  1.00 10.96      BA   C
ATOM   1567  O   LEU B  73     -14.291  29.292  -4.159  1.00 11.72      BA   O
ATOM   1568  N   LYS B  74     -14.465  27.562  -2.708  1.00 11.70      BA   N
ATOM   1569  CA  LYS B  74     -13.274  26.853  -3.242  1.00 11.73      BA   C
ATOM   1570  CB  LYS B  74     -12.971  25.637  -2.366  1.00 13.27      BA   C
ATOM   1571  CG  LYS B  74     -11.760  24.702  -2.939  1.00 14.76      BA   C
ATOM   1572  CD  LYS B  74     -12.334  23.249  -2.637  1.00 22.32      BA   C
ATOM   1573  CE  LYS B  74     -11.848  22.390  -1.527  1.00 22.93      BA   C
ATOM   1574  NZ  LYS B  74     -11.111  21.161  -2.054  1.00 27.26      BA   N
ATOM   1575  C   LYS B  74     -13.529  26.484  -4.718  1.00 11.13      BA   C
ATOM   1576  O   LYS B  74     -14.529  25.920  -5.090  1.00 11.44      BA   O
ATOM   1577  N   PRO B  75     -12.558  26.853  -5.581  1.00 10.74      BA   N
ATOM   1578  CA  PRO B  75     -12.732  26.554  -6.988  1.00 11.83      BA   C
ATOM   1579  CB  PRO B  75     -11.458  27.147  -7.664  1.00 11.27      BA   C
ATOM   1580  CG  PRO B  75     -11.198  28.389  -6.759  1.00 13.94      BA   C
ATOM   1581  CD  PRO B  75     -11.493  27.836  -5.334  1.00 12.92      BA   C
ATOM   1582  C   PRO B  75     -12.811  25.042  -7.221  1.00 11.52      BA   C
ATOM   1583  O   PRO B  75     -12.104  24.298  -6.533  1.00 12.23      BA   O
ATOM   1584  N   ASP B  76     -13.655  24.613  -8.133  1.00 11.55      BA   N
ATOM   1585  CA  ASP B  76     -13.722  23.175  -8.445  1.00 13.01      BA   C
ATOM   1586  CB  ASP B  76     -12.420  22.705  -9.105  1.00 13.70      BA   C
ATOM   1587  CG  ASP B  76     -12.633  21.493 -10.003  1.00 17.64      BA   C
ATOM   1588  OD1 ASP B  76     -13.755  20.996 -10.152  1.00 18.74      BA   O
ATOM   1589  OD2 ASP B  76     -11.641  21.028 -10.543  1.00 18.70      BA   O
ATOM   1590  C   ASP B  76     -14.022  22.327  -7.204  1.00 11.95      BA   C
ATOM   1591  O   ASP B  76     -13.401  21.246  -6.958  1.00 13.25      BA   O
ATOM   1592  N   ASP B  77     -15.023  22.786  -6.415  1.00 11.60      BA   N
```

```
ATOM   1593  CA  ASP B  77     -15.426  22.072  -5.207  1.00 11.66     BA   C
ATOM   1594  CB  ASP B  77     -15.848  23.067  -4.110  1.00 10.05     BA   C
ATOM   1595  CG  ASP B  77     -16.040  22.418  -2.746  1.00 10.58     BA   C
ATOM   1596  OD1 ASP B  77     -16.241  21.201  -2.726  1.00 11.04     BA   O
ATOM   1597  OD2 ASP B  77     -15.952  23.131  -1.743  1.00 10.71     BA   O
ATOM   1598  C   ASP B  77     -16.604  21.144  -5.595  1.00 11.01     BA   C
ATOM   1599  O   ASP B  77     -17.749  21.584  -5.706  1.00 11.76     BA   O
ATOM   1600  N   SER B  78     -16.322  19.852  -5.628  1.00 11.40     BA   N
ATOM   1601  CA  SER B  78     -17.290  18.846  -6.036  1.00 11.33     BA   C
ATOM   1602  CB  SER B  78     -16.625  17.459  -6.206  1.00 11.07     BA   C
ATOM   1603  OG  SER B  78     -16.153  16.931  -4.984  1.00 15.40     BA   O
ATOM   1604  C   SER B  78     -18.475  18.707  -5.052  1.00 10.63     BA   C
ATOM   1605  O   SER B  78     -19.571  18.206  -5.409  1.00 12.36     BA   O
ATOM   1606  N   ARG B  79     -18.316  19.173  -3.820  1.00 10.54     BA   N
ATOM   1607  CA  ARG B  79     -19.339  19.090  -2.750  1.00 11.65     BA   C
ATOM   1608  CB  ARG B  79     -18.708  19.379  -1.352  1.00 10.95     BA   C
ATOM   1609  CG  ARG B  79     -17.611  18.352  -0.972  1.00 11.06     BA   C
ATOM   1610  CD  ARG B  79     -16.859  18.802   0.268  1.00  7.67     BA   C
ATOM   1611  NE  ARG B  79     -16.169  20.068  -0.041  1.00  9.80     BA   N
ATOM   1612  CZ  ARG B  79     -15.220  20.637   0.713  1.00 11.93     BA   C
ATOM   1613  NH1 ARG B  79     -14.903  19.985   1.844  1.00 13.15     BA   N
ATOM   1614  NH2 ARG B  79     -14.636  21.767   0.349  1.00 10.92     BA   N
ATOM   1615  C   ARG B  79     -20.474  20.079  -2.982  1.00  9.39     BA   C
ATOM   1616  O   ARG B  79     -21.533  19.928  -2.386  1.00 11.48     BA   O
ATOM   1617  N   VAL B  80     -20.249  21.119  -3.804  1.00 10.56     BA   N
ATOM   1618  CA  VAL B  80     -21.265  22.114  -4.054  1.00 10.92     BA   C
ATOM   1619  CB  VAL B  80     -20.612  23.444  -4.445  1.00 11.14     BA   C
ATOM   1620  CG1 VAL B  80     -21.793  24.491  -4.808  1.00 12.79     BA   C
ATOM   1621  CG2 VAL B  80     -19.715  23.951  -3.278  1.00 12.23     BA   C
ATOM   1622  C   VAL B  80     -22.246  21.579  -5.069  1.00 10.18     BA   C
ATOM   1623  O   VAL B  80     -21.886  21.397  -6.239  1.00 12.37     BA   O
ATOM   1624  N   ILE B  81     -23.508  21.384  -4.677  1.00  9.68     BA   N
ATOM   1625  CA  ILE B  81     -24.499  20.816  -5.641  1.00  9.98     BA   C
ATOM   1626  CB  ILE B  81     -25.624  20.247  -4.825  1.00 12.96     BA   C
ATOM   1627  CG1 ILE B  81     -25.129  19.035  -3.967  1.00 12.15     BA   C
ATOM   1628  CD1 ILE B  81     -26.144  18.545  -2.927  1.00 13.75     BA   C
ATOM   1629  CG2 ILE B  81     -26.806  19.821  -5.761  1.00 14.42     BA   C
ATOM   1630  C   ILE B  81     -24.959  21.945  -6.569  1.00 11.49     BA   C
ATOM   1631  O   ILE B  81     -25.197  21.708  -7.797  1.00 12.90     BA   O
ATOM   1632  N   ALA B  82     -25.087  23.159  -6.043  1.00 10.53     BA   N
ATOM   1633  CA  ALA B  82     -25.565  24.312  -6.835  1.00 11.32     BA   C
ATOM   1634  CB  ALA B  82     -27.121  24.266  -7.013  1.00 12.66     BA   C
ATOM   1635  C   ALA B  82     -25.238  25.532  -5.992  1.00 11.11     BA   C
ATOM   1636  O   ALA B  82     -25.137  25.471  -4.765  1.00 11.04     BA   O
ATOM   1637  N   HIS B  83     -25.100  26.663  -6.675  1.00 11.25     BA   N
ATOM   1638  CA  HIS B  83     -24.854  27.943  -5.941  1.00  9.67     BA   C
ATOM   1639  CB  HIS B  83     -23.380  28.029  -5.501  1.00 12.01     BA   C
ATOM   1640  CG  HIS B  83     -22.446  28.066  -6.673  1.00 11.58     BA   C
ATOM   1641  ND1 HIS B  83     -21.889  29.224  -7.223  1.00 14.29     BA   N
ATOM   1642  CE1 HIS B  83     -21.188  28.863  -8.305  1.00 15.17     BA   C
ATOM   1643  NE2 HIS B  83     -21.198  27.544  -8.399  1.00 16.15     BA   N
ATOM   1644  CD2 HIS B  83     -22.033  27.038  -7.422  1.00 12.71     BA   C
ATOM   1645  C   HIS B  83     -25.169  29.075  -6.826  1.00 11.59     BA   C
ATOM   1646  O   HIS B  83     -25.024  29.040  -8.058  1.00 11.61     BA   O
ATOM   1647  N   THR B  84     -25.501  30.189  -6.207  1.00 12.04     BA   N
```

```
ATOM   1648  CA  THR B  84     -25.543  31.523  -6.890  1.00 10.82      BA   C
ATOM   1649  CB  THR B  84     -26.550  32.472  -6.236  1.00 11.72      BA   C
ATOM   1650  OG1 THR B  84     -26.032  32.784  -4.916  1.00 12.25      BA   O
ATOM   1651  CG2 THR B  84     -27.926  31.897  -6.132  1.00 10.63      BA   C
ATOM   1652  C   THR B  84     -24.154  32.117  -6.799  1.00 10.75      BA   C
ATOM   1653  O   THR B  84     -23.223  31.598  -6.169  1.00 13.03      BA   O
ATOM   1654  N   LYS B  85     -23.971  33.264  -7.453  1.00 12.88      BA   N
ATOM   1655  CA  LYS B  85     -22.794  34.128  -7.196  1.00 12.76      BA   C
ATOM   1656  CB  LYS B  85     -22.695  35.270  -8.271  1.00 15.51      BA   C
ATOM   1657  CG  LYS B  85     -22.663  34.693  -9.673  1.00 18.14      BA   C
ATOM   1658  CD  LYS B  85     -22.295  35.803 -10.662  1.00 23.07      BA   C
ATOM   1659  CE  LYS B  85     -22.333  35.366 -12.156  1.00 28.38      BA   C
ATOM   1660  NZ  LYS B  85     -22.047  33.908 -12.359  1.00 27.62      BA   N
ATOM   1661  C   LYS B  85     -22.952  34.803  -5.819  1.00 13.69      BA   C
ATOM   1662  O   LYS B  85     -24.083  34.856  -5.242  1.00 12.89      BA   O
ATOM   1663  N   LEU B  86     -21.858  35.443  -5.360  1.00 11.58      BA   N
ATOM   1664  CA  LEU B  86     -21.889  36.337  -4.189  1.00 12.13      BA   C
ATOM   1665  CB  LEU B  86     -20.500  36.431  -3.591  1.00 13.32      BA   C
ATOM   1666  CG  LEU B  86     -20.474  37.092  -2.188  1.00  9.89      BA   C
ATOM   1667  CD1 LEU B  86     -20.787  36.116  -1.091  1.00 12.73      BA   C
ATOM   1668  CD2 LEU B  86     -19.092  37.677  -1.989  1.00 11.72      BA   C
ATOM   1669  C   LEU B  86     -22.407  37.733  -4.575  1.00 11.07      BA   C
ATOM   1670  O   LEU B  86     -21.941  38.336  -5.537  1.00 14.73      BA   O
ATOM   1671  N   ILE B  87     -23.421  38.189  -3.864  1.00 11.93      BA   N
ATOM   1672  CA  ILE B  87     -24.018  39.529  -4.214  1.00 11.17      BA   C
ATOM   1673  CB  ILE B  87     -25.493  39.411  -4.785  1.00 11.67      BA   C
ATOM   1674  CG1 ILE B  87     -26.484  38.819  -3.755  1.00 13.44      BA   C
ATOM   1675  CD1 ILE B  87     -27.896  38.802  -4.167  1.00 13.35      BA   C
ATOM   1676  CG2 ILE B  87     -25.404  38.606  -6.115  1.00 12.76      BA   C
ATOM   1677  C   ILE B  87     -24.010  40.449  -3.042  1.00 11.73      BA   C
ATOM   1678  O   ILE B  87     -24.017  40.008  -1.883  1.00 12.77      BA   O
ATOM   1679  N   GLY B  88     -23.921  41.755  -3.339  1.00 12.33      BA   N
ATOM   1680  CA  GLY B  88     -24.090  42.779  -2.309  1.00 13.29      BA   C
ATOM   1681  C   GLY B  88     -25.456  43.414  -2.430  1.00 12.48      BA   C
ATOM   1682  O   GLY B  88     -26.294  43.020  -3.298  1.00 14.71      BA   O
ATOM   1683  N   SER B  89     -25.667  44.472  -1.622  1.00 13.83      BA   N
ATOM   1684  CA  SER B  89     -27.021  45.080  -1.690  1.00 15.80      BA   C
ATOM   1685  CB  SER B  89     -27.270  46.123  -0.599  1.00 15.40      BA   C
ATOM   1686  OG  SER B  89     -26.464  47.251  -0.886  1.00 19.64      BA   O
ATOM   1687  C   SER B  89     -27.360  45.672  -3.097  1.00 14.95      BA   C
ATOM   1688  O   SER B  89     -26.499  46.125  -3.898  1.00 15.24      BA   O
ATOM   1689  N   GLY B  90     -28.643  45.545  -3.357  1.00 15.18      BA   N
ATOM   1690  CA  GLY B  90     -29.226  45.974  -4.661  1.00 14.24      BA   C
ATOM   1691  C   GLY B  90     -28.890  45.040  -5.817  1.00 17.58      BA   C
ATOM   1692  O   GLY B  90     -29.278  45.308  -6.958  1.00 20.84      BA   O
ATOM   1693  N   GLU B  91     -28.193  43.929  -5.577  1.00 16.81      BA   N
ATOM   1694  CA  GLU B  91     -27.932  42.940  -6.602  1.00 16.20      BA   C
ATOM   1695  CB  GLU B  91     -26.471  42.482  -6.597  1.00 17.35      BA   C
ATOM   1696  CG  GLU B  91     -25.502  43.630  -6.831  1.00 18.66      BA   C
ATOM   1697  CD  GLU B  91     -24.049  43.164  -6.962  1.00 28.13      BA   C
ATOM   1698  OE1 GLU B  91     -23.444  42.633  -5.981  1.00 20.77      BA   O
ATOM   1699  OE2 GLU B  91     -23.480  43.358  -8.069  1.00 29.56      BA   O
ATOM   1700  C   GLU B  91     -28.865  41.758  -6.498  1.00 16.96      BA   C
ATOM   1701  O   GLU B  91     -29.540  41.542  -5.484  1.00 16.36      BA   O
ATOM   1702  N   LYS B  92     -28.934  41.005  -7.581  1.00 15.96      BA   N
```

```
ATOM   1703  CA  LYS B  92     -29.715  39.760  -7.631  1.00 18.04     BA   C
ATOM   1704  CB  LYS B  92     -31.064  39.931  -8.352  1.00 18.30     BA   C
ATOM   1705  CG  LYS B  92     -32.123  40.911  -7.702  1.00 21.94     BA   C
ATOM   1706  CD  LYS B  92     -33.482  41.174  -8.467  1.00 29.25     BA   C
ATOM   1707  CE  LYS B  92     -34.724  40.391  -7.893  1.00 33.95     BA   C
ATOM   1708  NZ  LYS B  92     -35.660  40.970  -6.746  1.00 30.51     BA   N
ATOM   1709  C   LYS B  92     -28.874  38.734  -8.410  1.00 16.78     BA   C
ATOM   1710  O   LYS B  92     -27.929  39.039  -9.220  1.00 15.88     BA   O
ATOM   1711  N   ASP B  93     -29.231  37.469  -8.173  1.00 14.82     BA   N
ATOM   1712  CA  ASP B  93     -28.676  36.458  -8.961  1.00 13.44     BA   C
ATOM   1713  CB  ASP B  93     -27.256  36.091  -8.521  1.00 12.76     BA   C
ATOM   1714  CG  ASP B  93     -26.543  35.239  -9.501  1.00 12.59     BA   C
ATOM   1715  OD1 ASP B  93     -26.461  35.638 -10.708  1.00 13.80     BA   O
ATOM   1716  OD2 ASP B  93     -26.059  34.145  -9.151  1.00 14.85     BA   O
ATOM   1717  C   ASP B  93     -29.548  35.231  -8.851  1.00 13.10     BA   C
ATOM   1718  O   ASP B  93     -29.998  34.869  -7.781  1.00 13.30     BA   O
ATOM   1719  N   SER B  94     -29.717  34.520  -9.956  1.00 12.18     BA   N
ATOM   1720  CA  SER B  94     -30.491  33.278  -9.991  1.00 12.54     BA   C
ATOM   1721  CB  SER B  94     -31.650  33.367 -11.025  1.00 13.98     BA   C
ATOM   1722  OG  SER B  94     -32.533  34.394 -10.629  1.00 13.38     BA   O
ATOM   1723  C   SER B  94     -29.671  32.115 -10.364  1.00 11.49     BA   C
ATOM   1724  O   SER B  94     -28.774  32.228 -11.202  1.00 11.76     BA   O
ATOM   1725  N   VAL B  95     -30.004  30.932  -9.827  1.00 11.28     BA   N
ATOM   1726  CA  VAL B  95     -29.327  29.715 -10.265  1.00 11.76     BA   C
ATOM   1727  CB  VAL B  95     -28.295  29.160  -9.211  1.00 13.91     BA   C
ATOM   1728  CG1 VAL B  95     -28.916  28.796  -7.920  1.00 15.24     BA   C
ATOM   1729  CG2 VAL B  95     -27.525  27.939  -9.787  1.00 17.87     BA   C
ATOM   1730  C   VAL B  95     -30.408  28.676 -10.560  1.00 11.21     BA   C
ATOM   1731  O   VAL B  95     -31.367  28.506  -9.775  1.00 11.16     BA   O
ATOM   1732  N   THR B  96     -30.254  27.945 -11.630  1.00  9.78     BA   N
ATOM   1733  CA  THR B  96     -31.129  26.828 -11.941  1.00  8.96     BA   C
ATOM   1734  CB  THR B  96     -31.649  26.984 -13.372  1.00  8.86     BA   C
ATOM   1735  OG1 THR B  96     -32.547  28.130 -13.290  1.00 11.01     BA   O
ATOM   1736  CG2 THR B  96     -32.477  25.698 -13.795  1.00  9.82     BA   C
ATOM   1737  C   THR B  96     -30.237  25.523 -11.857  1.00 10.66     BA   C
ATOM   1738  O   THR B  96     -29.125  25.514 -12.436  1.00 10.96     BA   O
ATOM   1739  N   PHE B  97     -30.764  24.465 -11.282  1.00 10.62     BA   N
ATOM   1740  CA  PHE B  97     -30.058  23.208 -11.256  1.00 10.49     BA   C
ATOM   1741  CB  PHE B  97     -29.334  23.011  -9.852  1.00 10.62     BA   C
ATOM   1742  CG  PHE B  97     -30.211  22.935  -8.731  1.00 11.15     BA   C
ATOM   1743  CD1 PHE B  97     -30.554  24.069  -7.990  1.00 11.32     BA   C
ATOM   1744  CE1 PHE B  97     -31.287  24.010  -6.856  1.00 14.06     BA   C
ATOM   1745  CZ  PHE B  97     -31.791  22.793  -6.418  1.00 17.06     BA   C
ATOM   1746  CE2 PHE B  97     -31.496  21.651  -7.120  1.00 18.33     BA   C
ATOM   1747  CD2 PHE B  97     -30.612  21.693  -8.242  1.00 12.79     BA   C
ATOM   1748  C   PHE B  97     -30.997  22.053 -11.594  1.00 11.88     BA   C
ATOM   1749  O   PHE B  97     -32.178  22.133 -11.412  1.00 11.95     BA   O
ATOM   1750  N   ASP B  98     -30.387  20.937 -11.962  1.00 11.16     BA   N
ATOM   1751  CA  ASP B  98     -31.098  19.771 -12.311  1.00 10.66     BA   C
ATOM   1752  CB  ASP B  98     -30.206  18.820 -13.059  1.00 13.41     BA   C
ATOM   1753  CG  ASP B  98     -29.961  19.231 -14.432  1.00 16.39     BA   C
ATOM   1754  OD1 ASP B  98     -30.731  20.034 -15.009  1.00 18.00     BA   O
ATOM   1755  OD2 ASP B  98     -28.961  18.746 -15.015  1.00 22.05     BA   O
ATOM   1756  C   ASP B  98     -31.605  19.035 -11.037  1.00 11.23     BA   C
ATOM   1757  O   ASP B  98     -30.857  18.731 -10.104  1.00 12.82     BA   O
```

```
ATOM   1758  N   VAL B  99     -32.889  18.725 -11.007  1.00 11.52      BA   N
ATOM   1759  CA  VAL B  99      -33.499  18.044  -9.868  1.00 12.32      BA   C
ATOM   1760  CB  VAL B  99      -35.072  18.163  -9.916  1.00 12.14      BA   C
ATOM   1761  CG1 VAL B  99      -35.763  17.312  -8.842  1.00 14.65      BA   C
ATOM   1762  CG2 VAL B  99      -35.536  19.622  -9.684  1.00 14.40      BA   C
ATOM   1763  C   VAL B  99     -32.925  16.611  -9.704  1.00 11.38      BA   C
ATOM   1764  O   VAL B  99     -32.910  16.088  -8.560  1.00 11.97      BA   O
ATOM   1765  N   SER B 100     -32.464  16.027 -10.823  1.00 11.82      BA   N
ATOM   1766  CA  SER B 100      -31.810  14.736 -10.759  1.00 13.27      BA   C
ATOM   1767  CB  SER B 100      -31.453  14.276 -12.197  1.00 14.14      BA   C
ATOM   1768  OG  SER B 100      -30.507  15.151 -12.789  1.00 18.24      BA   O
ATOM   1769  C   SER B 100     -30.548  14.763  -9.864  1.00 13.21      BA   C
ATOM   1770  O   SER B 100     -30.056  13.671  -9.525  1.00 15.64      BA   O
ATOM   1771  N   LYS B 101     -30.009  15.921  -9.476  1.00 12.64      BA   N
ATOM   1772  CA  LYS B 101      -28.890  15.938  -8.551  1.00 14.56      BA   C
ATOM   1773  CB  LYS B 101      -28.266  17.368  -8.582  1.00 13.97      BA   C
ATOM   1774  CG  LYS B 101      -27.566  17.601  -9.941  1.00 19.71      BA   C
ATOM   1775  CD  LYS B 101      -26.496  18.629  -9.915  1.00 30.06      BA   C
ATOM   1776  CE  LYS B 101      -25.594  18.439 -11.170  1.00 29.54      BA   C
ATOM   1777  NZ  LYS B 101      -24.486  19.451 -11.203  1.00 37.48      BA   N
ATOM   1778  C   LYS B 101     -29.299  15.608  -7.138  1.00 13.92      BA   C
ATOM   1779  O   LYS B 101     -28.417  15.398  -6.291  1.00 17.93      BA   O
ATOM   1780  N   LEU B 102     -30.603  15.587  -6.848  1.00 12.47      BA   N
ATOM   1781  CA  LEU B 102      -31.135  15.414  -5.460  1.00 12.23      BA   C
ATOM   1782  CB  LEU B 102      -32.235  16.432  -5.100  1.00 13.51      BA   C
ATOM   1783  CG  LEU B 102      -31.784  17.894  -5.327  1.00 11.38      BA   C
ATOM   1784  CD1 LEU B 102      -32.945  18.804  -4.983  1.00 17.77      BA   C
ATOM   1785  CD2 LEU B 102      -30.522  18.245  -4.492  1.00 14.77      BA   C
ATOM   1786  C   LEU B 102     -31.732  14.017  -5.322  1.00 12.29      BA   C
ATOM   1787  O   LEU B 102     -32.326  13.460  -6.292  1.00 13.00      BA   O
ATOM   1788  N   LYS B 103     -31.602  13.458  -4.123  1.00 13.06      BA   N
ATOM   1789  CA  LYS B 103      -32.100  12.108  -3.837  1.00 13.97      BA   C
ATOM   1790  CB  LYS B 103      -31.014  11.273  -3.121  1.00 14.49      BA   C
ATOM   1791  CG  LYS B 103      -31.216   9.756  -3.098  1.00 22.49      BA   C
ATOM   1792  CD  LYS B 103      -29.909   9.087  -2.554  1.00 27.58      BA   C
ATOM   1793  CE  LYS B 103      -28.599   9.893  -2.914  1.00 33.20      BA   C
ATOM   1794  NZ  LYS B 103      -27.312   9.416  -2.244  1.00 31.85      BA   N
ATOM   1795  C   LYS B 103     -33.269  12.259  -2.914  1.00 12.61      BA   C
ATOM   1796  O   LYS B 103     -33.259  13.001  -1.876  1.00 12.73      BA   O
ATOM   1797  N   GLU B 104     -34.315  11.546  -3.217  1.00 13.28      BA   N
ATOM   1798  CA  GLU B 104      -35.435  11.512  -2.293  1.00 14.02      BA   C
ATOM   1799  CB  GLU B 104      -36.557  10.634  -2.883  1.00 13.96      BA   C
ATOM   1800  CG  GLU B 104      -37.329  11.345  -4.032  1.00 18.78      BA   C
ATOM   1801  CD  GLU B 104      -38.564  10.524  -4.403  1.00 20.37      BA   C
ATOM   1802  OE1 GLU B 104      -39.521  10.620  -3.600  1.00 22.40      BA   O
ATOM   1803  OE2 GLU B 104      -38.565   9.819  -5.463  1.00 19.27      BA   O
ATOM   1804  C   GLU B 104     -35.034  11.008  -0.903  1.00 12.89      BA   C
ATOM   1805  O   GLU B 104     -34.211  10.106  -0.738  1.00 15.32      BA   O
ATOM   1806  N   GLY B 105     -35.663  11.601   0.119  1.00 15.17      BA   N
ATOM   1807  CA  GLY B 105      -35.456  11.135   1.476  1.00 16.57      BA   C
ATOM   1808  C   GLY B 105     -34.273  11.836   2.128  1.00 17.64      BA   C
ATOM   1809  O   GLY B 105     -33.999  11.595   3.320  1.00 21.46      BA   O
ATOM   1810  N   GLU B 106     -33.511  12.617   1.360  1.00 15.28      BA   N
ATOM   1811  CA  GLU B 106      -32.349  13.292   1.958  1.00 15.18      BA   C
ATOM   1812  CB  GLU B 106      -31.097  13.126   1.062  1.00 16.31      BA   C
```

ATOM 1813 CG GLU B 106 -29.863 13.832 1.615 1.00 21.72 BA C
ATOM 1814 CD GLU B 106 -28.507 13.208 1.220 1.00 29.28 BA C
ATOM 1815 OE1 GLU B 106 -28.487 12.298 0.337 1.00 31.34 BA O
ATOM 1816 OE2 GLU B 106 -27.439 13.619 1.840 1.00 28.39 BA O
ATOM 1817 C GLU B 106 -32.653 14.732 2.226 1.00 13.06 BA C
ATOM 1818 O GLU B 106 -33.306 15.406 1.426 1.00 16.27 BA O
ATOM 1819 N GLN B 107 -32.243 15.231 3.388 1.00 12.66 BA N
ATOM 1820 CA GLN B 107 -32.354 16.636 3.713 1.00 14.99 BA C
ATOM 1821 CB GLN B 107 -32.758 16.763 5.203 1.00 14.81 BA C
ATOM 1822 CG GLN B 107 -32.972 18.256 5.586 1.00 18.13 BA C
ATOM 1823 CD GLN B 107 -33.198 18.341 7.065 1.00 16.70 BA C
ATOM 1824 OE1 GLN B 107 -32.206 18.290 7.872 1.00 17.43 BA O
ATOM 1825 NE2 GLN B 107 -34.449 18.495 7.472 1.00 15.55 BA N
ATOM 1826 C GLN B 107 -31.004 17.315 3.526 1.00 16.59 BA C
ATOM 1827 O GLN B 107 -30.031 16.996 4.275 1.00 17.59 BA O
ATOM 1828 N TYR B 108 -30.916 18.230 2.565 1.00 12.37 BA N
ATOM 1829 CA TYR B 108 -29.665 18.967 2.255 1.00 11.34 BA C
ATOM 1830 CB TYR B 108 -29.775 19.332 0.747 1.00 10.13 BA C
ATOM 1831 CG TYR B 108 -29.743 18.070 -0.125 1.00 9.63 BA C
ATOM 1832 CD1 TYR B 108 -28.523 17.522 -0.505 1.00 10.50 BA C
ATOM 1833 CE1 TYR B 108 -28.492 16.337 -1.257 1.00 10.16 BA C
ATOM 1834 CZ TYR B 108 -29.686 15.727 -1.591 1.00 10.38 BA C
ATOM 1835 OH TYR B 108 -29.639 14.515 -2.336 1.00 11.96 BA O
ATOM 1836 CE2 TYR B 108 -30.896 16.295 -1.249 1.00 10.31 BA C
ATOM 1837 CD2 TYR B 108 -30.952 17.405 -0.489 1.00 10.66 BA C
ATOM 1838 C TYR B 108 -29.679 20.252 3.060 1.00 8.57 BA C
ATOM 1839 O TYR B 108 -30.692 20.616 3.645 1.00 10.44 BA O
ATOM 1840 N MET B 109 -28.544 20.960 3.051 1.00 9.14 BA N
ATOM 1841 CA MET B 109 -28.418 22.283 3.712 1.00 9.60 BA C
ATOM 1842 CB MET B 109 -27.288 22.290 4.741 1.00 9.33 BA C
ATOM 1843 CG MET B 109 -27.512 21.341 5.916 1.00 10.36 BA C
ATOM 1844 SD MET B 109 -28.952 21.682 6.941 1.00 12.16 BA S
ATOM 1845 CE MET B 109 -28.475 23.306 7.658 1.00 14.69 BA C
ATOM 1846 C MET B 109 -28.114 23.331 2.627 1.00 9.36 BA C
ATOM 1847 O MET B 109 -27.338 23.085 1.682 1.00 9.96 BA O
ATOM 1848 N PHE B 110 -28.797 24.488 2.810 1.00 9.81 BA N
ATOM 1849 CA PHE B 110 -28.390 25.638 2.056 1.00 9.02 BA C
ATOM 1850 CB PHE B 110 -29.521 26.230 1.186 1.00 10.17 BA C
ATOM 1851 CG PHE B 110 -30.660 26.880 1.953 1.00 10.65 BA C
ATOM 1852 CD1 PHE B 110 -30.573 28.241 2.289 1.00 10.43 BA C
ATOM 1853 CE1 PHE B 110 -31.629 28.846 2.995 1.00 10.97 BA C
ATOM 1854 CZ PHE B 110 -32.768 28.115 3.323 1.00 12.21 BA C
ATOM 1855 CE2 PHE B 110 -32.832 26.781 2.932 1.00 10.23 BA C
ATOM 1856 CD2 PHE B 110 -31.787 26.162 2.246 1.00 9.99 BA C
ATOM 1857 C PHE B 110 -27.844 26.674 2.990 1.00 8.72 BA C
ATOM 1858 O PHE B 110 -28.210 26.740 4.185 1.00 10.26 BA O
ATOM 1859 N PHE B 111 -26.934 27.513 2.488 1.00 9.36 BA N
ATOM 1860 CA PHE B 111 -26.264 28.491 3.430 1.00 9.30 BA C
ATOM 1861 CB PHE B 111 -25.235 27.741 4.345 1.00 9.78 BA C
ATOM 1862 CG PHE B 111 -24.440 26.694 3.559 1.00 9.74 BA C
ATOM 1863 CD1 PHE B 111 -24.935 25.413 3.382 1.00 10.10 BA C
ATOM 1864 CE1 PHE B 111 -24.211 24.497 2.641 1.00 10.53 BA C
ATOM 1865 CZ PHE B 111 -22.950 24.835 2.095 1.00 9.14 BA C
ATOM 1866 CE2 PHE B 111 -22.488 26.091 2.280 1.00 9.38 BA C
ATOM 1867 CD2 PHE B 111 -23.212 27.018 3.000 1.00 10.30 BA C

```
ATOM   1868  C   PHE B 111     -25.507  29.512   2.585  1.00 10.37      BA   C
ATOM   1869  O   PHE B 111     -25.276  29.349   1.359  1.00  9.61      BA   O
ATOM   1870  N   CYS B 112     -25.109  30.597   3.245  1.00  9.60      BA   N
ATOM   1871  CA  CYS B 112     -24.164  31.624   2.702  1.00  9.61      BA   C
ATOM   1872  CB  CYS B 112     -24.620  32.950   3.239  1.00 10.65      BA   C
ATOM   1873  SG  CYS B 112     -23.497  34.314   2.684  1.00  9.61      BA   S
ATOM   1874  C   CYS B 112     -22.766  31.328   3.231  1.00  9.61      BA   C
ATOM   1875  O   CYS B 112     -22.584  30.963   4.383  1.00  9.92      BA   O
ATOM   1876  N   THR B 113     -21.779  31.407   2.310  1.00  9.68      BA   N
ATOM   1877  CA  THR B 113     -20.402  31.136   2.639  1.00  9.83      BA   C
ATOM   1878  CB  THR B 113     -19.704  30.276   1.626  1.00  9.16      BA   C
ATOM   1879  OG1 THR B 113     -19.593  31.004   0.382  1.00 10.55      BA   O
ATOM   1880  CG2 THR B 113     -20.342  28.898   1.472  1.00  9.99      BA   C
ATOM   1881  C   THR B 113     -19.569  32.417   2.918  1.00  9.45      BA   C
ATOM   1882  O   THR B 113     -18.362  32.290   3.177  1.00 10.54      BA   O
ATOM   1883  N   PHE B 114     -20.205  33.601   2.991  1.00  9.37      BA   N
ATOM   1884  CA  PHE B 114     -19.419  34.774   3.405  1.00  8.70      BA   C
ATOM   1885  CB  PHE B 114     -20.264  36.033   3.310  1.00 10.61      BA   C
ATOM   1886  CG  PHE B 114     -19.517  37.311   3.560  1.00  9.40      BA   C
ATOM   1887  CD1 PHE B 114     -19.245  37.717   4.878  1.00 11.56      BA   C
ATOM   1888  CE1 PHE B 114     -18.444  38.873   5.190  1.00 12.82      BA   C
ATOM   1889  CZ  PHE B 114     -18.068  39.655   4.051  1.00 13.28      BA   C
ATOM   1890  CE2 PHE B 114     -18.285  39.251   2.755  1.00 11.31      BA   C
ATOM   1891  CD2 PHE B 114     -19.043  38.081   2.479  1.00 12.28      BA   C
ATOM   1892  C   PHE B 114     -18.939  34.541   4.844  1.00  9.96      BA   C
ATOM   1893  O   PHE B 114     -19.696  33.994   5.627  1.00  9.92      BA   O
ATOM   1894  N   PRO B 115     -17.673  34.929   5.220  1.00  9.60      BA   N
ATOM   1895  CA  PRO B 115     -17.140  34.500   6.522  1.00  9.64      BA   C
ATOM   1896  CB  PRO B 115     -15.803  35.300   6.614  1.00 12.40      BA   C
ATOM   1897  CG  PRO B 115     -15.416  35.337   5.132  1.00 13.66      BA   C
ATOM   1898  CD  PRO B 115     -16.628  35.527   4.340  1.00 11.07      BA   C
ATOM   1899  C   PRO B 115     -18.092  34.904   7.669  1.00  8.91      BA   C
ATOM   1900  O   PRO B 115     -18.495  36.058   7.875  1.00 10.09      BA   O
ATOM   1901  N   GLY B 116     -18.459  33.893   8.421  1.00  9.19      BA   N
ATOM   1902  CA  GLY B 116     -19.312  34.036   9.590  1.00  8.76      BA   C
ATOM   1903  C   GLY B 116     -20.778  33.956   9.352  1.00  8.43      BA   C
ATOM   1904  O   GLY B 116     -21.544  33.702  10.307  1.00 11.75      BA   O
ATOM   1905  N   HIS B 117     -21.236  34.073   8.105  1.00  8.21      BA   N
ATOM   1906  CA  HIS B 117     -22.648  34.126   7.847  1.00  9.42      BA   C
ATOM   1907  CB  HIS B 117     -22.935  34.687   6.445  1.00  9.26      BA   C
ATOM   1908  CG  HIS B 117     -22.644  36.149   6.355  1.00  7.82      BA   C
ATOM   1909  ND1 HIS B 117     -23.095  36.901   5.301  1.00  9.42      BA   N
ATOM   1910  CE1 HIS B 117     -22.621  38.134   5.433  1.00 10.04      BA   C
ATOM   1911  NE2 HIS B 117     -22.014  38.250   6.608  1.00  9.44      BA   N
ATOM   1912  CD2 HIS B 117     -21.977  36.981   7.182  1.00  9.18      BA   C
ATOM   1913  C   HIS B 117     -23.399  32.802   8.022  1.00  9.08      BA   C
ATOM   1914  O   HIS B 117     -24.604  32.847   8.302  1.00 10.45      BA   O
ATOM   1915  N   SER B 118     -22.707  31.687   7.923  1.00  9.02      BA   N
ATOM   1916  CA  SER B 118     -23.454  30.419   8.001  1.00 10.68      BA   C
ATOM   1917  CB  SER B 118     -22.583  29.243   7.491  1.00 12.51      BA   C
ATOM   1918  OG  SER B 118     -21.552  29.051   8.362  1.00 15.43      BA   O
ATOM   1919  C   SER B 118     -23.936  30.099   9.408  1.00 11.02      BA   C
ATOM   1920  O   SER B 118     -24.815  29.246   9.543  1.00 10.76      BA   O
ATOM   1921  N   ALA B 119     -23.495  30.831  10.413  1.00  9.63      BA   N
ATOM   1922  CA  ALA B 119     -24.030  30.616  11.771  1.00 10.12      BA   C
```

```
ATOM   1923  CB  ALA B 119     -23.323  31.544  12.822  1.00 12.45      BA   C
ATOM   1924  C   ALA B 119     -25.554  30.865  11.757  1.00 10.11      BA   C
ATOM   1925  O   ALA B 119     -26.332  30.141  12.398  1.00 11.33      BA   O
ATOM   1926  N   LEU B 120     -26.009  31.890  11.069  1.00  9.15      BA   N
ATOM   1927  CA  LEU B 120     -27.428  32.247  11.009  1.00 10.97      BA   C
ATOM   1928  CB  LEU B 120     -27.578  33.748  11.363  1.00 10.75      BA   C
ATOM   1929  CG  LEU B 120     -27.154  34.126  12.783  1.00 10.29      BA   C
ATOM   1930  CD1 LEU B 120     -27.469  35.596  13.018  1.00 12.17      BA   C
ATOM   1931  CD2 LEU B 120     -27.911  33.226  13.822  1.00 13.38      BA   C
ATOM   1932  C   LEU B 120     -28.038  32.051   9.654  1.00 10.29      BA   C
ATOM   1933  O   LEU B 120     -29.272  31.858   9.571  1.00 10.12      BA   O
ATOM   1934  N   MET B 121     -27.261  32.074   8.594  1.00  9.32      BA   N
ATOM   1935  CA  MET B 121     -27.785  32.064   7.216  1.00  9.59      BA   C
ATOM   1936  CB  MET B 121     -27.084  33.074   6.291  1.00  9.54      BA   C
ATOM   1937  CG  MET B 121     -27.164  34.501   6.862  1.00  8.98      BA   C
ATOM   1938  SD  MET B 121     -26.591  35.743   5.699  1.00 10.54      BA   S
ATOM   1939  CE  MET B 121     -28.016  35.781   4.545  1.00 11.28      BA   C
ATOM   1940  C   MET B 121     -27.663  30.660   6.668  1.00  8.62      BA   C
ATOM   1941  O   MET B 121     -26.754  30.319   5.974  1.00  9.80      BA   O
ATOM   1942  N   LYS B 122     -28.620  29.821   7.147  1.00  9.56      BA   N
ATOM   1943  CA  LYS B 122     -28.626  28.413   6.732  1.00  9.61      BA   C
ATOM   1944  CB  LYS B 122     -27.681  27.541   7.555  1.00 11.26      BA   C
ATOM   1945  CG  LYS B 122     -28.098  27.113   8.951  1.00 10.58      BA   C
ATOM   1946  CD  LYS B 122     -28.297  28.276   9.918  1.00 12.38      BA   C
ATOM   1947  CE  LYS B 122     -28.657  27.664  11.289  1.00 13.34      BA   C
ATOM   1948  NZ  LYS B 122     -28.841  28.802  12.315  1.00 14.09      BA   N
ATOM   1949  C   LYS B 122     -30.053  27.898   6.886  1.00 11.06      BA   C
ATOM   1950  O   LYS B 122     -30.830  28.453   7.652  1.00 10.61      BA   O
ATOM   1951  N   GLY B 123     -30.376  26.845   6.149  1.00  9.18      BA   N
ATOM   1952  CA  GLY B 123     -31.657  26.174   6.229  1.00  9.46      BA   C
ATOM   1953  C   GLY B 123     -31.576  24.858   5.519  1.00  8.71      BA   C
ATOM   1954  O   GLY B 123     -30.560  24.420   5.076  1.00  9.86      BA   O
ATOM   1955  N   THR B 124     -32.723  24.178   5.492  1.00  9.53      BA   N
ATOM   1956  CA  THR B 124     -32.816  22.827   4.884  1.00 10.37      BA   C
ATOM   1957  CB  THR B 124     -33.581  21.884   5.826  1.00  8.60      BA   C
ATOM   1958  OG1 THR B 124     -34.929  22.357   6.006  1.00  9.91      BA   O
ATOM   1959  CG2 THR B 124     -32.941  21.839   7.199  1.00 10.67      BA   C
ATOM   1960  C   THR B 124     -33.464  22.865   3.528  1.00 11.15      BA   C
ATOM   1961  O   THR B 124     -34.247  23.768   3.213  1.00 10.75      BA   O
ATOM   1962  N   LEU B 125     -33.158  21.854   2.732  1.00 10.75      BA   N
ATOM   1963  CA  LEU B 125     -33.850  21.680   1.420  1.00 10.40      BA   C
ATOM   1964  CB  LEU B 125     -32.967  22.229   0.306  1.00 10.90      BA   C
ATOM   1965  CG  LEU B 125     -33.550  22.088  -1.123  1.00 10.20      BA   C
ATOM   1966  CD1 LEU B 125     -33.111  23.248  -1.980  1.00 11.93      BA   C
ATOM   1967  CD2 LEU B 125     -33.112  20.776  -1.801  1.00 12.78      BA   C
ATOM   1968  C   LEU B 125     -34.133  20.168   1.247  1.00 10.80      BA   C
ATOM   1969  O   LEU B 125     -33.255  19.339   1.534  1.00 11.30      BA   O
ATOM   1970  N   THR B 126     -35.329  19.866   0.767  1.00  9.69      BA   N
ATOM   1971  CA ATHR B 126     -35.632  18.471   0.490  0.50 10.44      BA   C
ATOM   1972  CA BTHR B 126     -35.751  18.506   0.602  0.50 11.08      BA   C
ATOM   1973  CB ATHR B 126     -36.157  17.700   1.757  0.50  9.77      BA   C
ATOM   1974  CB BTHR B 126     -36.604  18.097   1.831  0.50 12.17      BA   C
ATOM   1975  OG1ATHR B 126     -36.167  16.302   1.552  0.50 10.20      BA   O
ATOM   1976  OG1BTHR B 126     -37.869  18.771   1.831  0.50 17.79      BA   O
ATOM   1977  CG2ATHR B 126     -37.616  17.989   2.053  0.50 13.51      BA   C
```

```
ATOM   1978  CG2BTHR B 126     -35.885  18.460   3.136  0.50  9.03     BA   C
ATOM   1979  C   THR B 126     -36.565  18.349  -0.685  1.00 11.28     BA   C
ATOM   1980  O   THR B 126     -37.358  19.263  -0.986  1.00 10.80     BA   O
ATOM   1981  N   LEU B 127     -36.500  17.172  -1.334  1.00 12.31     BA   N
ATOM   1982  CA  LEU B 127     -37.560  16.861  -2.315  1.00 14.47     BA   C
ATOM   1983  CB  LEU B 127     -37.183  15.664  -3.193  1.00 15.89     BA   C
ATOM   1984  CG  LEU B 127     -36.057  15.928  -4.151  1.00 14.36     BA   C
ATOM   1985  CD1 LEU B 127     -35.576  14.633  -4.783  1.00 17.72     BA   C
ATOM   1986  CD2 LEU B 127     -36.596  16.795  -5.367  1.00 17.37     BA   C
ATOM   1987  C   LEU B 127     -38.898  16.459  -1.690  1.00 14.78     BA   C
ATOM   1988  O   LEU B 127     -38.981  15.893  -0.561  1.00 16.76     BA   O
ATOM   1989  N   LYS B 128     -39.977  16.725  -2.384  1.00 15.29     BA   N
ATOM   1990  CA  LYS B 128     -41.232  16.100  -1.962  1.00 16.87     BA   C
ATOM   1991  CB  LYS B 128     -41.982  17.058  -1.015  1.00 18.80     BA   C
ATOM   1992  CG  LYS B 128     -43.290  16.488  -0.474  1.00 25.04     BA   C
ATOM   1993  CD  LYS B 128     -43.975  17.491   0.476  1.00 31.02     BA   C
ATOM   1994  CE  LYS B 128     -45.186  16.865   1.140  1.00 33.04     BA   C
ATOM   1995  NZ  LYS B 128     -44.824  16.521   2.543  1.00 36.46     BA   N
ATOM   1996  C   LYS B 128     -42.044  15.830  -3.190  1.00 17.62     BA   C
ATOM   1997  O   LYS B 128     -42.034  16.581  -4.168  1.00 18.77     BA   O
ATOM   1998  OXT LYS B 128     -42.840  14.831  -3.193  1.00 19.21     BA   O
ATOM   1999 CU    CU F   1    -12.589  17.767 -12.503  1.00 19.72       CU
ATOM   2000 CU    CU G   1    -46.986  26.786 -12.948  1.00 16.77       CU
ATOM   2001 CU    CU I   1    -20.359  26.330  -9.881  1.00 28.14       CU
ATOM   2002 CU    CU J   1    -12.454  -9.224  -8.502  1.00 20.80       CU
ATOM   2003 CU    CU C   1     -3.365  12.626 -25.893  1.00 11.79       CU
ATOM   2004 CU    CU D   1    -24.028  36.223   3.615  1.00 12.77       CU
ATOM   2005  O3  TRS E   1    -14.395  17.729 -14.212  1.00 18.99        O
ATOM   2006  C3  TRS E   1    -13.744  18.792 -14.981  1.00 17.71        C
ATOM   2007  C   TRS E   1    -13.303  20.054 -14.270  1.00 19.95        C
ATOM   2008  N   TRS E   1    -12.245  19.647 -13.311  1.00 23.64        N
ATOM   2009  C2  TRS E   1    -12.646  20.904 -15.391  1.00 20.56        C
ATOM   2010  O2  TRS E   1    -13.751  21.432 -16.119  1.00 22.04        O
ATOM   2011  C1  TRS E   1    -14.578  20.634 -13.603  1.00 21.59        C
ATOM   2012  O1  TRS E   1    -14.110  21.779 -12.870  1.00 25.97        O
ATOM   2013  O3  TRS H   1    -20.199  24.487  -8.099  1.00 30.83        O
ATOM   2014  C3  TRS H   1    -19.170  25.140  -7.327  1.00 26.67        C
ATOM   2015  C   TRS H   1    -18.054  25.603  -8.297  1.00 28.27        C
ATOM   2016  N   TRS H   1    -18.705  26.526  -9.288  1.00 27.07        N
ATOM   2017  C2  TRS H   1    -16.960  26.287  -7.442  1.00 28.50        C
ATOM   2018  O2  TRS H   1    -16.584  25.377  -6.397  1.00 27.89        O
ATOM   2019  C1  TRS H   1    -17.533  24.348  -9.027  1.00 30.24        C
ATOM   2020  O1  TRS H   1    -16.299  24.679  -9.651  1.00 35.18        O
ATOM   2021  O3  TRS K   1     -0.029  20.230 -16.490  1.00 18.22        O
ATOM   2022  C3  TRS K   1      0.277  21.622 -16.799  1.00 20.71        C
ATOM   2023  C   TRS K   1      0.043  22.527 -15.536  1.00 22.13        C
ATOM   2024  N   TRS K   1      0.628  21.762 -14.406  1.00 21.69        N
ATOM   2025  C2  TRS K   1      0.814  23.848 -15.561  1.00 22.32        C
ATOM   2026  O2  TRS K   1      2.222  23.659 -15.573  1.00 19.28        O
ATOM   2027  C1  TRS K   1     -1.480  22.744 -15.300  1.00 22.41        C
ATOM   2028  O1  TRS K   1     -1.683  23.173 -13.933  1.00 25.94        O
ATOM   2029 CL    CL L   1     -5.194   0.875 -23.597  1.00 15.73       CL
ATOM   2030  O   HOH M   1    -22.510  17.883  -0.926  1.00 10.81        O
ATOM   2031  O   HOH M   2     -2.165   4.196 -13.909  1.00 10.99        O
ATOM   2032  O   HOH M   3    -20.520  31.438   6.133  1.00 10.83        O
```

```
ATOM   2033  O   HOH M   4      -1.385  26.078 -24.065  1.00 10.91           O
ATOM   2034  O   HOH M   5      -2.078   1.726 -17.768  1.00  9.95           O
ATOM   2035  O   HOH M   6      -8.473  19.636 -27.883  1.00 11.85           O
ATOM   2036  O   HOH M   7       0.962  15.797 -29.987  1.00  9.05           O
ATOM   2037  O   HOH M   9     -36.002  34.541   2.125  1.00 13.19           O
ATOM   2038  O   HOH M  10     -13.390  21.275 -21.901  1.00 12.95           O
ATOM   2039  O   HOH N   1     -20.833  19.771   7.832  1.00 12.95           O
ATOM   2040  O   HOH N   2     -12.967  13.183 -12.294  1.00 12.62           O
ATOM   2041  O   HOH N   3      -8.107  15.983 -28.633  1.00 10.13           O
ATOM   2042  O   HOH N   4     -15.976  25.929  -0.964  1.00 12.98           O
ATOM   2043  O   HOH N   5      -2.220   5.034 -11.270  1.00 10.43           O
ATOM   2044  O   HOH N   6     -21.514  14.876 -20.808  1.00 10.05           O
ATOM   2045  O   HOH N   7      -1.070  17.610 -15.517  1.00 14.59           O
ATOM   2046  O   HOH O   1     -25.593  24.437  10.325  1.00 13.43           O
ATOM   2047  O   HOH O   2     -36.340  21.029   4.046  1.00 16.61           O
ATOM   2048  O   HOH O   3      -4.551  14.538 -35.314  1.00  9.72           O
ATOM   2049  O   HOH O   4      -1.042   7.397 -10.154  1.00 11.14           O
ATOM   2050  O   HOH O   5     -24.206  34.295  11.020  1.00 14.60           O
ATOM   2051  O   HOH O   6     -17.046  30.997   5.078  1.00 16.55           O
ATOM   2052  O   HOH O   7      -6.842  16.636 -17.845  1.00 15.56           O
ATOM   2053  O   HOH O   8     -21.835  20.585  10.202  1.00 15.34           O
ATOM   2054  O   HOH O   9      -9.130   4.100 -28.845  1.00 14.12           O
ATOM   2055  O   HOH O  10     -24.649  20.864   7.999  1.00 15.01           O
ATOM   2056  O   HOH O  11     -31.453  33.201   8.486  1.00 15.99           O
ATOM   2057  O   HOH O  12     -17.633  19.030   5.741  1.00 13.66           O
ATOM   2058  O   HOH O  13     -30.825  30.499  11.327  1.00 17.02           O
ATOM   2059  O   HOH O  14     -18.513   0.628 -25.118  1.00 13.84           O
ATOM   2060  O   HOH O  15       2.199   1.315 -19.230  1.00 12.43           O
ATOM   2061  O   HOH P   1     -24.615  26.082  -9.539  1.00 15.99           O
ATOM   2062  O   HOH P   2     -40.846  23.157  -6.349  1.00 15.67           O
ATOM   2063  O   HOH P   3      -6.651   5.194 -30.153  1.00 13.38           O
ATOM   2064  O   HOH P   4      -1.401  -0.970 -18.666  1.00 15.35           O
ATOM   2065  O   HOH P   5     -24.888  26.928  11.187  1.00 17.48           O
ATOM   2066  O   HOH P   6     -22.602   4.558  -7.668  1.00 14.83           O
ATOM   2067  O   HOH P   7      -7.308  29.148 -20.073  1.00 14.00           O
ATOM   2068  O   HOH Q   1     -22.907  16.084  -2.926  1.00 14.58           O
ATOM   2069  O   HOH Q   2     -20.612  18.932 -28.178  1.00 12.41           O
ATOM   2070  O   HOH Q   3     -38.257  31.921 -11.324  1.00 11.56           O
ATOM   2071  O   HOH Q   4      -3.317  27.564 -21.347  1.00 14.77           O
ATOM   2072  O   HOH Q   5     -32.592  30.613   7.106  1.00 17.55           O
ATOM   2073  O   HOH Q   6       1.301  15.395 -15.162  1.00 15.21           O
ATOM   2074  O   HOH Q   7     -23.330  14.643 -18.717  1.00 16.37           O
ATOM   2075  O   HOH Q   8      -3.464   8.371  -9.145  1.00 13.93           O
ATOM   2076  O   HOH Q   9     -27.671  15.912   3.558  1.00 15.78           O
ATOM   2077  O   HOH Q  10      -8.100  19.013 -30.500  1.00 13.47           O
ATOM   2078  O   HOH Q  11     -21.091  24.632   9.247  1.00 19.56           O
ATOM   2079  O   HOH Q  12     -31.312  44.929   5.835  1.00 18.02           O
ATOM   2080  O   HOH Q  13     -15.097  29.927  -6.741  1.00 15.55           O
ATOM   2081  O   HOH Q  14     -33.325  37.145  -7.814  1.00 14.78           O
ATOM   2082  O   HOH Q  15     -44.506  21.975  -9.864  1.00 18.12           O
ATOM   2083  O   HOH Q  16       6.041  19.012 -20.273  1.00 16.12           O
ATOM   2084  O   HOH Q  17       2.897  10.134 -12.310  1.00 15.76           O
ATOM   2085  O   HOH Q  18     -13.806  19.761  -2.624  1.00 17.22           O
ATOM   2086  O   HOH Q  19      -0.970  11.033 -10.705  1.00 18.93           O
ATOM   2087  O   HOH Q  20      -9.203  16.896 -31.994  1.00 16.71           O
```

```
ATOM   2088  O   HOH Q  21     -1.511  24.748 -26.645  1.00 15.99           O
ATOM   2089  O   HOH Q  22    -20.120  15.875 -29.718  1.00 15.15           O
ATOM   2090  O   HOH Q  23      1.183  21.917 -24.797  1.00 16.33           O
ATOM   2091  O   HOH Q  24    -29.923  38.732  12.574  1.00 17.44           O
ATOM   2092  O   HOH S   1     -7.436  -3.420 -17.844  1.00 16.28           O
ATOM   2093  O   HOH S   2    -17.981  10.472  -9.064  1.00 19.24           O
ATOM   2094  O   HOH S   3     -8.127  16.514 -34.583  1.00 15.19           O
ATOM   2095  O   HOH S   4     -9.301  22.548 -16.206  1.00 18.79           O
ATOM   2096  O   HOH S   5    -23.220  22.932   9.574  1.00 18.06           O
ATOM   2097  O   HOH S   6    -24.914  14.483   5.038  1.00 17.43           O
ATOM   2098  O   HOH S   7    -18.936  24.075 -26.528  1.00 15.72           O
ATOM   2099  O   HOH S   8    -17.117  18.142 -14.499  1.00 17.81           O
ATOM   2100  O   HOH S   9      3.628   5.705 -17.611  1.00 21.70           O
ATOM   2101  O   HOH S  10    -25.921  32.222 -10.866  1.00 17.15           O
ATOM   2102  O   HOH S  11    -10.962  29.011   6.364  1.00 19.32           O
ATOM   2103  O   HOH R   1    -17.757  27.706  10.444  1.00 19.59           O
ATOM   2104  O   HOH R   2    -14.150  11.448 -10.491  1.00 18.99           O
ATOM   2105  O   HOH R   3      3.235  20.543 -14.637  1.00 18.35           O
ATOM   2106  O   HOH R   4    -27.484  21.119 -12.347  1.00 17.77           O
ATOM   2107  O   HOH R   5    -25.198  14.723  -3.702  1.00 21.03           O
ATOM   2108  O   HOH R   6    -33.591  16.634 -13.560  1.00 16.17           O
ATOM   2109  O   HOH R   7    -20.849   8.264 -30.333  1.00 16.63           O
ATOM   2110  O   HOH R   8    -35.273  37.125  -4.236  1.00 16.72           O
ATOM   2111  O   HOH R  10     -7.066  11.893 -11.155  1.00 19.81           O
ATOM   2112  O   HOH R  11     -4.758  -2.311 -23.346  1.00 16.31           O
ATOM   2113  O   HOH R  12    -34.369  15.291  -0.919  1.00 20.24           O
ATOM   2114  O   HOH R  13    -40.156  20.804 -15.225  1.00 17.21           O
ATOM   2115  O   HOH R  14    -18.475  -2.099  -6.192  1.00 15.81           O
ATOM   2116  O   HOH R  15      1.479   8.869 -10.359  1.00 13.93           O
ATOM   2117  O   HOH R  16    -28.020  28.673 -13.370  1.00 20.77           O
ATOM   2118  O   HOH R  17    -17.929  45.633  -2.149  1.00 17.99           O
ATOM   2119  O   HOH R  19    -21.995  13.898   1.680  1.00 19.40           O
ATOM   2120  O   HOH R  20      3.028  23.610 -18.084  1.00 18.31           O
ATOM   2121  O   HOH T   1     -0.761  17.920 -31.126  1.00 12.45           O
ATOM   2122  O   HOH T   2    -32.453  28.087   9.963  1.00 16.90           O
ATOM   2123  O   HOH T   3     -8.527  14.037 -12.112  1.00 17.75           O
ATOM   2124  O   HOH T   4    -10.557  25.487 -29.822  1.00 18.73           O
ATOM   2125  O   HOH T   5    -32.575  37.084 -10.404  1.00 15.44           O
ATOM   2126  O   HOH T   6    -44.312  13.929  -8.179  1.00 21.48           O
ATOM   2127  O   HOH T   7    -16.680  17.993   3.434  1.00 21.53           O
ATOM   2128  O   HOH T   8    -39.342  27.852   0.753  1.00 21.03           O
ATOM   2129  O   HOH T   9    -25.048  11.537 -25.955  1.00 17.48           O
ATOM   2130  O   HOH T  10     -1.719   1.773 -15.043  1.00 21.18           O
ATOM   2131  O   HOH T  11      4.480  20.893 -19.031  1.00 20.48           O
ATOM   2132  O   HOH T  12    -21.044  32.180  -4.783  1.00 22.11           O
ATOM   2133  O   HOH T  13    -16.653  12.138 -11.168  1.00 19.96           O
ATOM   2134  O   HOH U   2     -4.836  -4.639 -16.787  1.00 19.32           O
ATOM   2135  O   HOH U   3    -18.099  -4.662  -6.878  1.00 16.76           O
ATOM   2136  O   HOH U   4    -18.919  18.185   8.943  1.00 20.16           O
ATOM   2137  O   HOH U   5    -30.455  36.194  11.212  1.00 20.65           O
ATOM   2138  O   HOH U   6    -43.521  20.322 -12.148  1.00 16.75           O
ATOM   2139  O   HOH U   7    -34.420  13.489  -8.214  1.00 21.56           O
ATOM   2140  O   HOH U   8    -29.521   3.004 -15.755  1.00 18.13           O
ATOM   2141  O   HOH V   1    -33.695  40.556  10.112  1.00 21.59           O
ATOM   2142  O   HOH V   2    -12.324  27.448 -23.227  1.00 20.10           O
```

```
ATOM   2143  O   HOH V   3     -16.423  -0.190  -6.400  1.00 19.46          O
ATOM   2144  O   HOH V   4     -40.549  32.938  -9.993  1.00 16.37          O
ATOM   2145  O   HOH V   5       2.109  -1.429 -28.892  1.00 18.98          O
ATOM   2146  O   HOH V   6     -48.964  26.843 -11.461  1.00 17.61          O
ATOM   2147  O   HOH V   7     -23.987  30.517 -10.117  1.00 19.75          O
ATOM   2148  O   HOH V   8     -19.680  23.331 -19.957  1.00 19.58          O
ATOM   2149  O   HOH V   9     -26.530  24.901 -11.345  1.00 18.75          O
ATOM   2150  O   HOH V  10     -26.115  29.538  15.363  1.00 22.29          O
ATOM   2151  O   HOH V  11     -38.741  21.580   3.344  1.00 20.06          O
ATOM   2152  O   HOH V  12     -34.346   9.778  -5.451  1.00 20.58          O
ATOM   2153  O   HOH V  13     -12.561 -11.077 -10.052  1.00 21.18          O
ATOM   2154  O   HOH V  14     -27.283  13.412  -2.701  1.00 20.44          O
ATOM   2155  O   HOH V  15      -9.243  25.551   3.744  1.00 21.24          O
ATOM   2156  O   HOH V  16     -25.576  14.960 -23.254  1.00 17.70          O
ATOM   2157  O   HOH V  17     -12.466  -4.300  -9.133  1.00 17.22          O
ATOM   2158  O   HOH V  18     -12.338  23.852 -13.018  1.00 21.24          O
ATOM   2159  O   HOH V  19     -29.634  17.313   7.084  1.00 22.51          O
ATOM   2160  O   HOH V  20       5.598  15.122 -18.802  1.00 21.66          O
ATOM   2161  O   HOH V  21     -10.006  28.669 -19.777  1.00 19.65          O
ATOM   2162  O   HOH V  22     -12.110  -2.209 -21.954  1.00 21.45          O
ATOM   2163  O   HOH V  23       7.656   5.832 -20.233  1.00 18.94          O
ATOM   2164  O   HOH W   1     -17.623  31.220   7.718  1.00 20.70          O
ATOM   2165  O   HOH W   3     -38.198  22.657 -14.766  1.00 16.39          O
ATOM   2166  O   HOH W   4     -19.088  -5.898  -9.369  1.00 23.18          O
ATOM   2167  O   HOH W   5     -11.626  18.632 -32.858  1.00 20.35          O
ATOM   2168  O   HOH W   6     -37.845  13.473  -0.132  1.00 23.13          O
ATOM   2169  O   HOH W   7     -16.513  -3.149 -15.080  1.00 21.11          O
ATOM   2170  O   HOH W   8       0.608   2.001 -31.192  1.00 19.32          O
ATOM   2171  O   HOH W   9     -26.033   3.641 -12.403  1.00 17.41          O
ATOM   2172  O   HOH W  10     -25.802  15.654  -6.372  1.00 22.13          O
ATOM   2173  O   HOH W  11       2.664  12.866 -12.102  1.00 20.32          O
ATOM   2174  O   HOH W  12     -21.673  20.131 -25.859  1.00 18.92          O
ATOM   2175  O   HOH W  13      -7.116  17.971 -15.215  1.00 22.99          O
ATOM   2176  O   HOH W  14     -16.587  29.714   9.499  1.00 30.11          O
ATOM   2177  O   HOH W  15     -19.633  21.809  -7.736  1.00 23.00          O
ATOM   2178  O   HOH W  16     -25.763  22.399 -10.496  1.00 21.21          O
ATOM   2179  O   HOH W  17     -14.083  -2.815 -20.401  1.00 24.10          O
ATOM   2180  O   HOH X   1     -23.795  17.254  -7.379  1.00 21.68          O
ATOM   2181  O   HOH X   2     -36.414  18.215   5.425  1.00 22.86          O
ATOM   2182  O   HOH X   3     -17.439  -6.501 -11.656  1.00 23.44          O
ATOM   2183  O   HOH X   4     -21.988  45.223  -3.722  1.00 20.13          O
ATOM   2184  O   HOH X   5     -27.584  48.665   6.928  1.00 23.86          O
ATOM   2185  O   HOH X   6      -2.756  -3.280 -18.770  1.00 21.56          O
ATOM   2186  O   HOH X   7     -24.477  18.138 -20.671  1.00 21.49          O
ATOM   2187  O   HOH X   8     -40.497  36.916   3.238  1.00 21.42          O
ATOM   2188  O   HOH X   9       8.966  19.362 -24.880  1.00 20.88          O
ATOM   2189  O   HOH X  10     -23.697  16.074   8.956  1.00 23.60          O
ATOM   2190  O   HOH X  11      -8.599  -3.005 -28.451  1.00 23.12          O
ATOM   2191  O   HOH X  12     -31.443  43.066  -4.296  1.00 22.20          O
ATOM   2192  O   HOH X  13     -23.613  12.171 -14.740  1.00 22.10          O
ATOM   2193  O   HOH X  14     -11.320  -2.378 -25.817  1.00 21.79          O
ATOM   2194  O   HOH X  15     -16.339  20.680  -9.078  1.00 21.91          O
ATOM   2195  O   HOH X  16     -43.554  17.364 -17.963  1.00 23.55          O
ATOM   2196  O   HOH X  17     -21.761  14.017 -14.268  1.00 24.63          O
ATOM   2197  O   HOH Y   1     -35.669  17.258   8.899  1.00 22.05          O
```

```
ATOM   2198  O   HOH Y   2     -32.587  38.945  12.158  1.00 20.08          O
ATOM   2199  O   HOH Y   3     -40.096  32.455  -7.404  1.00 20.96          O
ATOM   2200  O   HOH Y   4      -9.791  24.095 -14.103  1.00 26.73          O
ATOM   2201  O   HOH Y   5     -14.915  39.523   6.992  1.00 23.62          O
ATOM   2202  O   HOH Y   6     -49.362  23.161 -11.901  1.00 18.92          O
ATOM   2203  O   HOH Y   7      -5.083  27.289 -26.513  1.00 20.73          O
ATOM   2204  O   HOH Y   8     -13.601  18.863  -5.245  1.00 21.94          O
ATOM   2205  O   HOH Y   9     -27.493  42.106 -10.079  1.00 21.32          O
ATOM   2206  O   HOH Y  10     -11.001  10.984 -36.713  1.00 19.82          O
ATOM   2207  O   HOH Y  11     -24.624   3.239 -20.884  1.00 18.66          O
ATOM   2208  O   HOH Y  12      -9.048  27.172   5.904  1.00 24.00          O
ATOM   2209  O   HOH Y  13      -0.238  19.139 -13.253  1.00 23.65          O
ATOM   2210  O   HOH Y  14     -17.407  14.641   1.205  1.00 20.10          O
ATOM   2211  O   HOH Y  15      -7.079  16.550 -12.747  1.00 23.95          O
ATOM   2212  O   HOH Y  17     -33.933  38.763   4.405  1.00 25.10          O
ATOM   2213  O   HOH Y  18      -9.260  31.270   6.033  1.00 28.93          O
ATOM   2214  O   HOH Y  19     -16.702  27.839  13.117  1.00 28.18          O
ATOM   2215  O   HOH Y  20     -14.821  41.702   5.200  1.00 22.58          O
ATOM   2216  O   HOH Y  21      -8.412  25.868   1.198  1.00 28.42          O
ATOM   2217  O   HOH Y  22     -10.970  14.110 -10.698  1.00 25.28          O
ATOM   2218  O   HOH Z   1       4.227  16.849 -14.885  1.00 22.60          O
ATOM   2219  O   HOH Z   2     -11.191  30.135 -10.002  1.00 21.87          O
ATOM   2220  O   HOH Z   3     -15.628   1.812  -4.329  1.00 20.69          O
ATOM   2221  O   HOH Z   4     -14.680  15.445 -31.568  1.00 28.30          O
ATOM   2222  O   HOH Z   5     -10.884  38.058  -2.736  1.00 21.25          O
ATOM   2223  O   HOH Z   6       5.989   4.546 -18.312  1.00 23.34          O
ATOM   2224  O   HOH Z   7     -16.323  22.525 -11.425  1.00 24.40          O
ATOM   2225  O   HOH Z   8     -23.821   0.494  -9.268  1.00 27.78          O
ATOM   2226  O   HOH Z   9     -13.678  17.506  -0.941  1.00 23.08          O
ATOM   2227  O   HOH Z  10     -24.417  12.737 -17.383  1.00 23.32          O
ATOM   2228  O   HOH Z  11      -8.600  26.446 -13.236  1.00 22.57          O
ATOM   2229  O   HOH Z  12     -14.825  28.330 -17.581  1.00 25.49          O
ATOM   2230  O   HOH Z  13     -34.155  44.033   8.540  1.00 22.43          O
ATOM   2231  O   HOH Z  14     -36.249  44.239  -0.546  1.00 23.25          O
ATOM   2232  O   HOH Z  15      -9.507  28.901 -13.727  1.00 23.77          O
ATOM   2233  O   HOH Z  17     -18.176  21.827 -13.394  1.00 25.81          O
ATOM   2234  O   HOH Z  19     -14.850  40.497   1.476  1.00 20.80          O
ATOM   2235  O   HOH Z  20      -1.096   5.299 -34.106  1.00 23.94          O
ATOM   2236  O   HOH Z  21     -30.788  13.564   5.307  1.00 22.57          O
ATOM   2237  O   HOH Z  22     -32.814  47.461  11.041  1.00 24.07          O
ATOM   2238  O   HOH Z  23     -38.615  17.887   6.636  1.00 23.21          O
ATOM   2239  O   HOH Z  24     -24.060  17.508 -29.875  1.00 23.59          O
ATOM   2240  O   HOH Z  25     -19.662  21.364  11.837  1.00 26.32          O
ATOM   2241  O   HOH Z  26       1.733   1.385 -15.470  1.00 25.79          O
ATOM   2242  O   HOH Z  27     -15.238  19.241   7.100  1.00 25.69          O
ATOM   2243  O   HOH Z  28     -40.177  20.520 -17.999  1.00 26.12          O
ATOM   2244  O   HOH Z  29     -25.162  27.347  13.891  1.00 26.01          O
ATOM   2245  O   HOH a   1     -29.131  -7.163 -12.501  1.00 31.46          O
ATOM   2246  O   HOH a   2     -42.178  27.037 -12.200  1.00 18.87          O
ATOM   2247  O   HOH a   3      -7.501  -2.315 -14.111  1.00 27.61          O
ATOM   2248  O   HOH a   4     -17.432  48.418  -1.772  1.00 23.79          O
ATOM   2249  O   HOH a   5     -18.537  26.108 -23.379  1.00 20.64          O
ATOM   2250  O   HOH a   6     -33.409  47.380   0.223  1.00 24.71          O
ATOM   2251  O   HOH a   7     -40.723  31.880  -3.163  1.00 23.15          O
ATOM   2252  O   HOH a   8      -7.798  -5.801 -28.449  1.00 19.36          O
```

```
ATOM   2253  O   HOH a   9     -31.877  25.489 -18.299  1.00 22.08           O
ATOM   2254  O   HOH a  10     -36.903   8.446   0.033  1.00 21.49           O
ATOM   2255  O   HOH a  11     -17.631  48.338   2.261  1.00 23.37           O
ATOM   2256  O   HOH a  12     -27.892  -4.302 -18.921  1.00 20.45           O
ATOM   2257  O   HOH a  13     -33.070  48.916  14.821  1.00 31.11           O
ATOM   2258  O   HOH a  14     -40.457  25.548  -0.650  1.00 28.88           O
ATOM   2259  O   HOH a  15     -30.831  47.368  -1.878  1.00 25.07           O
ATOM   2260  O   HOH a  16      -4.876  -2.854 -20.424  1.00 23.18           O
ATOM   2261  O   HOH a  17     -12.117  22.574   5.278  1.00 30.19           O
ATOM   2262  O   HOH a  18     -19.428  14.302 -12.692  1.00 24.17           O
ATOM   2263  O   HOH a  19     -12.330  26.167 -11.464  1.00 24.95           O
ATOM   2264  O   HOH a  20     -10.761  -4.932 -12.705  1.00 24.40           O
ATOM   2265  O   HOH b   1     -19.382  30.346   9.146  1.00 23.79           O
ATOM   2266  O   HOH b   2     -22.332  27.120  10.247  1.00 25.31           O
ATOM   2267  O   HOH b   3     -37.655  15.532 -11.825  1.00 25.71           O
ATOM   2268  O   HOH b   4     -17.747  29.381  -7.849  1.00 31.29           O
ATOM   2269  O   HOH b   5      -9.458  24.378  -5.683  1.00 25.89           O
ATOM   2270  O   HOH b   6       5.543  21.255 -16.173  1.00 25.40           O
ATOM   2271  O   HOH b   7     -12.367  14.256 -32.613  1.00 27.52           O
ATOM   2272  O   HOH b   8     -24.032  51.474   2.622  1.00 22.68           O
ATOM   2273  O   HOH b   9     -42.605  13.778 -15.461  1.00 29.72           O
ATOM   2274  O   HOH b  10     -22.245  15.671 -16.494  1.00 27.52           O
ATOM   2275  O   HOH b  11     -10.191  26.890  -0.433  1.00 23.91           O
ATOM   2276  O   HOH c   1     -25.866  10.333 -18.323  1.00 20.86           O
ATOM   2277  O   HOH c   2     -23.734  47.044  -3.153  1.00 24.67           O
ATOM   2278  O   HOH c   3     -19.525  38.013  -7.114  1.00 22.02           O
ATOM   2279  O   HOH c   5     -26.377   0.613 -21.878  1.00 21.74           O
ATOM   2280  O   HOH c   6      -9.462  19.921 -14.702  1.00 22.60           O
ATOM   2281  O   HOH c   7     -11.419  29.234   9.075  1.00 30.43           O
ATOM   2282  O   HOH c   8     -37.051  41.800  -1.236  1.00 22.27           O
ATOM   2283  O   HOH c   9       4.755   2.373 -28.722  1.00 26.25           O
ATOM   2284  O   HOH c  10     -21.986  16.880  -5.192  1.00 24.31           O
ATOM   2285  O   HOH c  11     -30.446  38.056 -11.766  1.00 25.12           O
ATOM   2286  O   HOH c  12     -38.349  37.810   1.744  1.00 29.82           O
ATOM   2287  O   HOH c  13     -36.589  23.226 -17.089  1.00 34.13           O
ATOM   2288  O   HOH c  14     -46.663  17.171 -12.132  1.00 21.15           O
ATOM   2289  O   HOH c  15       5.529  10.082 -11.852  1.00 24.90           O
ATOM   2290  O   HOH c  16     -14.394  26.717 -10.031  1.00 25.26           O
ATOM   2291  O   HOH c  17      -4.829  29.237 -24.084  1.00 28.76           O
ATOM   2292  O   HOH c  18     -13.832  29.312  -8.984  1.00 25.44           O
ATOM   2293  O   HOH c  19       8.869   9.106 -29.396  1.00 23.06           O
ATOM   2294  O   HOH d   1     -41.331  26.020  -5.382  1.00 25.32           O
ATOM   2295  O   HOH d   2     -10.081  41.384  -3.506  1.00 24.95           O
ATOM   2296  O   HOH d   3     -25.693  17.475 -24.211  1.00 21.08           O
ATOM   2297  O   HOH d   4     -40.544  15.560   1.727  1.00 23.02           O
ATOM   2298  O   HOH d   5     -26.916  12.775 -24.636  1.00 21.61           O
ATOM   2299  O   HOH e   1     -13.806  27.904 -25.699  1.00 28.08           O
ATOM   2300  O   HOH e   2     -20.648  23.852 -17.339  1.00 24.59           O
ATOM   2301  O   HOH e   3     -18.757  24.044 -29.109  1.00 24.80           O
ATOM   2302  O   HOH e   4     -21.788   4.648 -28.837  1.00 22.34           O
ATOM   2303  O   HOH e   6     -23.944  49.196  -1.254  1.00 26.24           O
ATOM   2304  O   HOH e   7     -21.522  50.616  -1.066  1.00 22.44           O
ATOM   2305  O   HOH e   8      -9.652  20.764 -32.123  1.00 27.01           O
ATOM   2306  O   HOH e   9     -39.938  25.820  -3.228  1.00 28.42           O
ATOM   2307  O   HOH e  10     -46.226  20.081 -12.047  1.00 26.84           O
```

```
ATOM   2308  O   HOH e  11     -17.953  15.584  -3.604  1.00 27.61           O
ATOM   2309  O   HOH e  12     -15.201  11.068 -32.086  1.00 29.02           O
ATOM   2310  O   HOH e  13      -4.987   5.214 -32.711  1.00 25.74           O
ATOM   2311  O   HOH e  14     -14.736  49.437   0.746  1.00 23.71           O
ATOM   2312  O   HOH e  15     -20.958  28.526  12.575  1.00 31.56           O
ATOM   2313  O   HOH e  16     -32.167  49.931   1.240  1.00 26.39           O
ATOM   2314  O   HOH e  17     -27.499   9.937 -16.286  1.00 27.90           O
ATOM   2315  O   HOH e  18     -14.915   8.446  -4.404  1.00 23.41           O
ATOM   2316  O   HOH e  19     -13.558  23.694   9.533  1.00 29.20           O
ATOM   2317  O   HOH e  20      -7.802  30.520 -26.483  1.00 26.98           O
ATOM   2318  O   HOH e  21     -40.870  37.727   5.946  1.00 25.74           O
ATOM   2319  O   HOH e  22     -47.879  21.429 -10.252  1.00 25.36           O
ATOM   2320  O   HOH f   1     -24.516  12.539 -29.906  1.00 24.61           O
ATOM   2321  O   HOH f   2     -19.591  25.322  12.359  1.00 32.69           O
ATOM   2322  O   HOH f   3     -42.582  22.992  -3.320  1.00 25.14           O
ATOM   2323  O   HOH f   4     -46.499  31.800  -8.078  1.00 30.15           O
ATOM   2324  O   HOH f   5     -34.635  46.759   8.412  1.00 30.26           O
ATOM   2325  O   HOH f   6     -25.876  15.093 -20.139  1.00 24.72           O
ATOM   2326  O   HOH f   7     -19.360  14.894  -1.342  1.00 27.71           O
ATOM   2327  O   HOH f   8     -17.489  22.159 -30.522  1.00 29.27           O
ATOM   2328  O   HOH f   9     -28.671  25.689 -15.317  1.00 27.68           O
ATOM   2329  O   HOH f  10     -19.780  49.293   3.637  1.00 20.21           O
ATOM   2330  O   HOH f  11       1.081   4.387 -35.609  1.00 28.33           O
ATOM   2331  O   HOH f  12     -19.461  46.426  -4.195  1.00 24.96           O
ATOM   2332  O   HOH f  13     -40.562  33.972   3.519  1.00 33.71           O
ATOM   2333  O   HOH f  14       9.215  11.598 -31.394  1.00 24.71           O
ATOM   2334  O   HOH f  15     -13.867  21.909   7.295  1.00 29.96           O
ATOM   2335  O   HOH f  16     -14.323  28.028   9.094  1.00 30.40           O
ATOM   2336  O   HOH f  17     -11.775  28.432 -12.422  1.00 28.72           O
ATOM   2337  O   HOH f  18     -17.383  28.695 -23.593  1.00 31.39           O
ATOM   2338  O   HOH f  19     -24.658  10.079  -9.101  1.00 28.35           O
ATOM   2339  O   HOH f  20     -27.971  14.489 -12.152  1.00 32.57           O
ATOM   2340  O   HOH f  21       8.094   3.026 -20.522  1.00 29.99           O
ATOM   2341  O3  TRS g   1     -13.129  15.785  -8.550  1.00 38.20           O
ATOM   2342  C3  TRS g   1     -14.245  15.390  -9.319  1.00 36.32           C
ATOM   2343  C   TRS g   1     -14.270  16.293 -10.543  1.00 35.85           C
ATOM   2344  N   TRS g   1     -13.083  16.108 -11.453  1.00 32.42           N
ATOM   2345  C2  TRS g   1     -15.551  16.000 -11.339  1.00 36.49           C
ATOM   2346  O2  TRS g   1     -16.676  16.637 -10.743  1.00 42.41           O
ATOM   2347  C1  TRS g   1     -14.189  17.735 -10.018  1.00 34.75           C
ATOM   2348  O1  TRS g   1     -13.770  18.583 -11.073  1.00 27.24           O
ATOM   2349  O   HOH h   1     -42.589  28.615  -8.385  1.00 24.31           O
```